Re-engineering the tropane alkaloid biosynthesis pathway in potato.

Matthew Hooper BSc (Hons) MRes

A thesis submitted for the degree of

Doctor of Philosophy

Heriot Watt University

August 2018

Abstract

Tropane alkaloids are a group of nitrogenous compounds that have a role in the treatment of multiple medical conditions. Many members of the Solanaceae produce these high valued compounds, such as the commercial source *Duboisia*. However, potato (*Solanum tuberosum*) does not produce tropane alkaloids. High levels of compounds which share tropane alkaloid precursors do accumulate in potato tissues (the nortropane alkaloids). The aim of this project is to investigate whether the range of alkaloids synthesised in potato can be enhanced by utilising biotechnological approaches to re-engineer the biochemical pathways, overcoming lesion points within potato.

Transgenic lines have been developed to investigate whether metabolic flux can be diverted away from the nortropane alkaloids and towards the precursors of the high value tropane alkaloids. Transgenic lines which over-express *tropinone reductase I*, have been shown to accumulate the precursor tropine, after the application of exogenous tropinone, and within leaf disc assays tropine accumulation reached 161.00 ± 3.61 μg/g FW in transgenic lines compared to 0.63 ± 0.05 μg/g FW in *Désirée* controls. Similarly, *tropinone reductase II* down-regulating lines have shown a decrease in the accumulation of pseudotropine, a nortropane alkaloid precursor; however, there was no statistically significant increase in tropine accumulation. Pseudotropine accumulation in down-regulating transgenic lines reached 1.64 ± 0.27 μg/g FW, compared to 5.24 ± 0.44 μg/g FW in *Désirée* controls. Other regions of the biosynthetic pathway were investigated through recombinant protein expression assays to generate a more in-depth understanding and identify further lesions in this pathway within potato. These assays showed that the annotated *hyoscyamine-6β-hydroxylase* within the potato genome browsers were not able to convert hyosycamine to the downstream tropane alkaloids, when compared to a bona-fide h6h enzyme from *Datura*.

I would like to dedicate this to my friends and family who have supported me throughout this process. I can not thank you all enough.

Acknowledgements

Firstly, I would like to acknowledge the support I have received from my supervisors. Dr. Raymond Campbell being there to bounce ideas off and offer advice when things were not going to plan with cloning issues that were encountered. Dr. Mark Taylor and Professor Derek Stewart for offering continued guidance and advice throughout this process and ensuring that I was on top of everything.

It would be remiss of me to not acknowledge my parents Martin and Jackie whom have taken an interest in this and asked questions to try and lead me down other trains of thought. My best pals Tilly and Duncan whom have offered an ear when I have needed to let loose and talk through things which were causing stress and have helped me change my lifestyle massively over the last 2 years. I would also like to thank the new friends I have made at the Dundee Roadrunners whom have opened my eyes to a new activity which has been extremely beneficial in relieving the stress that this project has bought on and the last few years certainly would not have been as fun without them.

I'd also like to thank and acknowledge the help and support received from the rest of the Taylor Group as well as the staff in the LC-MS facility at The James Hutton Institute for their ability to listen to my issues and offer advice as well as offer help with harvesting and tissue culture. So, my sincerest thank-you to: Dr. Laurence Ducreux, Dr. Wayne Morris, Dr. Almudena Trapero-Mozos, Dr. William Allwood, Dr. Alexandre Foito and Dr. Sabine Freitag.

I could go on, but there are too many people to name – sincerely to everyone who has offered help, advice and lent an ear – I can not thank-you enough!

ACADEMIC REGISTRY

Research Thesis Submission

Name*:*			
School:			
Version: *(i.e. First, Resubmission, Final)*		Degree Sought:	

Declaration

In accordance with the appropriate regulations I hereby submit my thesis and I declare that:

1) the thesis embodies the results of my own work and has been composed by myself
2) where appropriate, I have made acknowledgement of the work of others and have made reference to work carried out in collaboration with other persons
3) the thesis is the correct version of the thesis for submission and is the same version as any electronic versions submitted*.
4) my thesis for the award referred to, deposited in the Heriot-Watt University Library, should be made available for loan or photocopying and be available via the Institutional Repository, subject to such conditions as the Librarian may require
5) I understand that as a student of the University I am required to abide by the Regulations of the University and to conform to its discipline.
6) I confirm that the thesis has been verified against plagiarism via an approved plagiarism detection application e.g. Turnitin.

* *Please note that it is the responsibility of the candidate to ensure that the correct version of the thesis is submitted.*

Signature of Candidate*:*		Date:	

Submission

Submitted By *(name in capitals):*	
Signature of Individual Submitting:	
Date Submitted:	

For Completion in the Student Service Centre (SSC)

Received in the SSC by *(name in capitals):*			
Method of Submission *(Handed in to SSC; posted through internal/external mail):*			
*E-thesis Submitted (**mandatory for final theses)***			
Signature:		Date:	

Table of contents

List of tables

Tables in the Appendix:

List of figures

Figures in the appendix:

Abbreviations

<	Less than
>	More than
µg/g	microgram/gram
35s CaMV	*35s Cauliflower Mosaic Virus*
B.C	Before Christ
BRIC	Brazil, Russia, India and China
CDS	Coding Sequence
cDNA	complementary DNA
CID	Collision Induced Dissociaton
DAO	Diamine Oxidase
ddH_2O	double distilled water
Ds	*Datura stromonium*
DNA	Deoxyribonucleic acid
DW	Dry Weight
ef-Iα	*elongation-factor-Iα*
FW	Fresh Weight
gadph	*Glyceraldehyde 3-phosphate dehydrogenase*
GCMS	Gas Chromatography Mass Spectrometry
h6h	*hyoscyamine-6β-hydroxylase*
HPLC-UV	High Performance Liquid Chromotography Ultra Violet
IPTG	Isopropyl β-D-1-thiogalactopyranoside
KCl	Potassium chloride
LLE	Liquid-Liquid Extraction
LB	Lysogeny Broth
LOD	Limit Of Detection
LOQ	Limit of Quantification
mg/kg	milligrams/kilogram
MRM	Multiple Reaction Monitoring
MS 20	Murashige Skoog 20
m/z	mass/charge ratio
NADP(H)	Nicotinamide Adenine Dinucleotide Phosphate
nptII	*Neomycin phosphotransferase II gene*
PAV	Presence Absence Varients

PCR	Polymerase Chain Reaction
PDA	Photo-Diode Array
pmt	*putrescine-N-methyltransferase*
QqQ-LC-MS/MS	Triple Quadrupole Liquid Chromatography Mass Spectrometer
RNA	Ribonucleic acid
RT-qPCR	Real Time quantitative Polymerase Chain Reaction
SAM	S-adenosylhomocysteine
SASA	Science and Advice for Scottish Agriculture
SDR	Short chain dehydrogenase/reductase
SnRKI	*sucrose-non-fermenting-I related protein kinase*
SOC	Super Optimal broth with Catabolite supression
SPE	Solid-Phase Extraction
St	*Solanum tuberosum*
TBS-T	Tris-Buffered Saline with Tween
t/ha	tons/hectare
TLC	Thin Layer Chromotography
trI	*tropinone reductase I*
trII	*tropinone reductase II*
TRL	Tropinone Reductase Like
USA	United States of America
VIGS	Virus Induced Gene Silencing
WHO	World Health Organisation
Ws	*Withania somnifera*

Chapter 1: General Introduction

1.1 Natural products from plants

Natural products are broadly defined as *'chemical compounds produced by living organisms'* (Abdel-lateif *et al*, 2016). Natural products have a role in an organism's physiology and can provide secondary benefits to the organism. Within plants, many natural products are secondary metabolites; these are chemical compounds which are not involved in the regular maintenance of the life cycles of the plants which synthesise them (Oksman-Caldentey and Inzé, 2004).

During the early 1900s, plant-derived medicines from the root, leaves and bark accounted for 80% of medicines used. It is also estimated that currently 60% of anticancer compounds are produced from natural products (Abdel-lateif *et al*, 2016). There continues to be great emphasis on elucidating the pathways for the production of plant natural products as some synthetic drugs, in particular antimicrobials cause a number of negative side effects (Abdel-lateif *et al*, 2016). The World Health Organisation (WHO) have generated a list of 252 essential drugs, of these 11% are produced from natural products of flowering plants, which in 2002 were valued at US$30 billion just in the USA (Oksman-Caldentey and Inzé, 2004).

More than 200,000 natural plant products have been discovered, and these can be divided into groups dependent on their chemical composition (Springob and Kutchan, 2009). One of the diverse groups is the alkaloids, and all the groups are produced through complex biosynthetic routes. A simple definition of an alkaloid was offered by Pelletier in 1983: '*a cyclic compound containing nitrogen in a negative oxidation state which is of limited distribution in living organisms*' (Roberts and Wink, 1998). The alkaloids are one of the most diverse groups of natural products, with humans having exploited these plant natural products for centuries (see section 1.3). Alkaloid diversity begins with the amino acid they are derived from; for example, the benzylisoquinoline alkaloids are derived from two tyrosine molecules whilst the pyrrollzidine alkaloids are composed of a necine base (hydroxymethylpyrrilizadine) which is esterified (Springob and Kutchan, 2009) during biosynthesis.

1.2 Definition and occurrence of tropane alkaloids.

Since 1983 the definition of tropane alkaloids has been refined to include the presence of two or more hydroxyl groups (Molyneux *et al*, 2002) along with the tropane ring which is the defining feature of these compounds (Figure 1.1, Philipov and Doncheva, 2013). The tropane alkaloids are a group of secondary metabolites produced by some members of the plant families Solanaceae, Erythroxylaceae, Convolvulaceae, Proteaceae and Rhizophoraceae (Jirschitzka *et al*, 2012; Philipov and Doncheva, 2013). *Erythroxylum*, more commonly known as the coca plant belongs to the family Erythroxylaceae and has been found to contain hygrine and cocaine. The plant family Convolvulaceae which includes *Calystegia sepium* is a source of nortropane alkaloids, known as the calystegines (Christen, 2000). *Triunia montana* (a member of the proteaceae) have been found to contain tropane alkaloids with side chains connected at either C2 or C4, such as darlingine (Yang *et al*, 2017) and *Bruguiera sexangula* (Rhizophoraceae) contain the alkaloid brugine (Griffin and Lin, 2000). In 2003 it was reported that there were over 12,000 known chemical alkaloid structures (Hashimoto and Yamada, 2003), but this figure increased to just over 27,000 by 2014, although there is uncertainty as to the validity of some of these compounds (Amirkia and Heinrich, 2014). Of these, over 200 are known to belong to the tropane alkaloids (Philipov and Doncheva, 2013).

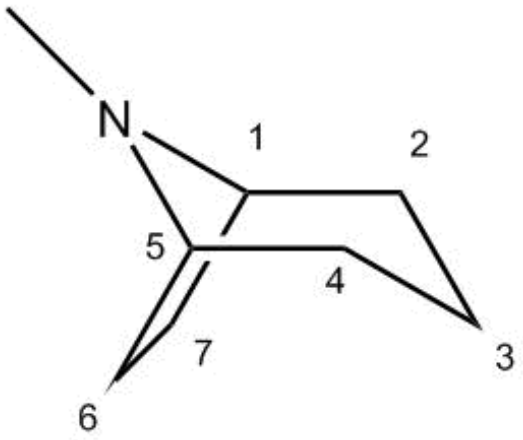

Figure 1.1: **Tropane alkaloid backbone.**

Schematic of the tropane alkaloid backbone showing the seven carbon atoms; adapted from Philipov and Doncheva (2013)

1.3 History

Tropane alkaloids have been used for their inherent pharmaceutical properties throughout history, having been first used for their hallucinogenic properties, but now more for their action as anticholinergics or stimulants (Griffin and Lin, 2000).

Some of the earliest evidence that indicates that humans were using plants which produced tropane alkaloids is from 4000 year old Assyrian clay tablets, where *Atropa belladonna* and other plants are mentioned (Wink, 1998). In both India and China, the use of alkaloid producing plants in medicine has been described as far back as 900 B.C and 3000 B.C respectively (Wink, 1998). Tropane alkaloids were first introduced into European medical practices by Romany immigrants with references being made in the 17th Century (Griffin and Lin, 2000), but it was not until 1819 when the term alkaloid was used to describe these compounds by the German chemist, Carl Meiβner.

Methods for extracting purified alkaloids became available from 1830 onwards with hyoscyamine amongst the first to be extracted (Grynkiewicz and Gadzikowska, 2008). Around 1860 Western Civilisation first experienced specific tropane alkaloid preparations. These were preparations of scopolamine and hyoscyamine made by Australian Aborigines using the leaves and twigs of *Duboisia hopwoodii*, and was known as ‘pituri’ (Bernard, 1952), which during expeditions by Western botanists to Australia in the early to mid-1800s, were collected. This allowed investigations into the physiological effects of tropane alkaloids to occur.

During World War II, the leaf of the current commercial tropane alkaloid producing plants was first studied for its alkaloid composition. *Duboisia myoporoides* and *Duboisia leichhardtii* were found to contain scopolamine and hyoscyamine in higher concentrations than the sources being used at the time (*Atropa belladonna* and *Hyoscyamus* spp.) (Barnard, 1952), this resulted in them being adopted as an industrial source for tropane alkaloids.

1.4 Recent uses.

More recently, the use of plant derived drugs is on the increase, particularly those based on the tropane alkaloid skeleton such as scopolamine which has been shown to help in the treatment of motion sickness and hyoscyamine in the treatment of gastrointestinal disorders (Hashimoto *et al*, 1993; Oksman-Caldentey, 2007).

Atropine, a tropane alkaloid which is formed by the racemization of (-)-hyoscyamine, has uses in both ophthalmology and cardiology, where it is used for its analgesic and antispasmodic properties on the parasympathetic nervous system (Khanam *et al*, 2001; Palazon *et al*, 2003). Dependent on the dose administered, atropine can be used to treat both bradycardia and tachycardia. For the treatment of bradycardia, which is when an individual has a low regular heart rate, atropine is administered in low concentrations where it increases the firing of the sino-ventricular node. In cases of tachycardia, where a patient's resting heart rate is over 100 beats per minute, atropine treatment at higher doses inhibits the sino-atrial node and reduces the heart rate. In both cases, and to varying degrees, atropine blocks the acetylcholine receptors within the heart muscular walls and can slow the heartbeat. The effects between both scopolamine and atropine have upon the central nervous system differ greatly, and this is thought to be due to the enhanced permeability of scopolamine to cross the blood-brain barrier.

Scopolamine can cause drowsiness and fatigue making it effective as a motion sickness medication (Christen, 2000). According to Kumar *et al* (2010), the use of scopolamine through transdermal delivery systems for motion sickness was expected to have a market value of US$31.5 billion in 2015. In contrast the nortropane arm of the biosynthesis pathway, which leads to the production of the calystegines, which display strong glycosidase inhibition (Kaiser *et al*, 2006), is much less valued compared to the tropane alkaloids. The Brazil, Russia, India and China (BRIC) Diabetes Drugs Market report (Markets and Markets, 2018) indicated that diabetes mediation was worth US$8.7 billion in 2014. This value is solely for diabetes medication and includes both the oral and injectable markets.

Glycosidase inhibitors can be used in the treatment of diabetes, as they block the breakdown of glucosides, reducing glucose release. Molyneux *et al*, (1993) demonstrated that a complex of Calystegine B_1 (27%) and B_2 (73%) from extracts of *Calystegia sepium* displayed potent inhibitory characteristics against β–glucosidase, with 50% inhibition being seen at a calystegine complex concentration of 0.6 µg/ml. Currently the nortropane alkaloids are not extracted for use as glycosidase inhibitors. However, due to the inhibition exhibited above, there is interest in utilising these compounds as antiviral or anticancer medication which could see their economic value and interest increase (Schimming *et al*, 2005).

1.5 Biosynthetic Pathway.

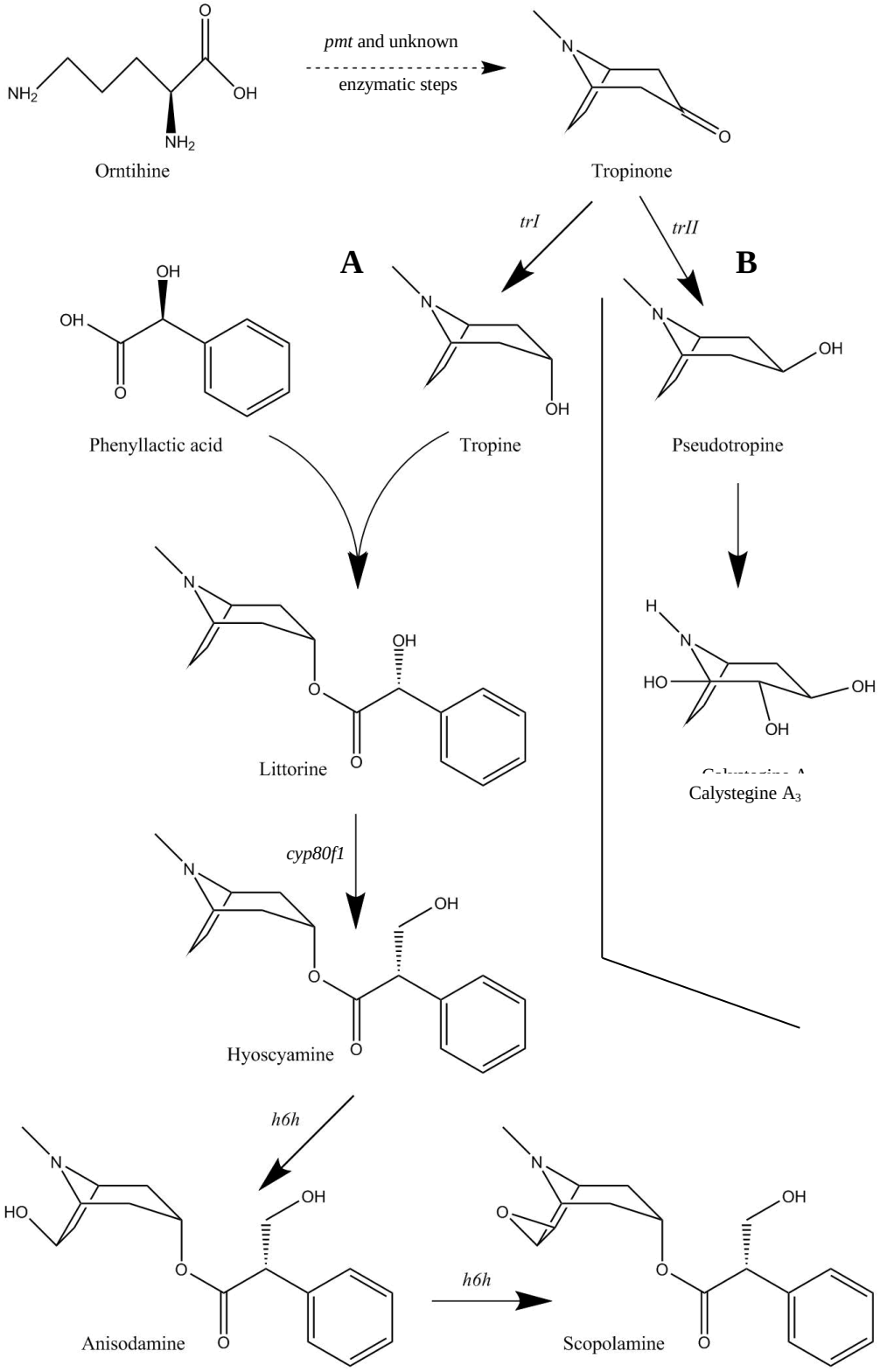

Figure 1.2: **Tropane and nortropane alkaloid biosynthetic pathway in the Solanaceae.** The tropane alkaloid pathway can be seen with the formation of tropine catalysed by the trI (EC 1.1.1.206) enzyme, with subsequent catlysisation by the enzymes cyp80F1 (Q1A1B0-1) and h6h (EC 1.14.11.11) (**A**). Whereas, the nortropane arm can be seen from tropinone and the action of trII (EC 1.1.1.236), leading to pseudotropine formation (**B**). In both cases pmt (EC 2.1.1.53) is responsible for the formation of tropinone from ornithine.

1.5.1 The shared pathway within the Solanaceae.

The formation of tropane alkaloids begins with the precursor amino acid L-ornithine (Philipov and Doncheva, 2013) which, in a reaction catalysed by *ornithine decarboxylase*, is decarboxylated to form putrescine. Putrescine undergoes methylation via the catalytic activity of *putrescine N-methyltransferase* (*pmt*) (Stenzel *et al,* 2006; Hashimoto *et al,* 1989) to produce *N*-methylputrescine. *N*-methylputrescine is the substrate for *N*-methylputrescine oxidase (a diamine oxidase (DAO)) which catalyses an oxidative deamination reaction to produce *N*-methyl-Δ^1-pyrrolinium (Hashimoto 1990; Dewick, 2009). The mechanisms behind the conversion of *N*-methyl-Δ1-pyrrolinium to tropinone are yet to be elucidated (Rocha *et al,* 2002), however, *N*-methyl-Δ1-pyrrolinium is the substrate which is considered to be the branch point for other alkaloid synthesis pathways such as the formation of cocaine in the Erythroxylaceae (Schmidt *et al,* 2015).

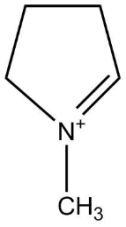

Figure 1.3: **Chemical structure of *N*-methyl-Δ^1-pyrrolinium**.
This is the metabolite at the diversion point for the production of tropane alkaloids in the Solanaceae and Erythroxylaceae.

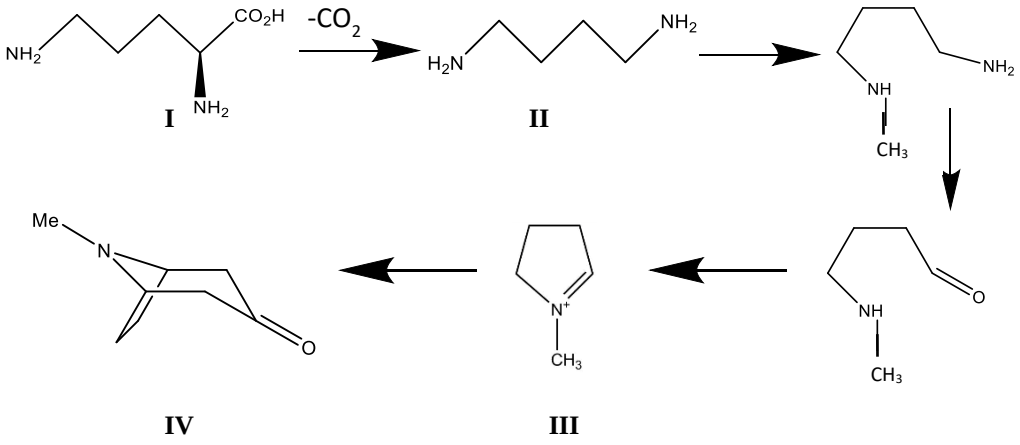

Figure 1.4: **The first steps in the formation of tropinone**.
Representation of the biosynthetic pathway for the formation of tropinone (IV) from L-ornithine (I) via *N*-methylputrescine (II) and the *N*-methyl-Δ^1-pyrrolinium (III) cation.

Tropinone serves as the substrate for two NADP(H) (Nicotinamide Adenine Dinucleotide Phosphate) dependent tropinone reductases (trI and trII) which have different stereospecificities (Nakajima *et al*, 1993; Robins *et al*, 1991). It is these stereospecifities which indicate which arm of the pathway (as shown in Figure 1.2) substrate flux is diverted to and refers to the isomer of the molecule present. In both cases the chemical formula is the same, but it is the orientation of the molecules which differs. Both trI and trII act upon the same 3α-hydroxyl group in tropinone and convert it to the 3α-hydroxytropane of tropine or 3β-hydroxyl of pseudotropine respectively (Figure 1.5). Both trI and trII belong to the short-chain dehydrogenase/reductase (SDR) family of enzymes, with the enzymes in this family sharing low sequence similarity (up to 30%) and are generally of about 300 amino acids in length (Brock *et al*, 2008). However, the similarity between trI and trII within the SDR family has been reported as 64% across 260 amino acid residues (Nakajima *et al*, 1993). There is evidence for the presence of trI in *Solanum tuberosum*; however, its activity is poor, with speculation that its function is not devoted to tropane alkaloid biosynthesis (Kaiser *et al*, 2006). Manipulation of the trI arm of the tropane alkaloid biosynstheis pathway will be investigeated in Chapter 5, whereas, Chapter 6 is concerned with manipulation of both the trII nortropane alkaloid arm and trI arm.

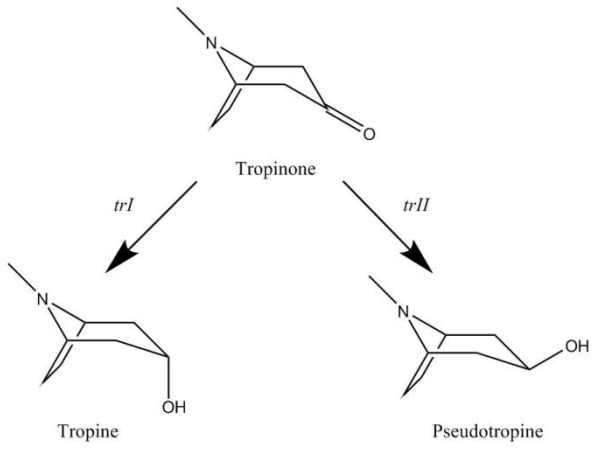

Figure 1.5: **The tropinone branch point.**

Schematic showing the two compounds tropine (bottom left) and pseudotropine (bottom right) formed from tropinone (top middle) catalysed by trI and trII respectfully.

1.5.2 The tropane alkaloid arm

The formation of tropine from tropinone is catalysed by trI, which is the start of the pathway to the high value tropane alkaloids hysocyamine and scopolamine. Tropine undergoes a condensation reaction with phenyllactate to form littorine (Lanoue *et al*, 2002 and Dewick, 2009), however the enzyme(s) which catalyse this reaction are currently unknown. It is hypothesised that a co-enzyme A ester is involved, with Robins *et al*, (1994), suggesting the use of an '*activated ester, such as co-enzyme A thioesters, or an alkaloidal ester'* as a substrate for the formation of littorine from work conducted on transformed root cultures of *Datura stromonium* and *Duboisia leichhardti.*

Early suggestions were that the conversion of littorine to hyoscyamine required co-enzyme B_{12} as a cofactor, however this compound is not found in higher plants. This speculation was due to the similarity found in the conversion of methylmalonyl CoA to succinyl-CoA (Leete, 1990; Ollangnier *et al,* 1998). Vitamin B_{12} is a source of 5`-deoxyadenosyl radicals in bacteria and animals; S-adenosylmethionine (SAM) exhibits a similar function in plants (Ollangnier *et al,* 1998). Ollangnier *et al*, (1998) have also demonstrated that in the presence of exogenous SAM in *Datura stramonium* root cultures, hyoscyamine levels increased to 61% (compared to 3.5% in SAM deficient cultures), as measured by GC-MS (Gas Chromatography-Mass Spectometry).

More recently a cytochrome P450 (*cyp80f1*) known as littorine mutase/monoxygenase has been identified, which catalyses the conversion of littorine to hyoscyamine (Li *et al*, 2006). In these experiments, the cytochrome P450 gene function was tested by virus induced gene silencing (VIGS) assays. Experimentally, *in vitro* it was found that (R)-littorine was mainly converted to hyoscyamine aldehyde and (2'R,3'R)-3'-hydroxylittorine by *cyp80f1* as shown in Figure 1.6. *In vivo* experiments demonstrated that the suppression of this cytochrome P450 via VIGS resulted in littorine accumulation, whereas, overexpression of *cyp80f1* in the roots of *Nicotiana benthamiana* supplemented with littorine showed a significant increase in hyoscyamine. Figure 1.6 depicts the two potential routes for the conversion of littorine to hyoscyamine.

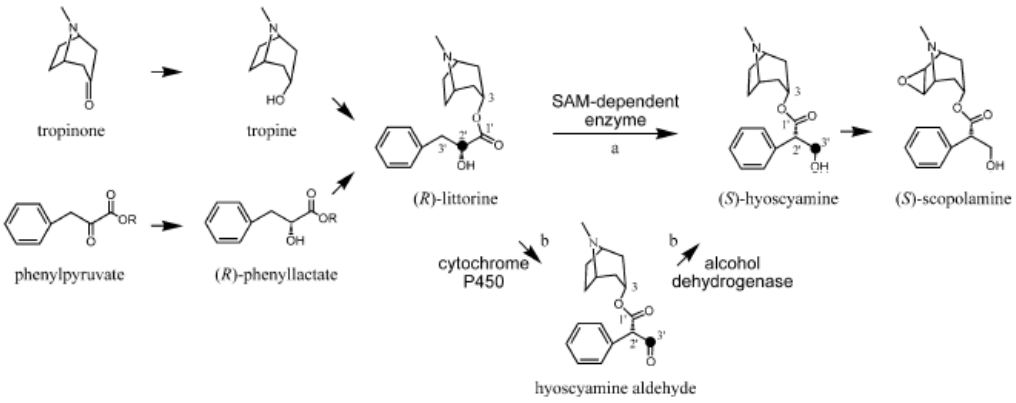

Figure 1.6: **The two proposed routes for the formation of hyoscyamine from littorine**. Schematic of the biosynthesis pathway from tropinone to scopolamine via 2 proposed routes – the SAM mediated pathway (upper route) or through use of *cyp80f1* (Li *et al*, 2006)

The final step in the biosynthesis of scopolamine is the hydroxylation and epoxidation of hyoscyamine to scopolamine via an intermediate 6β-Hydroxy-hyoscyamine (anisodamine) with both reactions catalysed by the enzyme hysocyamine-6β-hydroxylase (h6h) (Rocha *et al*, 2002). The first step of this reaction is to introduce a 6β-hydroxyl group onto C6 of the tropane ring. Once this intermediate is formed, the same enzyme catalyses the formation of scopolamine; by closing the epoxide ring (Humphrey and O'Hagan, 2001). This is the removal of the hydrogen bound to oxygen at the C7 position of the tropane skeleton, and the oxygen then becoming bound to the C6 and C7 closing the ring (as shown in Figure 1.7). This will be investigated in Chapter 4.

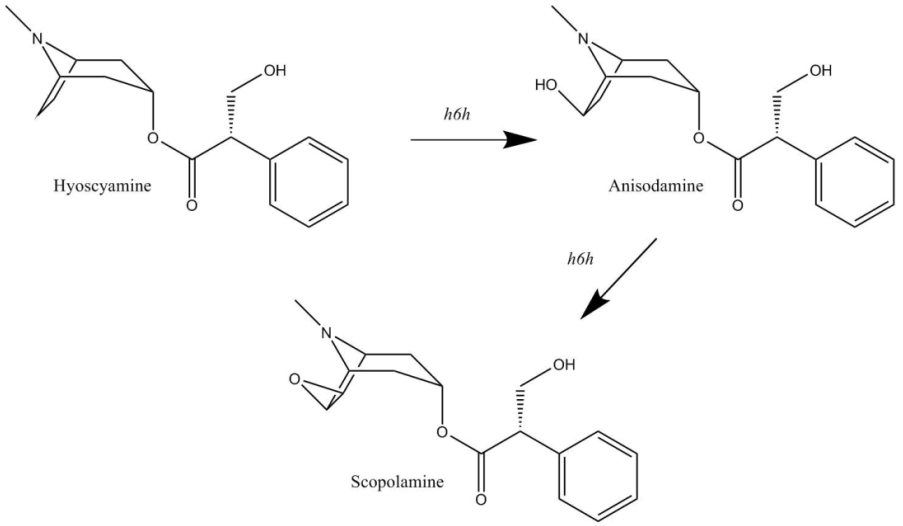

Figure 1.7: **Representation of the biosynthesis of scopolamine from hyoscyamine**. Hyoscyamine being converted to scopolamine via the intermediate anisodamine (6β-hydroxy-hyoscyamine) by the enzyme h6h.

1.5.3 The notropane alkaloid arm

Previous studies have shown that *Solanum tuberosum* (potato) tissues completely lack tropane alkaloids (Keiner and Dräger, 1999). However, alkaloids in the form of nortropanes are known to accumulate in some tissues (Griffiths *et al*, 2008 and Richter *et al*, 2005). The first step in the nortropane alkaloid specific pathway is the formation of pseudotropine from tropinone, catalysed by the enzyme trII (Richter *et al*, 2005). Within these studies it was ascertained that pseudotropine accumulated quicker than tropine, confirming the trII activity levels shown within potato (Dräger, 2006). Transcripts for *trII* have been shown to be present in all parts of *Solanum tuberosum*; however, some tissues do not exhibit trII enzyme activity due to unknown regulatory factors (Keiner *et al*, 2002). The calystegines, the biosynthetic compounds of pseudotropine, are a diverse group of compounds which all share the same tropinone background, with the difference between the compounds being the location and number of hydroxyl groups present, thus they are a family of polyhydroxy-nortropanes (Griffiths *et al*, 2008).

There have been studies focused on the distribution of calystegines across some Solanaceous and Convolvulaceae plant tissues and these centre around nine of the most common (A_3, A_5, A_6, B_1, B_2, B_3, B_4, C_1 and N_1), (Bekkouche *et al*, 2001; Schimming *et al*, 2005). These studies have documented the distribution of calystegines in potato tissues with levels reaching up to 316 mg/kg DW (Dry Weight) in the tuber flesh and up to 2581 mg/kg DW within the tuber peel (Friedman *et al*, 2003). Griffiths *et al*, (2008) analysed 4 *Phureja* and 5 *Tuberosum* (*Solanum tuberosum* Group *Phureja* and *Tuberosum*) lines and found that the concentration of calystegines were 100-fold higher in tuber sprouts than tuber flesh, and 8 times that of the peel for group *Tuberosum*, with similar results reported for calystegine concentration in *Phureja* lines. Calystegine levels are also known to decrease as the plant matures and tuberises (Keiner and Dräger, 1999). Due to the ability of calystegines to act as glycosidase inhibitors the determination of alkaloid levels within the edible tuber has been extensively investigated. Friedman *et al*, (2003) and Petersson *et al*, (2013) determined the calystegine content of eight and thirteen potato cultivars respectively from the flesh and peel of the tuber individually as well as the tuber as a whole. They showed that there is significant variability in the calystegine content between cultivars studied.

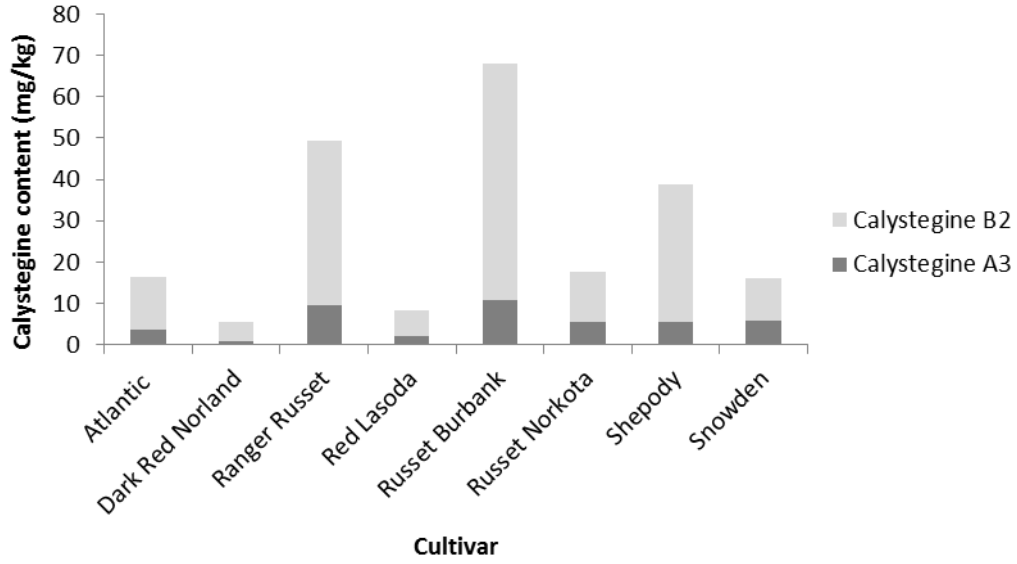

Figure 1.8: **Calystegine content in eight potato cultivars.**

Total fresh weight calystegine content (mg/kg) of tubers from eight potato cultivars as described by Friedman *et al*, (2003).

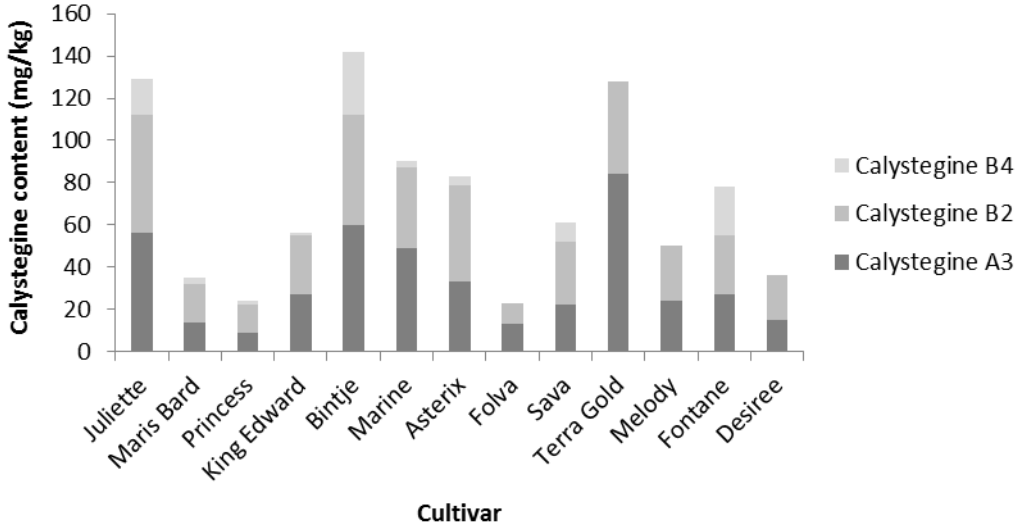

Figure 1.9: **Calystegine content from thireteen potato cultivars.**

Total fresh weight calystegine content (mg/kg) of tubers from thirteen potato cultivars as described by Petersson *et al*, (2013).

Petersson *et al*, (2013) noted that calystegine A_3 and B_2 are found at similar levels between cultivars (Figure 1.9), however this differs from the finding of Friedman *et al*, (2003) (Figure 1.8). This highlights that the levels of calystegines within potato are variable, with possible genetic and/or environmental reasons for the differences. One such external consideration for variability of calystegines is the storage conditions of potato tubers. In a summary, Keiner and Dräger (1999) describe this variability from

two previous studies; the first conducted by Nash *et al*, (1995) reported a calystegine level of 100 µg/g in fresh potato peel, with the rest of the tuber being one tenth of this. Whereas, Asano *et al*, (1995) find that between 3.4 and 7 µg/g fresh whole tuber mass was calystegine. Keiner and Dräger (1999) deduced from this and other studies that calystegine content decreased within the sprouts, and that sprouts of eight months of age have approximately half the calystegine levels of those from tubers after five months of storage. Within tuber sprouts they demonstrated that after exogenous tropinone application, only pseudotropine was detected within sprouts. There were no tropane or nortropane alkaloids found within control assays.

1.6 Production in the Solanaceae

The Solanaceae family contains nearly 3000 species (Christen, 2000) and are comprised of two sub-families, the Solanoidea and the Cestroideae (Griffin and Lin, 2000). These sub-families can be further divided into seven tribes (which is a secondary taxonomic rank between family and genus (IAPT, 2012). Tribe members are capable of producing tropane alkaloids in different quantities and specificities. The sub-family Solanoidea consists of four tribes: the Datureae, Solandreae, Solaneae and the Hyoscyameae with the remaining three tribes belong to the sub-family, Cestroideae. These remaining three are the Anthocercideae, Nicandreae and the Salpiglossidae (shown in Figure 1.10) (Griffin and Lin, 2000).

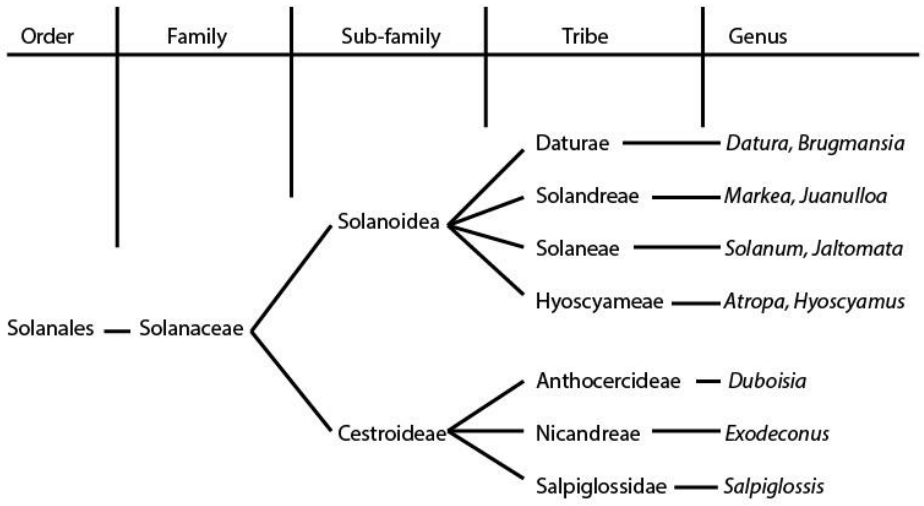

Figure 1.10: Tribes within the Solanaceae.

Diagrammatic representation of the lineage through the various taxonomic levels of tropane alkaloid producing members of the Solanaceae.

The alkaloids produced by tribe members of this family can be separated into five different sub-groups: miscellaneous alkaloids, (such as hygrine and tropinone), monosubstituted tropanes (tropine, littorine), 3-6 disubsitituted tropanes (3,6-dihydroxytropane), 3-substituted-6,7-epoxytropanes (scopine and scopolamine) and lastly 3,6,7-trisubstituted tropanes (meteloidine) (Doncheva *et al*, 2006).

Tropane alkaloid biosynthesis is known to take place in the roots with subsequent transport and accumulation in the leaves from which they are harvested (Hashimoto *et al*, 1986). More specifically, the formation of *N*-methylputrescine from ornithine occurs in the root pericycle, whilst tropinone and tropine biosynthesis and conversion occurs in the endodermal cells (Ziegler and Facchini, 2008). Once tropine has been synthesised, it is transported to the root pericycle for hyoscyamine and scopolamine synthesis and these are then exported (Ziegler and Facchini, 2008).

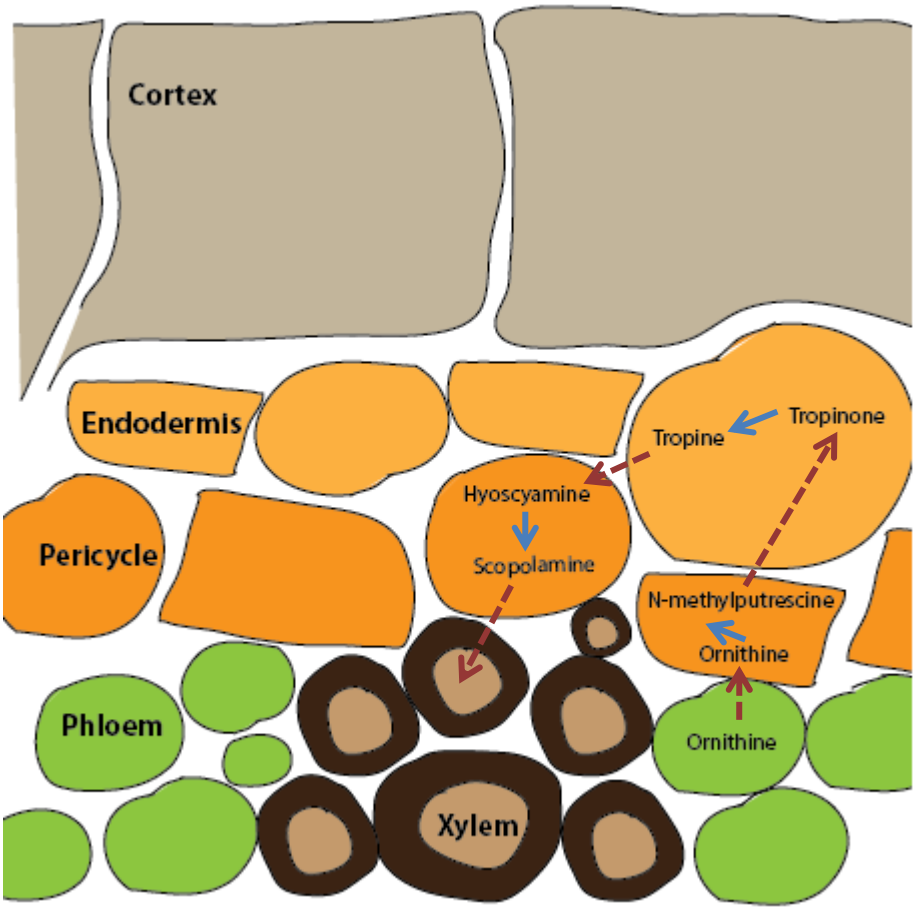

Figure 1.11: **Movement of tropane alkaloid metabolites during biosythesis.**

Diagrammatic representation for the pathway of metabolite movement during tropane alkaloid biosynthesis within the roots of producing species. Red dashed arrows show the perceived metabolite translocation between cellular tissue types and the blue arrows show enzymatic reactions. (Adapted from Ziegler and Facchini (2008))

Leaves from commercial *Duboisia* hybrids typically contain 2-4% DW tropane alkaloids (Ciba Foundation, 1988), with generally 60% scopolamine and 30% hyoscyamine. The remaining 10% is comprised of associated alkaloids. Through commercial cultivation, in some countries, varieties are able to accumulate up to 6% dry weight in their leaves, producing a total tropane alkaloid yield of 1t/ha (Palazon *et al*, 2008). Commercially, tropane alkaloids are extracted from hybrid cultivars of *Duboisia leichhardtii x myoporoides*, which are native to Queensland and surrounding regions of Australia (Dräger, 2006; Griffin and Lin, 2000).

Hybrids of *Duboisia leichhardtii x myoporoides* are the main source of production of these high valued tropane alkaloids. The interest in obtaining tropane alkaloids commercially began in earnest in 1940, initially from wild plant species before progressing onto a more industrial scale. In the early 1950's, the pharmaceutical company Boehringer Ingelheim launched Buscopan® (Ohlendorf, 1996). The way in which Buscopan® works is through the application of an antispasmodic action to the muscle lining of the gastrointestinal tract, making it suitable in the treatment of Irritable Bowel Syndrome (IBS). *Duboisia* hybrids are cultivated at altitudes exceeding 500 metres above sea level, but there is regional variation in the tropane alkaloid produced. This variation in tropane alkaloid accumulation has been attributed to the variety differences of *Duboisia myoporoides*. The southern pyridine variety exhibiting limited tropane alkaloid accumulation. The southern varieties produce higher concentrations of the pyridine alkaloids nicotine and anabasine (Gritsanapan and Griffin, 1991). Structurally, this different class of alkaloids do not exhibit the skeleton shown in Figure 1.1, but contain the structure in Figure 1.12 (Plunkett, 1991). For example scopolamine is the main tropane alkaloid produced in a region to the North of Gosford, New South Wales, whereas hysocyamine is the predominant tropane alkaloid when plants are grown to the South of Gosford (Gritsanapan and Griffin, 1991), with anabasine and nicotine being the dominant alkaloids when grown in regions of Queensland (Griffin and Lin, 2000).

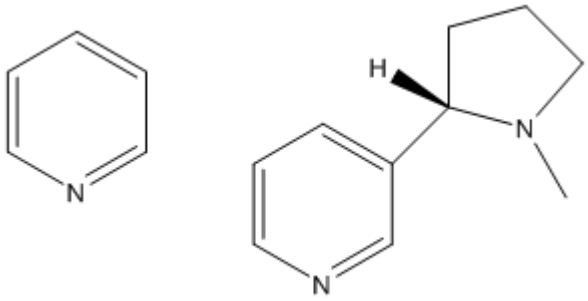

Figure 1.12: Represenation of pyridine alkaloids.

Left is a schematic of the pyridine ring, which is the common feature in pyridine alkaloids. Right is the chemical skeleton of the pyridine alkaloid nicotine.

In the late 1940s it was noted that it was possible to isolate *Duboisia* 'types' which are adapted to a wide range of environmental conditions and can produce tropane alkaloids of interest singularly, or proportionally together depending on the environmental and genetic nature of the material (Barnard, 1952). Field trials conducted by Boehringer Ingelheim, showed changes due to 'genotype x site interactions' as well as the age of the plant resulting in a decrease in yield of all alkaloid types produced. This led to identification of hybrid clones in which tropane alkaloid production was less impacted by the effect of external factors (Ohlendorf, 1996).

It has been suggested that tropane alkaloids such as hyoscyamine and scopolamine can be used as ecophysiological markers (Vanhaelen *et al*, 1991). It has been shown that the ratio between these two tropane alkaloids decreases through plant development (Table 1.1 and 1.2). Altitude and water stress have also been shown to influence accumulation of tropane alkaloids, depending on the vegetative cycle of the plant. For example *Datura metel* plants grown at lower altitudes had decreased accumulation of tropane alkaloids, whereas *Datura inoxia* grown at altitude had decreased tropane alkaloid accumulation due to slower growth rates (Vanhaelen *et al*, 1991). Water stress has been shown to generally increase alkaloid content and conversely alkaloid levels decrease during wet periods (Vanhaelen *et al*, 1991), this is similar to the findings of Griffin and Lin, (2000).

From 1950 to 2010 average rainfall in New South Wales has fallen from ~600 to ~500mm per year, and there has been an average increase of daily temperatures across Australia of 0.7^{o}C from 1960 (NSW Government, 2011). Due to the changing

environmental conditions, and as demand for tropane alkaloids is increasing, it is becoming of greater importance to try and ascertain other sources for the commercial production of tropane alkaloids, with work conducted on hairy root cultures of *Hyoscyamus niger* (Jaremicz *et al*, 2014) as well as other Solanaceous species with a view towards industrial production of tropane alkaloids.

		Stage			
Light Period (h)	**Alkaloid**	**3**	**4**	**5**	**6**
16	Scopolamine (S)	3	13.5	11	12
	Hyoscyamine (H)	0.5	3	8.5	17
	Total	3.5	16.5	19.5	29
	S/H ratio	6	4.5	1.3	0.7
9	Scopolamine (S)	2	4	9	7
	Hyoscyamine (H)	0.05	3	5	9
	Total	2.5	7	14	16
	S/H ratio	4	1.3	1.8	0.8

Table 1.1: **Tropane alkaloid yield during differnet light regimes**.

Scopolamine and hyoscyamine yield at different growth stages and under different day lengths from *Datura metel* (mg/100g DW leaves). Stage 3 – flower bud appearance, Stage 4 – first flower bloom, Stage 5 – fruit maturation, Stage 6 – 3 to 5 month old plant.

Site	**Altitude (m)**	**Roots**	**Stem**	**Leaves**	**Flower**	**Fruit**	**Seeds**
Bombay	Sea level	0.27	0.19	0.25	0.69	0.06	0.09
Poona	563	0.52	0.29	0.32	0.86	0.79	0.1
Pachmari	716	0.71	0.43	0.54	0.95	0.084	0.14
Darjeeling	2166	0.89	0.46	0.58	0.99	0.097	0.19

Table 1.2: Tropane alkaloid content in six tissues at different altitudes.

Tropane alkaloid content as a percentage dry weight from *Datura metel* tissues when grown at different altitudes (adapted from Vanhaelen *et al*, 1991).

The development of tropane alkaloids within the plant has been implicated in both plant and herbivore defensive mechanisms (Wink, 1998; Nash and Watson, 1995; Freitas *et al*, 1996). This has been indicated through various studies, and is not limited to the tropane alkaloid arm of the pathway. Wink (1988) discussed how alkaloids can be toxic to some vertebrates and arthropods, with atropine being utilised as an insect repellent. Nash and Watson, (1995) demonstrated that Lepidoptera (an order of insects

which includes butterflies and moths) feed on members of the Solanaceae. These insects ingest calystegines and other glycosidase inhibitors to make themselves more unpalatable to predators and so reduce the rate of predation upon them. Freitas *et al* (1996), built further on this by showing that the storage of tropane alkaloids by larvae of *Placidula* led to strong rejection by vertebrates, and that this is probably a primitive trait to help in the survival of the young.

It has been suggested that methyl jasmonate has a part to play in the tropane alkaloid biosynthesis pathway (Kang *et al*, 2004). Up-regulation of the genes along the tropane alkaloid biosynthetic pathway has been achieved through incidents of wounding from herbivorous insects. When *Dendrobium nobile* was treated with methyl jasmonate, *trI* mRNA levels were found to be enhanced (Chen *et al*, 2013), this is a homologous gene to the putative *trI* from *Solanum tuberosum* or the known *trI* from other Solanaceous species. Levels of scopolamine have been shown to increase in *Brugmansia suaveolens* when treated with methyl jasmonate, which resulted in a decrease in herbivory compared to control plants (Arab *et al*, 2012). Other studies which looked at the effects of methyl jasmonate on the production of tropane alkaloids found that *pmt* and *h6h* expression levels increased, which lead to an increase in hyoscyamine, N-methyl-putrescine and nicotine concentrations in the species being studied (Kang *et al*, 2004; Ryan *et al*, 2015).

There is some evidence to suggest that calystegines can be degraded by microbes in the rhizosphere. A single strain of *Rhizobium meliloti* (strain 41) was reported to convert calystegines due to the presence of the pRme41a plasmid (Tepfer *et al*, 1988). *R. meliloti* 41 was able to catabolise calystegines to use them as a carbon and nitrogen sources, whereas *R. meliloti* 41 deficient in the pRme41a plasmid could not. This catabolic selectivity within strains of *Rhizobium* infers that calystegines, through nutritional selection, can have a minor effect on the ecology of the rhizosphere. This effect is minor as pRme41a deficient bacteria are able to continue the symbiotic relationship with *Medicago* hosts, and that calystegine catabolism is not linked to the routine nitrogen fixation within the rhizosphere.

1.7 Evolution in plants.

Phylogenetic comparisons between members of the Solanaceae and Erythroxylaceae suggest that the last common ancestor is likely to have been in existence approximately 120 million years ago (Magallon and Castillo, 2009). This suggests either that the tropane alkaloid biosynthesis pathway is ancient and/or that it has evolved independently in these two families. Jirschitzka *et al,* (2012) support this second theory as they demonstrated that the tropinone reduction step in the biosynthetic pathway is catalysed by members of two different enzymatic classes in the Solanaceae and Erythroxylaceae. In the Solanaceae, this reaction is catalysed by two tropinone reductases (trI and trII) which belong to the short-chain dehydrogenase/reductase enzyme family (SDRs) whereas in the Erythroxylaceae a methylecgonone reductase (an aldo-keto reductase) catalyses this step. Furthermore, Jirschitzka *et al,* (2012) argue that as biosynthesis occurs in the roots and then the metabolites are translocated to the leaves in the Solanaceae whereas the site for biosynthesis in the Erythroxylaceae is in the young leaves, which gives extra emphasis on the different evolutionary lineage. Figure 1.13 shows the chemical structure of cocaine, a tropane alkaloid produced by *Erythroxylum coca*, a member of the Erythroxylaceae.

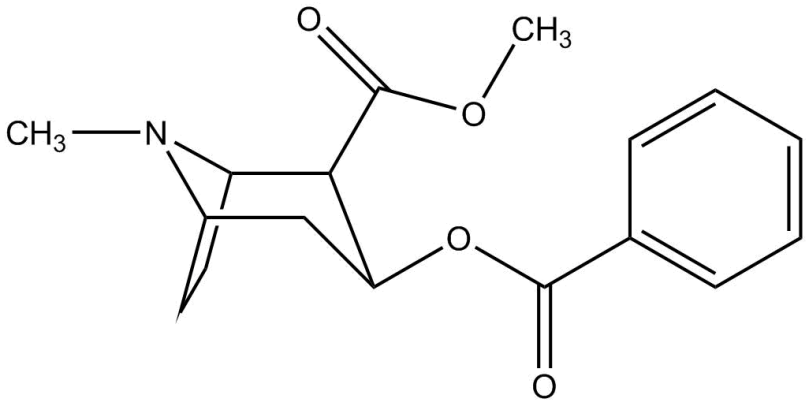

Figure 1.13: **Chemical structure of cocaine**.
Cocaine is produced by *Erythroxylum coca* (from the Erythroxylaceae), with the tropane skeleton visible on the left-hand side of the structure.

1.8 The short-chain dehydrogenase/reductase superfamily.

Both trI and trII belong to the SDR enzyme superfamily, one of the most ancient protein families known, with examples present in all current taxonomic domains of life (Moummou *et al*, 2012). Within these domains there is protein sequence divergence,

with typically only 15 – 30% residue identity between sequences (Kallberg *et al*, 2002). There are however universal characteristics that all the SDRs share. These characteristics include the YxxxK catalytic motif, 'Rossmann-fold' β-sheets with α-helices on each side and other conserved cofactor binding motifs (Moummou *et al*, 2012; Kallberg *et al*, 2002).

There are reported to be 7 different types of SDRs; one sub-type, the tropinone reductase-like SDRs (TRLs) have been grouped with the classical SDRs, which also includes the true tropinone reductase group 'SDR65C' with these groups having been characterised by the SDR nomenclature initiative (Reinhardt *et al*, 2014). Although the TRL sub-group of SDRs show similarity to known active tropinone reductases, there has been limited functionality demonstrated with only *Cochlearia officinalis* tropinone reductase (Brassicaceae) and *Dendrobium nobile* trI (Orchidaceae) catalysing the conversion of tropinone to both tropine and pseudotropine (in the case of *Co*tr) and tropine in the case of *Dn*trI (Reinhardt *et al*, 2014). Other annotated TRL enzymes (such as those from *Arabidopsis thaliana*) are unable to catalyse the reduction of tropinone, but have been shown to have an effect on lipophilic and monoterpene ketones, suggesting that there is limited binding space within the active sites (Reinhardt *et al*, 2014). It has also been suggested that specific His and Glu residues in trI and trII respectively are critical in ensuring tropinone is correctly orientated for the reaction to take place (Brock *et al*, 2008).

1.9 *Solanum tuberosum*: the potato.

The origins of the modern cultivated potato stem from its domestication in the Andean region of South America (The Potato Genome Sequencing Consortium, 2011) around 8000 years ago (Ortiz and Mares, 2017). Whilst the New World was discovered by Columbus in 1492, it was not until the 1530's that the potato made its way to European shores with the first historical recording of the potato being from 1537 (Hawkes and Francisco-Ortega, 1993). The use of potato as a food source suffered early scepticism in Europe due to its lack of adaptation to the longer day lengths in the more northerly geographic region, leading to the production of small tubers. Additionally, botanists of the time noticed its similarity to other members of the Solanaceae and suspected that it may be poisonous (Brown, 1993). Once this initial scepticism was overcome, potato became an important staple for the masses and in particular the poorer

classes of the time, due to its un-burdensome needs from planting to harvest. Some anecdotal links between the rise of the use of potato as a food source and the population explosion seen in Ireland between 1790 and 1845 have been attributed to the ease in production and the lack of interest from higher societal classes (Brown, 1993). More recently the potato has become known as a food security crop and China, which is the world's largest producer and consumer of potato, is turning to it as its main source of food security (Ortiz and Mares, 2017). Within the developed world production in 2009 reached 330 million tonnes (The Potato Genome Sequencing Consortium, 2011) which increased further to 376.8 million tonnes in 2016 (FAO, 2018).

The modern cultivated potato has become a staple food source due to its high nutrient content; it is rich in Vitamin C and B6 as well as containing high quantities of potassium, fibre and further B complex vitamins and other associated minerals (Ortiz and Mares, 2017).

Potato is a clonal crop with many different species and landraces under cultivation. Due to the clonal nature of reproduction and the relatively small number of species initially introduced to Europe, potato exhibits a 'narrow genetic base' (The Potato Genome Sequencing Consortium, 2011). This has led to some barriers through disease susceptibly and adverse effects attributed to inbreeding, when attempting to improve cultivars in the past (The Potato Genome Sequencing Consortium, 2011). Many potato cultivars are autotetraploid (containing four copies of the genome) and suffer from inbreeding depression. Potatoes contain a set of 12 non-homologous chromosomes with a total genome size of 844 megabases which encode for 39031 transcripts (The Potato Genome Sequencing Consortium, 2011). The duplication events which have led to the multiple copies of the genome being present are thought to have happened with the divergence of potato and grape ~ 89 million years ago, with a further duplication event occurring within potato ~ 67 million years ago (The Potato Genome Sequencing Consortium, 2011).

The resulting effect of these duplications towards inbreeding depression can be seen through frameshifts, the development of premature stop codons or even in presence/absence variants (PAV). Frameshifts have the ability to change gene function due to representation of different amino acids, thus resulting in different proteins being encoded; premature stop codons will cause translation to stop and as a result the protein

which is formed will be shorter in length and functionality will be affected. PAV are lines from the same species or cultivar in which a specific sequence is located in one genome, but missing from another (Springer *et al*, 2009).

1.10 Manipulation of the potato genome and tropane alkaloid biosynthesis pathway

As potato does not produce tropane alkaloids the pathway must be manipulated through genetic engineering by the introduction of known functional alkaloid biosynthetic genes. This process of increasing secondary metabolites by introducing a foreign gene to alter a biosynthetic pathway has been previously demonstrated to be effective in potato. Examples which demonstrate this have been shown on various biosynthetic pathways such as the carotenoid/flavonoid and starch pathway (Hichri *et al*, 2010; Simo *et al*, 2014). Ducreux *et al*, (2005) introduced the phytoene synthase gene *crtB* from *Erwinia uredovora* into *Solanum tuberosum* cultivar *Desiree* and *Solanum phureja*. Through this approach, Ducreux *et al*, (2005) showed that there was a 6.3 fold increase in carotenoid accumulation in cultivar *Desiree* (5µg up to 35 µg DW), and in *Solanum phureja* the increase was from 25 µg to 78 µg DW in the best line.

McKibbin *et al*, (2006) overexpressed the sucrose non-fermenting-1-related protein kinase (*SnRK1*) in *Solanum tuberosum* cv. Prairie. Using this approach they demonstrated that there was an increase of up to 167% *SnRK1* activity in 3 transgenic lines and this led to a decrease of up to 83% in glucose and a 30% increase in starch levels compared to wild type controls. These are only two cases out of many which help demonstrate that *Solanum tuberosum* is a viable candidate for genetic transformation.

Attempts to manipulate the tropane alkaloid biosynthesis pathway have been made in a number of Solanaceous species. Moyano *et al*, (2002) overexpressed *pmt* from *Nicotiana tabacum* in *stable Duboisia* hybrid hairy root transgenics resulting in a 2-4 fold increase in N-methylputrescine levels compared with the wild type. However there was no increase in downstream tropane alkaloid production. Jouhikainen *et al*, (1999) were concerned with enhancing scopolamine production in *Hyoscyamus muticus* through genetic engineering of root cultures. In their study, *h6h* from *Hyoscyamus niger* was transformed into *Hyoscyamus muticus* root cultures and they demonstrated that scopolamine content was raised to 17 mg/l, almost 100 times greater than experimental

controls. Rocha *et al*, (2002) utilised particle bombardment to produce stable transgenic lines of *Nicotiana tabacum* where two *Hyoscyamus niger* cDNAs which encoded *trI* and *h6h* were introduced. Although Rocha *et al*, introduced *trI* and *h6h* from *Hyoscyamus niger*, with the measurable effect primarily focused upon the nicotine biosynthesis pathway, with an almost 13 times increase in nicotine present (up to 149 µg/g FW (Fresh Weight) in controls to up to 1430 µg/g FW in transgenic lines).

1.11 Modular cloning methodology.

As *Solanum tuberosum* and the tropane alkaloid biosynthesis pathway are readily manipulated, it is worth discussing techniques for metabolic engineering. In recent years there have been new developments in molecular cloning techniques which allow the efficient recombination of vector and cassette sequences in a single restriction ligation reaction.

The most recent developments have stemmed from BioBrick, which was described and released by Knight (2003). The BioBrick system is based on the use of Type II restriction enzymes, such as EcoRI and XbaI. These enzymes create 4 base overhangs, or 'sticky ends'. Sequences with the complementary bases are able to recombine with. Further developments to this system have been made in the Golden Gate system, where Type IIS restriction enzymes are used. The differences between the Type II system of BioBrick and the Type IIS system of Golden Gate is that the Type IIS restriction enzymes are able to recognise non-palindromic sequences (that is sequences which do not read the same whether read from the 5' or 3' end). Type IIS enzymes cleave DNA outside of the enzyme recognition site (shown in Figure 1.14) (Patron *et al*, 2015). There are a potential 256 potential overhang sequences using Type IIS enzymes which allow the construction of multiple fragments of DNA using different combinations of overhang sequences. Following recombination, correctly ligated DNA products do not contain the enzyme recognition sites and therefore cannot be cut again by the restriction enzyme.

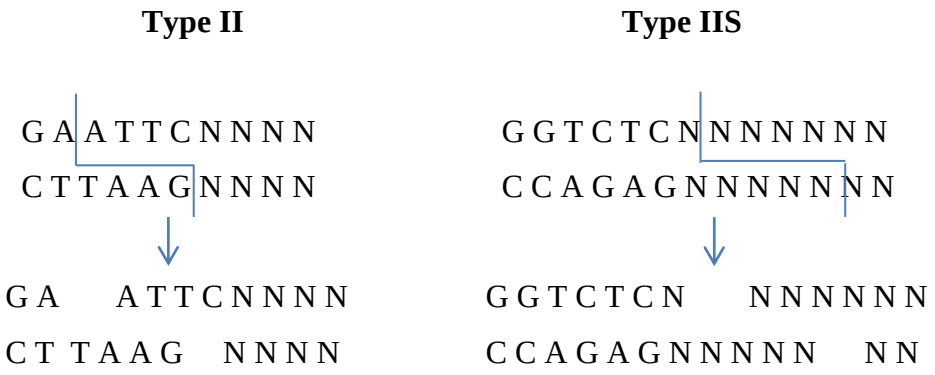

Figure 1.14: **Type II and Type IIS restriction edonuclease cut sites.**

Example of Type II and Type IIS enzyme cut sites used in the BioBrick and Golden Gate/GoldenBraid cloning systems. Left is a type II EcoRI recognition site and right BsaI used in the Type IIS system. The overhangs created are illustrated, N denotes unknown base depending on the system.

The original Golden Gate cloning system has been converted to allow 4 base overhangs or 'fusion sites' which are compatible across all parts that the system may require, whether promoter, terminator or coding sequence. This compatibility has been utilised in the MoClo and GoldenBraid 2.0 system, allowing for almost 100% interchangeability of parts between these systems (Patron *et al*, 2015). Both the MoClo and GoldenBraid 2.0 systems result in scarless recombination, unlike other methods such as Gateway cloning which in some cases leaves up to a 21 base scar between building blocks (Sarrion-Perdigones *et al*, 2013). Figure 1.15 illustrates the MoClo and GoldenBraid 2.0 syntax, showing the overhang fusion sites which are used in the potential part recombinations. An example of a simple promoter 5' UTR, coding sequence and 3' UTR, terminator is also shown below.

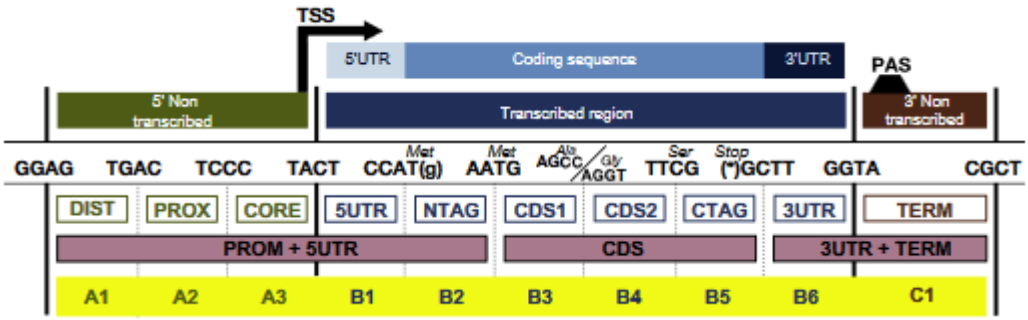

Figure 1.15: **GoldenBraid methodology**

A schematic of the methodology used within the GoldenBraid cloning system which shows the 4 nucleotide fusion sites at each junction as well as regions that parts represent from the GoldenBraid library (adapted from Patron *et al*, 2015).

GoldenBraid was developed by the Plant Genomics and Biotechnology group at the Instituto de Biología Molecular y Celular de Plantas at the Universitat Politècnica de València, Spain (https://gbcloning.upv.es). The vectors in the GoldenBraid system are based on previously reported plant vectors used in transformation which have been modified for the cloning system. The main changes are to the existing restriction sites used around the Multiple Cloning Site (MCS) (Sarrion-Perdigones *et al*, 2013).

The GoldenBraid system allows the production of GBparts by multiple labs to be deposited in a central location and to be used by others. The repository can be searched (https://gbcloning.upv.es/search/) for the cassette element required and requested (https://gbcloning.upv.es/order/) directly. This allows the easy exchange of GBparts and elements which are known to work between researchers saving valuable time and making cloning strategies more efficient.

The cloning strategy for assembling a binary transformation construct using the GoldenBraid system which can be used in *Agrobacterium tumefaciens* mediated transformations, is a three stage process and is outlined below in Figures 1.16 through 1.18.

Step 1: Domestication (the generation of GBpatches)

Domestication of a sequence refers to the addition of a 4 base overhang and the removal of Type IIS recognition sites used in the downstream cloning strategy within the sequence of interest. Using the software available at https://gbcloning.upv.es/do/domestication/ primer design is conducted for the first step in the GoldenBraid cloning strategy. The software allows the CDS of the gene being investigated to be adapted to the GBpatch (described in Figure 1.16) as well as introducing the restriction sites to allow ligation into pUPD2 (2.2.3.1). Once the GBpatch is ligated into pUPD2, it is referred to as a GBpart. pUPD2 is a high copy number T-vector and allows for easy characterisation through sequencing of the inserted synthesised gene fragment.

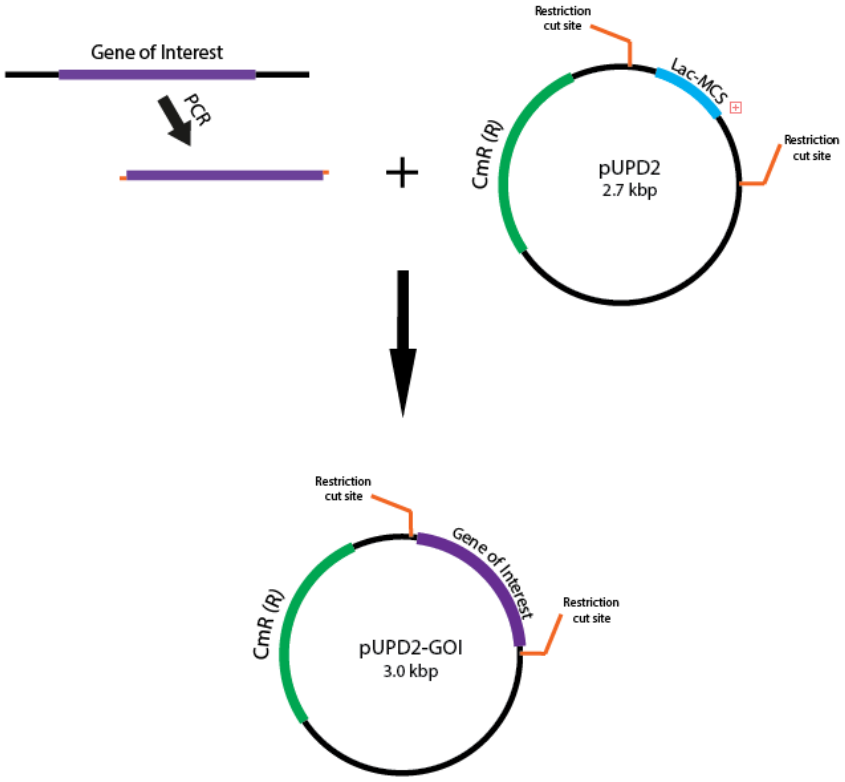

Figure 1.16: Domestication within GoldenBraid.

Domestication of a cloned gene fragment using the GoldenBraid 3.0 system. Gene fragments containing compatible restriction site overhangs designed using the GbCloning domestication software are ligated into the pUPD2 vector through a restriction endonuclease-ligation reaction using the restriction endonuclease BsmBI and T4 ligase. The completed construct is termed a GBpatch using the Goldenbraid nomenclature.

Step 2: Construction of the transcriptional unit

The GoldenBraid repository has GBparts for promotors, terminators and other useful sequences available that will allow the easy and rapid generation of a complete transcriptional unit with the GBpart containing the gene under investigation from Step 1. To produce the transcriptional unit, these GBparts are recombined into the α level plasmids (pDGB3_α) through the use of the restriction endonuclease BsaI. This reaction occurs in a single tube and can be transformed directly into *E. coli* once the reaction is complete. The 35s CaMV (Cauliflower Mosaic Virus) promoter is a strong constitutive promoter allowing for high levels of gene expression (Dutt *et al*, 2014).

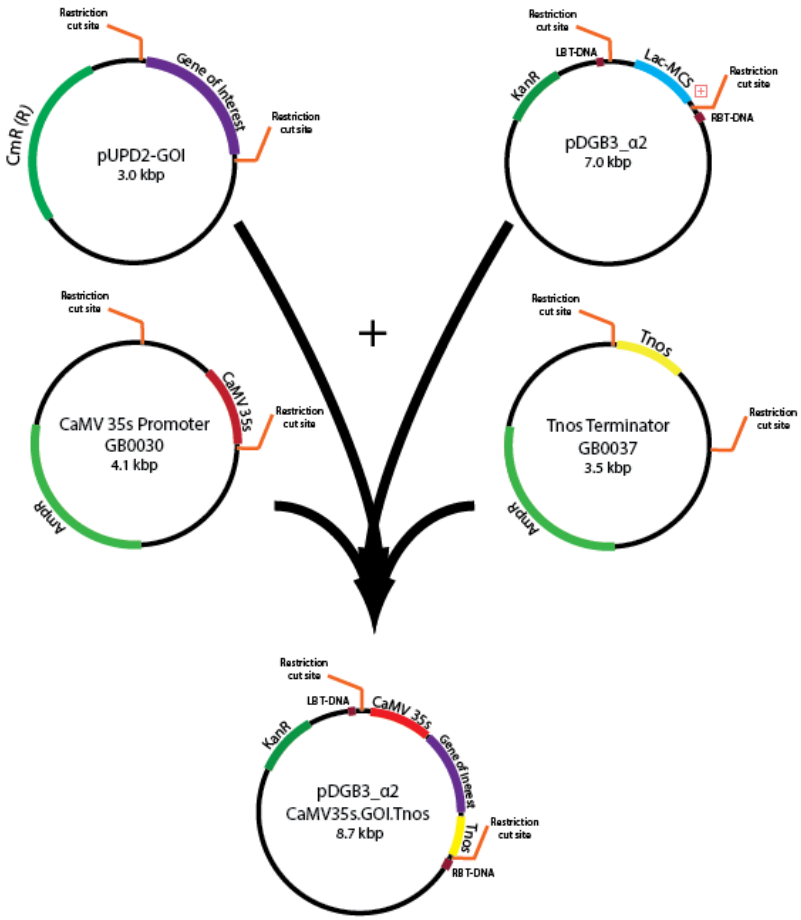

Figure 1.17: **Generation of transcriptional units**.

Construction of a transcriptional unit using a domesticated gene of interest and promoter and terminator GBparts. The pUPD2 vector containing the gene of interest is combined with two pre-prepared GBpart vectors containing the CaMV 35s promoter and Tnos terminator using an endonuclease–ligation reaction to in the presence of a pDGB3_α series 'destination' binary vector to form a functional gene cassette. The completed gene cassette is constructed in the correct orientation due to the specific overhangs produced by the Type IIS restriction enzymes used.

Step 3: Construction of multipartite constructs

The generation of multipartite constructs, that is, constructs with two or more transcriptional units can be achieved using a GoldenBraid cloning strategy. This strategy, in a single restriction endonuclease and ligation reaction is able to take complete transcriptional units from α level vectors, and insert them together into a **Ω** level destination vector. The strategy is outlined below, and is completed with the generation of the transcriptional units, due to the four base 'fusion tag' ensuring recombination occurs in the correct order.

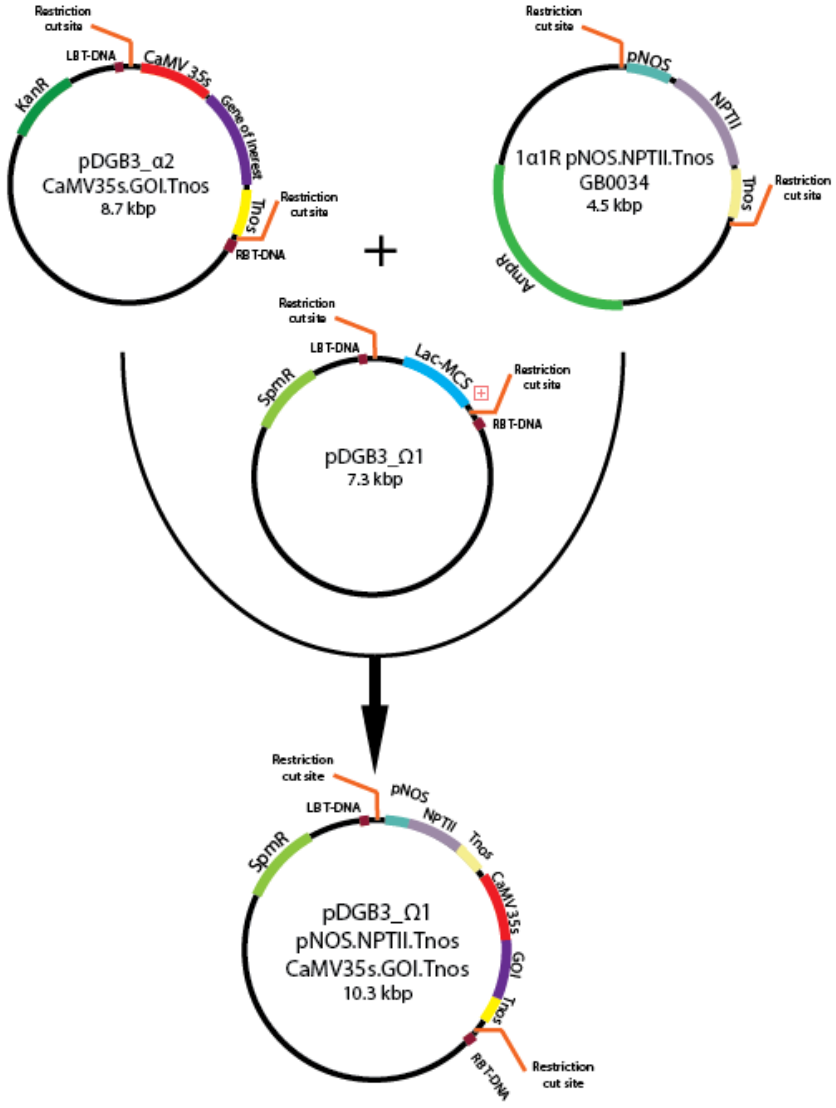

Figure 1.18: **Assembly of multiple units.**

Binary assembly of multiple transcriptional units into the pDGB3_ Ω1 vector. Using the pDGB3_α2 construct containing a transcriptional unit with the gene of interest and a second GBpart vector, pDGB1α_1R containing the *nptII* gene (GBpart, GB0034) a final restriction endonuclease and recombination reaction is used to generate the final construct in the pDGB3_Ω1 vector. The completed construct confers antibiotic selection in transformed explants.

1.12 Methods used for the detection of tropane alkaloids.

Many recent studies into tropane alkaloids have used Thin Layer Chromatography (TLC), High Performance Liquid Chromatography (HPLC), Gas Chromatography Mass Spectroscopy (GC-MS) and more recently Triple Quadrupole Liquid Chromatography Mass Spectroscopy (QqQ-LC-MS) to quantify the presence of alkaloids within samples (Dräger, 2002; Steenkamp *et al*, 2004; Zhou *et al*, 2017).

1.12.1 Thin Layer Chromatography

TLC can be applied to separate molecules of interest by a solvent on a stationary phase and then detected through specific derivatizing chemicals. The polarity of this stationary phase has been shown to have an effect on the separation and detection of tropane and nortropane alkaloids. Detection of calystegines using TLC shows differences in retention factor (R_f) values for the different classifications of calystegine as well mobile phases used in separation, summarised in Dräger (1995, 2002).

TLC has its advantages, such as high sample throughput, rapid analysis times, limited extraction and clean up requirements and finally, the availability of specific alkaloid detection and derivatizing chemicals (Kokotkiewicz *et al*, 2017). TLC has been demonstrated to be effective in both plant (Keiner and Dräger, 1999) and bacterial assays (Coa *et al*, 2015). Detection of tropane alkaloids uses the derivatizing solution, Dragendorff reagent, or a variation, the Dragendorff Munier reagent. Dragendorrf reagent contains a mixture of bismuth nitrate, acetic acid and potassium iodide which reacts with alkaloids present. In the presence of high nortropane alkaloid concentrations a light pink spot is produced (Dräger, 1995). Dragendorff Munier replaces the acetic acid with tartaric acid, producing a light purple spot on a yellow background to a sensitivity of 0.1 µg of tropine and pseudotropine (Keiner and Dräger, 1999). Calystegine detection via TLC uses a silver nitrate reagent for detection, with the LOD (limit of detection) being 5 µg/ml (Dräger, 2002).

1.12.2 HPLC-UV

HPLC-UV utilises UV detection to determine compounds within a sample being analysed. Whilst not as quantitatively accurate compared to other LC systems to be used in this study, the instrumentation is suitable for the detection and estimation of compounds of interest.

The use of photo-diode array detectors (PDA) for confirmation of the presence of tropane alkaloids in a multitude of sample preparations has been investigated thoroughly. Steenkamp *et al* (2004) demonstrated that the LOD and LOQ (limit of quantification) for PDA detection of both atropine and scopolamine were 1 µg/ml and 10 µg/ml respectively. Tamerdashev *et al*, (2012) also demonstrated that it is possible to determine the concentration of atropine and scopolamine from different *Datura metel* organs using an HPLC-UV system. The LOQ in this study was 3 µg/ml for both metabolites.

1.12.3 Gas Chromatography Mass Spectroscopy (GC-MS)

GC-MS has been previously used in studies primarily concerned with the extraction and quantification of the calystegines (Friedman *et al* 2003; Keiner *et al* 2000; Griffiths *et al* 2008); however, it has also been used to show if there is any change in metabolite flux towards the tropane alkaloid biosynthetic pathway during feeding assays (Keiner and Dräger, 1999). GC-MS involves sample extracts being derivitised in the presence of N-methyl-N-trimethylsilytrifluoroacetamide, producing silyated esters (Griffiths *et al* 2008; Keiner and Dräger 1999). These esters make it easier to detect the compound of interest using the specific chromatography.

Detection limits for metabolites along the tropane and nortropane alkaloid biosynthetic pathway have been described. The LOD for the calystegines has been reported as approximately 1µg/ml, with the LOQ being 10µg/ml (Keiner *et al* 2000, and Keiner and Dräger, 1999). The LOD for the tropane alkaloids tropine and tropinone is reported as 10µg/ml, whereas pseudotropine is 50µg/ml, suggesting that the GC-MS system was more sensitive for the calystegines than the tropane alkaloids being investigated in the Keiner and Dräger, (2000) study.

1.12.4 Agilent Triple-quadrupole LC-MS (QqQ-LC-MS)

A feature of the QqQ-LC-MS systems is that they need to detect and isolate multiple specific parent ions in a mixture, fragment them through collisions and then detect the unique representative product ions in the mixture and quantify them (Kitteringham *et al*, 2009). From their inception as radio frequency traps, quadrupole LC-MS has become more sophisticated allowing tandem mass spectrometry (MS/MS) to be implemented. This has enabled collision induced dissociation (CID) assays to be conducted (Perchalskl *et al*, 1982). Changes in radio frequencies (RF) cause ions to be ejected from the ion trap at different times due to increases in resonation (measured in kHz). This technique, known as 'resonant ejection' overcomes issues which can arise from mass/charge ratios and the influence other ions may have within the ion trap (March, 1997). In turn this increases the resolution of the mass scans.

Fragmentation patterns for individual metabolites can be coupled together to enable the detection of multiple metabolites within a sample. This is known as a multiple reaction monitoring (MRM) analysis. Ions which are being targeted need to be predetermined for this to take place (Kitteringham *et al*, 2009) and Figure (1.19) below, shows a schematic representation of this 'optimization' process through the three quadrupoles. Any QqQ-LC-MS machine is capable of being used for this type of analysis.

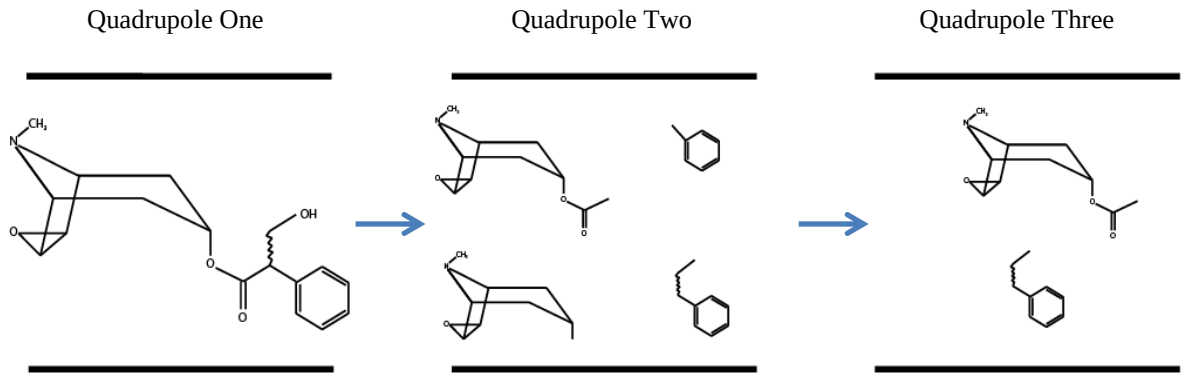

Figure 1.19: **Representation of metabolite fragmentation and detection through the three different quadrupoles of the QqQ-LC-MS.**

Parent ions are analysed in quadrupole one, (in this representation scopolamine is shown), before moving into the collision quadrupole where fragmentation takes place via CID. The fragments produced in quadrupole two are analysed for the abundance of each ion. The most abundant fragmented ions are then selected to be representative ions of the parent metabolite. In quadrupole three, selected daughter ions are screened for in the samples presented to quantitatively determine the amount of the initial parent present in the sample. The fragmented ions shown in quadrupole two are four generated from Zhou *et al*, (2017).

1.13 Extraction method differences

Consensus for the extraction of tropane alkaloids from plant material involves agitation in a diluted polar organic solvent (Jakabova *et al*, 2012; Chen *et al*, 2017). However, there are variations of this method which involve further steps, such as prolonged agitation in extraction buffer, or the resulting supernatant being solubilised under acidic conditions (El Bazoui *et al*, 2009). Differences between extraction methods for the tropane and nortropane alkaloids have been reported. Friedman *et al*, (2003), reported that non-acidified buffers work well for the extraction of nortropane alkaloids, whereas an acidified extraction buffer has been demonstrated to work well for tropane alkaloids (Chen *et al*, 2017; Cirlini *et al*, 2018). For both extraction methods there is no unique difference in preparation between samples for analysis on either LC or GC-MS systems.

Successful extraction methods must result in a high percentage recovery of the tropane and nortropane alkaloid profile from the tissues under analysis. As briefly discussed some extraction protocols require a more complex method for tropane and nortropane alkaloid extraction, which is followed by either a solid-phase extraction (SPE) or liquid-liquid extraction (LLE) clean up, to remove further interfering compounds which could impede detection. SPE and LLE clean-up has been shown, in some cases, to result in greater peak clarity during subsequent chromatography steps. SPE clean-up for samples generally use cation exchange resin columns (Dräger, 1995; Friedman *et al*, 2003), whereas LLE clean-up can be achieved using commercially available EXtrelut® columns (Merck, Germany) (Richter *et al*, 2007; Sramska *et al*, 2017).

Cation exchange resin columns have been used for the determination of calystegine (nortropane alkaloid) concentrations within different members of the Solanaceae. Dräger (1995) demonstrated that nortropane alkaloids can be extracted from root cultures of *Atropa belladonna*, whereas Friedman *et al*, (2003) extracted the same nortropane alkaloids from 8 different potato cultivars and in both cases the extracts were applied to a cation exchange resin column. The nortropane alkaloids are retained by these resin columns due to the charge of the secondary amino group (Mroczek *et al*, 2006). Most other molecules present flow through the resin column when washed, prior to the bound molecules of interest being eluted in an alkali solution.

LLE clean-up of tropane alkaloids on EXtrelut® columns has been reported to be successful (Richter *et al*, 2007), however Sramska *et al* (2017) were unable to use this approach. The purpose of these EXtrelut® columns is to allow a liquid-liquid clean-up of samples, permitting greater sensitivity in the detection system. Sramska *et al* (2017) reported that using EXtrelut® columns for clean-up results in less than half the initial spike amount of atropine being recovered from samples when comparing two differing extraction methods (16.5±2.6% from 40 mg kg^{-1} DW and 35.9±2.1% from 160 mg kg^{-1} DW). Whereas the best performing extraction method tested (which included longer ultra-sonication and a greater number of hexane washes) showed recovery rates of 45.1±2.3% from 40 mg kg^{-1} DW and 66.7±3.4% from 160 mg kg^{-1} DW respectively.

Comparisons between SPE and LLE have been conducted for alkaline based drugs, due to an interest from forensic laboratories (Juhascik and Jenkins, 2009). Whilst not using the same brand of SPE column as in previously cited studies, atropine and scopolamine had a limit of detection (LOD) of 50 ng/ml and 250 ng/ml respectively; however LLE purification of these samples was not undertaken in this study. A tropane alkaloid which did undergo both SPE and LLE in this study was cocaine (produced by *Erythroxylum coca*, a member of the family Erythroxylaceae), and this showed a similar LOD for both clean up methods (25 ng/ml).

1.14 Objectives.

There are limited sources of plants that produce natural tropane alkaloids. Increasing demand for and yield variability in these metabolites makes the development of a stable production platform more important. *Solanum tuberosum* offers the potential to increase and stabilise supply of the metabolites. *Solanum tuberosum* can be grown universally and contains tropane alkaloid precursors, up to the tropinone branch point. The tropinone branch point in potato represents the first known lesion of this pathway in *Solanum tuberosum*, where tropinone flux is diverted towards the nortropane alkaloids through trII activity. The objectives of this study are to elucidate and assess the functionality of the tropane alkaloid biosynthesis pathway within *Solanum tuberosum*, and understand why potato does not produce tropane alkaloids. The development of robust detection methods for tropane alkaloids and associated metabolites will also be undertaken for the platforms that are available. These detection methods will be deployed to determine metabolite accumulation primarily within leaves, however, other tissues will be investigated. This will be achieved through:

1. The development of a robust detection method for metabolites found along and associated with the tropane alkaloid biosynthesis pathway.
2. The generation of *trI* over-expression transgenics
3. The generation of *trII* down-regulation transgenics
4. The generation of co-transformed *trI* over-expression and *trII* down-regulating transgenics
5. Discern the functionality of annotated downstream tropane alkaloid genes from within the potato genome through recombinant protein assays.

Chapter 2: Materials and Methods

2.1 Media, antibiotics and buffers.

2.1.1 Bacterial culture media

Lysogeny Broth (LB) (pH 7.5):

Tryptone	1.0 % (w/v)
NaCl	1.0 % (w/v)
Yeast extract	0.5 % (w/v)

Super optimal broth with catabolite suppression (SOC) media (pH 7.0):

Tryptone	2.0 % (w/v)
Yeast extract	0.5 % (w/v)
Glucose	20 mM
$MgSO_4$	20 mM
$MgCl_2$	10 mM
NaCl	10 mM

2.1.2 Tissue culture media

MS 20 (Murashige and Skoog, 1962) (pH 5.7):

Sucrose	2.0 % (w/v)
Agar	0.8 % (w/v)
Murashige and Skoog basal medium (Melford)	0.5 % (w/v)

MS 30 (Murashige and Skoog) (pH 5.7):

As MS 20 media, except 3 % (w/v) Sucrose.

HB1 medium (MS30 plus the following) (pH 5.8):

α-naphthalene acetic acid (NAA)	0.2 mg l^{-1}
Gibberellic Acid (GA_3)	0.02 mg l^{-1}
Zeatin Riboside (ZR)	2.5 mg l^{-1}

4 ml^{-1} HB1 supplement is used per 1 l^{-1} MS30

HB2 medium (MS30 plus the following) (pH 5.8):

α-naphthalene acetic acid (NAA)	0.02 mg l^{-1}
Gibberellic Acid (GA_3)	0.02 mg l^{-1}
Zeatin Riboside (ZR)	2.00 mg l^{-1}

4 ml^{-1} HB2 supplement is used per 1 l^{-1} MS30

2.1.3 Antibiotics

Antibiotic	Conc. required for *E. coli* (µg ml)	Conc. required for *A. tumefaciens* (µg ml)	Conc. required for plant media (µg ml)	Conc. of stock (mg ml)
Ampicillin	50 - 100	-	-	100
Cefotaxime	-	-	500	125
Chloramphenicol	50 - 100	-	-	34
Kanamycin	50	50	100	12.5
Rifampicin	-	100	-	10
Spectinomycin	50 - 100	100	-	
Tetracycline	-	5	-	12.5
IPTG	32	-	-	20
X-Gal	32	-	-	20

All antibiotics were prepared in double distilled water (ddH_2O) with the exception of chloramphenicol which was dissolved in 100% ethanol and rifampicin which was dissolved in 100% methanol.

2.1.4 Buffers

Agrobacterium inoculation buffer

10 mM $MgCl_2$
10 mM MES buffer, pH 5.6
150 µM Actosyringone

Promega Ligation buffer (2x) (Promega, UK)

30 mM Tris.HCl, pH 7.8
10 mM $MgCl_2$
10 mM DTT
1 mM ATP

10x Platinum™Taq High Fidelity buffer (Invitrogen, USA)

600 mM Tris-SO_4 (pH 8.9)
180 mM $(NH_4)_2SO_4$
Total volume 1.25 ml

T4 DNA Ligase buffer (pH 7.4) (Promega, UK)

10 mM Tris-HCl
50 mM KCl
1 mM DTT
0.1 mM EDTA
50 % glycerol (v/v)

RNA Loading buffer

0.55 % (w/v) Bromophenol Blue
0.8 mM EDTA
0.23 M Formaldehyde
4 % (v/v) Glycerol
6 % (v/v) Formamide

10x Tris-Buffered Saline (TBS) (pH 7.5)

0.4 M Tris Base
2.75 M NaCl

1x TBS-Tween^{20}

50 ml 10x TBS
0.5 ml Tween^{20}
449.5 ml *dd*H_2O

10% SDS Protein Extraction Buffer

10 % (w/v) SDS

20x NuPAGE™ MOPS SDS Running Buffer (pH 7.7) (Invitrogen, USA)

50 mM MOPS
50 mM Tris-Base
0.1 % (w/v) SDS
1 mM EDTA

20x NuPAGE™ Transfer Buffer (pH 7.2) (Invitrogen, USA)

25 mM Bicine
25 mM Bis-Tris (free base)
1 mM EDTA

2.2 Plasmids

2.2.1 pGEM®-T Easy

pGEM®-T Easy (Promega, UK) is a high copy number vector containing the T7 and SP6 RNA polymerase promoters flanking a multiple cloning site (MCS) with the α-peptide coding region of *β-galactosidase* gene allowing blue/white screening of colonies, and ampicillin selectable marker (AmpR). pGEM®-T Easy are linearized vectors containing 3' and 5' terminal thymidine (T) overhangs allowing easy T/A cloning (section 2.5.3.4.1).

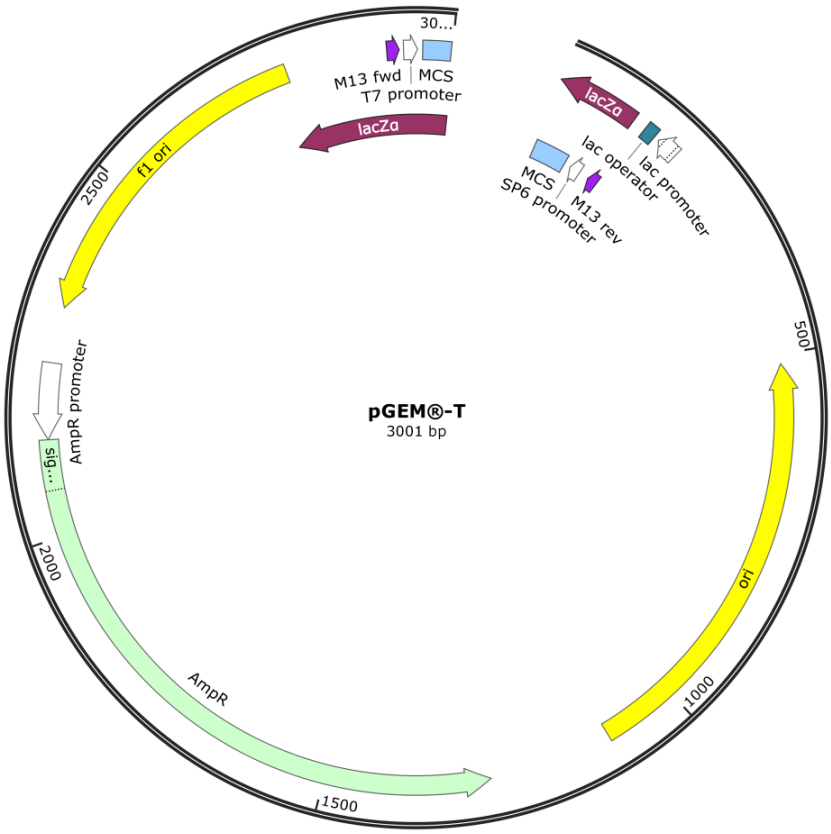

Figure 2.1: pGEM®-T Easy vector

Schematic of the pGEM®-T Easy vector. Vector maps generated using SnapGene ® Viewer 3.2.1

2.2.2 pET-28a$^{(+)}$ (Novagen®, Germany)

pET-28a$^{(+)}$ vectors (Novagen®, Germany) contain a T7 promoter, kanamycin selectable marker and a MCS which is flanked on both the 5' and 3' termini with a sequence encoding a histidine repeat enabling tagging of recombinant proteins for efficient purification and analysis. Figure 2.2 below shows the vector schematic with the four restriction endonuclease enzymes used in future studies labelled within the MCS.

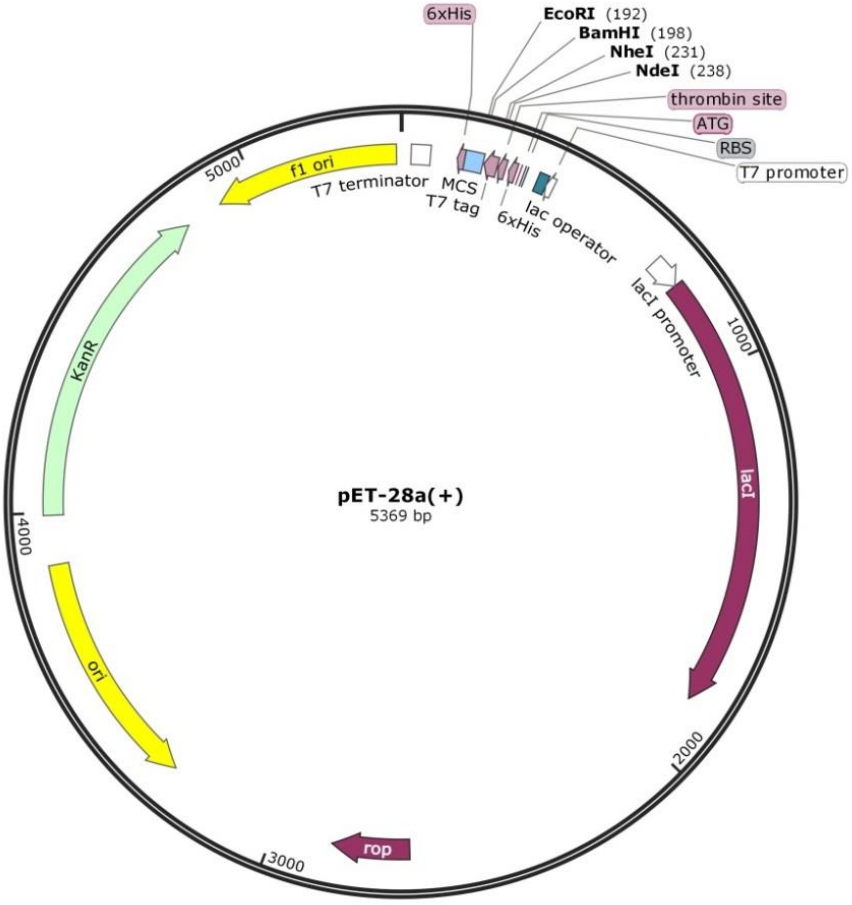

Figure 2.2: pET-28a$^{(+)}$ vector.

Schematic diagram of a pET-28a$^{(+)}$ plasmid. Vector maps generated using SnapGene ® Viewer 3.2.1

2.2.3 GoldenBraid

pUPD2

pUPD2 is the updated ‘domestication vector’ used in the GoldenBraid system. The backbone for this vector is pSB1C3 which is a high copy number plasmid and carries chloramphenicol resistance (CmR) (https://gbcloning.upv.es/pUPD/). Figure 2.3 below shows the plasmid map with key features annotated as well as the restriction endonuclease sites which allow cloning and recombination of cloned gene fragments.

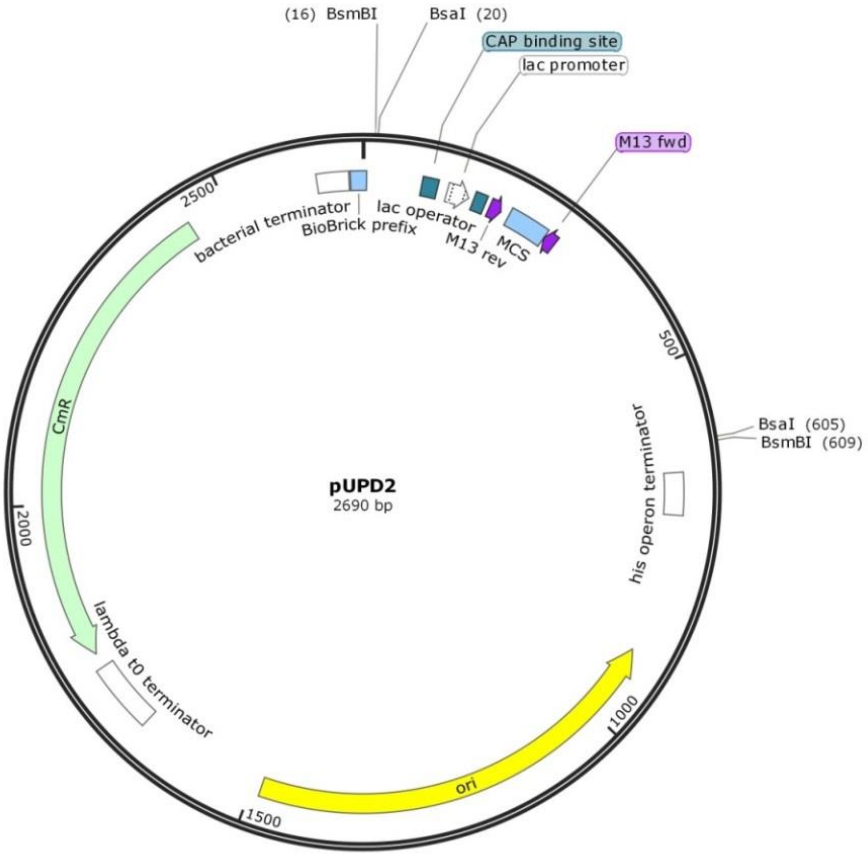

Figure 2.3: pUPD2 vector

Schematic of the pUPD2 GoldenBraid domestication vector annotated with regions of interest and restriction enzyme cut sites. Vector maps generated using SnapGene ® Viewer 3.2.1

pDGB1_α1R

pDGB1_α1R is a GoldenBraid alpha series binary vector used for the ligation of amplicons in the reverse orientation. This vector contains two Type II BsaI restriction sites used in the Goldenbraid system cloning and is a derivative of the plant vector pGreenII (Sarrion-Perdigones *et al*, 2013). pDGB1_α1R holds the sequence for kanamycin (KanR) resistance which is used as a selectable marker.

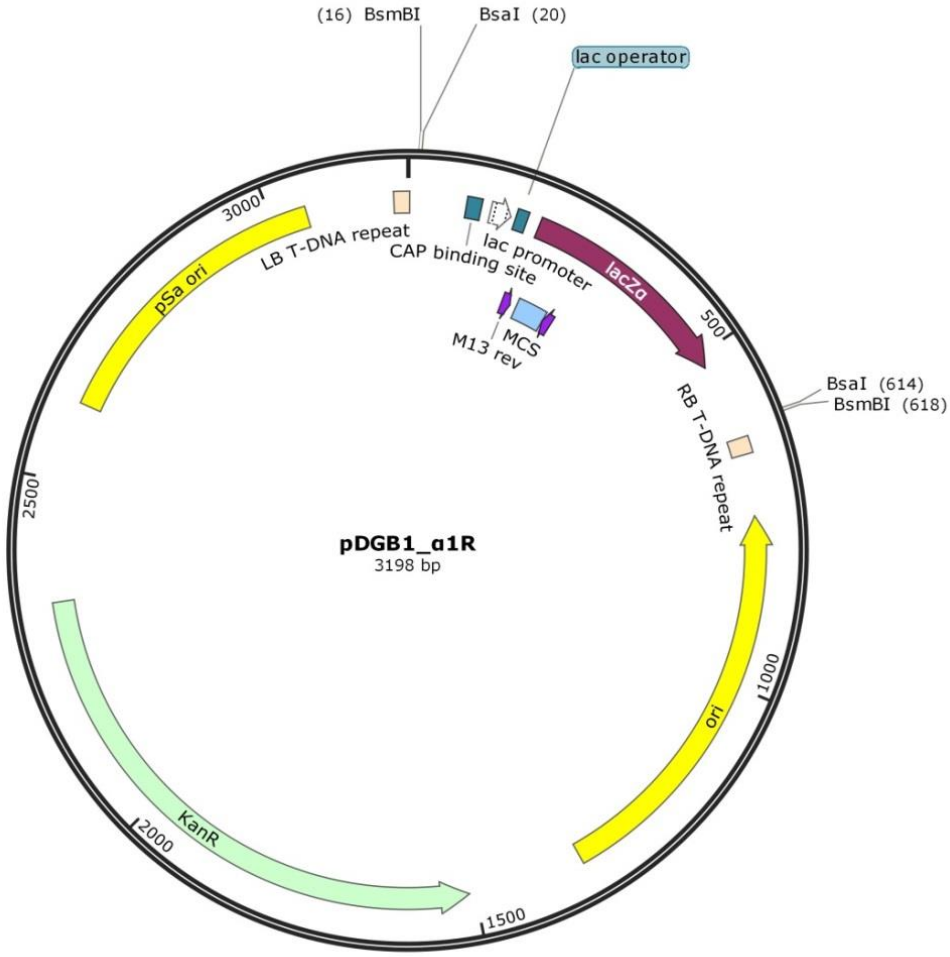

Figure 2.4: pDGB1_α1R vector

Schematic of pDGB1_α1R destination vector annotated with regions of interest and restriction enzyme cut sites. Vector maps generated using SnapGene ® Viewer 3.2.1

pDGB3_α series

pDGB3_α1 and pDGB3_ α2 are GoldenBraid binary vectors used for the recombination of GBparts and patches into functional transcriptional units enabling the generation of multipartite constructs. pDGB3_α series vectors are based on the pCAMBIA series vectors (Sarrion-Perdigones *et al*, 2013) Cloning is facilitated using a restriction endonuclease digestion and ligation reaction (section 2.5.3.4.3) utilising the Type II restriction enzyme, BsaI and T4 DNA ligase (Promega®, UK).

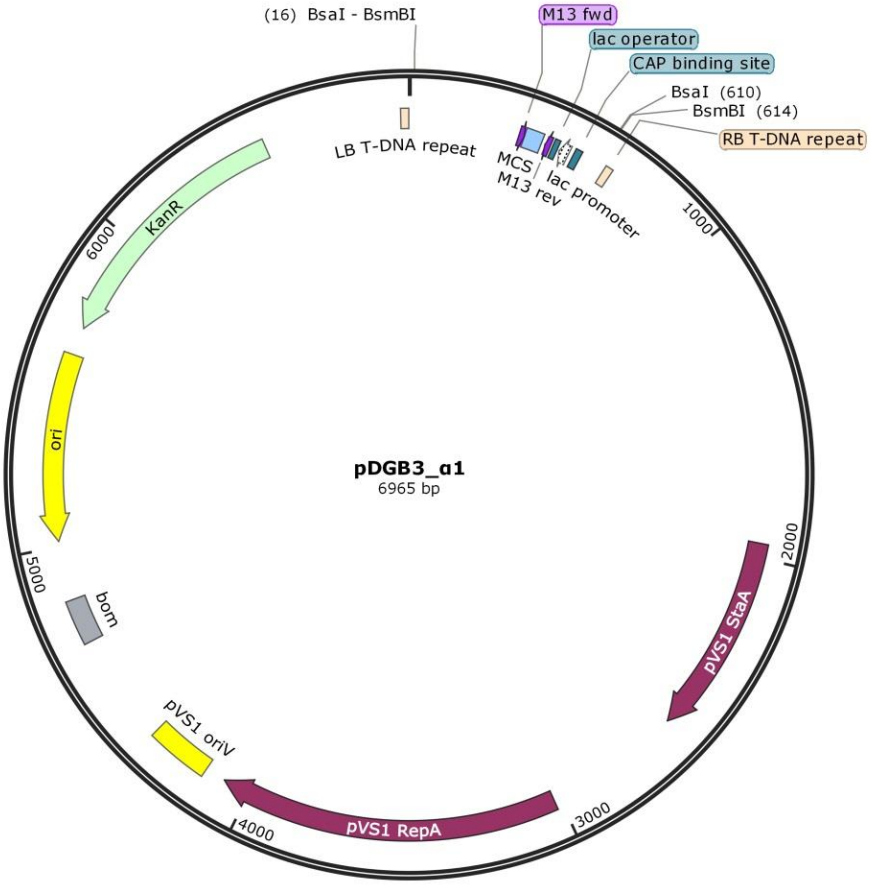

Figure 2.5: pDGB3_α vector

Schematic of pDGB3_α series destination vector annotated with regions of interest and restriction enzyme cut sites. Vector maps generated using SnapGene ® Viewer 3.2.1

pDGB3_Ω series

pDGB3_Ω1 and pDGB3_Ω2 are GoldenBraid Omega series binary vectors that can be used to generate multipartite constructs by the recombination of transcriptional units cloned in pDGB3_alpha series vectors. Amplicons are cloned into this destination vector using a restriction endonuclease digestion and ligation reaction (section 2.5.3.4.3) catalysed by the enzyme BsmBI and T4 DNA ligase (Promega®, UK). The pDGB3_Ω series vectors contain for a *SmR* gene encoding spectinomycin antibiotic resistance The vector backbone is based on the pCAMBIA series vectors (Sarrion-Perdigones et al, 2013).

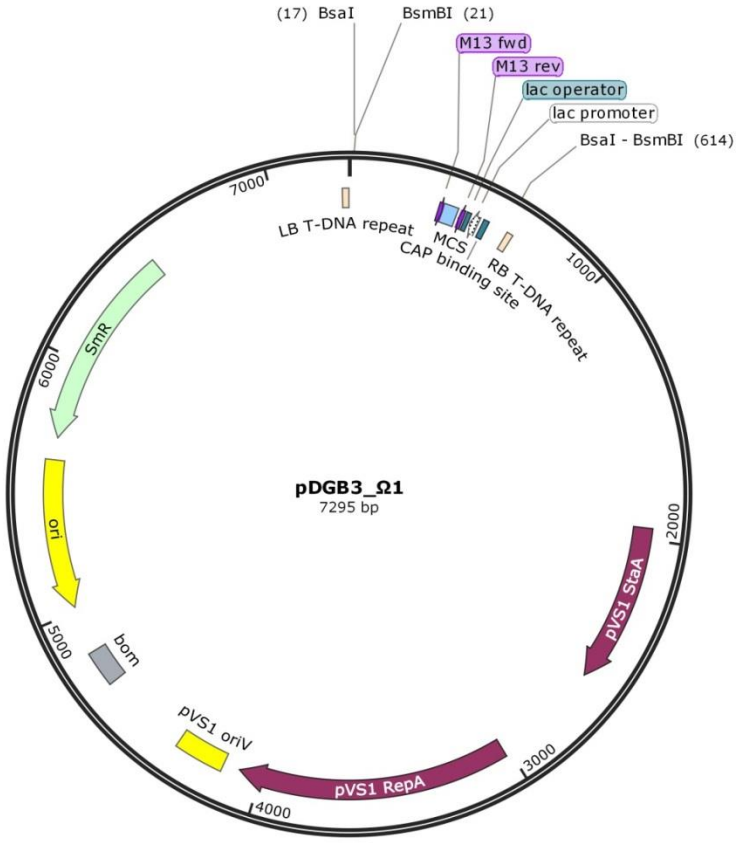

Figure 2.6: pDGB3_Ω vector.

Schematic of pDGB3_Ω series destination vector annotated with regions of interest and restriction enzyme cut sites. Vector maps generated using SnapGene ® Viewer 3.2.1

2.3 Bacterial Strains

2.3.1 *Escherichia coli* DH5a

Library efficiency® *Escherichia coli* DH5α (ThermoFisher™, UK) is a high yielding recombination supressing strain used for the propagation of plasmids. 'Library efficiency®' refers to the transformation efficiency of >1x10^8 cfu/µg plasmid DNA (colony forming units/µg), which is suitable for the transformation of low copy number constructs and blunt end ligations. The Φ80*lac*ZΔM15 genotype allows for blue/white colony screening due to α-complementation of the β-galactosidase gene when grown on media plates containing 32 µg/ml X-gal (5-bromo-4-chloro-3 indolyl-β-D-galactopyranoside) and 32 µg/ml IPTG.

2.3.2 *Escherichia coli* BL21 (DE3)

Chemically competent *Escherichia coli* BL21 (DE3) (Merck™) holds a chromosomal copy of the T7 RNA polymerase gene and is a lysogen of λDE3. This is controlled by the *lacUV5* promoter.

2.3.3 *Agrobacterium tumefaciens* AGL1

Electro-competent *Agrobacterium tumefaciens* strain AGL1 contains the binary helper plasmid pSoup used for for plasmid replication. pSoup is a Ti (tumour inducing) plasmid, which helps facilitate the transfer of the cloned gene cassette into the plant genome during transformation. Supplied by Dr. A Barakate of The James Hutton Institute, UK.

2.4 Plant material

All plant material was grown under glasshouse conditions in 15 or 30 cm diameter pots for potato plants and either 30 or 45 cm diameter pots for *Brugmansia aurea*, *Withania somnifera* and *Hyoscyamus niger* detailed in section 2.4.1. The compost mix used as a growth media was of the following composition: 85.05 % (v.v) Peat (Everris, UK); 7.01 % (v.v) Pavoir Sand (Geddes, UK); 7.01 % (v.v) Perlite (Westland Garden Health, UK); 0.25 % (w.v) Osmocote Exact 3-4 month (ICL, UK); 0.18 % (w.v) Limestone (Calcium) (Thomas Elliot Fertilisers, UK); 0.18 % Limestone

(magnesium) (Keith Singleton Horticultural Products, UK); 0.10 % (w.v) Osmocote Exact Start (ICL, UK); 0.04 % (w.v) Celcote wetting agent (LBS Horticulture, UK); 0.03 % (w.v) Exemptor insecticide (Bayer CropScience, UK). Glasshouse conditions were maintained at 18ºC daytime and 14ºC night time temperature, mean day length of 16 hours and light intensity varying between 400 and 1000 µmol $m^{-2}s^{-1}$. Plants were grown over the summer months (April to October) and shading into effect once the temperature rose above 25ºC, with the temperature monitored through the duration of growth by two temperature/humidity data loggers (DS1923 iButton®, Maxim, USA). These captured temperature and humidity data every hour and were changed fortnightly.

2.4.1 Growth and maintenance of *Brugmansia aurea*, *Withania somnifera* and *Hyoscyamus niger*

Several species of plants known to produce tropane alkaloids were bought from online horticultural retailers. *Brugmansia aurea* (Golden Angels Trumpets) were purchased as pot plants and re-potted upon arrival into large 40 cm diameter pots. *Withania somnifera* and *Hyoscyamus niger* seeds were purchased from Nickys Nursery, UK. Seeds were germinated on a damp towel at 4ºC then transferred to 20 cm diameter pots and grown under the standard glasshouse conditions as detailed in section 2.4.

Plants were watered daily and fed twice a week using Phostrogen All Purpose Plant Food (Bayer CropScience, UK) prepared as directed by the manufacturer. The All Purpose Plant Food contained 16 % (v.v) nitrogen; 10 % (v.v) phosphorous pentoxide; 24 % (v.v) potassium oxide; 2.5 % (v.v) magnesium oxide; 5.8 % (v.v) sulphur trioxide and trace amounts (combined total of 0.1436 % (v.v)) of micronutrients (copper, iron, manganese, molybdenum and zinc).

2.4.2 Maintenance of stock and transgenic potato material

Solanum tuberosum L. *cv Désirée* and *cv. Bintje* were purchased from Scottish Agricultural Science Agency (SASA) and maintained by axenic propogation on MS20 medium. Plants were subcultured using internodal sections from 3 to 4 week old tissue culture plantlets and grown in a growth cabinet maintained at 18ºC and under artificial light on a 16 hour light, 8 hour dark light cycle at 100 µmol m^{-2} s^{-1}.

2.4.3 Harvesting of plant material

Plant tissues were harvested into 15 ml Falcon™ tubes (Corning™) and flash frozen using liquid nitrogen. Harvested tissues were stored at -80°C until required for molecular and biochemical analysis.

2.5. Molecular Protocols

2.5.1 Nucleic acid extraction

Isolation of RNA

RNA was isolated from *Solanum tuberosum* cultivar *Désirée* root, stem and leaf tissue and cultivar *Bintje* leaf tissue using a Tri-reagent (Sigma-Aldrich) extraction method following the manufacturer's protocol. The extracted total RNA was then purified and DNase I treated using an RNeasy Mini Kit (Qiagen, Germany).

Isolation of genomic DNA

Genomic DNA was isolated from *Solanum tuberosum* cultivar *Désirée* and cultivar *Bintje* leaf tissue using an AquaGenomic™ MoBiClo (MultiTarget Pharmaceuticals LLC, USA) kit following the manufaturers protocol.(https://www.mobitec.com/cms/products/bio/06_dna_prot_tools/aquagenomic.pdf?pdf=aquagenomic.pdf).

Extraction of Plasmid DNA from bacterial cultures

Plasmid DNA was isolated from 4 ml of bacterial culture grown overnight at 37°C with the appropriate antibiotics using the Wizard Plus SV Miniprep DNA purification system (Promega, USA) following the manufacturer's protocol. The extraction procedure is based on the alkaline lysis of bacterial cells with the plasmid DNA being absorbed onto a silica membrane in the presence of a high salt buffer. Endonucleases are then removed by washing with buffer PB and salts removed by washing with the ethanol based PE buffer. Purified DNA was then eluted in a low salt buffer EB (10 mM Tris.HCL pH 8.5).

2.5.2 Analysis of nucleic acids

Quantification of nucleic acids by spectrophotometry

Concentrations of DNA and RNA were estimated using a NanoDrop® ND-1000 full-spectrum UV/Vis spectrophotometer (NanoDrop®, USA) measuring 1 µl of highly concentrated aqueous nucleic acid solution at up to 50-times higher concentrations than using a standard cuvette spectrophotometer (NanoDrop®, 2007). The NanoDrop uses a modified Beer-Lambert equation to correlate the calculated absorbance with concentration. DNA and RNA samples were measured at 260 and 280 nm absorbance, with a ratio of 1.8 being accepted as 'pure' for DNA and 2.0 for RNA.

Gel electrophoresis

Agarose gels were prepared by mixing 0.4 to 1 g of agarose with 50 ml of 1X Tris-borate/EDTA (TBE) buffer. This mixture was heated in a microwave on low power for 1 minute at a time, before being mixed and re-heated until all agarose had dissolved. The resulting mixture was cooled to ca. 60ºC before adding 1 µl of 10 mg ml^{-1} ethidium bromide. The gel was then cast in a gel tank with the required size comb and allowed to set under a fume hood for 1 hour. Once set the comb was removed and sufficient TBE buffer added to ensure the gel was fully submerged. Samples were then loaded onto the gel, in the lanes formed by the comb, and separated for 40 to 50 minutes by electrophoresis at 40 V. Imaging of the gel was made under UV light, using the UVITech transiluminator (UVITech, Cambridge, UK).

DNA and RNA quality determination by gel electrophoresis

DNA and RNA were separated and analysed by electrophoresis on ethidium bromide stained agarose gels to check quality using the method in section 2.5.2.2. To either 1% or 2% (w/v) agarose gels (for DNA and RNA respectively) stained with ethidium bromide, 5 µl of nucleic acid samples were added to lanes and separated. Total RNA samples had 1 µl of RNA loading buffer (section 2.1.4) added and were denatured at 70ºC for 10 minutes prior to loading in the gel. Both were visualised under UV light as in section 2.5.2.2.

DNA recovery from agarose gels

Vector and DNA fragments (from PCR and restriction endonuclease digestions) were separated by electrophoresis using ethidium bromide stained agarose gels and the desired band excised under UV illumination. Excised bands were purified using a Wizard® SV Gel and PCR clean up system (Promega, USA) following the manufacturer's protocol. Samples were eluted in between 20 and 50 µl of SDW and stored at 4°C until required for downstream applications.

2.5.3 Enzymatic manipulation of nucleic acids

Polymerase Chain Reaction (PCR)

PCR was conducted using two different types of Taq polymerase. For routine PCR to determine presence/absence and length of amplicons a non-proof reading Go*Taq*® G2 DNA polymerase (Promega, USA) was used. Whereas for PCR reactions where the product was to be sequenced, used for generation of recombinant proteins or in transformations, Platinum™ *Taq* DNA Polymerase High Fidelity (Invitrogen) was used. This polymerase has 3' to 5' exonuclease proof reading activity allowing nucleotide incorporation errors to be corrected, making it suitable for cloning applications.

Routine PCR reactions were carried out in a volume of 25 µl containing 1 unit (U) of Promega Go*Taq*® G2 DNA polymerase, 5 µl of 5x Green Go*Taq*® reaction buffer, and between 20 and 75 ng of template DNA per reaction. Also included were gene specific forward and reverse primers at a final concentration of 0.4 µM and the four deoxynucleotides (dNTPs) adenine, cytosine, guanine and thymine at a final concentration of 0.4 mM. The reaction contained $MgCl_2$ at a final concentration of 1 mM and was bought up to the final reaction volume with *dd*H_2O. Thermal cycling conditions used to generate the PCR fragments were as follows: 2 minutes denaturation at 94°C followed by 20 to 35 cycles of 94°C for 30 sec, 30 sec at the desired melting temperature (Tm) for the primer pair used (this was generally 5°C below primer melting point), and a 60 sec extension time per 1 kb of expected fragment at 72°C. Positive (where possible) and negative controls were included with each reaction.

PCR reactions using high fidelity Taq polymerase were carried out in a total reaction volume of 25 µl and as per the manufacturer's instructions, with each reaction containing 0.1 µl (5 U/µl) of Platinum® Taq DNA Polymerase High Fidelity, 2.5 µl of High Fidelity PCR buffer, gene specific forward and reverse primers at a final concentration of 0.2 µM, dNTPs at a final concentration of 0.2 mM and up to 50 ng of template DNA used per reaction. The final reaction contained MgSO4 at a final concentration of 2 mM and a final reaction volume of 25 µl with *dd*H_2O. Thermal cycling conditions were as follows: 2 min denaturation at 94^oC followed by 25 to 35 cycles of 94^oC for 15 sec, 30 sec at the desired melting temperature (Tm) for the primer pair used (this was generally 5^oC below primer melting point) and 60 sec extension time per 1 kb of expected fragment at 68^oC.

Restriction endonuclease digestion reactions

Plasmid DNA preparations (0.5 to 1 µg) underwent routine restriction endonuclease digestion in the presence of 5 to 10 units of enzyme, as well as at the appropriate temperature (normally 37^oC) and in the recommended buffer as per manufacturer's guidelines for 3 to 4 hours. Digested plasmid was visualised by ethidium bromide stained Tris-borate (TBE) agarose gel electrophoresis (section 2.5.2.2). In some instances digested fragments were excised from the gel and this was purified using the Promega Wizard® SV Gel & PCR clean up system (USA) as per manufacturer's protocol. This purified fragment was then used in subsequent ligation reactions.

cDNA synthesis

cDNA was synthesised from purified RNA samples for RT-qPCR analysis. During the project two methods were used for this purpose, these being Invitrogen™ SuperScript™ III Reverse Transcriptase or the TaKaRa CloneTech RNA to cDNA EcoDry™ Premix (Double Primed) lyophilized master mix. Once synthesis was complete all cDNA was diluted to 10ng/µl through the addition of ddH_2O.

cDNA was synthesised using the Invitrogen™ SuperScript™ III Reverse Transcriptase and up to 5 µg of DNase I treated total RNA. To the RNA, 1 µl of both Oligo(dT)20 (concentration) and 1 µl of dNTP mix (10 mM) was added, then the total volume was bought up to 13 µl with RNase free water. This mixture was then heated at

65ºC for 5 minutes then incubated on ice for a further minute. For the reverse transcription step of this protocol, 4 µl of First Strand Buffer (5x), and 1 µl of each of the following 0.1 M DTT, RNaseOUT™ (40 U/µl) and Superscript™ III RT (200 U/µl) was added. The mixture was then mixed by pipette and then heated at 50ºC for 60 minutes, before the enzyme deactivated by incubating at 70ºC for 15 minutes.

A second method used for synthesising cDNA was using a TaKaRa CloneTech RNA to cDNA EcoDry™ Premix (Double Primed) beads kit. 5 µg of DNase I treated total RNA in a final volume of 20 µl RNase-free H_2O was added to the lyophilized EcoDry™ Premix. The mixture was then mixed by pipetting and centrifuged to remove any potential air bubbles before heating at 42ºC for 60 minutes prior to deactivating the enzyme at 70ºC for 10 minutes.

2.5.3.4 Ligation reactions

pGEM®-T Easy (Promega, USA)

PCR synthesised DNA fragments containing adenine (A) overhangs were ligated into pGEM®-T Easy, using T4 DNA ligase (Promega, USA). T4 DNA ligase catalyses the formation of new bonds between the 5' phosphate residue and the 3' hydroxyl groups of fragment and plasmids. To ensure greater ligation efficiency the incubation conditions used were different to the manufacturer's guidelines. The thermal conditions were 10 cycles of 25ºC for 30 minutes, 22ºC for 30 minutes and 16ºC for 30 minutes with a final holding stage of 16ºC. The reaction mixture comprised of 1 µl T4 DNA Ligase buffer, 1 µl T4 DNA Ligase (3 U/µl), 1 µl pGEM®-T Easy (50 ng), a variable amount PCR product (depending on concentration and ratio being used) in a final reaction volume of 10 µl made up with with ddH_2O. Once complete, the ligation mixture was transformed into E.coli competent cells as detailed in section 2.5.4.1.

pET-28a$^{(+)}$ (Novagen)

DNA fragments were ligated into the linearised plasmid vector pET-28a$^{(+)}$ using a T4 DNA ligase (Promega, USA) catalysed reaction. For each sample, 75 ng of linearised vector was mixed with 40 ng of DNA fragment,1 µl T4 DNA ligase and 2 µl 10x ligase buffer (section 2.1.4) before being bought to a total volume of 20 µl with

ddH_2O. Samples were then incubated in a thermal cycler at conditions of 10 cycles of 25ºC for 30 minutes, 22ºC for 30 minutes and 16ºC for 30 minutes. Once complete, 5 µl of the reaction mixture was used for transformation into competent *E. coli* cells.

Ligations in the GoldenBraid system

Restriction ligation reactions were carried out in a 0.5 ml PCR tube, to this, 75 ng destination vector and 75 ng of each of the required GBparts and GBpatches were added. To this, 1 µl of 10 U/µl restriction endonuclease (either BsaI or BsmBI (both Promega, USA) depending on site being cleaved), 1 µl of 3 U/µl T4 DNA ligase and 1 µl T4 Ligase buffer were added. *dd*H20 was then added to a final total volume of 10 µl and the samples incubated in a thermocycler at 37ºC for 30 minutes, followed by 75 cycles of 37ºC for 2 minutes and 16ºC for 5 minutes respectively and held at 16ºC for 30 minutes. 2 µl of the ligation mixture was transformed into heat-shock *E. coli* as per the protocol in section 2.5.4.1. The reaction conditions described above are the same for each level of the GoldenBraid system as described in chapter 1.11.

2.5.3.2 Design of primers

Gene specific primers for PCR were designed by submitting the sequence in FASTA format (5' to 3' orientation) into the online software Primer3 programme (http://primer3.ut.ee/). Primer sequences were then purchased from Eurofins genomics (Germany) and re-suspended in *dd*H_2O to a final concentration of 100 µM upon arrival.

2.5.3.3 RT-qPCR (Universal Probe Library)

RT-qPCR was performed using cDNA prepared as described in section 2.5.3.3. Primers and probe sequences were designed using The Roche Universal Probe Library Assay Design Centre (https://lifescience.roche.com/en_gb/brands/universal-probe-library.html). All qRT-PCR reactions were performed using an Applied Biosystems StepOne Plus Real Time PCR system. 50 ng total cDNA was used as template in all reactions, which were composed of 12.5 µl 2x FastStart Universal Probe Master Mix (Rox) (Roche, UK), 10 µM Universal Probe, and 20 µM of both forward and reverse primer before being made up to a final volume of 25 µl with *dd*H_2O. Thermocycling conditions were as follows, denaturation stage of 95ºC for 10 mins, 40 cycles of 95ºC

for 15 sec and 60ºC extension for 1 min. Samples were ran in triplicate, using *elongation factor-1α* (*ef-1α*) as an endogenous control. This gene can be used as a control as it encodes a ubiquitous protein which is utilised in protein synthesis by binding aminoacyl-transfer RNA to ribosomes (Stürzenbaum and Kille, 2001) and has been shown to be highly consistent between different tissue samples and growth stages (Nicot *et al*, 2005; Ross *et al*, 2011). Calculations of relative expression levels for transgenic lines manipulating the *Solanum tuberos*um *tropinone reductase II* were performed using the Pfaffl method (Pfaffl, 2001). For transgenic lines which over-expressed a non-endogenous *tropinone reductase I* within *Solanum tuberosum*, the $2^{-\Delta C_T}$ has been shown to describe the relative expression levels of the introduced gene (Schmittgen and Livak, 2008).

2.5.3.4 Sequencing of DNA

Sequencing was performed by the Genome Technology Service at The James Hutton Institute, Dundee, UK. Plasmid templates were purified using the Promega Wizard® SV Miniprep DNA Purification System (USA) (section 2.5.1.3) and quantified by Nanodrop ND-1000 (Nanodrop, USA) (section 2.5.2.1). PCR templates were purified using the Promega Wizard® SV Gel & PCR clean up system (USA) and visualised by agarose gel electrophoresis. For plasmid templates, concentration for sequencing reactions ranged between 40 and 250ng/µl and for PCR templates the concentration range was between 1 and 50 ng/µl depending on fragment size. Sequencing reactions were conducted on a capillary based Applied Biosystems AB3730 DNA Analyser and the raw data visualised using the sequencing analysis software, Sequencher (version 5.2.4) (Gene Codes Corporation, USA).

2.5.3.5 Recombinant protein induction

The pET-28a$^{(+)}$ vector coupled with *E.coli* BL21 (DE3) is a powerful tool for the cloning and expression of recombinant proteins within *E. coli* where genes are expressed by a bacteriophage T7 RNA polymerase transcription signals from the host cell. Initial cloning and induction is performed in *E. coli* strain BL21 (DE3) hosts which do not exhibit basal T7 RNA polymerase activity due to the presence of a *lac* repressor, thereby preventing expression of the introduced gene without the addition of 1 mM IPTG (Isopropyl β-D-1-thiogalactopyranoside). Simultaneously the addition of IPTG

and substrate which the protein would act on was added at a final concentration of 100 mg/l. From here the cultures were allowed to grow at 16ºC, 22ºC, 28ºC and 37ºC for 48 hours with samples taken at 0, 24 and 48 hours post induction. Once samples were taken, the cell culture was centrifuged to pellet the cells (9400 x g for 5 minutes) and the supernatant was removed to a fresh Eppendorf for further metabolite analysis (as described in section 2.6.3). The pelleted cells underwent protein extraction and western blot analysis to check for induction as described in section 2.5.3.9.

2.5.3.6 Protein extraction and Western Blot

Crude protein extraction was conducted on pelleted cells (from 2 ml of inducted cultures (9400 x g for 5 minutes) by applying 500 µl SDS buffer, re-suspending the pellet and boiling for 10 minutes at 95ºC. Once boiled, the suspension was centrifuged (9400 x g for 5 minutes at 4ºC) to pellet cell debris; the supernatant was then moved to a fresh eppendorf. 26 µl of supernatant was then used for the western blotting.

To the supernatant being run on the gel 10 µl Novex NuPAGE SDS Running Buffer and 4 µl Novex NuPAGE Reducing Agent (Invitrogen, UK) were added. The samples were then denatured for 5 minutes at 90ºC whilst the gel and running buffers were prepared.

A Novex NuPAGE 4-12% Bis-Tris 15 well pre-cast gel (Invitrogen, UK) was placed in the running chamber and was surrounded with Novex NuPAGE MOPS SDS running buffer (one litre was made by adding 50 ml buffer to 950 ml *dd*H_2O). Once the samples where denatured they were pipetted into the wells of the gel, following manufacture's advice regarding well volume. 10 µl of Precision Plus Protein Dual Colour Standard (BioRAD, USA) was added to a well in the gel as a size marker. The gel was then run at 200V for 35 minutes.

After the protein sample had been run and separated on the gel, the gel was removed from its housing and washed in *dd*H_2O. Proteins were transferred from the gel to a nitrocellulose membrane (Novex 0.45 um pore size (Invitrogen, UK)), and the set up for this stage can be seen in Figure 2.7. All materials which were used in this transfer step were wetted prior to use in transfer buffer (50 ml Novex NuPAGE Transfer Buffer (20x), 850 ml *dd*H_2O and 100 ml methanol). The transfer was completed over 1 hour at 35V.

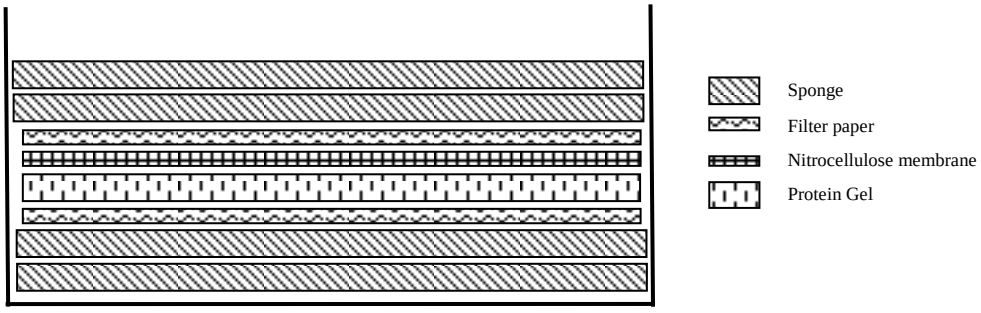

Figure 2.7: Schematic representation of the completed protein transfer cell.

Once protein transfer had been completed, the membrane was briefly washed in TBS-T buffer (see Appendix x for recipes). To 100 ml of TBS-T, 5 g of dry non-fat milk was added and shaken until completely dissolved. The membrane was incubated in 15 ml of this blocking solution for 1 hour at room temperature before two successive 5 minute washes in 15ml TBS-T. To another 25 ml of the milk solution 2.5 µl of 6x-HisTag Monoclonal Antibody (Invitrogen, UK) raised in Mouse (*Mus*) was added (dilution 1:10000). This was applied to the membrane and left on a shaker at 4^{o}C overnight.

The next day the membrane underwent 4 successive 5 min washes in 15 ml TBS-T before addition of the secondary antibody. In this case the secondary antibody was a goat anti-mouse IgG-HRP (Santa Cruz Biotechnology, USA) with 2.5 µl being added to 25 ml TBS-T milk solution (1:10000 dilution). This was left to incubate for 1 hour at room temperature. After this, the membrane underwent 4 successive 5 min washes in 15 ml TBS-T to remove excess antibody. Detection of any antibody tagged proteins used the chemiluminescent substrate SuperSignal™ West Femto (Thermo Scientific™, USA) as per the manufacturers protocol. Imaging of the membrane was done under UV with the SYNGENE G:BOX ™ (Synoptics, UK).

2.5.4 Bacterial Protocols

2.5.4.1 Heat shock transformation of competent *E.coli* (strains DH5α and BL21 (DE3))

100 µl aliquots of competent cells stored at -80ºC were thawed on ice (DH5α from ThermoFisher™, UK and BL21 from Merck™) for 5 minutes. To this, 2 µl of ligation reaction was added to 50 µl of competent cells and incubated on ice for between 5 and 30 minutes depending on the strain of *E.coli* (BL21 (DE3) and DH5α). After incubation, tubes were heated for 30 sec or 45 sec at 42ºC then incubated on ice for a further 2 min. 900 µl of warmed SOC media was then added to this mixture and further incubated at 37ºC for 2 hours and shaking at 250 rpm. Following incubation, 200 µl of the bacterial culture was spread over LB agar plates with appropriate antibiotic selection for the plasmid vector and once dried, inverted and incubated overnight at 37ºC to allow colony growth. Vectors which allowed blue/white colony screening were grown on LB plates containing IPTG and Xgal in addition to the antibiotic selection; plates were placed at 4ºC for 3 hours to enhance any colouration present.

2.5.4.2 Transformation of electro-competent Agrobacterium

Transformation of electro-competent *Agrobacterium tumefaciens* AGL1 (supplied by Dr. A Barakate, The James Hutton Institute) was performed using a Bio-Rad electroporator following the manufacturer's protocol. 40 µl of electro-competent Agrobacterium cells were gently thawed on ice for 5 minutes. 1 µl of plasmid DNA (50ng/µl) was then added, mixed using a pipette, then transferred to a pre-chilled Bio-Rad electroporation cuvette (Bio-Rad; 0.2 cm electrode gap) placed in the electroporator with the following conditions. 200 Ω resistance; 25 kV voltage; 25 µF capacitance. A single pulse was applied to the cuvette then 500 µl of warmed SOC medium (section 2.1.1) added, decanted into a sterile 1.5 ml eppendorf tube and incubated at 28ºC for 4 hours at 250 rpm. Following incubation, cells were plated onto LB plates containing the appropriate antibiotics inverted, and incubated at 28ºC for 3 days.

2.5.4.3 Preservation of bacterial cultures

After cultivation *E. coli* and *Agrobacterium tumefaciens* bacterial cultures were stored as glycerol stocks. These were made by mixing 1200 µl of bacterial culture (OD_{600} between 0.6 – 0.8) with 650 µl 50% glycerol (w/v). Samples were then inverted to ensure mixing before being snap frozen in liquid nitrogen and stored at -80ºC until needed.

2.5.4.4 Generation of bacterial cultures for transient and stable inoculation

For production of stable transgenics *Agrobacterium tumefaciens* cultures containing the binary transformation vectors (generated in section 2.5.3.4.3) were grown overnight in lysogeny broth media at 28ºC at 250 rpm. Following incubation, 20 µl of acetosyringone was added at a final concentration of 0.2 mM the incubated for another 4 hours at 28ºC. The OD_{600} was measured using a spectrophotometer (Amersham Bioscience Ultrospec 2100pro (UK)) and cells used for plant transformation when the OD_{600} was between 0.5 and 0.8.

2.5.4.5 Tissue culture of generated transgenic lines

Tissue culture was carried out in a laminar flow cabinet cleaned with 75% (v/v) ethanol, prior to work being carried out to ensure sterile conditions. Internodal sections from 5 week old potato plantlets cv. *Désirée* and cv. *Bintje* were taken, sections were between 5 and 10 mm long were cut longitudinally. Internodes were collected stored in liquid MS30 media for ca. 1 hour until enough explants were harvested (~ 100 per transformation required). Samples were moved to a petri dish containing the MS30 media and explants and 100 µl of freshly prepared Agrobacterium culture added (OD_{600} between 0.6 and 0.8) and incubated in the dark at 24ºC for 20 minutes at 50 rpm. After incubation, explants were removed and dried on Whatman™ filter paper before being transferred to callus induction media (HB1 (section 2.1.2)) at a maximum density of 100 explants per plate. Plates were then incubated for 2-3 days in low light conditions.

After this initial growth period, explants were transferred to fresh HB1 media containing the antibiotics cefotaxime and kanamycin as selection, at a density of 20 per plate and then allowed to further incubate in the growth cabinet for 7 days under 16:8

hour light conditions. Following this 7 day period, the media was again changed every 14 days until calli formation.

Once calli were present, explants were moved onto regeneration media (HB2 (section 2.1.2)) containing kanamycin and cefotaxime at a density of 20 explants per plate and subcultured every 14 days until shoots start to appear on the calli. As the shoots appear (ca. 4 to 6 weeks) and the calli grow the number of explants per plate were reduced accordingly.

Shoots over 1 cm in length were excised and assigned an identification number according to corresponding calli and plate number. Samples were transferred to fresh MS20 media containing cefotaxime and kanamycin. Shoots which exhibited root formation from the base of the shoot were subcultured onto fresh media and the presence of the transgene tested by PCR analysis (section 2.5.3.1). PCR positive lines were propagated for further replication.

2.6 Biochemical Analysis

2.6.1 Chlorophyll and Carotenoid extraction

Chlorophyll and carotenoid contents of transgenic leaf material were determined spectrophotometrically according to Miazek and Ledakowicz, 2013. The following method was carried out in low light conditions. 100 mg of ground, freeze dried leaf material was weighed out into a 15 ml Falcon® tube. To this, 5 ml of 95% ethanol was added and samples vortexed for 30 seconds then incubated at 60^{o}C for 1 hour followed by another 30 seconds of mixing. Samples were then centrifuged at 2800 x g for 2 minutes to form pellet and 100 µl of supernatant transferred to a cuvette containing 900 µl 95% ethanol. Spectrophotometer readings were taken at 470, 648 and 664 nm. To calculate the concentrations of Chlorophyll A, Chlorophyll B and Carotenoids in µg/g the following equations were used (Miazek and Ledakowicz, 2013):

Chlorophyll A = ((13.36 x 664nm reading – 5.19 x 648nm reading) x 10)/weight (g)

Chlorophyll B = ((27.43 x 648nm reading – 8.12 x 664nm reading) x 10)/weight (g)

Carotenoid = ((1000 x 470nm reading) x 10)-(1.82 x Chlorophyll A value)-(85.02 x Chlorophyll B value)/198

2.6.2 Extraction of tropane alkaloids from plant tissue

Plant tissue was collected, frozen in liquid nitrogen and lyophilised in a CHRiST® Gamma I-16 LSC freeze dryer (0.700 mbar vacuum and -49ºC condenser temperature). Samples were then ground to a fine powder using a mortar and pestle and stored in 15 ml Falcon® tubes. 40 mg of sample was removed and placed in a 2 ml eppendorf tube and two 3mm tungsten carbide beads (QiaGEN, USA) were added. The samples were then further homogenised in a QiaGEN TissueLyzerII (QiaGEN, USA) for 1 min and at a frequency of 20/s (kHz).

1.5 ml extraction buffer (49% MeOH, 49% ddH_2O and 2% Formic Acid) was added and the samples vortexed for 60 sec to ensure they were thoroughly mixed, then incubated on a blood rotator at 30 rpm for 1 hour at 4ºC. Samples were then centrifuged at 3000 x g for 15 minutes at 4ºC to pellet the tissue. 1 ml of supernatant removed and dried at 40ºC using a rotary evaporator until 300 µl was remaining. The samples were then frozen and dried using a freeze drier.

For samples which were expected to be high in calystegine content the formic acid was omitted from the extraction buffer as described in Petersson *et al*, (2013). When ready for analysis on the Agilent QqQ-LC-MS/MS, samples were re-suspended in 200 µl of 50% methanol which was spiked with reserpine (10 µM final concentration) used as an internal standard (ITSD).

2.6.3 Extraction of tropane alkaloids from media

Tropane alkaloids from bacterial biotransformation experiments were extracted whilst still in LB media. To ensure that there was no bacterial cells in the extract, 2ml of LB broth was removed from the culture and centrifuged at 9400 x g for 10 minutes at 4ºC. From this, the supernatant was removed and the pellet retained for western analysis. 200 µl of the supernatant was removed and analysed on the QqQ-LC-MS/MS with the addition of 10 µl reserpine (10 µM) as an ITSD.

2.6.4 HPLC

Methods were developed for using the HPLC which was equipped with the UI-100 Universal Chromatography Interface (Dionex, USA), Gynkotek UVD340U, Ultimate 3000 Autosampler (Dionex, USA) and using Chromeleon 6.60 SP9 (Build 1566) Software (Dionex, USA). The running method used in the first instance was previously described in Pietsch *et al* (2008), and can be seen below in Table 2.1. UV detection wavelengths of 207, 225, 250 and 280 nm were used for the detection of peaks within the samples Buffer A = 100% Acetonitrile, Buffer B = 0.01 M phosphate buffer (pH 6.5). Modifications were made to the running conditions, with Buffer B changing from 0.01 M Phosphate buffer (pH = 6.5) to 0.1% TFA, which was run under the same gradient. A Cronus CRONUSIL-S ODS2 5µm 25x0.46 cm (Labhut, UK) column was used.

Time (mins)	Buffer A %	Buffer B %
00:00	10	90
15:00	10	90
37:30	75	25
46:30	75	25
50:00	10	90

Table 2.1: **HPLC running conditions.**
Time and percentage composition of both buffers used during the run of a sample on the HPLC.

2.6.5 ThermoFisher Scientific's *OrbiTrap*™ LC-MS system.

For the analysis of the TAs a LTQ OrbiTrap™ XL (ThermoFisher Scientific, Germany) system was used. This system was equipped with an Aceela PDA Detector, Acella Autosampler and Acella 600 pump. The column used was a Synergi 4µm C18 Hydro-RP80 150 x 2.0 mm (Phenomenex, USA) which was kept at 30^{o}C. The running method consisted of two mobile phases. A: *dd*H_20 with 0.1% formic acid and B: methanol with 0.1% formic acid. The buffer gradient can be seen in Table 2.2 below. Data from runs were extracted and analysed through Xcalibur (ThermoFisher Scientific, USA). The injection volume was 5 µl.

Time (mins)	Mobile Phase A (%)	Mobile Phase B (%)
00:00	100	0
03:00	100	0
17:00	0	100
22:00	0	100
23:00	100	0
29:00	100	0

Table 2.2: LCMS running conditions.

Time and percentage composition of both mobile phases for during the run of a sample on the OrbiTrap™ LCMS system. There is a gradient of mobile phase B from 00:04 to 00:16 minutes, before stabilisation until 00:23 when mobile phase A is returned to 100% over the course of 1 minute.

2.6.6 QqQ-LC/MS

An Agilent Technologies™ 6460 Triple Quad LC/MS was used for a targeted analysis of the tropane alkaloids. The mobile phases, column and gradient conditions were the same as described previously for the Orbitrap™-LC/MS (Section 2.6.5). The Triple Quad LC/MS was equipped with the following Agilent Technologies™ Infinity 1260 series components: Diode Array Detector (DAD), Thermostatted Column Compartment (TCC), Automatic Loading Sampler (ALS) and a Quaternary Pump.

Individual metabolites which are to be analysed on the QqQ-LC/MS system underwent initial optimisation to generate fragment patterns which would allow for the generation of a multiple reaction monitoring reaction (MRM) and is further detailed in Chapter 3.

2.7 Statistical methods

T-test statistical analysis was conducted using the IBM SPSS® platform (Version 22). Comparisons between individual lines and controls (*Désirée* and Empty Vector) with significant differences have been shown where appropriate.

Chapter 3: Detection method development

3.1 Introduction

Robust and highly sensitive quantification methods for tropane and nortropane alkaloid analysis from different plant tissues and microbial sources were developed as important tools to be used throughout this project.

3.1.1 Composition of alkaloids and extraction from plant material

As previously discussed in Chapter 1, tropane alkaloids such as hyoscyamine and scopolamine are synthesised in the roots of some solanaceous plants. These compounds are then translocated to the leaves where they are stored (Mano *et al*, 1986). As tropane alkaloids are found throughout the plant, extraction from above and below ground tissues have been studied. Jakabova *et al*, (2012) extracted tropane alkaloids from five above ground tissues of four *Datura* species. Across the four species analysed, there was no consensus as to where the highest concentrations of the tropane alkaloids scopolamine or hyoscyamine (measured as atropine) were located. For example, in *Datura inoxia* scopolamine was the most abundant tropane alkaloid in all plant tissues tested. The highest concentrations of atropine was found in stems of fruit producing plants, whereas in *Datura stramonium* and *Datura stramonium* var. *tatula* all organs contained higher concentrations of atropine compared to scopolamine with var. *tatula* displaying up to 2.5-fold more total tropane alkaloids compared to *D. stramonium*. Kohnen *et al*, (2017) analysed root, stem and leaf samples from *Duboisia myoporoides* at three time points through plant development. It was found that whilst tropane alkaloid concentration increased in all tissues as the plant developed, scopolamine concentration in the leaves showed the greatest increase from 5.5 mg/g^{-1} DW (6 weeks post planting from cutting) to 14.8 mg/g^{-1} DW (6 months post planting from cutting), whereas in the roots it was hyoscyamine which showed the highest concentration at 6 months (4.2 mg/g^{-1} DW). These studies indicate that depending on the tissue of interest, tropane alkaloid concentrations are widely variable, and accurate quantification requires robust analytical methods.

Chemically, alkaloids are basic molecules, due in part, to the free electron pair located on the amine nitrogen atom bound to C1 and C5 of the tropane skeleton (El-Sakka, 2010). This aspect of their chemistry results in the alkaloids being readily soluble in polar organic solvents (Christen, 2007). A range of extraction and recovery

methods have been developed for tropane and other classes of alkaloids, and these were summarised in section 1.13.

3.1.2 A new LC-MS system for detection of tropane alkaloids.

Whilst GC-MS, TLC, HPLC-UV have been used for the detection of tropane alkaloids in previous studies and have been introduced in the chapter 1, the use of the ThermoFisher Scientific OrbiTrap™ LC-MS system has only recently started to be used for the detection of these metabolites (Romera-Torres *et al*, 2018).

3.1.3 ThermoFisher Scientific's OrbiTrap™ LC-MS system (hereafter OrbiTrap™).

The Orbitrap™ system achieves its 'ion trapping' through the generation of an electrical potential being applied to a central wire and its cylindrical housing. This generates an electric field, attracting ions that have insufficient velocity to escape the field and results in them becoming trapped (Makarov, 2000). Although a rudimentary version of this technique has been used since 1923, this was known as a 'Kingdon trap'; the technique was re-visited in 2000, and it was improved upon for accurate mass determination so that its use became more widespread.

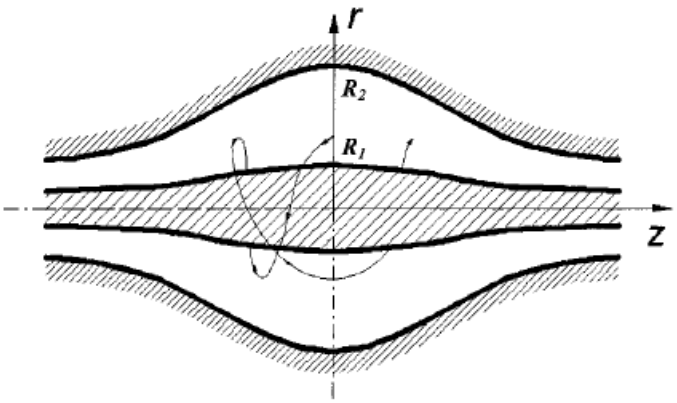

Figure 3.1.1: OrbiTrap™ electrode field scheme.

Example of ion trajectory within the OrbiTrap™ electrode field. Z denotes the symmetrical plane (Z = 0), and R is the radius from the central point of the electrostatic field. R_1 is indicating the position of the central electrode and R_2 shows the outer electrode. (Makarov, 2000).

OrbiTrap™ systems display a high degree of sensitivity and mass accuracy for ions within samples. The high degree of mass accuracy in conjunction with associated software (ThermoScientific™ Xcalibur™ version 2.2.44 (2011)) assists with determination of the elemental formulae and structure of unknown molecules within the samples (Makarov and Scigelova, 2010). Therefore the OrbiTrap™ system provides a powerful detection approach for the metabolites that have been produced by an engineered metabolic pathway. It is hoped that the chromatography and detection methods developed on the OrbiTrap™ can be translated to the quantitatively accurate Triple-Quadrupole LC-MS/MS.

3.1.4 Agilent Triple-Quadrupole (QqQ) LC-MS/MS tropane alkaloids fragmentation patterns in literature

The structural similarity of tropane alkaloids stems from the nitrogen containing tropane skeleton, previously described in Chapter 1.2 and Chapter 3.1. Therefore fragmentation patterns (see Chapter 1.12.4) generated from the QqQ-LC-MS/MS that can be used to discriminate between different tropane and nortropane alkaloids will be dependent on the nature of other parts of the molecule including any side groups added to this skeleton. For example, it is possible to discriminate between hyoscyamine and scopolamine due to the presence of the epoxide oxygen ring on the tropane skeleton at C-6 and C-7 of scopolamine. The fragments derived from this will exhibit an m/z of 138 in scopolamine compared to 124 in hyoscyamine.

Recent developments in detection techniques through using the QqQ-LC-MS/MS systems have shown that the fragmentation of the higher valued tropane alkaloids, hyoscyamine and scopolamine yields the patterns shown in Table 3.1.1. These fragments can be selected for individually, so that if they are detected within a sample once it has been fragmented the peak generated will correspond to a known panel of metabolite. The abundance of this peak compared to a standard sample enables accurate quantification. The process of fragmentation, detecting, quantifying and monitoring these peaks through the duration of the chromatography is referred to as Multiple Reaction Monitoring (MRM).

Molecule	*m/z*	Fragments generated (*m/z*)	Reference
Atropine	290.2	142.1 124.0 103.0 93.0 91.0 77.0 67.0	Chen *et al*, (2017)
		142.0 124.0 93.0 67.0	Zhou *et al*, (2017)
Anisodamine	306.1	158.0 140.0 122.0 121.0 79.0	Zhou *et al*, (2017)
Scopolamine	304.0	156.0 138.0 121.0 110.0 103.0 98.0 79.0	Chen *et al*, (2017)
		156.0 138.0 121.0 103.0 79.0	Zhou *et al*, (2017)

Table 3.1.1: Known tropane alkaloid fragmentation patterns.

Fragmentation patterns for the three larger tropane alkaloids atropine (racemic hyoscyamine), anisodamine and scopolamine with parent ion mass (m/z), fragments yielded and literature reference.

3.2 Materials and Methods

3.2.1 Extraction methods.

In assays below, two extraction methods are compared. Method S is refered to in section 2.6.2 and method V is adapted from Vorst *et al*, 2005.

Extraction buffer in method V is comprised of 62.5% MeOH, 37.375% *dd*H2O and 0.125% Formic Acid. 1.5 ml of extraction buffer was added to the ground sample and then vortexed for 60 seconds to allow for thorough mixing. The sample was then placed in an ultrasonication bath for 10 minutes, before being centrifuged at 3000 x g for 15 minutes to pellet tissues. Supernatant was removed and filtered through a 0.45 µm syringe filter prior to being dried in a rotary evaporator at 40oC. Samples were then re-suspended in 100 µl 50% MeOH.

Extraction method S uses 1.5 ml extraction buffer (49% MeOH, 49% *dd*H_2O and 2% Formic Acid) was added and the samples vortexed for 60 sec to ensure they were thoroughly mixed, then incubated on a blood rotator at 30 rpm for 1 hour at 4^oC. Samples were then centrifuged at 3000 x g for 15 minutes at 4^oC to pellet the tissue. 1 ml of supernatant removed and dried at 40^oC using a rotary evaporator until 300 µl was remaining. The samples were then frozen and dried using a freeze drier, before being re-suspended in 100 µl 50% MeOH.

3.3 Results

3.3.1 Thin Layer Chromatography (TLC)

TLC was developed as a potential rapid screening method for the detection of tropane alkaloids from bacterial assays. The TLC plate in Figure 3.3.1 shows bands stained a pink/red hue for 30µl of 10mM, 25mM and 50mM hyoscyamine hydrobromide as well as a brown band for 50mM tropinone. This level of sensitivity was estimated to be insufficient to be used in the bacterial assays which are discussed in Chapter 4. The level of sensitivity was lower than previously reported for this method (Coa *et al*, 2015), where sensitivity at 250µl of 0.2mM hyoscyamine was achieved.

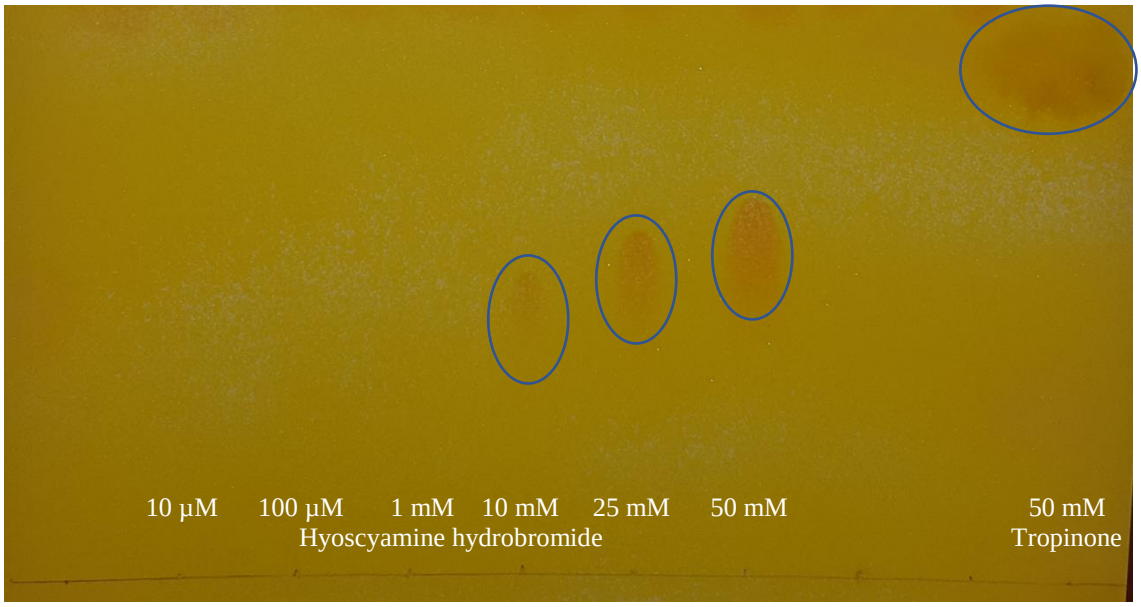

Figure 3.3.1: Alkaloid detection by TLC

TLC plate which has been sprayed with Dragendorff Munier reagent to detect various concentrations (10µM to 50mM) of hyoscyamine hydrobromide and a single concentration of tropinone (50mM). White bands have been overlaid on the figure above to indicate the leading edge of the band being detected of each visualised lane.

3.3.2 HPLC-UV

Methods for detection of tropane alkaloids using HPLC-UV were developed to overcome sensitivity issues presented by TLC. This technique was tested with the aim of providing a more sensitive determination of tropane alkaloids in samples from bacterial expression assays.

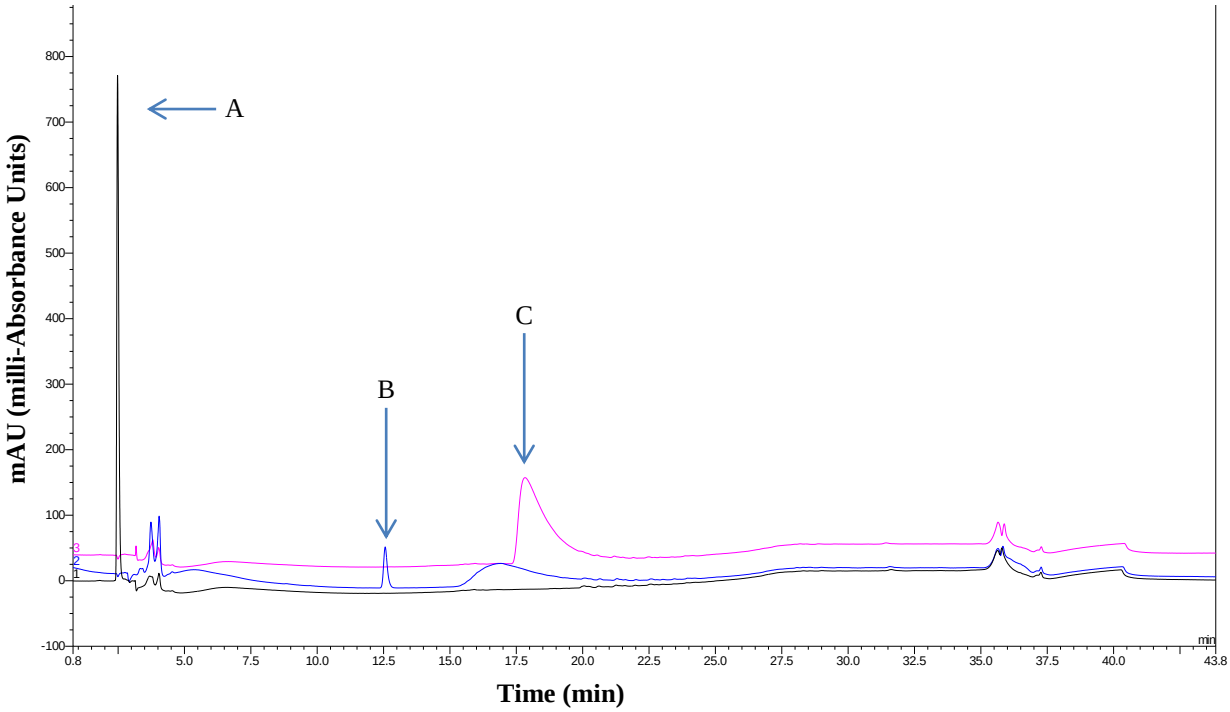

Figure 3.3.2: HPLC Chromatogram using tropane alkaloid standards

Chromatogram of metabolite standards which were used in the bacterial experiments (described in chapter 4). 5 µl of a 1 mg/ml of standard was injected with detection at 207nm, peaks for the tropane alkaloids being detected can be seen labelled, A = hyoscyamine, B = anisodamine and C = scopolamine.

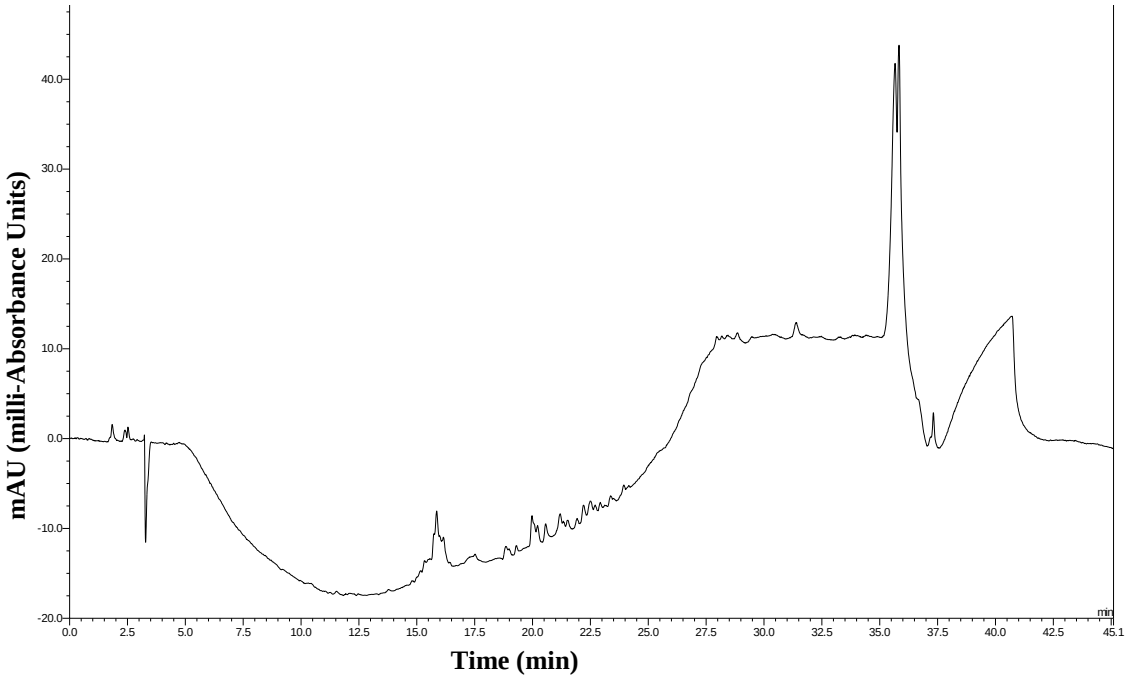

Figure 3.3.3: HPLC Chromatogram of media spiked with tropane alkaloids.

Chromatogram of LB media spiked with hyoscyamine for the detection of tropane alkaloids in the whole cell biotransformation experiments. It appears that there is masking of the hyoscyamine by the constituents of the LB media, so either Solid-Phase Extraction (SPE) or Liquid-Liquid Extraction (LLE) would be required to remove interfering compounds from these samples

Figure 3.3.2 shows an overlapped chromatogram of tropane alkaloid standards which will be under investigation in subsequent assays. The chromatogram shows that the tropane alkaloids hyoscyamine (black trace), anisodamine (blue trace) and scopolamine (pink trace) can be detected and there are peaks which are unique to each of them allowing for differentiation. Whilst the tropane alkaloids can be detected when run as standards, Figure 3.3.3 shows that there is a masking affect for media samples which have had hyoscyamine added and run under the same conditions. This indicates that the composition of the LB media which will be used in whole cell biotransformation assays (discussed in chapter 4) masks the detection of the peaks for hyoscyamine.

3.3.3 ThermoFisher Scientific's OrbiTrap™ LC-MS system

As it was clear that components of the LB media interfered with the detection of tropane alkaloids using HPLC, a system which allowed for greater sensitivity was used for the development of sample extraction and chromatography conditions. The OrbiTrap™ LC-MS/MS system was used for the elucidation of both these processes, with retention times for metabolites being shown in Table 3.3.1.

Compound	Retention Time (minutes)
Ornithine	1.61
Calystegine A_3	1.76
Tropinone	2.22
Tropine	2.35
Phenylalanine	8.73
Scopolamine	10.42
Atropine	11.45

Table 3.3.1: **Column retention times for tropane alkaloids**

Retention times for TAs and associated compounds used in method development using the OrbiTrap™ LC-MS system. A chromatogram of these compounds can be seen in Figure 3.3.4.

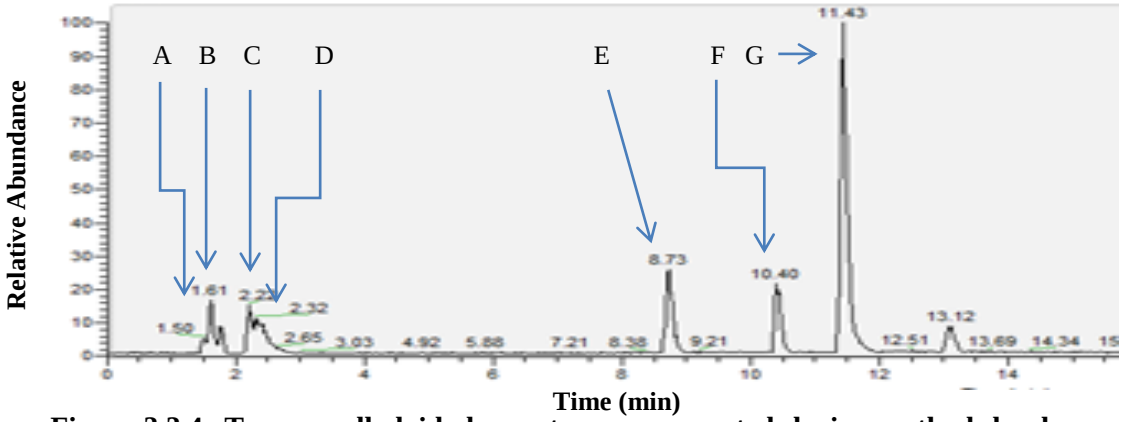

Figure 3.3.4: Tropane alkaloid chromatogram generated during method development on the OrbiTrap™.

Chromatogram of the compounds summarised in Table 3.3.1 from the OrbiTrap™. There is a clustering of the smaller molecular weight compounds (such as ornithine, tropinone and tropine) being eluted within the first three minutes, during which the mobile phase is *dd*H_2O + 0.1% formic acid (Phase A). A = ornithine, B = calystegine A3, C = tropinone, D = tropine, E = phenylalanine, F = scopolamine, G = atropine.

Within the first three minutes the clustering of the smaller molecular weight metabolites of interest indicated that they are not well retained or separated on the column compared to the relatively higher molecular weight tropane alkaloids hyoscyamine and scopolamine. Although the smaller metabolites elute relatively quickly using this method, the ability to detect them individually is not affected.

3.3.3.1 Comparison of extraction methods.

A reliable method for the extraction of tropane alkaloids from plant tissues was developed and validated. This was done through the comparison of two published extraction methods (method S described in section 2.6.2; and the method V described in Vorst *et al*, (2005)) and using the OrbiTrap™ for detection. The analysis was conducted on 100 mg extracts of *Datura stromonium* leaves and the results can be seen in Figure 3.3.5. For each metabolite, the average relative peak abundance of three injections for each *Datura* leaf sample has been given. These extraction methods show that there are significant differences in the detection of the metabolites; ornithine ($P = 0.0011$), littorine ($P = 0.0009$), phenylalanine ($P = 0.0138$) and phenylpyruvic acid ($P = 0.0038$) between the methods, with the other metabolites under initial investigation showing no significant difference in detectability. There is also no significant difference seen between the samples using method S, whereas there is between the extractions which

used the Vorst *et al* (2005) method, which are indicated in Figure 3.3.6. This shows method S is more reliable because there is less variability and in most cases comparable recoverability for the metabolites associated with the tropane alkaloid biosynthesis pathway, such as phenylalanine, showing greater stability in the extraction.

Figure 3.3.6 shows two chromatograms from a single injection of the sample 'V3'. This demonstrates that there are also other metabolites co-eluting at the same retention times as the metabolites of interest in this study. The lower chromatogram indicates the masses and the relative intensity of metabolites which are eluted from the column between ten and twelve minutes. The peaks of m/z 304.15 and 290.17 relate to atropine (hyoscyamine) and scopolamine. Due to the nature of the plant extract being analysed and the structural similarity of the higher molecular weight, more economically valuable tropane alkaloids. It can be suggested that the peak with an m/z of 306.17 probably relates to the intermediate anisodamine which has a reference mass of 305.37.

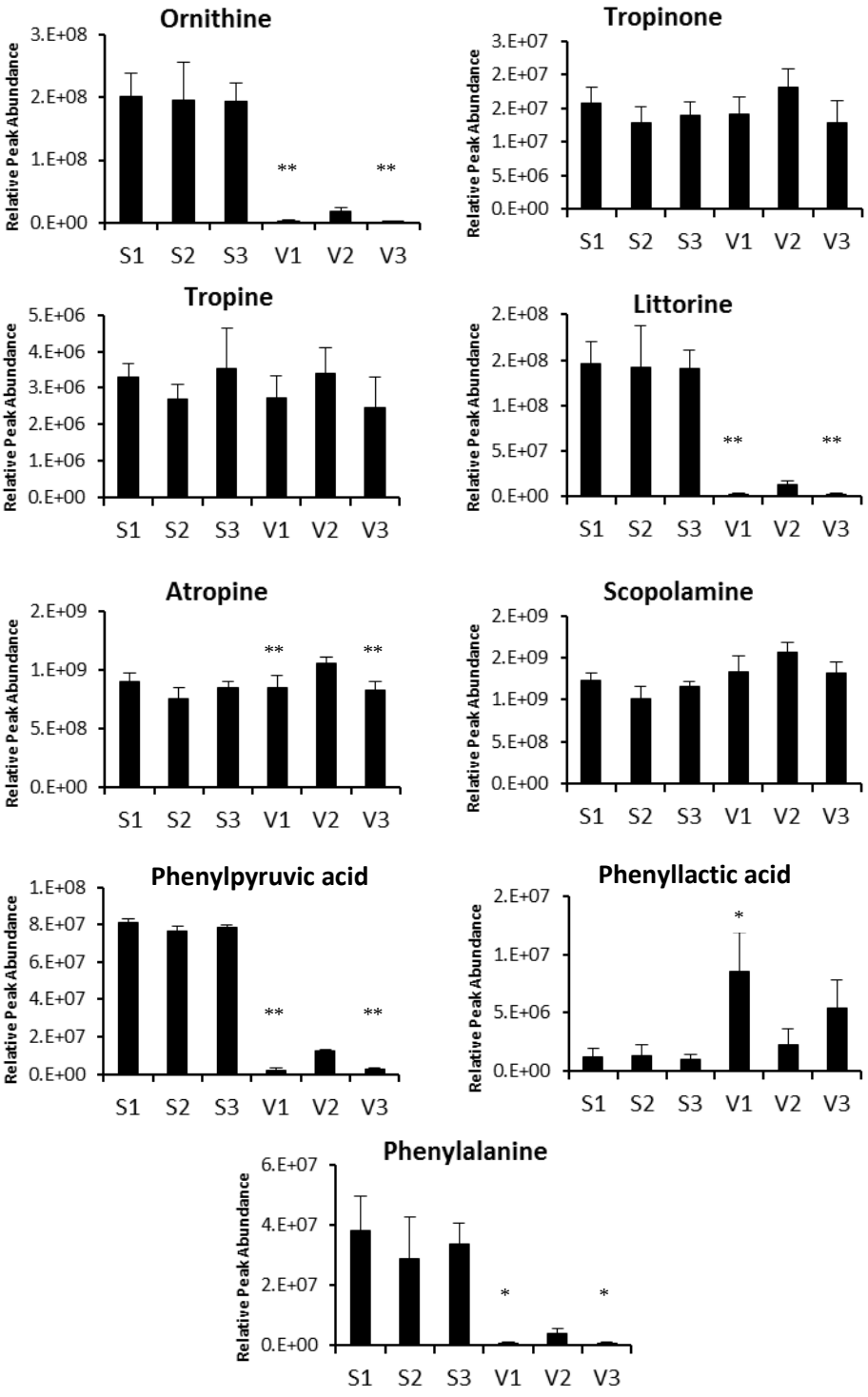

Figure 3.3.5: **Extraction methods differences on Tropane alkaloid recovery.**

Recovery of tropane alkaloids from extracts of *Datura* leaf using two different extraction methods: S = method described in 2.6.2, V = Vorst *et al*, 2005. Each bar shows the average peak area for compounds being detected from three injections of each extract. Error bars represent standard deviation between each injection (n = 3). * indicates a significant difference where $P < 0.05$, ** indicates a significant difference where $P < 0.01$ when compared to V2 injections.

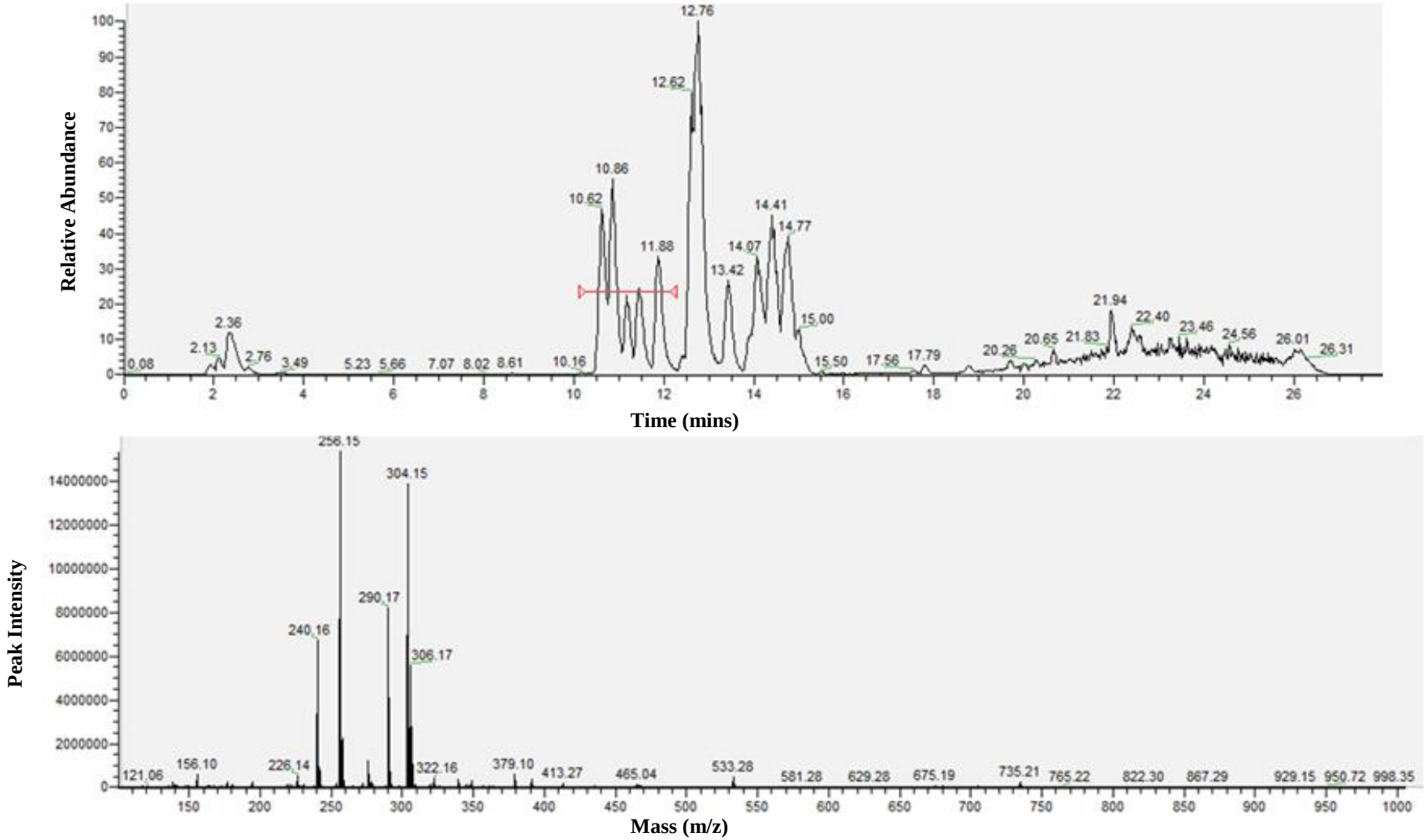

Figure 3.3.6: Chromatogram and detailed peak analysis from an extract analysed on the OrbiTrap™.

Top: Chromatogram of the compounds eluted from a single injection of a spiked sample using one of the potential extraction methods under investigation (extraction method as described in Vorst *et al*, 2005). Bottom: m/z and abundance of compounds found under the peaks highlighted by the red bar in the top chromatogram. This enables the determination of the presence or absence of compounds of interest whilst masked by others.

3.3.4 Agilent QqQ-LC-MS/MS

With chromatography for the detection of tropane alkaloids developed using the OrbiTrap™ LC-MS system a method for the quantitative detection of tropane alkaloids and associated metabolites was optimised.

Table 3.3.2 outlines the conditions to generate the product ions required for detection of each of the metabolites which are to be quantified within associated studies (Chapters 4, 5 and 6). The product ions given are the ones used in the MRM method for the detection and quantification of these metabolites, along with the fragmentation voltages and collision energies required to generate these product ions. A schematic representation of the fragmented ions produced by this process can be seen in Figure 3.3.7, where the four ions produced from scopolamine can be seen, the other metabolites undergo the same process and the masses of all fragments produced can be found in appendix A.3.2.

Once the metabolites which were to be investigated within this project had undergone optimisation using QqQ-LC-MS/MS, the linear range for quantification needed to be determined. To do this a mixture of metabolite standards was produced, serially diluted and then 5 µl of each dilution was injected in triplicate. This process was required to validate the MRM to be used in subsequent analysis. These were subsequently tested using both *Datura* leaf and potato tuber sprouts, and the results of this assay can be seen in Figure 3.3.8.

Metabolite	Retention Time (mins)	Mass (m/z^{+1})	Product Ions	Fragmentation Voltage (V)	Collision Energy (eV)
Ornithine	1.75	133.10	116.10	83	4
			70.10		16
Tropinone	2.65	140.10	82.10	121	20
			56.10		48
Pseudotropine	2.71	141.10	96.10	102	20
			124.10		16
Calystegine A3	1.98	160.10	142.10	98	8
			79.10		20
Calystegine B2	1.89	176.10	158.10	89	4
			140.10		8
Tropine	2.71	142.10	98.10	136	24
			58.20		28
Littorine	15.95	290.20	93.10	141	32
			142.10		28
Hyoscyamine	15.71	290.20	124.10	131	24
			77.10		68
Anisodamine	14.85	306.20	140.10	121	24
			77.10		80
Scopolamine	14.44	304.20	156.10	121	12
			138.10		12
Reserpine (ITSD)	19.51	609.30	195.10	250	41
			174.10		45

Table 3.3.2: **Tropane alkaloids ions optimised for the QqQ-LC-MS/MS.**

List of parent and fragment ions for metabolites from the tropane alkaloids biosynthesis pathway under investigation and used in the MRM. Also included are the fragmentation voltages and collision energies used to generate the observed fragment ions. See A.3.2 or a complete list of all fragments produced for each metabolite of interest.

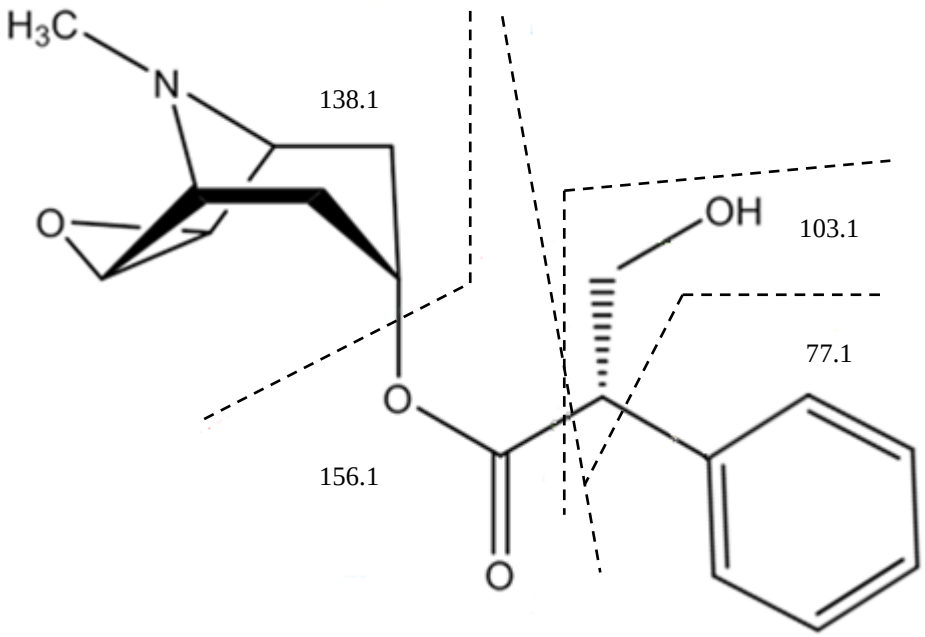

Figure 3.3.7: Fragmentation of scopolamine.

Schematic representation of the one of the tropane alkaloids, scopolamine showing the fragments produced by the QqQ-LC-MS/MS as well as their respective masses.

Metabolite	Slope	Intercept	R^2
Ornithine	5646.89	334.42	0.99
Labelled Ornithine	11531.99	877.38	1.00
Tropinone	22721.94	28682.47	0.99
Calystegine A3	14950.69	-7138.12	0.99
Tropine	30626.44	16584.28	0.98
Phenylalanine	107562.83	10163.79	1.00
Littorine	55695.74	36461.28	0.99
Hyoscyamine	150563.81	94885.50	0.99
Anisodamine	58827.89	47832.83	0.99
Scopolamine	64568.69	56966.47	0.99

Table 3.3.3: Generated standard curve data for metabolites under investigation.

Slope, Intercept and Linear Correlation of metabolites during the MRM method development.

Table 3.3.3 shows the standard curve data produced for the MRM being used in this study. These are a result of the injections of a metabolite mixture at eight concentrations from 0.01 to 20 ppm. The linear correlations are within an acceptable range for the metabolites to be detected across this broad concentration range.

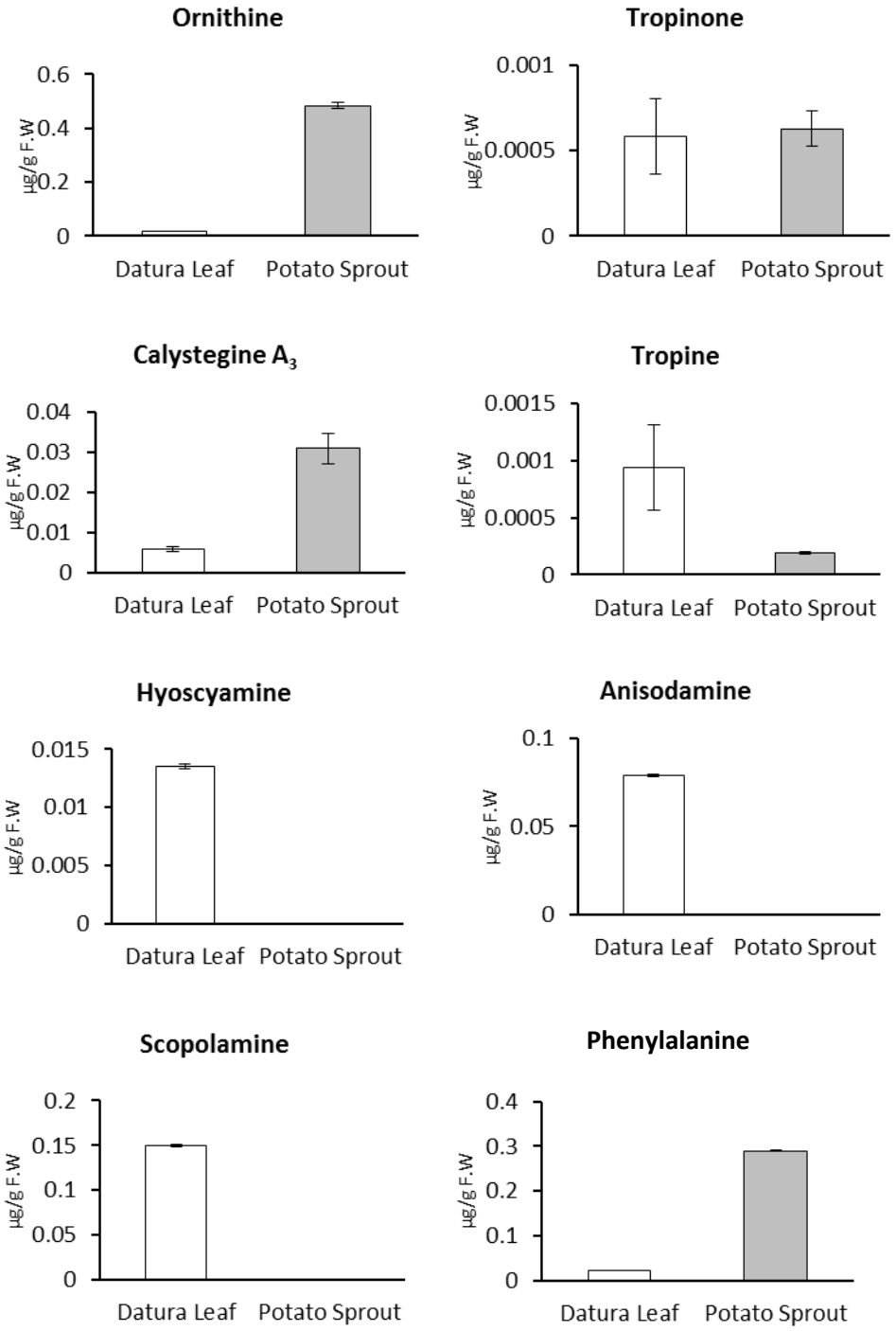

Figure 3.3.8: Multiple Reaction Monitoring metabolite detection

Detection of metabolites of interest from freeze dried *Datura* leaf and *Solanum tuberosum* cultivar *Desiree* sprout, using an MRM with most of the metabolites of interest from the tropane alkaloids biosynthesis pathway. This is a single sample for each which has undergone two injections, with the error between these injections being shown (technical replicates, n = 2).

Whilst initially suggested for the removal of interfering compound from the LB media of planned bacterial expression assays, the possibility that samples may need to undergo LLE (Liquid-Liquid Extraction) purification was investigated using *Datura* leaf and *Solanum tuberosum* tuber sprouts. Figure 3.3.9 A and B shows the effects of sample clean up after using the EXtrelut® NT-1 columns, when run on the Agilent QqQ-LC-MS/MS. Samples underwent this LLE clean-up technique to determine if metabolites which could interfere with the detection of the tropane alkaloids being investigated are able to be removed and then the tropane alkaloids can be concentrated prior to undergoing detection. There are both *Datura* leaf and *Solanum tuberosum* samples which have and have not undergone LLE on the EXtrelut® NT-1 column. The samples which were to undergo LLE purification had exogenous atropine added to them to determine if there was retention on the column for this tropane alkaloid. Within the *Datura* leaf sample (Figure 3.3.9, A), there is a clear elevated level of hyoscyamine from the sample which underwent LLE, however, there are no other tropane alkaloids present in a comparable level to the sample which did not undergo LLE. In Figure 3.3.9 B, the comparison from *Solanum tuberosum* sprout tissue indicates that the precursors to the tropane alkaloids biosynthesis pathway and the endogenous metabolites of the nortropane alkaloids pathway are present in higher levels within the sample which has not undergone the LLE protocol. The levels of hyoscyamine retained were also lower within the sprout sample which underwent the LLE, compared to the *Datura* sample; however, this could be due to the presence of endogenous atropine within *Datura.*

Figure 3.3.9 also shows that without any manipulation to the tropane and nortropane alkaloid pathway the metabolites prior to the tropinone branch point are detectable in *Solanum tuberosum* sprout tissue, whereas, in *Datura* leaf samples the metabolites from both the tropane and nortropane biosynthesis pathways are detectable. Appendix table 3.3 (A.3.3) gives a numerical representation for the results displayed in Figure 3.3.9 as some of the values are too small to visualise.

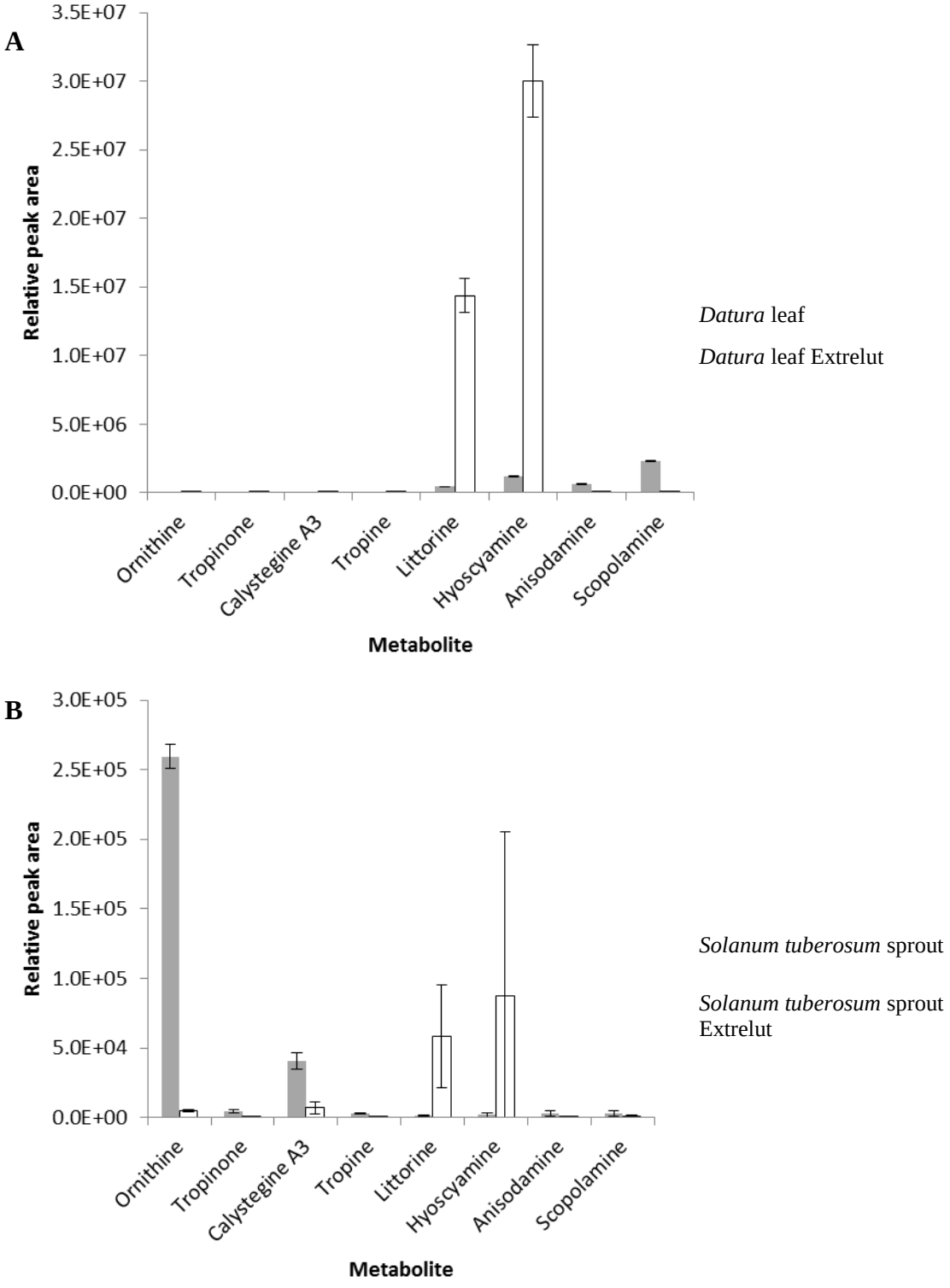

Figure 3.3.9: Effects of LLE on metabolite recovery.

Comparison of peak areas from *Datura* leaf (A) and *Solanum tuberosum* cultivar *Desiree* sprout (B) samples run on the QqQ-LC-MS/MS. Samples highlighted by ■ have not undergone LLE, whilst those denoted by □ have undergone LLE on the EXtrelut® NT-1 columns. Samples which underwent LLE had exogenous atropine applied to determine the recovery of this compound after clean up. There is an indication that whilst atropine is able to be recovered in both the *Datura* and potato samples, the further downstream metabolites such as scopolamine in the *Datura* sample do not appear to be as well detected in the samples which underwent LLE.

3.4 Discussion

The development of a rapid method for the detection of tropane and nortropane alkaloids from bacterial recombinant protein and transgenic assays was necessary. This would allow for high sample through-put, whilst reducing the demand upon the LC-MS facility. Previously, Dräger (1995 and 2002), Keiner and Dräger (1999) and Kokotkiewicz *et al*, (2017) have suggested that TLC is a suitable tool for this rapid screening; however it was found that the sensitivity achieved was unsuitable for the requirements of the planned assays within this study. The detection of metabolites of interest was conducted to a low concentration, however, to achieve a comparable level of sensitivity to Keiner and Dräger (1999) and Kokotkiewicz *et al*, (2017), a 500 µl loading of 0.1mM of hyoscyamine would needed to have been applied and detected on the TLC plate. This leads to technical difficulties, as the ability to efficiently spot this volume would not have been able to be conducted easily, nor would using a more concentrated sample preparation to reduce the required volume. Although this technique should be able to be optimisable, limitations with not knowing concentrations of tropane alkaloids potenitally produced in assays this technique could be applied too, and the availablilty of equipment with greater sensistivity means that for the purposes of the project this technique was not followed up on.

Similarly, the masking of compounds seen in Figure 3.3.3, by the LB media in samples run on the HPLC-UV indicated that a clean-up protocol needed to be considered if the HPLC-UV was to be used. The purification of samples by LLE was examined and tested on samples run on the Agilent QqQ-LC-MS-MS system and is discussed further below. To overcome the issues which were presented from the TLC and HPLC-UV, the development of detection methods which allowed for greater sensitivity and metabolite selection were undertaken.

The OrbiTrap™ offered greater qualitative sensitivity, as it was able to give an indication of the presence of, and accurate mass values for metabolites within a sample. Whilst being able to give accurate mass readings, if there are metabolites within a sample which had no reference mass size, the OrbiTrap™ is able to fragment these unknown metabolites. Then based on the fragmentation size and pattern of the unknown peaks chemical formulae can be suggested, to later check against reference standards. These suggested formulae are then able to be screened against suspected metabolites

and then checked against a reference standard, which should give the same peak and retention time. This is one of the unique features of this detection apparatus and allows it to stand out as a highly accurate investigative tool for use in manipulated pathway interactions. However, whilst the OrbiTrap™ allows for an accurate qualitative determination of alterations to metabolomic pathways, the QqQ-LC-MS/MS system can give greater quantification to the same samples.

Metabolites which have been optimised from the tropane alkaloid biosynthesis pathway using the QqQ-LC-MS/MS within this study, give parent and fragment ions for the high value tropane alkaloids which are consistent with the recently published ions generated in Chen *et al*, (2017) and Zhou *et al*, (2017) as described in Table 3.1.1, and A.3.2. The overlap in these ions indicates that although different systems were being used, the reproducibility of the product ions produced by CID was as expected. With this information, there is confidence that the product ions which are given for the other metabolites along the biosynthetic pathway will be able to be replicated. Therefore the quantitative and robust method for known and expected metabolites along the biosynthetic pathway suggests that the QqQ-LC-MS/MS system was of more use due to the quantifiable nature of the data provided and the high accuracy and specificity that the system is able to provide.

Whilst moving towards detection apparatus which exhibit greater sensitivity, the development of suitable extraction and running methods for use on the OrbiTrap and the QqQ-LC-MS/MS systems was required and accomplished with the adaptation of previously published methods. Once the chemistry and packing material of the chromatographic column to be used in the separation of tropane and nortropane alkaloids in this study was selected, the chromatographic method could be developed.

The method used was adapted to the column, as retention and separation of metabolites within the column is affected by the solvents and gradients used. The final separation method, as described in 2.5.3.5, was adapted from Jakabova *et al*, (2012), with the formic acid concentration being reduced from 1% to 0.1% (v/v), as well as mobile phase A being held at 100% for the first three minutes. A reduction in formic acid was applied to the mobile phases so as to reduce the interactions between the formic acid and the calystegines. This change was found to have a positive effect on the detection of the calystegines. Mobile phase A was held for three minutes to allow the

smaller metabolites under investigation to be eluted from the column with some separation occurring, whereas, if a gradient of methanol mobile phase was used, these small metabolites eluted with the column breakthrough.

A change in the gradient phase through an extension from three to seventeen minutes was implemented so that 100% mobile phase B is reached over fourteen minutes compared to the ten minutes in the Jakabova *et al* (2012) study. This extension was applied to increase the methanol concentration within the column more slowly which allowed for greater separation of the tropane alkaloids hyoscyamine, anisodamine and scopolamine. Whereas in Jakabova *et al*, (2012) where 90% mobile phase B is the highest level of methanol, 100% was used in this study with an extended plateau at this stage, ensuring that the retained metabolites are eluted off the column in between samples. In the method developed for the LC-MS/MS systems, the plateau of 100% phase B is for only five minutes, before the phases are returned to 100% A over one minutes, for a further six minute period, ensuring the column has been re-equilibrated for the next sample injection.

The adaptation in the running method was required, as stated for the lower molecular weight metabolites, such as ornithine, tropine, pseudotropine and the calystegines, but also due to initial uncertainty as to the interaction of hyoscyamine, anisodamine and scopolamine with the column. In the study conducted by Jakabova *et a*l, (2012) the separation and detection of atropine and scopolamine was investigated, giving an indication of the retention times expected for these metabolites. Figure 3.3.4 shows that there is clear separation for the tropane alkaloids hyoscyamine, anisodamine and scopolamine, yet the lower molecular weight precursors and nortropane alkaloids can be detected but not separated. Whilst there is this co-elution of lower weight metabolites, there is no detrimental effect on the detection and quantification of these products in the MRM which has been developed.

The method for extraction of metabolites from the tropane alkaloid biosynthetic pathway was required to recover metabolites from plant material with a high efficiency. There are numerous methods described for metabolite extraction (Keiner and Dräger, 2000; Vorst *et al*, 2005 and Jakabova *et a*l, 2012) and in some cases metabolite detection is conducted by GC-MS. From the two methods which were trialled in this project, method S, (as described in 2.6.2) is overall more effective in extracting the

lower molecular weight metabolites of interest as well as not showing any significant difference in extraction and recoverability of the higher molecular weight (and more economically important) tropane alkaloids. The ability to extract the early, low molecular weight metabolites was important in the development of the extraction method as this is the area of the biosynthetic pathway which is predicted to see the greatest effect in transgenic work to be undertaken. Whilst there was no significant difference in the extractability of the higher molecular weight tropane alkaloids between method S and the method described in Vorst *et al*, (2005) the lower molecular weight metabolite and pathway precursor ornithine and tropane alkaloid intermediate littorine were retained and detected significantly better from extracts using method S (P values <0.01 and <0.001 respectively (n=3)). This can be seen in Figure 3.3.5 where the relative peak abundance for each of the metabolites is shown. For the metabolites extracted using method S there was no significant difference between each of the 3 extracts tested, whereas for metabolites extracted using the Vorst method, there were significant differences shown between extracts V1 and V3 when they were compared to extract V2 for the metabolites littorine, ornithine, phenylpyruvic acid and atropine (racemic hyoscyamine) (P <0.01), and phenylalanine and phenyllactic acid (P <0.05). Method S and the method described by Vorst *et al* (2005), differ with respect to solvent used with 1:1 methanol:H_2O (v/v) with no formic acid in S, compared to 62.5:37.5 (v/v) with 0.125% formic acid in Vorst *et al*, (2005). This difference in ornithine recovery is in agreement with the findings of Friedman *et al*, (2003) who suggest that non-acidified buffers are better suited for the nortropane alkaloids, which are lower in molecular weight compared to tropane alkaloids. It has been shown that the non-acidified buffer used in method S, did not have any detrimental effect on tropane alkaloid recovery.

To understand the differences between the two extraction methods trialled and the variability within the samples, during the extraction method development (Figure 3.3.5), the addition of a known quantity of metabolite and the recovery of this from the sample would be a useful tool. These, however, were not undertaken in the development of the extraction protocol, due to machine time constraints, but will be discussed due to the use through determining if LLE purification is suitable.

The LLE purification protocol which has been trialled in this method development was previously described as successful by Richter *et al*, (2007). However, more recently Sramska *et al*, (2017) found that less than half the initial spiked amount

of hyoscyamine was retained and recovered from the purification columns in the studies they undertook. This shows similarity to the results which are indicated in Figure 3.3.9, in particular the differences between the detectability of the high value tropane alkaloids in the *Datura* samples which have undergone LLE and those that have not. Having followed the protocol in Richter *et al,* (2007) it was unclear as to why similar results were not seen, this lead to the belief that the characteristics of the column had changed in the time between the two studies. Through personal communication with a representative of Merck Millipore Technical Services, it was confirmed that the packing material of the EXtrelut® columns had changed after the assays were undertaken by Richter *et al*, and prior to the work in this study and the assays of Sramska *et al* being conducted. Therefore the LLE purification method hoped to be utilised for plant and bacterial samples was no longer suitable for this study.

A single 100mg sample of *Datura stromonium* leaf and potato sprout was extracted using method S and run on the QqQ-LC-MS/MS to determine if the metabolites along the tropane alkaloid and nortropane alkaloid biosynthesis pathway could be detected from both sources within the MRM developed. Figure 3.3.8 shows that whilst there is variation between the two samples with regards the concentration of individual metabolites this can be explained through the tissues which have been extracted. *Datura* leaf is not the site of tropane alkaloid biosynthesis (Hashimoto *et al,* 1986), however the leaves are the storage sites for the alkaloids, so the reduced levels of ornithine, calystegine and increased tropane alkaloids compared to the potato sprout where the nortropane alkaloid biosynthesis pathway is active, indicative of the higher calystegine level. Although this experimental data set is extremely small with only a single extraction and two injections into the machine it highlights that the metabolites along the tropane alkaloid and nortropane alkaloid pathway are able to be detected from different tissue types and the extraction method is suitable for these compounds.

3.4 Moving forward

With the development of a robust and repeatable extraction and detection method for the Agilent QqQ-LC-MS/MS, there is confidence in the ability to discern any metabolite changes to the tropane alkaloid biosynthetic pathway in transgenic lines being produced and any tropane alkaloid conversion during recombinant protein assays.

If this study was repeated and to increase the throughput of screening assays, the development of spectrophotometric techniques could be an advancement. Utilising a spectrophotometric plate reader, multiple samples could be read in tandem and in replication, thus discerning any tropane alkaloid changes within them. These samples could then be followed up using the more sensitive QqQ-LC-MS/MS technique for determination of individual metabolite content.

Chapter 4: Functional characterisation of a candidate gene encoding *hyoscyamine-6β-hydroxylase* from potato

4.1 Introduction

It is known that there is a lesion in the tropane alkaloid biosynthesis pathway at the tropinone branch point within potato, due to the limited expression and/or enzyme activity of trI (Keiner and Dräger, 1999). However, there is little understanding as to the presence and functionality of any downstream genes which are responsible for the production of high value tropane alkaloids. The purpose of the work described in this Chapter is to investigate if any of these downstream genes are present within the potato genome and elucidate any functionality, which may be present, whilst also ensuring that a limited MRM detection method which was developed in Chapter 3 can be applied to bacterial assays.

In members of the Solanaceae which produce the high value tropane alkaloids hyoscyamine and scopolamine, *littorine mutase/monoxygenase (cyp80f1)* and *hyoscyamine-6β-hydroxylase* (*h6h*) are known to be expressed in the cells of the root pericycle. Expression and conversion of hyoscyamine to scopolamine has also been reported in cultured cells of *Datura stramonium*, leaves of *Hyoscyamus muticus* and shoots of *Datura metel* (Pramod *et al*, 2010a) suggesting that the h6h enzyme is functional in these tissues and alkaloid biosynthesis can occur. Functional expression analysis of *h6h* has been undertaken in a number of solanaceous species such as *Hyoscyamus niger* (Rocha *et al*, 2002), *Datura metel* (Pramod *et al*, 2010b), *Anisodus tanguticus* (Liu *et al*, 2005) and *Atropa belladonna* (Li *et al*, 2012). The formation of hyoscyamine requires the re-arrangement of littorine, and this is catalysed by a cytochrome P450; cyp80f1 (Li *et al*, 2006). cyp80f1 activity results in the formation of hyoscyamine aldehyde which is then reduced via an alcohol dehydrogenase to form hyoscyamine

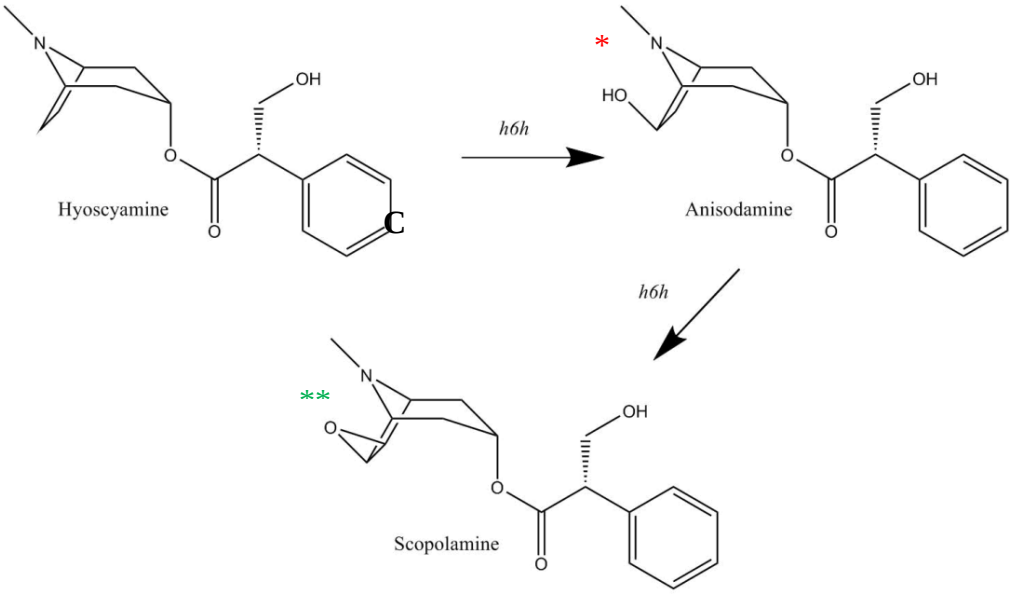

Figure 4.1.1: Conversion of hyoscyamine to scopolamine by h6h.

Schematic representation of the conversion of hyoscyamine (A) through the intermediate anisodamine (B) to the final high value tropane alkaloid scopolamine (C). h6h catalyses the introduction of a 6β-hydroxyl group onto the tropane ring (indicated by the *), with h6h then closing and forming an epoxide ring through the removal of the hydrogen atoms at C7 and on the introduced hydroxyl group (denoted by the **) (Humphrey and O'Hagan, 2001).

To assess the functionality of annotated *h6h* genes from *Brugmansia candida* and *Anisodus actuangulus*, recombinant protein expression assays have been developed (Cardillo *et al*, 2017; Coa *et al*, 2015). This has been shown to be a useful tool in the determination of protein functionality and in some cases conversion through whole cell biotransformation assays has yielded the downstream tropane alkaloids; anisodamine and scopolamine. Cardillo *et al,* (2017) have shown that conversion to anisodamine and scopolamine can occur in the presence and absence of co-factors (such as sodium ascorbate and 2-oxoglutarate) but the percentages of substrate conversion are remarkably different. Utilising the *h6h* cDNA sequence from *Brugmansia candida* and in the presence of co-factors, 82.16 ± 5.28 % hyoscyamine was converted to anisodamine and 12.82 ± 4.28 % to scopolamine, whereas in the absence of these co-factors conversion was 5.22 ± 0.18 % and 0.67 ± 0.39 % respectively after 25 hours. Coa *et al,* (2015) also demonstrated that *E. coli* expressing a S14P/K97A mutant of *Anisodus actuangulus* h6h yielded 100 % hyoscyamine conversion to scopolamine after 48 hours, when compared to *E. coli* cells which expressed the wild type *Anisodus acutangulus h6h* gene, only 75 % was converted to the intermediate anisodamine and

the remaining 25 % to scopolamine. S14P/K97A *Aa*h6h mutants have mutations at the Ser14 and Lys97 amino acids, which are conserved within h6h of solanaceae members. Although these amino acids are outside the binding regions for co-factors and substrates, it is speculated that changes in these regions can have an effect on enzyme activity through interactions with other residues resulting in changes in enzyme conformation (Coa *et al*, 2015).

Using the recombinant h6h protein from *Atropa belladonna* in functional assays, Li *et al*, (2012) demonstrated that the affinity for *Ab*h6h to hydroxylate hyoscyamine is lower than that of other tropane alkaloid producing species such as *Hyoscyamus niger* and *Anisodus tanguticus*. The K_m values for the h6h proteins assayed were 52.1 ± 11.5 µM *(Ab*h6h*)*, 35 µM (*Hn*h6h) and 15.1 ± 0.3 µM (*At*h6h). As well as *Ab*h6h exhibiting a lower affinity for hysocamine in the hydroxylation step, the K_m and V_{max} values for the epoxidation step of the reaction (the formation of scopolamine from anisodamine) indicate that *Ab*h6h is not as efficient as the h6h from the other sources. The V_{max} value for the epoxidation step was 0.1% that of the V_{max} for the hyoscyamine hydroxylation step. Li *et al*, (2012) concluded from this that the epoxidation step is slower than the hydroxylation step within *Atropa belladonna*, but it is not known if this is universal across TA producing species for this part of the pathway.

Enhancement of tropane alkaloid production in members of the solanaceae has also been achieved through the overexpression of *h6h*. *Duboisia* hybrid hairy root cultures were shown to exhibit an increase in the content of scopolamine present from 74.3 and 74.9 % in control lines to between 76.0 and 89.7 % in transformed overexpression lines (Palazon *et al*, 2003). Rahman *et al*, (2006) overexpressed *h6h* in hairy root cultures of the non-hybrid, *Duboisia leichhardtii* and observed scopolamine production rates of 38.2 mg l^{-1} after 6 weeks growth using an initial 9 mg of fresh roots, but when using a *Duboisia* hybrid (similar to that of the Palazon *et al* study), 74.5 mg/l scopolamine was produced after 4 weeks and with 100 mg fresh roots. Rahman *et al*, (2006) also noted that dramatic increases in scopolamine production rates were seen when combining *h6h* with *putrescine N-methyltransferase* (*pmt*) and this yielded 411.2 mg/l scopolamine from *Hyoscyamus niger* root cultures. This suggests that exogenous expression of *h6h* and associated genes may have a greater enhancement effect for increasing the production of high value tropane alkaloids from current production sources.

The potato, *Solanum tuberosum* as discussed in Chapter 1, does not produce high value tropane alkaloids, such as hyoscyamine and scopolamine, due in part to the aforementioned lesion at the tropinone branch point. However, in wild potato species there has been shown to be homology between 2-oxoglutarate-dependent dioxygenases within the species *Solanum chacoense* Bitt. and *h6h* from *Hyoscyamus niger* (60 % similarity and 44% amino acid identity) (Lantin *et al*, 1999). As h6h is a 2-oxogluterate-dependent enzyme (Kanegae *et al*, 1994) like the dioxygenase found in the wild potato species, it is possible that the *Solanum tuberosum* genome may hold orthologues of *h6h*, but the reaction products are not detected because of a lack of substrate being produced, due to the trI lesion. Through the process of wounding as well as plant defence response elicitors the expression of an h6h-like protein was induced within potato (Nakane *et al*, 2003), suggesting that *h6h* orthologues are present within the potato genome.

This study will, in the first instance, search the potato genome for *h6h* orthologues, and then attempt to synthesise, express and determine functionality of these through whole cell biotransformation assays. This will allow us to determine if they are functional or if they represent another lesion along the tropane alkaloid biosynthesis pathway. *In planta* functional assays will be undertaken in parallel to determine if there is any endogenous activity.

4.2 Materials and Methods

4.2.1 Generation and characterisation of h6h recombinant plasmids

Figures 4.2.1, 4.2.2 and 4.2.3 detail the process of generating plasmids capable of producing recombinant h6h proteins through the pET-28a^{+} expression vectos.

4.2.2 Biological Replication

Bacterial transformation assays for each temperature and construct were carried out in triplicate (n = 3). For the hyosycamine plate feeding assay on *Solanum tuberosum* cultivar *Désirée* plantlets, replication occurred with n = 3 for control plantlets and plantlets with roots, and n = 4 for plantlets which did not have roots.

Figure 4.2.1: Translated *Sth6h*_A amino acid sequence in pET-28a$^+$

Translated pET-28a$^+$ *St*h6h_A sequence within the final plasmid. The red line denotes the histidine tag residues and the black line indicates the *St*h6h_A start codon. Sequence analysis was conducted to ensure that the h6h was in the correct reading frame within the plasmid. Figure produced using the online software ExPASy translate (www.expasy.org/translate/)

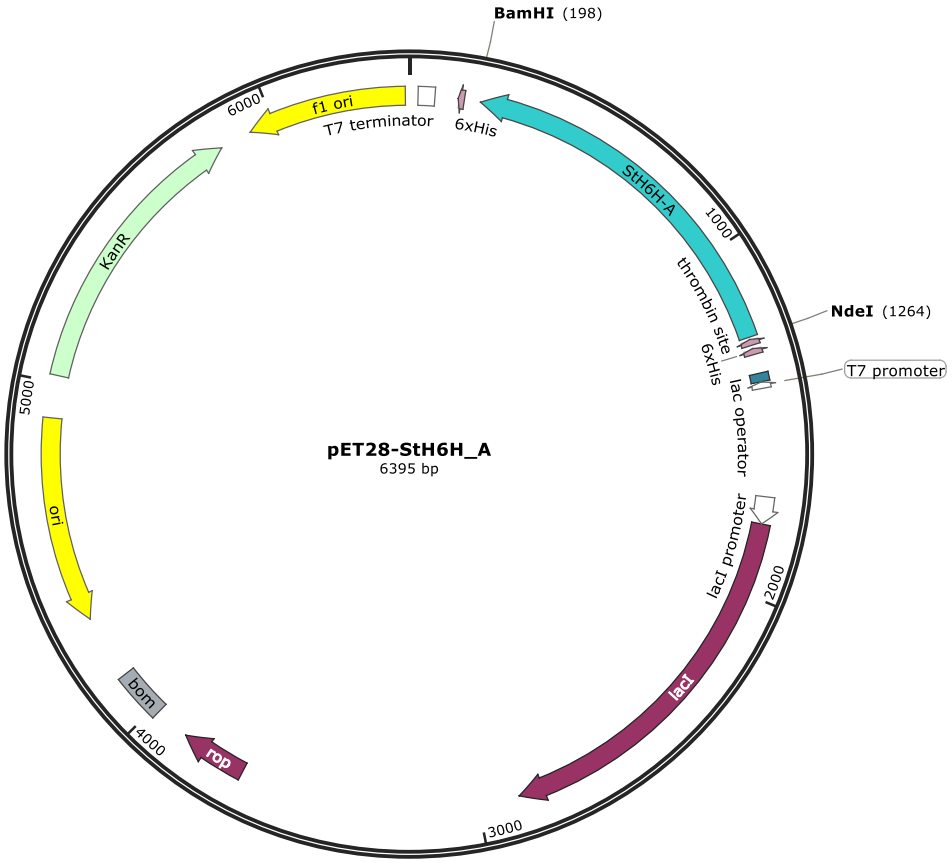

Figure 4.2.2: Diagram of the completed pET28a^{+}-Sth6h_A vector.

The BamHI/NdeI restriction endonuclease digestion sites are shown on the diagram and yield a 1066 and 5329 base fragments, as can be seen in figure 4.2.6. Vector maps generated using SnapGene ® Viewer 3.2.1

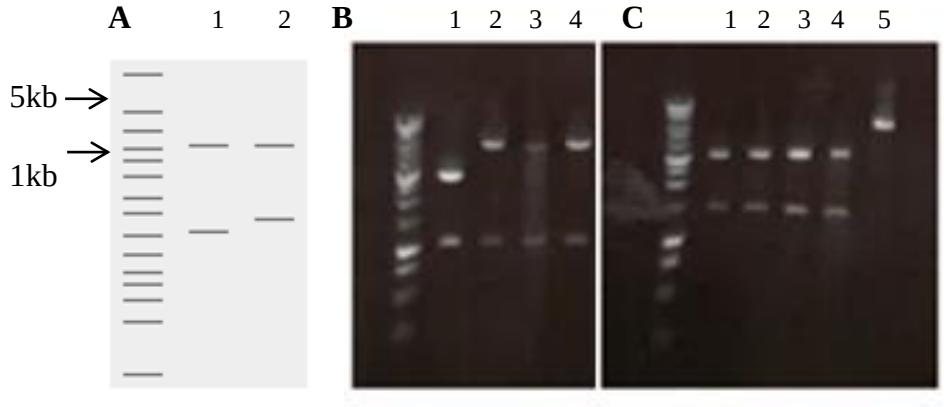

Figure 4.2.3: Virtual and enzymatic digestion of pET-28a+ vectors

A: Virtual digestion map showing the expected band sizes for two of the pET-28a^{+} h6h plasmids (lane 1 = pET-28a^{+} *St*h6h_A; lane 2 = pET-28a^{+} *Ds*h6h), produced using the online software Benchling (www.benchling.com). B: BamHI/NdeI restriction endonuclease digestion of pET-28a^{+} *St*h6h_A (lane 1 = pGEM-T_Sth6h_A, lane 2/3/4 = pET-28a^{+} *St*h6h_A) C: EcoRI/NheI restriction endonuclease digestion of pET-28a^{+} *Ds*h6h with respective controls (lane 1/2/3/4 = pET-28a^{+} *Ds*h6h, lane 5 = pET-28a^{+} control).

4.3 Results

Using a keyword search within the potato genome browser (www.SpudDB.com) for ‘hyoscyamine’ two sequences were returned with high similarity to the h6h sequence of tropane alkaloid producing species. These sequences were PGSC0003DMT400070444 (NCBI Gene Accession number: XM_006340300.2) and PGSC0003DMT400069454 (NCBI Gene Accession number: XM_006352681.2) and will be respectively referred to as *Sth6h*_A and *Sth6h*_B through the rest of this work. To ensure that the sequences returned via SpudDB from potato were homologous to bonafide *h6h* sequences from tropane alkaloid producers; these sequences underwent BLASTp analysis within the NCBI. With these genes identified within the potato genome, a phylogenetic analysis was conducted against species which are known producers of TAs and it can be seen that there is a close relationship with the sequences from potato and *Hyoscyamus aureus* for *Sth6h*_A and *Datura inoxia* and *Duboisia* for *Sth6h*_B, shown in Figure 4.3.1.

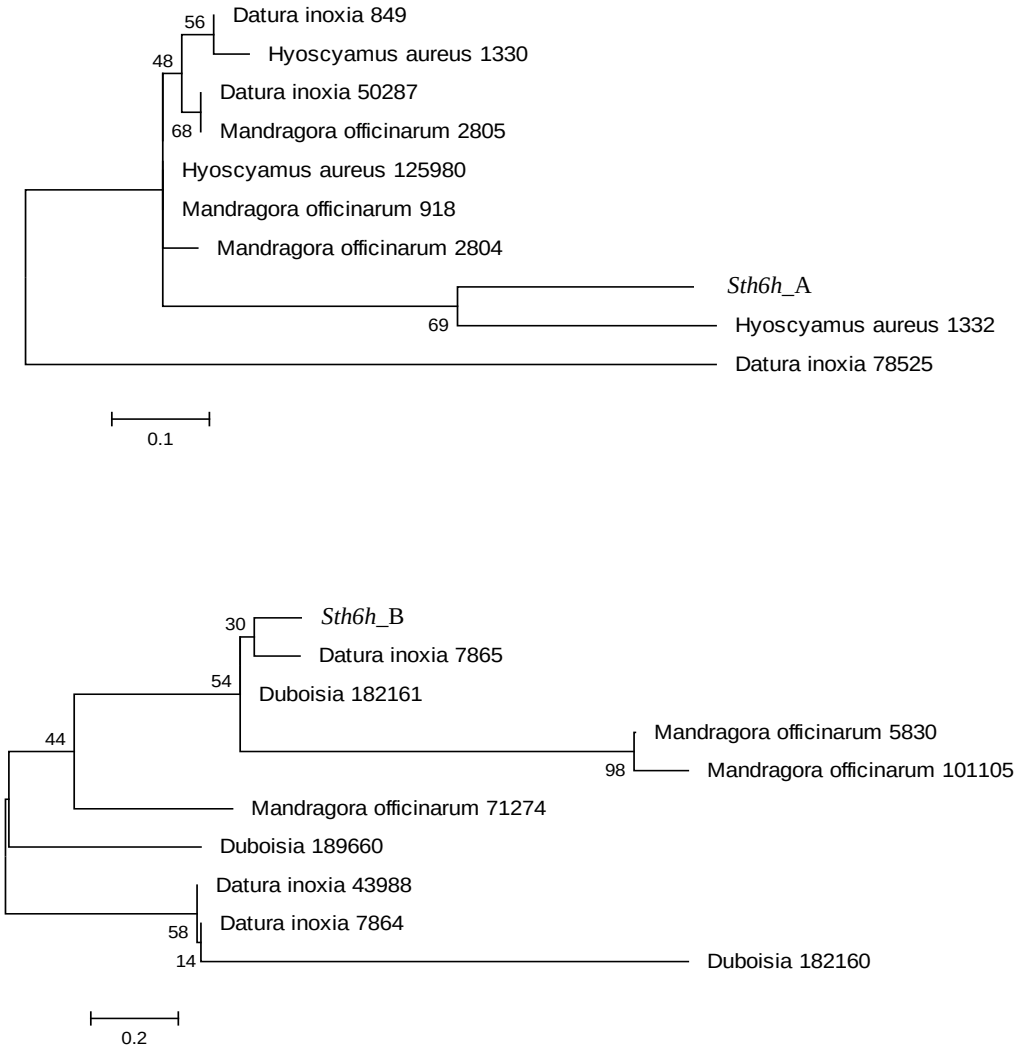

Figure 4.3.1: Phylogentic relationships between *h6h* from potato and tropane alkaloid producers.

Phylogenetic relationships between *Sth6h*_A in panel A, and *Sth6h*_B in panel B compared to nucleotide contigs of *h6h* genes from tropane alkaloid producing species. These contigs have been generated from a $BLAST_n$ analysis by Daniel Schlesinger (ARO, Israel), with the trees produced with MEGA6 using Maximum Likelihood method with 1000 replications.

The phylogenetic relationships and coding sequence similarities (shown in Figure 4.3.2) between the two *h6h* genes from potato and tropane alkaloid producing species suggest that there is potential for the potato *h6h* genes to share h6h activity. The regions highlighted for both the Fe^{2+} and 2-oxogluterate substrate binding domains are the areas which are important for the catalytic activity of the enzyme (Jaber-Vazdekis *et al*, 2009 and Dehghan *et al*, 2013). This analysis stimulated further studies to understand how well these potato orthologues are expressed within potato tissue. Interestingly, there is 93% sequence similarity between the *Sth6h*_A and the predicted *h6h* sequence from *Solanum lycopersicum* (XM_004527798.2).

qRT-PCR analysis showed that the expression profiles for these two *h6h* potato orthologues varied across growth stages of *Solanum tuberosum* cultivar *Désirée* from both leaf and root tissues. These genes were both highly expressed in root tissue (Figure 4.3.3.A) compared to leaf at all time points (Figure 4.3.3.B), correlating with the site of tropane alkaloid biosynthesis in plant species which produce tropane alkaloids (Hashimoto *et al,* 1991). The error bars for the two *Sth6h* genes analysed in both tissues show large variation at certain time points. In the samples from roots, large error bars appear during the Tuber Initiation stages (T.I I and T.I II). In leaf tissue, the largest error bars can be seen in the Vegitative Growth stage III (V.G III). The size of the error bars in both cases, could be caused by a number of reasons such as; the quality of the extracted RNA used in the assays; physiological changes within the tissues at the time of harvest and extraction or there are inhibitory factors within the reaction mixtures from cDNA synthesis through to the qRT-PCR.

As these genes are expressed *in planta*, functional analysis was undertaken. The cDNA representing these genes were cloned from potato root and ligated into the recombinant protein expression vector pET-28a^{+} (Chapter 2.2.2) with *h6h* from *Datura stromonium* being used as a positive control in downstream assays. Figure 4.3.4, shows that after protein induction with 1 mM IPTG, there was production of the histidine tagged recombinant h6h protein. The signal seen in Figure 4.3.4 is of the chemiluminescent detection solution working against the secondary antibody. This indicates that the h6h protein from all sources was induced and expressed over the 48-hour time period, and that the protein generated was of the expected molecular weight.

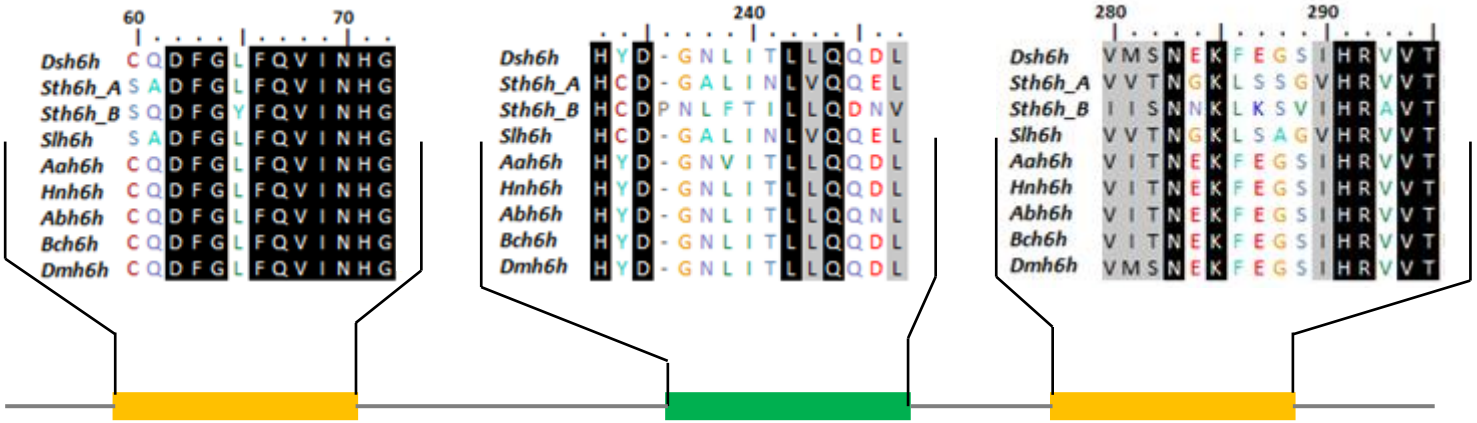

Figure 4.3.2: **h6h amino acid aligments between species within the solanaceae**.

Schematic of amino acid alignment with 2-oxogluterate and iron binding domains expanded to show differences between species within the solanaceae that can and can not produce tropane alkaloids. The species which do not produce tropane alkaloids are *St*h6h_A, *St*h6h_B and *Sl*h6h (XP_004251246.1), with *Ds*h6h (ALD59774.1), *Aa*h6h (ABM74185.1), *Ab*h6h (AEN79443.1), *Hn*h6h (BAA05630.1), *Bc*h6h (ACB40931.1), *Dm*h6h (AAQ04302.1) all producing tropane alkaloids. Amino acids with 100% similarity are highlighted in black, and those with > 50% similarity are highlighted in grey. Coloured amino acids highlight differences. Protein length is between 360 - 365 amino acids. The orange boxes represent the regions which contain the Fe^{2+} binding domains and the green box representing the 2-oxogluterate substrate binding domains. Alignments produced using BioEdit version 7.2.5

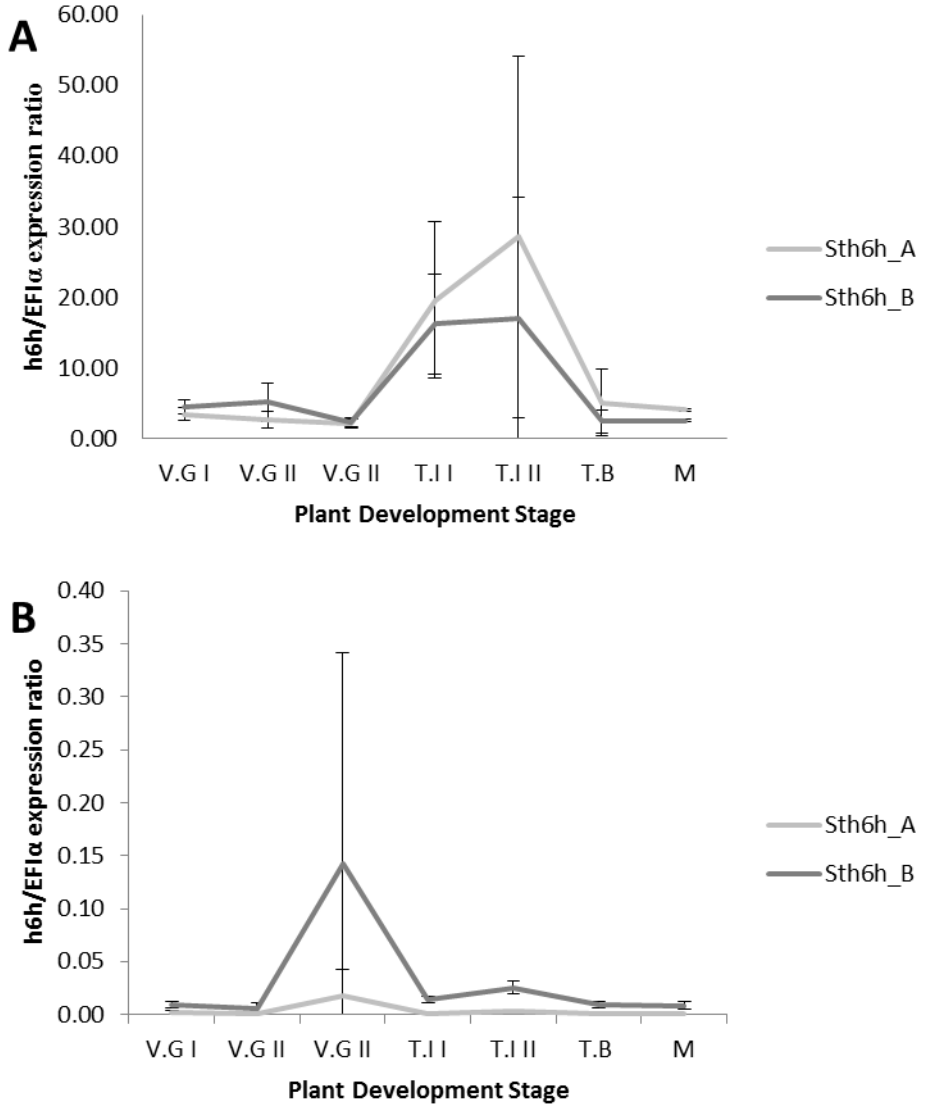

Figure 4.3.3: qRT-PCR time course analysis of *h6h* in potato tissue.

A = qRT-PCR analysis of *Sth6h*_A and *Sth6h*_B relative expression levels from *Solanum tuberosum* cultivar *Désirée* roots. This indicates that both *h6h* genes under investigation within potato are expressed well in the roots with expression reaching its highest levels during tuber induction. **B** = qRT-PCR analysis of *Sth6h*_A and *Sth6h*_B relative expression levels from *Solanum tuberosum* cultivar *Désirée* leaf. This indicates that the expression levels of the two *h6h* genes from Solanum tuberosum are not well expressed within the leaves. (V.G – Vegetative Growth, T.I – Tuber Induction, T.B – Tuber bulking, M – Maturation). Growth stage definitions taken from Patil *et al*, (2016), three replicates were used at

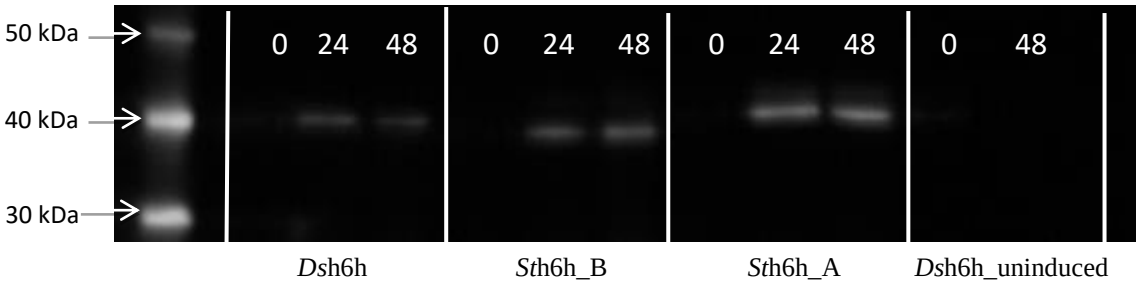

Figure 4.3.4: Western blot analysis of histidine tagged recombinant h6h

Protein extracted from IPTG induced *E. coli* strain BL21 cells over a 48 hour time course. For the three h6h proteins under investigation it can be seen that there is protein expression after 24 and 48 hours, giving proteins of the expected molecular weight (*D*sh6h – 41.5 kDa, *St*h6h_A – 41.1 kDa and *St*h6h_B – 40.3 kDa); un-induced *D*sh6h is used as a control to ensure there is no basal protein expression within the BL21 cell cultures. Primary antibody: 6x-His Tag Monoclonal antibody raised in mouse (*Mus*), Secondary antibody: Anti-mouse IgG HRP, raised in Goat (*Capra*).

With these h6h proteins being expressed within bacterial cell cultures, metabolite conversion assays were carried out. Figure 4.3.5 and 4.3.6, show that there was conversion of hyoscyamine to both anisodamine and scopolamine over the 48 hour time period for *D*sh6h at both 16 and 28^{o}C, whereas for both *St*h6h_A and *St*h6h_B there was no metabolite conversion detected over the same time period. This suggests that whilst the CDS encodes for a protein that was induced and expressed, there is no evidence of h6h activity for the potato protein in contrast to that observed with the control *D*sh6h. With regards to *D*sh6h conversion assays, at 16 and 28^{o}C there were detectable levels of scopolamine present within the cells cultures after 48 hours as well as no detectable hyoscyamine within the 16^{o}C assay after 48 hours. Assays at 24 and 37^{o}C were also conducted and showed that there was conversion to anisodamine for *D*sh6h at both temperatures, as well as further conversion to scopolamine detectable at 24^{o}C, although this was lower than the levels detected in both the 16 and 28^{o}C assays. For both *St*h6h assays at these temperatures there was no conversion detected (data not shown).

With recombinant protein assays for *St*h6h demonstrating that the *h6h* sequences under investigation were not functional within the bacterial system, *in planta* feeding assays were undertaken to determine if h6h exhibits activity *in planta*. During a pilot study using cultivar *Désirée* plantlets, root growth appeared to be suppressed in plants which were grown on hyoscyamine spiked MS20 media. Although this data is not shown due to the small scale of the experiment, for the subsequent *in planta* assays, *Désirée* plantlets were sub-cultured onto fresh spiked media with and without roots to negate possible inhibition effects from the hyoscyamine.

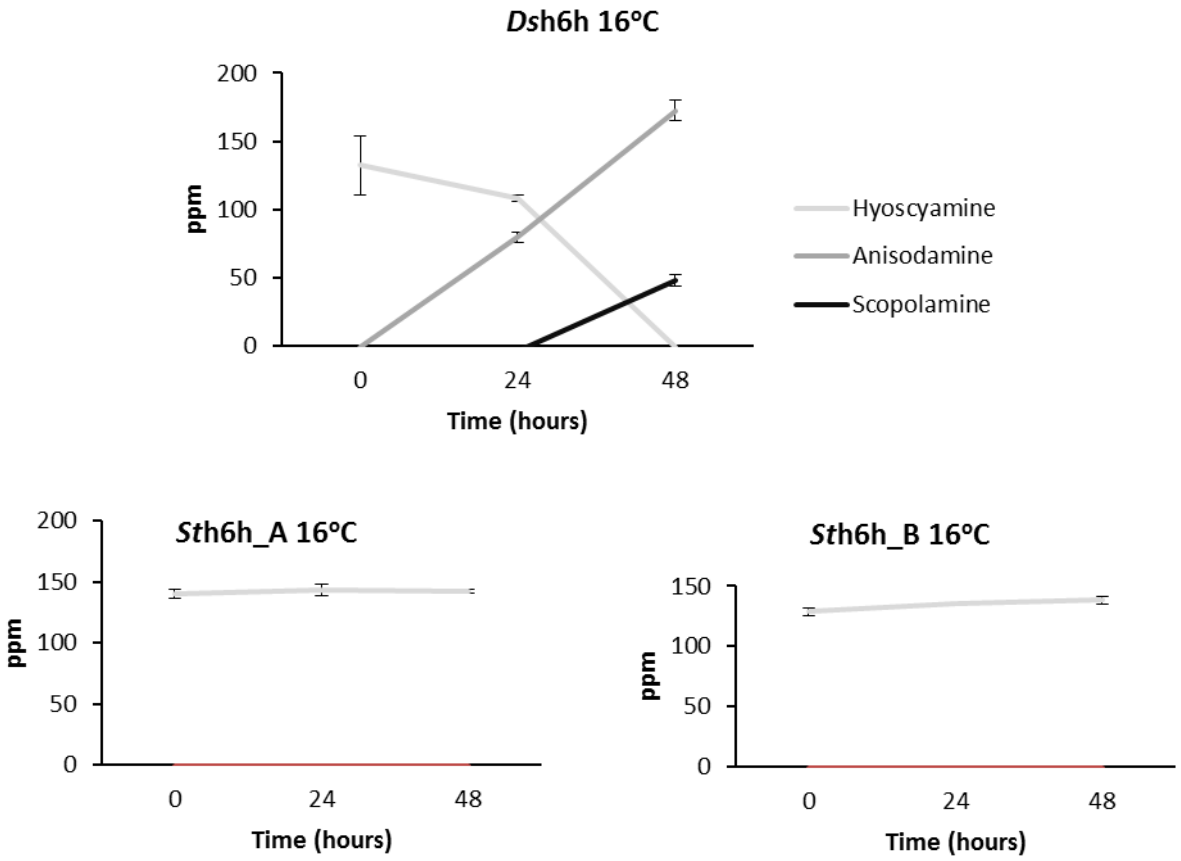

Figure 4.3.5: Tropane alkaloid biotransformation by *Ds*h6h and *St*h6h at 16°C.

Panels representing the change in tropane alkaloid level over the 48 hour time course, for h6h recombinant protein assays at 16°C. In the *Datura stromonium* control assays, it can be seen that hyoscyamine is converted into anisodamine and scopolamine over the 48 hour time course. However, in both of the *Solanum tuberosum* h6h assays at this temperature, no conversion is detected. The results at each time point are the averages of 3 replicates and the s.e.m is shown (n=3).

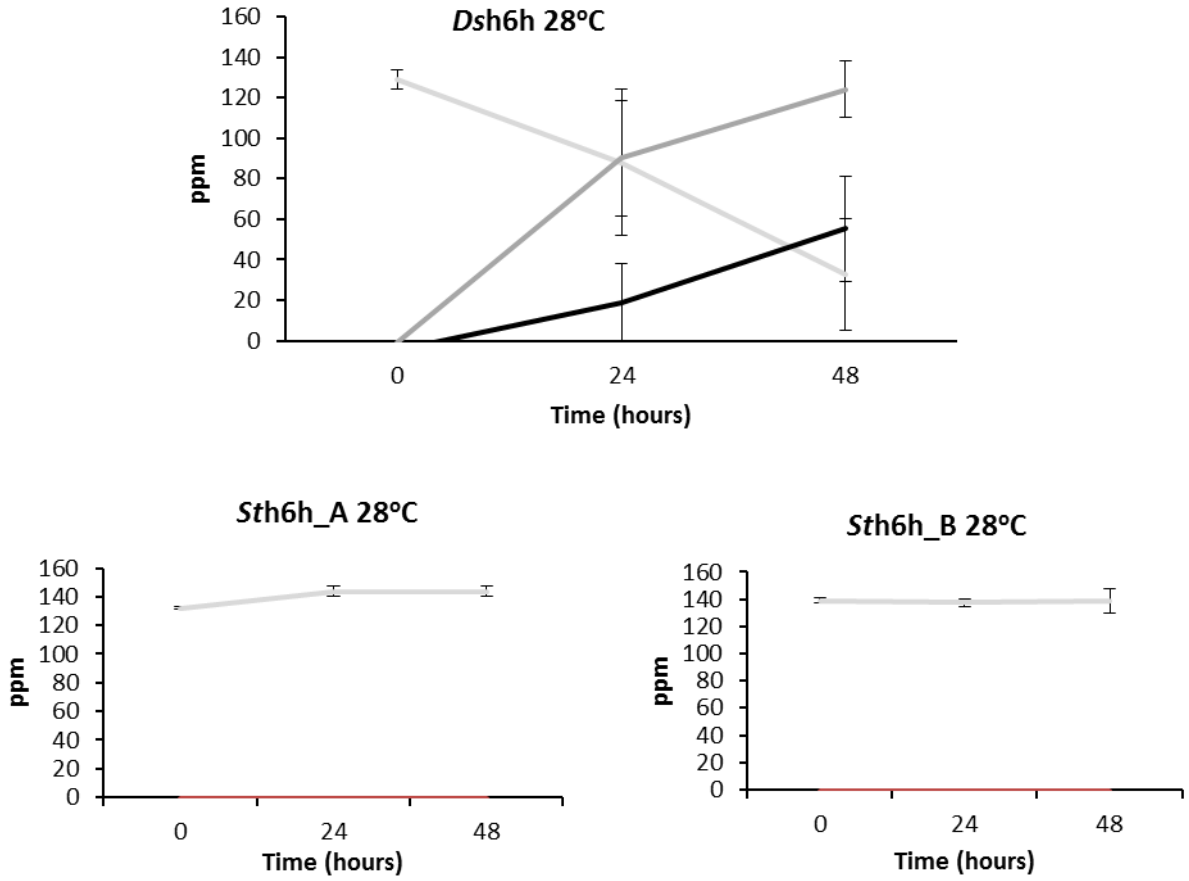

Figure 4.3.6: Tropane alkaloid biotransformation by *Ds*h6h and *St*h6h at 28ºC.

Panels representing the change in tropane alkaloid level over the 48 hour time course, for h6h recombinant protein assays at two temperatures 28ºC. In the *Datura stromonium* control assays, it can be seen that hyoscyamine is converted into anisodamine and scopolamine over the 48 hour time course. However, in both of the *Solanum tuberosum* h6h assays at this temperature, no conversion is detected. The results at each time point are the averages of 3 replicates and the s.e.m is shown (n=3).

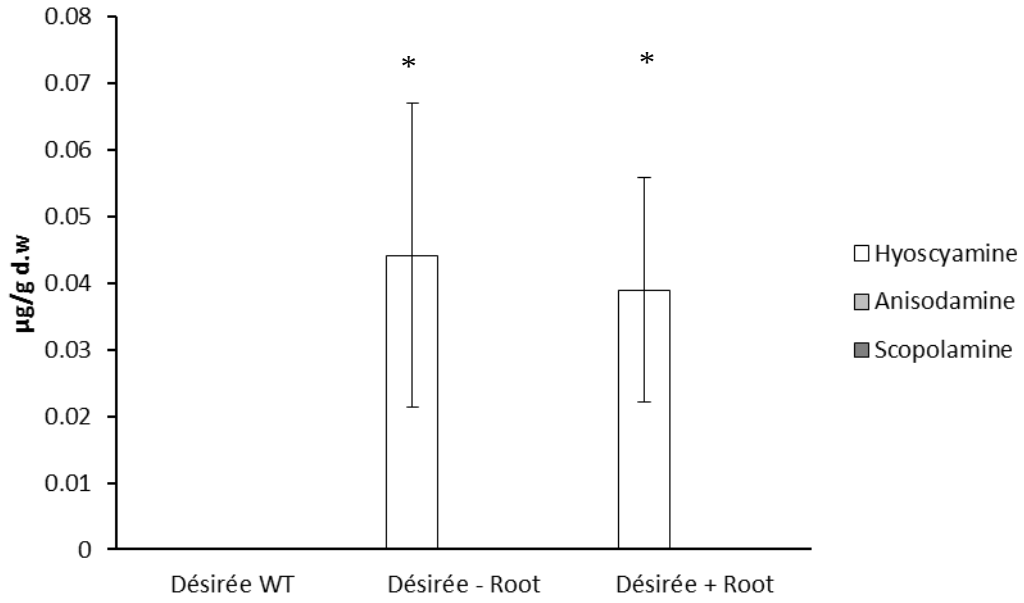

Figure 4.3.7: Functional assay to determine *In planta* h6h activity.

In planta functional assay to determine if there is any endogenous h6h activity within *Solanum tuberosum* cultivar *Désirée* plantlets. The plantlets in this assay were grown on MS20 in the presence or absence of hyoscyamine, as well being sub-cultured with roots still intact (*Désirée* plus roots (n = 3)) or as a fresh nodal cutting (*Désirée* and no roots (n = 4)). There was no anisodamine or scopolamine detected in plants grown in the presence of hyoscyamine. * indicates a significant difference to control plantlets (n = 3) where $P < 0.05$.

The *in planta* assay shown in Figure 4.3.7 demonstrates that whilst there is uptake of hyoscyamine from the tissue culture media, there is no conversion into the downstream metabolites. The analysis of plantlets and other tissues has been shown to be an effective way to determine the functionality of h6h. This approach has been utilised by both Khanam *et al*, (2001) and Kai *et al*, (2012). In their respective studies, Khanam *et al*, (2001) were concerned with the production of tropane alkaloids in shoot cultures of *Duboisia myoporoides*, whereas, Kai *et al*, (2012) investigated the effects of over-expressing *trI* and *h6h* in *Anisodus acutangulus*. Whilst in these previous studies, there was no application of exogenous hyoscyamine, Rocha *et al*, (2002) expressed *h6h* from *Hyoscyamus niger* in *Nicotiana tabacum* and assessed functionality through the application of 1 mM hyoscyamine in detached leaf assays. Within this system there was uptake of hyoscyamine into the leaves but this was not uniform across the lines tested; 3000 µg/g compared to 600 µg/g FW in the best and worst lines respectively. Subsequent conversion to anisodamine and scopolamine was weak, with these two tropane alkaloids accounting for a total of 342 µg/g FW from the best line in the Rocha *et al*, (2002) study.

4.4 Discussion

Previously, the functional characterisation of *h6h* has been conducted for multiple species within the Solanaceae (Cao *et al*, 2015; Kai *et al*, 2011; Cardillo *et al*, 2017; Li, van Belkum and Vederas, 2012; Hashimoto, Matsuda and Yamada, 1993; Jaber-Vazdekis *et al*, 2009; and Pramod, Singh and Jayabaskaran, 2010b), determining the effects of exogenous elicitors (Kang *et al*, 2004) as well as required reaction co-factors (Cardillo *et al*, 2017) on this important enzymatic step in the tropane alkaloid biosynthesis pathway.

The principle aim of this study was to determine whether a functional *h6h* gene that catalyses the hydroxylation and epoxidation steps of the tropane alkaloid biosynthesis pathway could be identified from potato. Within the potato genome sequence two genes were identified that were annotated as *h6h* genes. These sequences were cloned and expressed within a bacterial expression system to determine if they catalysed the hydroxylation and epoxidation of hyoscyamine to the final metabolite scopolamine.

Phylogenetic analysis and CDS alignments have been used to show that nucleotide *h6h* sequence similarity between active genes from tropane alkaloid producers and those found within potato. The two sequences annotated from potato show a relationship to sequences from other Solanaceous species in which tropane alkaloid biosynthesis occurs. Within the phylogenetic trees shown in Figure 4.3.1, the branch support (also known as bootstrap values) between *Sth6h*_A and *Hyoscyamus aureus* 1332 is 69, this is just below the accepted relationship level of 70, which indicates a convincing level of support (Lee, 2000). Due to this it cannot be strictly inferred that there is a true relationship between these two *h6h* sequences, however it does produce an interesting avenue for investigation. The branch support between *Sth6h*_B and the *h6h* contig from *Datura inoxia* is not indicative of a strong phylogenetic relationship as it returns a bootstrap value of 30. The previous branch which contains the *Duboisia h6h* and a branch support of 54, gives a little more strength to the possibility of a loose phylogenetic relationship, but not enough to completely accept the relationship. Bootstrap values are used to indicate the variability in distribution within the sequence data through resampling the data multiple times (Felsenstein, 1998). In the case of this study 1000 replicates were used in the

development of the phylogenetic trees, which for the *Sth6h*_B/*Datura inoxia* 7865 node resulted in a bootstrap value of 30, indicating that node was reproduced 300 times out of the 1000 replicates.

There is 65.9% nucleotide sequence identity for *St*h6h_A and 61.8% sequence identity for *St*h6h_B when compared to *Ds*h6h which was used as a control within this study. Whilst there are large areas of shared sequence identity between the sequences from potato and those from the tropane alkaloid producing species presented, differences within the 2-oxogluterate substrate and iron binding domains in Figure 4.3.2 could be indicative of why no h6h activity could be detected for those potato genes across the four temperatures tested. Other regions exhibiting sequence differences can influence the activity of the potato h6h sequences, however it is unclear as to the effect these have.

The *E. coli* recombinant biotransformation assays conducted to determine the functionality of the two *St*h6h orthologues within this study have shown that there is no h6h activity when compared to an active h6h. The *Ds*h6h used within these assays, showed activity at all the temperatures tested, although to varying degrees. Comparison of this active h6h to previous studies has shown that it follows a similar pattern to the wild type results described in Cao *et al*, (2015). At 16^{o}C, Cao *et al*, demonstrated that the wild type *Anisodus actuangulus h6h* catalysed the hydroxylation of hyoscyamine into anisodamine after 8 hours with 100% efficiency. The epoxidase activity of this enzyme however, appeared to be limited with 25% of the intermediate anisodamine being converted into scopolamine after 24 hours, with this level being maintained for the duration of the experiment. Whilst Cao *et al*, (2015) saw 100% conversion of hyoscyamine after 8 hours, in the assay at 16^{o}C it took 48 hours to reach this level of conversion. The levels of scopolamine, from the epoxidation of anisodamine, continued to rise from 24 to 48 hours, suggesting that the reaction was not complete. Similar results were seen in the *Ds*h6h assays at 28^{o}C. The similarities between the *Ds*h6h control used in this assay and the results from the Coa *et al*, (2015) study indicate *Ds*h6h was a suitable control to determine if the reaction conditions were appropriate to indicate any *St*h6h activity.

Cofactors such as ascorbate and catalase have been shown to be required for the efficient catalysis of substrates within some organisms. Catalase is required within organisms to keep hydrogen peroxide levels below toxic levels and *E. coli* is able to

produce endogenous catalase for this purpose. The oxygen produced from the catalysis of hydrogen peroxide is used in the conversion of hyoscyamine into anisodamine Previous research conducted by Cardillo *et al*, (2017) discounted issues related to reaction co-factors being omitted as they demonstrated that bacterial strains produce catalase to a sufficient level that exogenous catalase is not required to be added. Therefore, there are no negative effects on the hyoscyamine conversion rates during their study. They have shown that omission of 2-oxogluterate limited the biotransformation efficiency of hyoscyamine to anisodamine with 95% remaining unconverted after 25 hours and no scopolamine being detected. In the two *D*sh6h assays shown in Figures 4.3.5 and 4.3.6, show there is almost 100% conversion of hyoscyamine over the 48 hours the assay was allowed to continue. Therefore, whilst supplementing the culture media used in the assays within this study, may have shown an improvement in the reaction efficiency of the positive control, and possibly allowed for an increase in the amount of scopolamine produced, it is doubtful that the *St*h6h assays which showed no hydroxylation activity would exhibit activity.

The translated recombinant proteins used in this assay were produced with an N-terminus Histidine tag. Histidine tags are six or more histidine residues and are relatively small in size (about 2.5 kDa) (Booth *et al*, 2018). Histidine tags are useful as 90% of determined protein structures have been elucidated through the use of a protein tag, and the histidine tag represents a large portion of these (Booth *et al*, 2018). The histidine tag has been shown to decrease the substrate affinity and kinetic parameters 8-fold in the GNAT enzyme superfamily, when compared to untagged enzymes (Booth *et al*, 2018). The distribution of histidine tagged proteins within bacterial cells has been shown to be uneven, when expressed at 37ºC over 12 hours (Park *et al*, 2015). Interference of the histidine tag on recombinant protein expression and function has been shown to be variable. The impact of the histidine tag on proteins expressed in this assay may be a contributory factor in why the *St*h6h expressed proteins did not convert hyoscyamine. With the knowledge that the proteins from the assays in this study were expressed and hyoscyamine conversion in the *Datura stromonium* control assay, there is evidence that substrate binding occurred. With this it can be said that, at least *D*sh6h protein structure was not affected by the presence of the histidine tag, this is unable to be confirmed for the two *St*h6h proteins. Whilst it may be speculated that enzyme kinetics may have been decreased due to the presence of the histidine tag, which is similar to the results described in Booth *et al*, (2018) without experimental comparisons

of the kinetics of untagged enzymes this cannot be proven. Comparison of untagged to tagged *St*h6h protein may elicit differences due to the removal of the tag and is an avenue for further research.

In planta Solanum tuberosum cultivar *Désirée* plantlet feeding assays were deployed to determine if there was conversion of hyoscyamine into the downstream metabolites. Plantlets were sub-cultured with and without roots and subsequently grown on MS20 media with hyoscyamine hydrobromide added. Plantlets with and without roots were used to alleviate concerns that hyoscyamine may inhibit the root development and uptake of hyoscyamine into the plantlets which was seen in a small pilot study. Plantlets without roots had the developed roots removed 2 mm above the highest root prior to sub-culturing onto the MS20 hyoscyamine hydrobromide media used in the assay. Figure 4.3.7 shows that for the plants grown on hyoscyamine enriched media there is a significant uptake of the alkaloid into the plant system compared to the plantlets grown on MS20, however, there was no detectable anisodamine or scopolamine in these samples. Rocha *et al,* (2002) investigated the functional expression of *Hn*h6h in *Nicotiana tabacum*. This was achieved through the generation of transgenic lines and then feeding detached leaves hyoscyamine and measuring the conversion to anisodamine and scopolamine. *Nicotiana tabacum*, like potato does not produce these tropane alkaloids, therefore any conversion in the controls would indicate a functional h6h enzyme. Rocha *et al,* (2002) showed that there was uptake of hyoscyamine into the leaves of the controls, but no further conversion was detected. However, two of the generated *h6h* transgenic lines did show limited conversion to anisodamine and scopolamine. Rocha *et al,* (2002) may have seen better results if they had utilised roots as this is the site of tropane alkaloid biosynthesis. The controls show similarities to the *in planta* assays conducted within this study, through the uptake of hyoscyamine into the tissues being studied, but no downstream conversion.

With the results of the bacterial recombinant expression and *in planta* assays, it can be suggested that whilst there are annotated *h6h* sequences within the potato genome, these genes are not functional and represent a further lesion on the tropane alkaloid biosynthesis pathway within this crop.

Chapter 5: Over-expression of *Withania somnifera* t*ropinone reductase I* in *Solanum tuberosum* cultivar *Désirée.*

5.1 Introduction

Within the Solanaceae, *tropinone reductase I* (*trI)* has been studied extensively due to its importance in the production of the tropane alkaloids (Nakajima *et a*l, 1993; Kaiser *et al*, 2006; Küster *et al*, 2017). trI catalyses the conversion of tropinone to tropine (also known as 3α-tropanol and seen in Figure 5.1.1), a precursor for the formation of the economically important tropane alkaloids hyoscyamine and scopolamine, shown in Figure 1.7 (Kaiser *et al*, 2006).

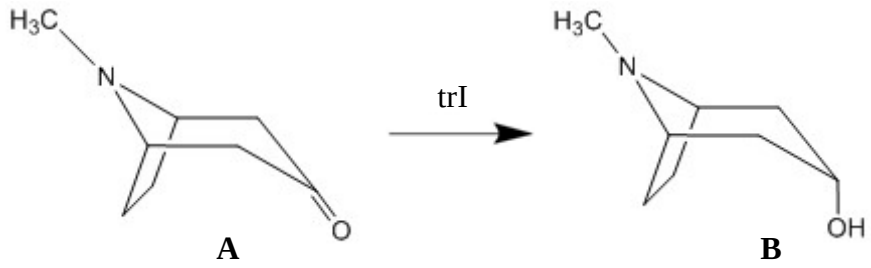

Figure 5.1.1: **Conversion of tropinone to tropine.**

Schematic representation of the conversion of tropinone (A) to tropine (B). trI is responsible for the NADPH dependent reduction of oxygen located on the 3rd carbon of the tropane alkaloid skeleton (see Figure 1.1), producing tropine.

As described in Chapter 1.8 trI is a member of the short-chain dehydrogenase/reductase (SDR) family of enzymes. This enzyme family shares conserved amino acid motifs (Moummou *et al*, 2012) and between the two tropinone reductase enzymes (trI and trII) from *Datura* there are 167 identical amino acids resulting in 64% sequence identity. Comparisons of the trI amino acid sequence from Solanaceous species shows that the conserved regions of the SDR family are present, even in species in which the production of tropane alkaloids is non-existent. This comparison can be seen in Figure 5.1.2, taken from Kushwaha *et al*, (2013).

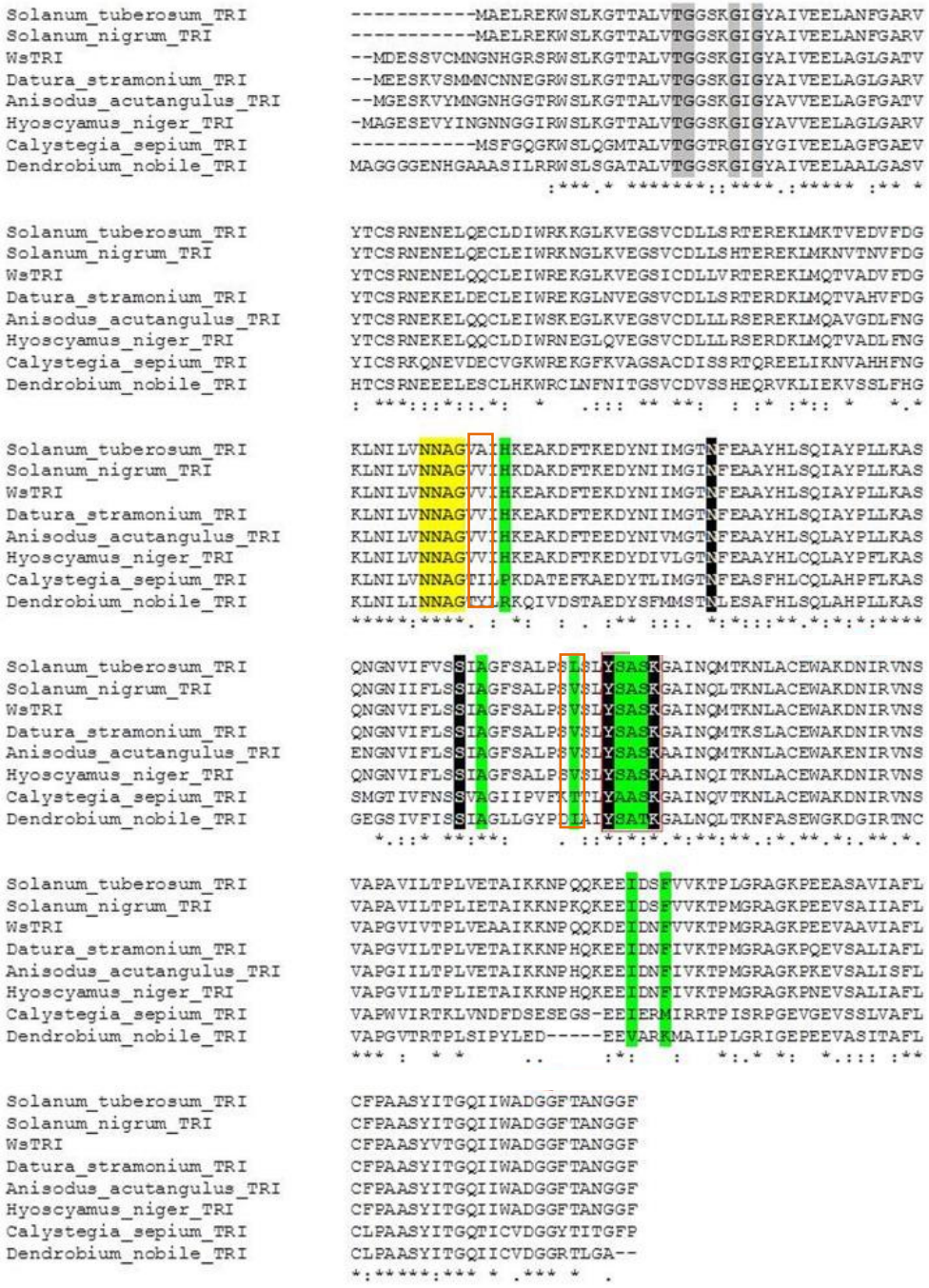

Figure 5.1.2: trI protein sequence alignment.

Protein sequence alignment of Solanaceous trI sequences from producers of tropane alkaloids and potato. Highlighted residues indicate amino acids involved in the following; Grey – co-factor binding, Green – tropinone binding, Black – the catalytic tetrad, Yellow – conserved SDR motif, along with the enclosed YxxxK region. Figure reproduced from Kushwaha *et al*, (2013).

Kushwaha *et al*, (2013) have also bought together information from other studies which look at trI activity either from recombinant protein (expressed in *E. coli*) or purified native plant protein. Although the Kushwaha *et al*, (2013) study is primarily focused on *Withania somnifera* trI as a recombinant protein, they show that trI from this species has a Michaelis Constant (K_m) of 1.27 (mM) compared to trI from other species

such as *Hyoscyamus niger* (1.01), *Datura stromonium* (0.117) and *Solanum tuberosum* (0.188), indicating that the substrate is required in a slightly greater concentration for optimal recombinant enzyme activity. This has led to speculation that along with gene expression and protein levels, the concentration and availability of tropinone within tissues could be a factor for tropine formation *in planta* (Dräger, 2006; Kushwaha *et al*, (2013)). It is noted in Kaiser *et al,* (2006), that the specific activity at optimal pH for the purified recombinant *St*trI protein (530 ± 55 pk_at/mg at pH 6.0) is considerably lower than that of *Ds*trI (864,000 pk_at/mg at pH 7.0). It has been hypothesised that this reduction in catalytic activity is a result of amino acid differences which participate in tropinone binding. Within the *St*trI sequence two of the amino acids which are involved in substrate binding are A101 and L159, however, these differ to the trI sequences from species which show high catalytic activity. *Datura stromonium* has V110 and V168, and *Hyoscyamus niger* has V111 and V169 respectively in these positions when aligned against each other. These differences are highlighted by the orange boxes in the sequence alignment shown in Figure 5.1.2.

Inactivity of trI within *Solanum tuberosum* has previously been demonstrated to be the primary bottleneck in any potential flux through the tropane alkaloid biosynthesis pathway (Keiner and Dräger, 1999). Studies into trI activity within potato have recently been conducted through both the over-expression and down-regulation of the endogenous potato *trI*. This work, conducted by Küster *et al* (2017) has shown that through *SttrI* over-expression, and in the presence of exogenous tropinone there is an increase in tropine formation, when compared to control lines (up to 75 µg/g compared to 25 µg/g FW). Conversely down regulated *trI* lines still exhibit trace amounts of tropine formation, but this was comparable to the control lines. This, according to the authors, suggests that *trI* from potato is expressed and active *in vivo,* although this arm of the pathway is less active than the nortropane alkaloid arm. Therefore, tropine does not accumulate in potato tissues to comparable levels seen within members of the solanaceae which produce tropane alkaloids, as the catalysis of tropinone is directed towards pseudotropine

The aim of this study is to determine if the transgenic expression of a non-potato *trI* gene displaying high tropinone catalytic properties results in tropinone conversion towards the tropane alkaloid biosynthesis pathway via tropine production, as seen in Figure 1.2. The potential removal of this bottleneck in potato is the first step to re-engineering the tropane alkaloid biosynthesis pathway.

5.2 Materials and Methods:

5.2.1 Production of transformation vectors.

The *WstrI* coding sequence was synthesised and transformation vectors were generated. After confirmation that these plasmids contained the gene cassettes in the correct orientation by Sanger sequencing and restriction endonuclease digestion (Figure 5.2.1), they underwent transformation into *Agrobacterium tumefaciens* (section 2.5.4.2). *Agrobacterium* mediated transformation into *Solanum tuberosum* cultivar *Désirée* was used to produce transgenic lines (sections 2.5.4.4 and 2.5.4.5).

Genomic DNA was extracted from *Agrobacterium* transformed calli which were producing shoots (2.5.1) prior to undergoing PCR (2.5.3) to determine if the *WstrI* gene cassette had been inserted into the *Solanum tuberosum* genome, shown in Figure 5.2.2 and 5.2.3.

Once lines had undergone initial characterisation for transgene presence, as outlined by Figures 5.2.2 and 5.2.3, RNA from lines positive for the transgene was extracted (2.5.1). The RNA was checked both by gel electrophoresis (Chapter 2.5.2) as seen in Figure 5.2.4, and spectrophotometrically (Chapter 2.5.2) as in Table 5.2.1.

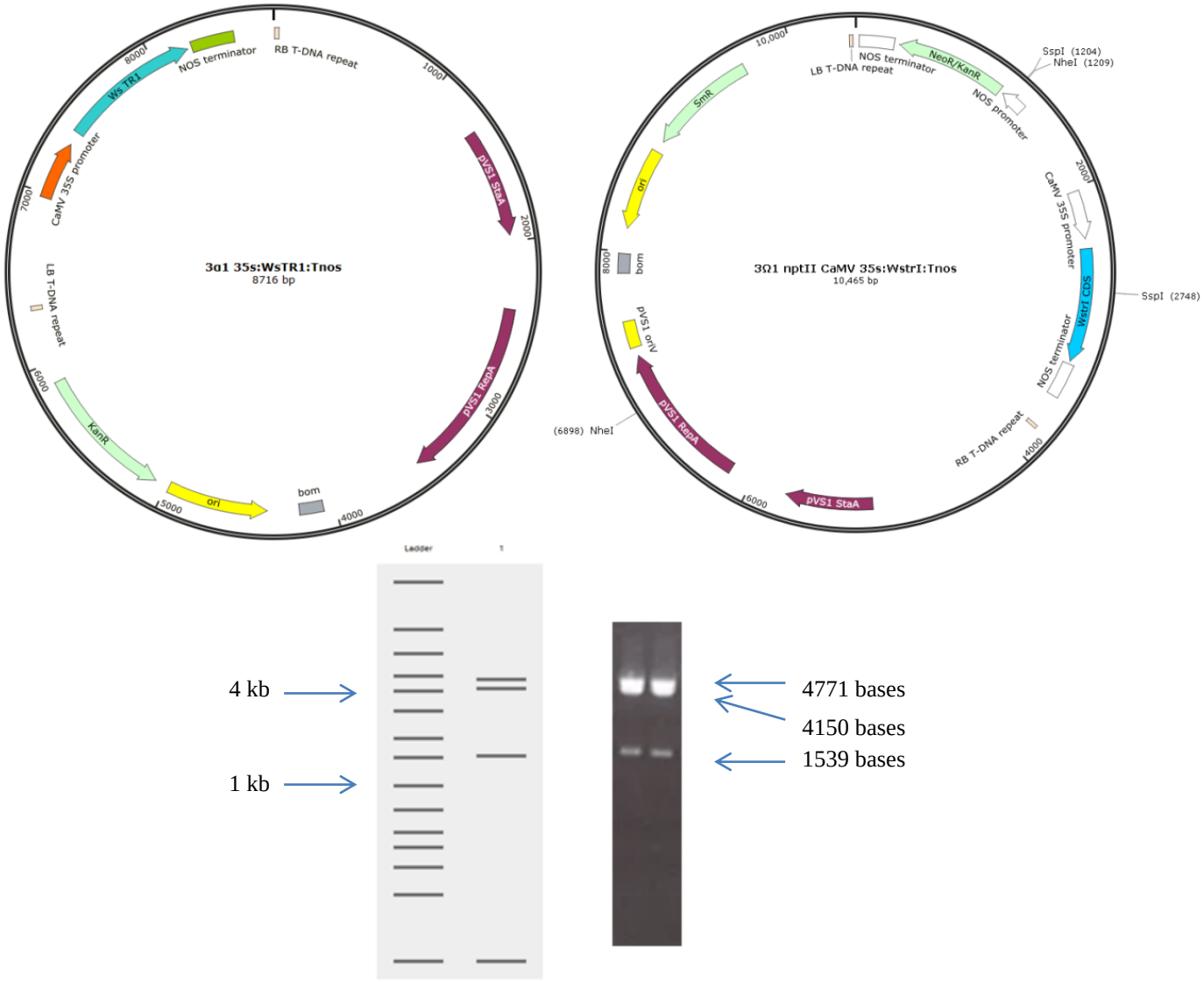

Figure 5.2.1: Manufactured plasmid vectors and expected enzymatic digestion pattern. Top left: Complete 3α1 destination vector containing the 35sCaMV:*WstrI:*Tnos gene cassette, produced using the GoldenBraid cloning strategy described in sections 1.11 and 2.5.3.4.3. Top right: Final 3Ω1 destination vector containing the transgenic selectable marker gene *nptII* as well as the 35sCaMV:*WstrI*:Tnos gene cassette from the 3α1 vector. The vector diagram also includes the diagnostic restriction endonuclease cut sites for SspI and NheI which will be used to determine if the recombinant ligation reaction has been successful. These two vectors were generated using the GoldenBraid cloning methodology detailed in chapter 1.11 and 2.5.3.4.3. Bottom left: Predicted restriction digestion map for the finalised 3Ω1 Tnos:*nptII*:Pnos 35sCaMV:*WstrI*:Tnos transformation vector using SspI/NheI. Lane 1 - DNA ladder; Lane 2 - shows predicted band size of completely digested vector which are 4771/4150/1539/5 bases. Bottom right: Image of ethidium bromide stained electrophoresis gel showing the expected banding pattern of the complete transformation vector. The band expected at 5 bases is too small to be resolved and imaged on the gel, which is why it is unable to be seen in the image. The two bands visible at the top of the image which represent the 4771/4150 fragments. Vector maps generated using SnapGene® Viewer 3.2.1and predicted digestion image generated using Benchling online software (www.benchling.com).

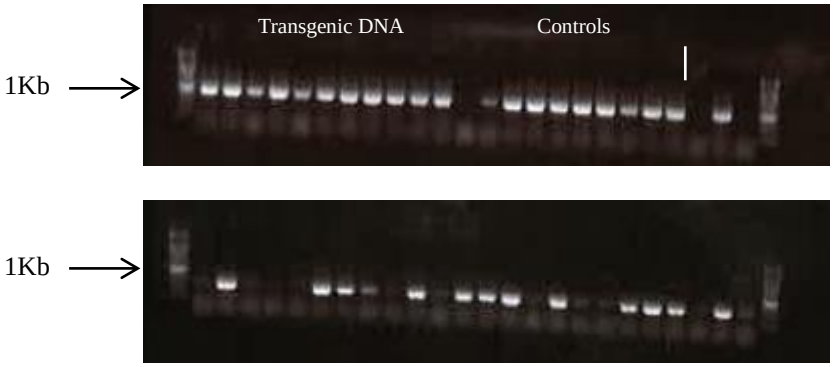

Figure 5.2.2: gDNA electrophoresis in characterisation of transgenics.

Top: Electrophoresis image of genomic DNA which has undergone PCR to test for the presence of *ef-1α* which is being used as a loading control. The band produced is 917bp which can be seen below the main 1kb band of the DNA ladder. Bottom: Electrophoresis image of the same genomic DNA samples, testing for the presence of the *nptII* gene (which confers kanamycin resistance to the plantlet). A 600bp fragment is expected for this reaction product. Primer sequences can be seen in appendix A.5.2.1.

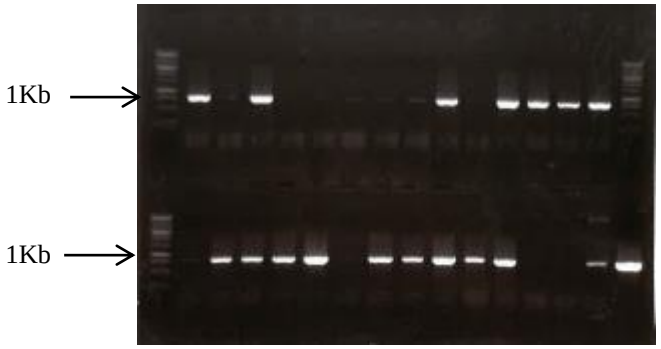

Figure 5.2.3: Characterisation via PCR for positive *WstrI* transgenic lines.

Electrophoresis image of genomic DNA which has undergone PCR to test for the presence of *WstrI* from samples positive for the presence of *nptII*. Positive lines went forward for RT-qPCR analysis for *WstrI* expression level characterisation. Primer sequences can be seen in appendix A.5.2.1.

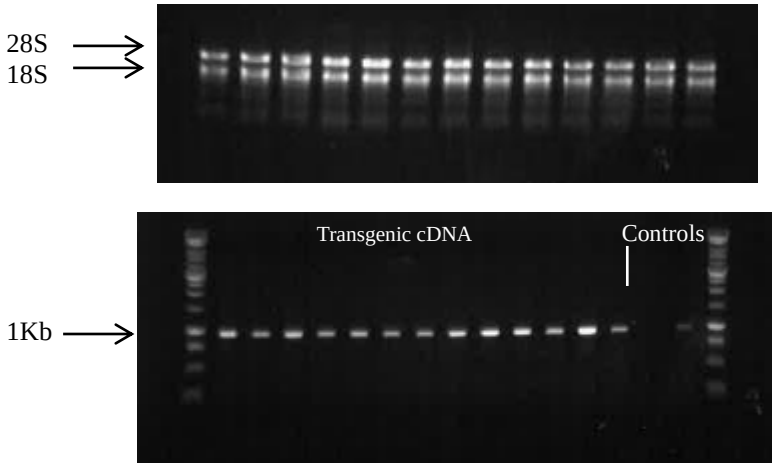

Figure 5.2.4: RNA extraction and cDNA characterisation prior to qRT-PCR analysis Top: Ethidium bromide stained agarose gel image to visually check the integrity of RNA extracted from *WstrI* positive plantlets determined in 5.2.7. The bands shown point to the presence of the 28S and 18S ribosomal RNA sub-units from extracted samples. The presence of these two bands in an approximate 2:1 intensity ratio and lack of smearing indicate the RNA has not been degraded during extraction. RNA quality was also determined by spectrophotometer with a representative example of this being seen in table 5.2.1 Bottom: Electrophoresis image of *ef-1α* PCR conducted on cDNA from the RNA extracted from plantlets prior to undergoing RT-qPCR. This reaction was 25 cycles, to show that the cDNA synthesis reaction was uniform across the reactions, through using *ef-1α* as a control.

Sample	ng/µl	A260	A280	260/280	260/230
WstrI/A*strII* 20.1	757.44	18.94	8.87	2.14	1.13
WstrI/nptII 47.1	354.04	8.85	4.36	2.03	1.04
WstrI/A*strII*/*nptII* 3.2	478.05	11.95	5.74	2.06	1.11
Désirée WT A	494.76	12.37	5.71	2.17	1.41
WstrI/nptII 16.1	284.71	7.12	3.39	2.10	1.74
WstrI/A*strII* 36.1	498.01	12.45	5.80	2.15	1.74
WstrI/A*strII* 6.1	642.72	16.07	7.49	2.15	1.74
WstrI/nptII 18.3	439.83	11.00	5.12	2.15	1.43

Table 5.2.1: Representitive spectrophotometer readings from RNA extracts.
Reproduced table of the read out from the Nanodrop® ND-100 spectrophotometer showing the concentration of RNA present in the sample (ng/µl) as well as 260/280 and 260/230 purity ratios.

5.2.2 Biological replication

In all assays within the Chapter there are four biological replications (n = 4)

5.3 Results:

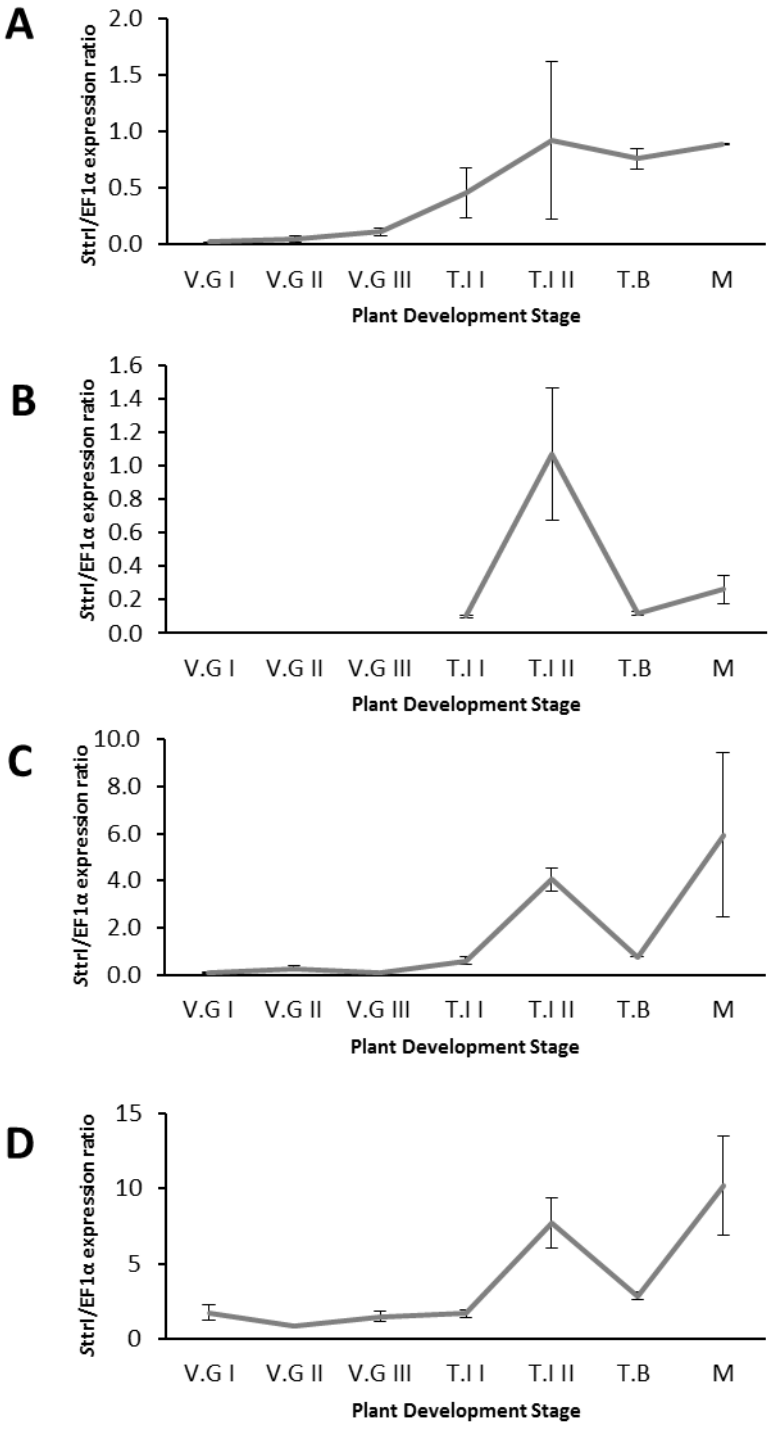

Figure 5.3.1: *trI* time course expression data from four tissues.

qRT-PCR expression data of *SttrI* from four different tissues during seven stages of plant development. Each panel represents a different tissue, with A – root; B – tuber; C – stem and D – leaf. Developmental stages relate to the following with average height given as an indicator: V.G – Vegetative Growth (stage I (27.0 cm) to III (61.8 cm)), T.I – Tuber Initiation (stage I (93.2 cm) and II (109.5 cm)), T.B – Tuber Bulking (131.6 cm) and M – Maturation/Senescence (128.2 cm). The definitions of growth stages are taken from Patil *et al*, (2016). Three replicates were used at each growth stage, with the standard error being represented by the error bars.

RT-qPCR analysis of *trI* expression from potato displayed in Figure 5.3.1 shows that the endogenous gene exhibits a different expression pattern within all of the four tissues tested throughout plant development. It appears that the highest relative expression level, compared to the endogenous control *elongation factor-1α* (*ef-1α*) occurs during tuber initiation II (T.I II), in all tissues tested. In the roots, which has been established as the site of tropane alkaloid biosynthesis (Hashimoto *et al,* 1986), the ratio of *trI/ef-1α* expression is c.a 1.0. As *trI* is expressed at significant levels in roots, corresponding trI enzyme activity might be expected. However, evidence for trI activity in potato roots has not been reported.

The phylogenetic analysis of tropinone reductases from members of the solanaceae and other plant families shows that tropinone reductases fall into three distinct groups (Figure 5.3.2). Group I are the *tropinone reductase I* genes from only members of the solanaceae, Group II are *tropinone reductase II (trII)* genes from the solanaceae, and Group III contains those genes exhibiting tropinone reductase activity, but belonging to other plant families.

Whilst Kushwaha *et al*, (2013) conducted alignments of the trI amino acid sequences from producers of tropane alkaloids and included the potato trI sequence; it is of interest to include other non-tropane alkaloid producing species to highlight any consistent similarities between these sequences. The nucleotide and CDS alignments in Figures 5.3.3 and 5.3.4 highlight sequence similarities of known *trI* genes from members of the solanaceae, these being the sequences which have a black background. The differences in nucleotide sequences are displayed by the colour of the base shown, with bases being represented by: green = adenine, red = thymine, blue = cytosine and black = guanine.

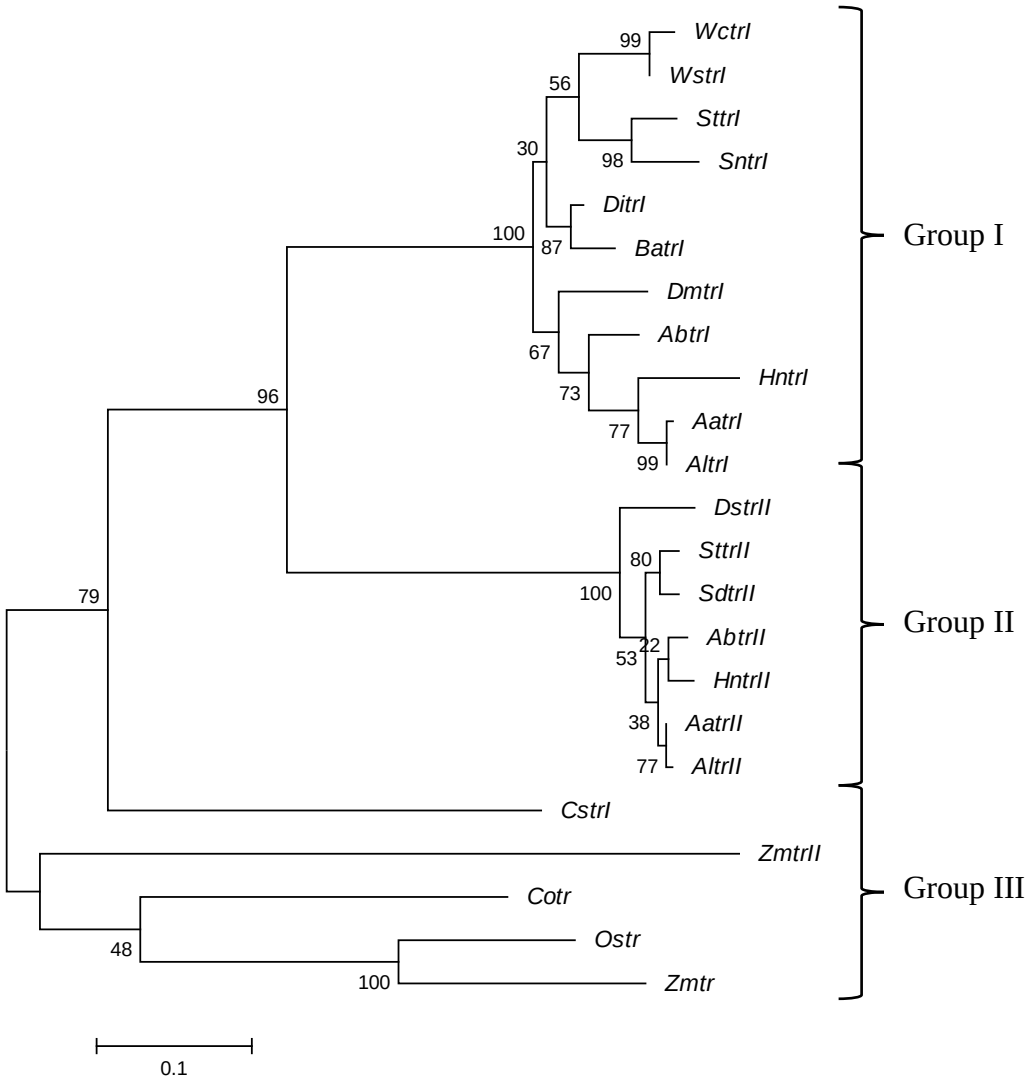

Figure 5.3.2: Phylogentic tree detailing tropinone reductase clusters across species which exhibit reductase activity.

Phylogenetic relationships between *tropinone reductases* of members of the Solanaceae and other plant families which exhibit tropinone reduction activity. Three distinct clades are visible from the dendrogram, with *trI* clustering in Group I, *trII* clustering in Group II and tropinone reductases from other families and species which exhibit activity clustering in Group III. GenBank Accession Numbers: *Dm*trI – AQU12716.1, *Wc*trI – AGB56644.1, *Aa*trI – ACB71202.1, *Di*trI –AIN39992.1, *Ab*trI – AFP55030.1, *St*trI – CAC34420.1, *Sn*trI – CAQ19734.1, HntrI – BAA13547.1, SttrII – CAC19810.1, *Ab*trII – AGH24753.1, *Sd*trII – CAQ19732.1, *Aa*trII – ACB71203.1, *Ws*trI – AGY46257.1, *Al*trII – AGL76990.1, *Ba*trI – AIN39993.1, AltrI – AGL76989.1, DstrII – AAA33282.1, *Hn*trII – AAB09776.1, *Cs*trI – CAD20555.1, *Co*tr – CAO02390.1, *Os*tr –ABF95192.1, *Zm*tr – ACG34080.1, *Zm*trII – NP_001147765.1. Figure produced using MEGA6 utilising the Maximum Likelihood method with 1000 replications.

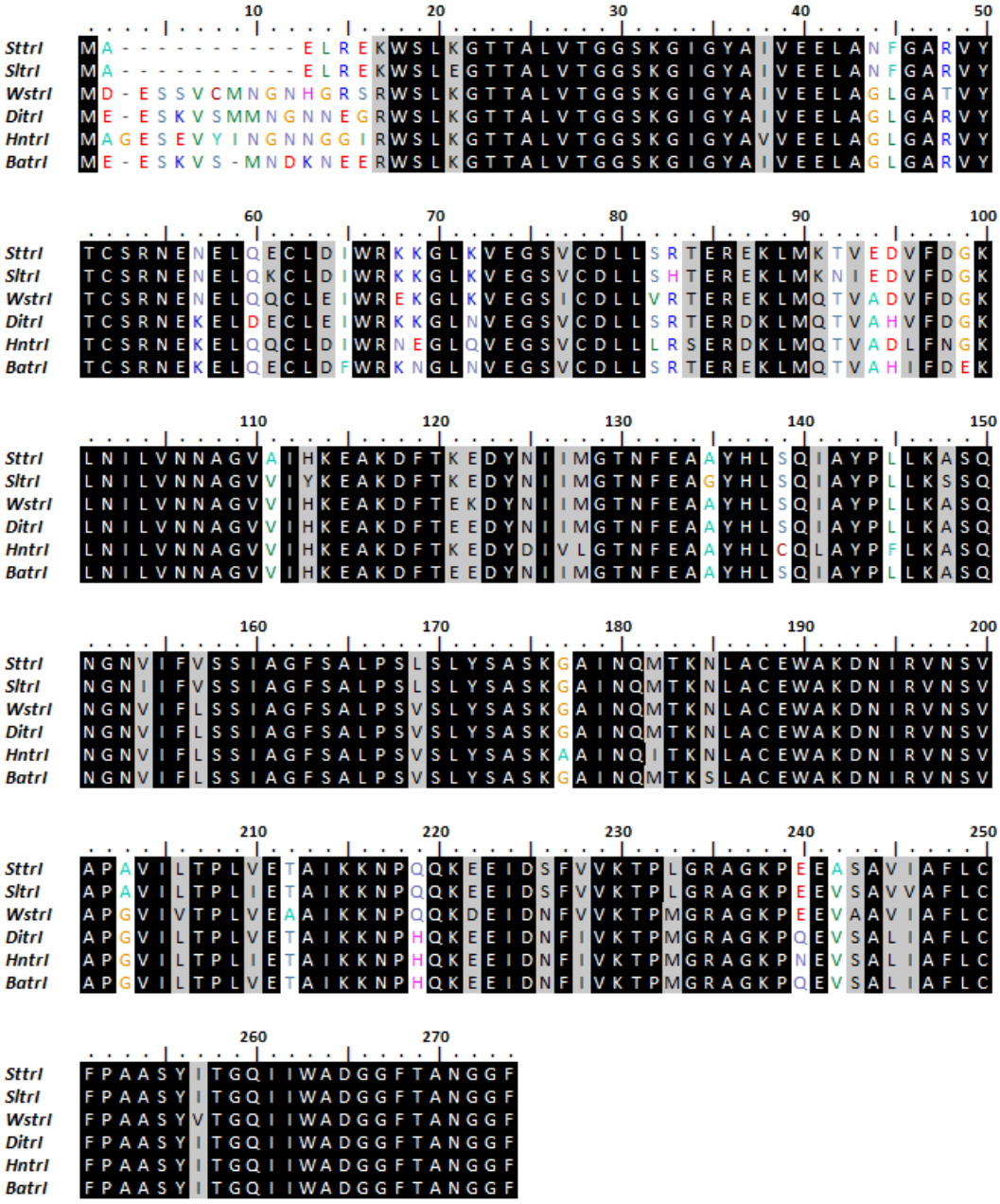

Figure 5.3.3: Amino acid sequence alignement of Solanaceous trI.

Multiple sequence alignment of Solanaceous *trI* amino acid sequences from *Solanum tuberosum* – *SttrI* (NP_001275290.1), *Solanum lycopersicum* - *SltrI* (XP_004249378.1), *Datura inoxia* –*DitrI* (AIN39992.1), *Brugmansia arborea* – *BatrI* (AIN39993.1), *Withania somnifera* - *WstrI* (AGY46257.1) and *Hyoscyamus niger* – *HntrI* (BAA13547.1). Identical amino acids are highlighted in black and the coloured amino acids show differences. Figure produced using BioEdit version 7.2.5.

trI from *Withania somnifera* has high recombinant enzyme activity (Kushwaha *et al*, 2013) and catalyse tropinone production efficiently. This trI enzyme has the four critical amino acids required for tropinone reduction and a sequence identity of 87.2% compared to *SttrI*. For these reasons, this gene was selected for the production of *trI* over-expression transgenic lines.

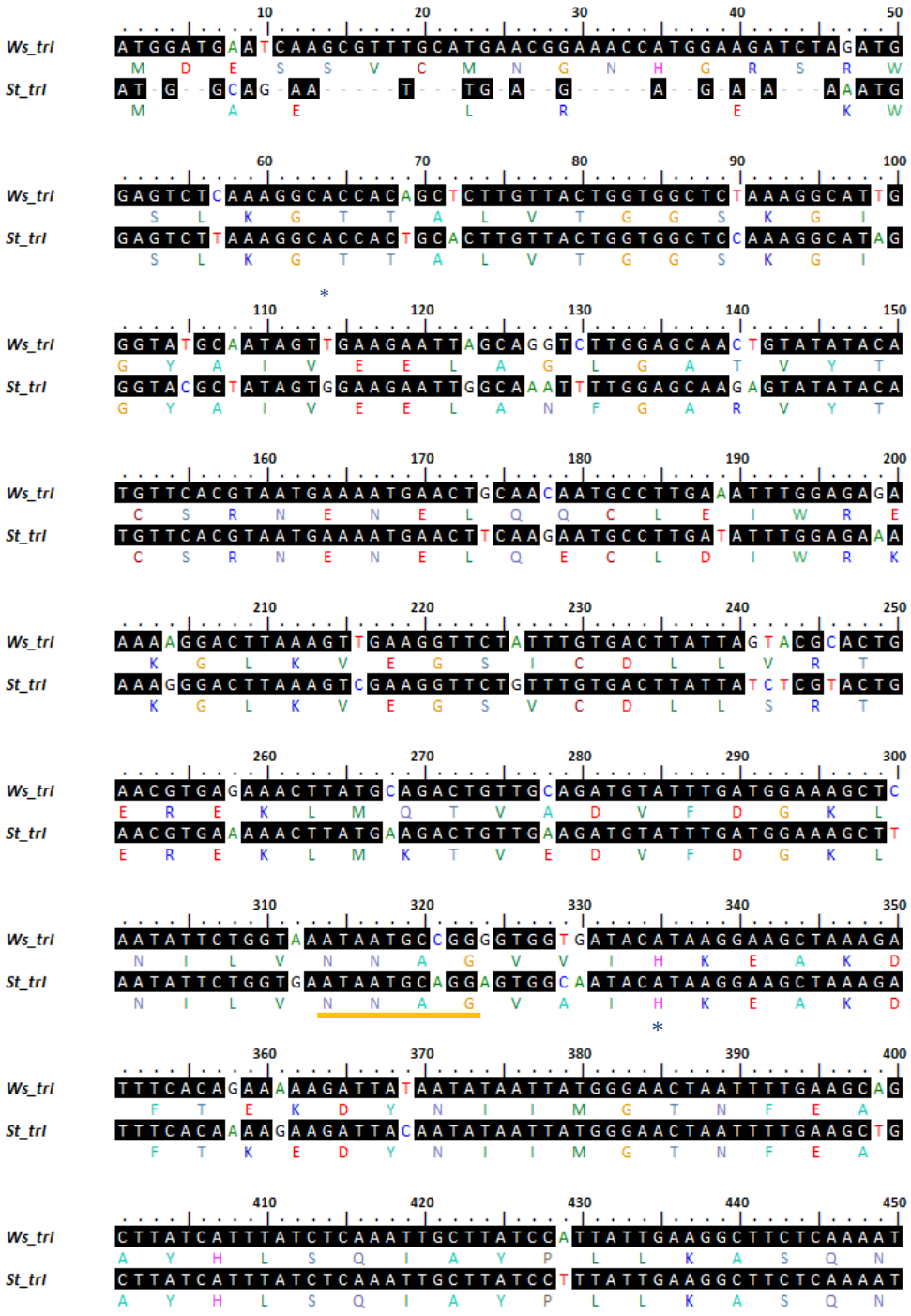

* continued on next page

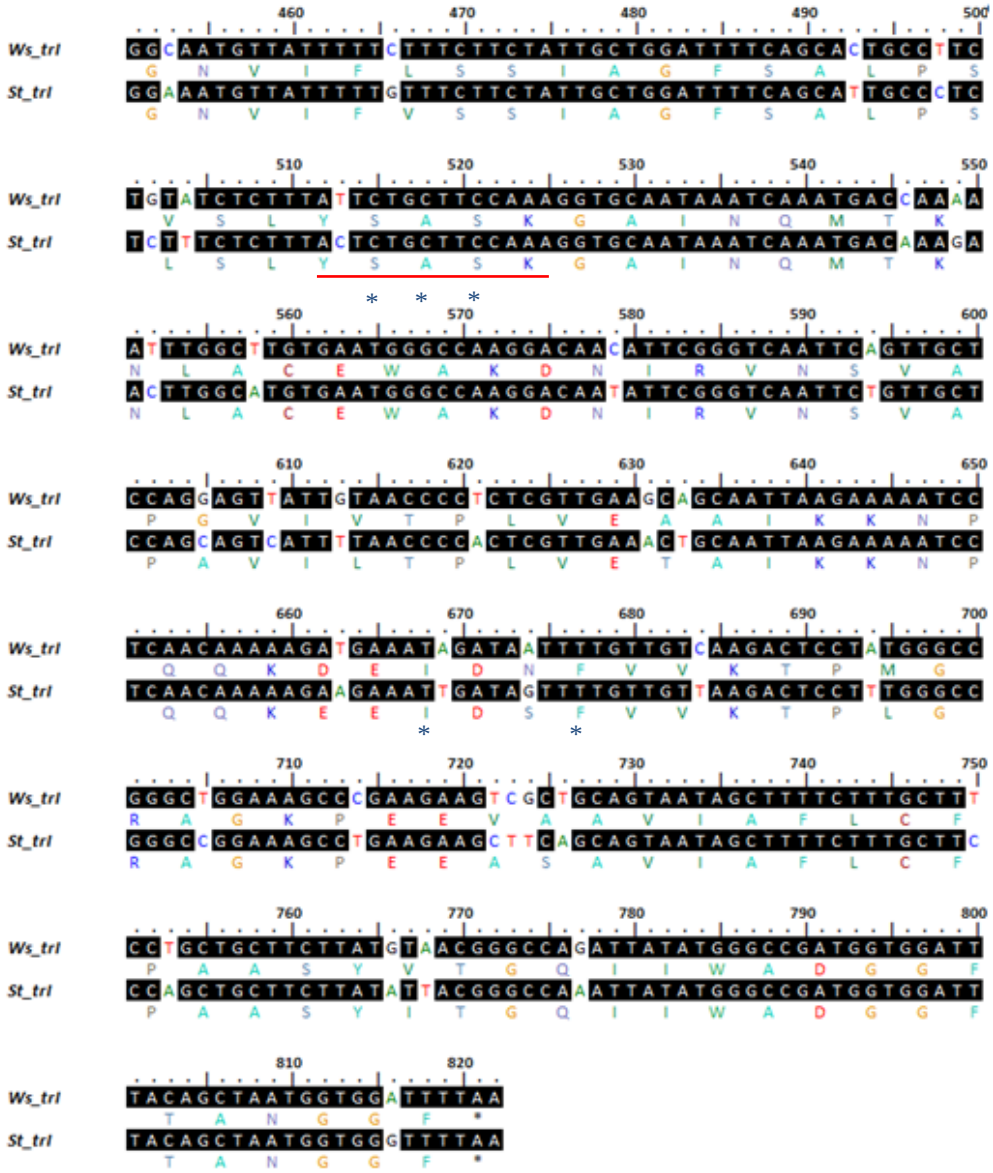

Figure 5.3.4: ***Withania somnifera*** **and potato** ***trI*** **amino acid sequence alignment**.

Sequence alignment of *trI* from *Solanum tuberosum* (NM_001288361.1) and *Withania somnifera* (KF360055.1). Both the nucleotide and amino acid sequences are aligned indicating that whilst there may be nucleotide differences between the two sequences in places, the translated protein sequence may be identical. Identical nucleotides are highlighted in black and the coloured bases show nucleotide differences. Orange underline shows conserved SDR region, Red underline indicates the YxxxK SDR motif and the blue asterisk (*) shows the regions of the sequence which participate in tropinone binding. Figure produced using BioEdit version 7.2.5.

5.3.1 Transgene characterisation.

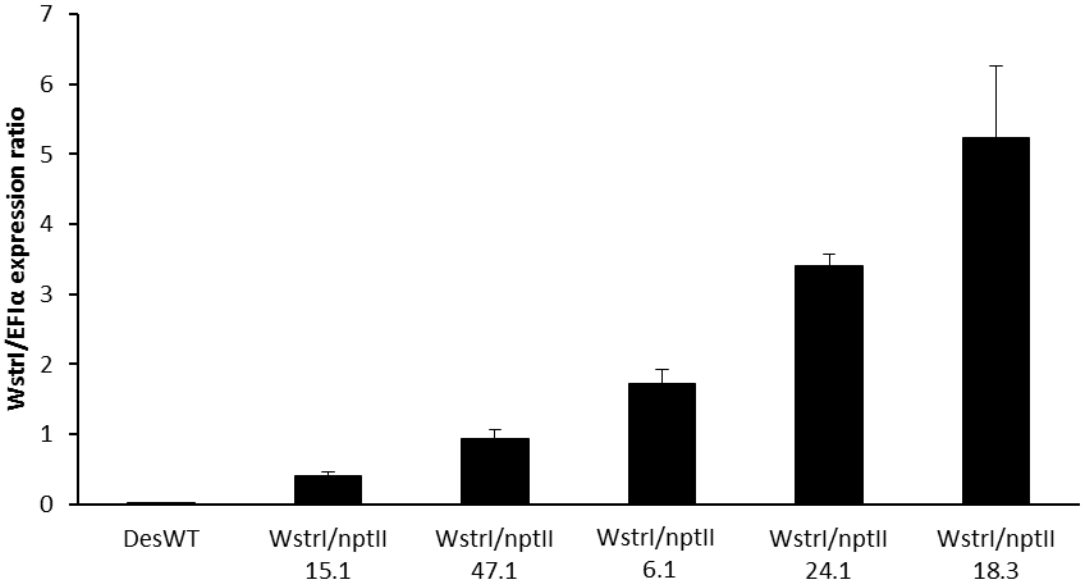

Figure 5.3.5: ***WstrI* transgene characterisation** qRT-PCR expression ratios between *WstrI* and *ef-1α* from the five transgenic lines which were investigated further due to exhibiting consistent expression ratios. Expression levels from 18 plantlets were tested, with the data from these shown in Appendix A.5.2.2. Error bars represent the standard error between technical replicates in the RT-qPCR analysis.

Figure 5.3.5 shows that there is variation in the *WstrI*/*ef-1α* expression ratios between transgenic lines produced. Comparison to the constitutively expressed *ef-1α* indicates that *WstrI* expression is 5.00 ± 1.02 times higher than *ef-1α* in line *WstrI/nptII* 18.3, whereas in line *WstrI/nptII* 15.1 the expression ratio is 0.41 ± 0.04.

These lines were grown in the glasshouse as detailed in Chapter 2.4 from May through to August of 2017, with four biological replicates in a randomised block design. Weekly height measurements were taken for all plants grown during this period, with the average height for the transgenic lines grown shown in Figure 5.3.6. Four of the five lines grown did not show any significant growth differences when compared to the *Désirée* and Empty Vector controls, however, there was one line, *WstrI/nptII* 15.1 which appeared to be stunted and grew slower than the other lines. *WstrI/nptII* 15.1 reached an average height of 90.0 ± 15.3 cm, compared to 156.5 ± 5.2 cm for cultivar *Désirée*.

5.3.2 Growth and Phenotypic Characterisation

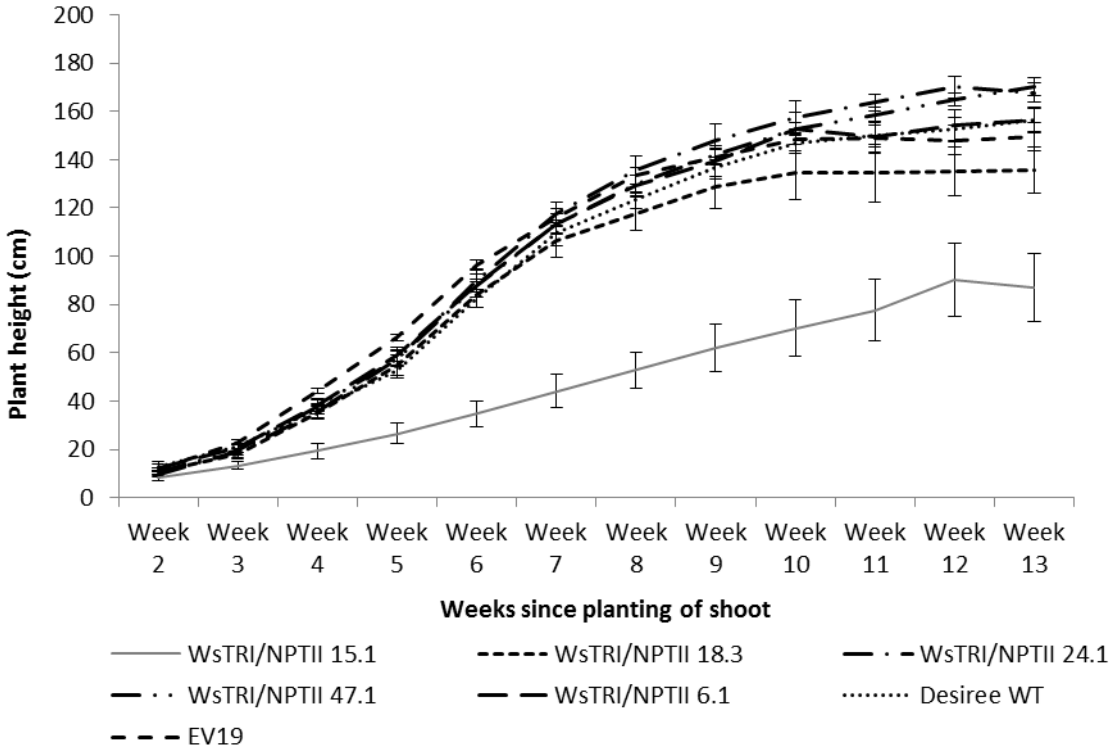

Figure 5.3.6: Plant height measurements during growth of *WstrI* transgenics.

Average weekly plant height measurements for the five *WstrI/nptII* transgenics lines grown in glasshouse conditions. This indicates that four of the five lines grown did not exhibit any adverse growth effects which could result in stunting when compared to the controls, whilst there was one line (*WstrI/nptII* 15.1) that only grew to an average height of 90 ± 15 cm. These are the average of the 4 biological replicates with the Standard Error being shown (n = 4). Cultivar *Désirée* and an Empty Vector (EV) transgenic were also grown as experimental controls.

The growth parameters measured in Figures 5.3.6, 5.3.7 and 5.3.8 indicate that four out of the five *WstrI/nptII* transgenic lines under investigation within this study, did not suffer any adverse phenotypic effects as a result of the *Agrobacterium* transformation process. This is shown through the height chart in Figure 5.3.6, the non-significant differences in biomass produced across the four tissues harvested and finally the carotenoid and chlorophyll abundance in Figure 5.3.8. Conversely, there were highly significant differences in the biomass of the four tissues harvested from *WstrI/nptII* 15.1 when compared to the transgenic and control lines. Whilst, there did not appear to be any difference in carotenoid or chlorophyll content, data from further analysis for this line will not be shown.

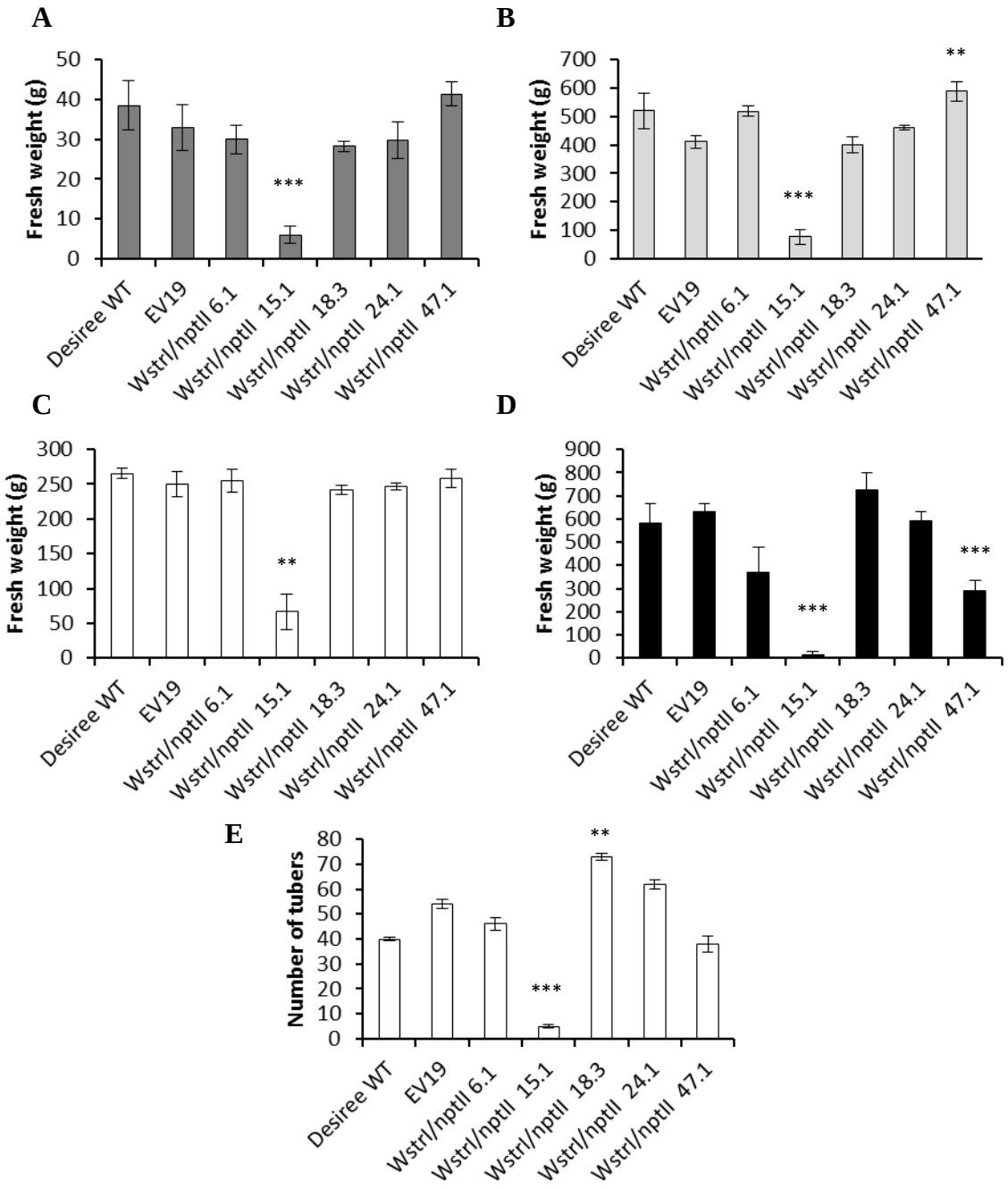

Figure 5.3.7: **Harvested fresh weight potato organ data**.

Panel A = root, B = stem, C = leaf, D = tuber mass, E = tuber number. As indicated in Figure 5.3.6, *WstrI/nptII* 15.1 shows a highly significant decrease in fresh weight when compared to the control lines, ** indicates a significant difference where $P < 0.01$ and *** indicates a significance of $P < 0.001$ ($n = 4$).

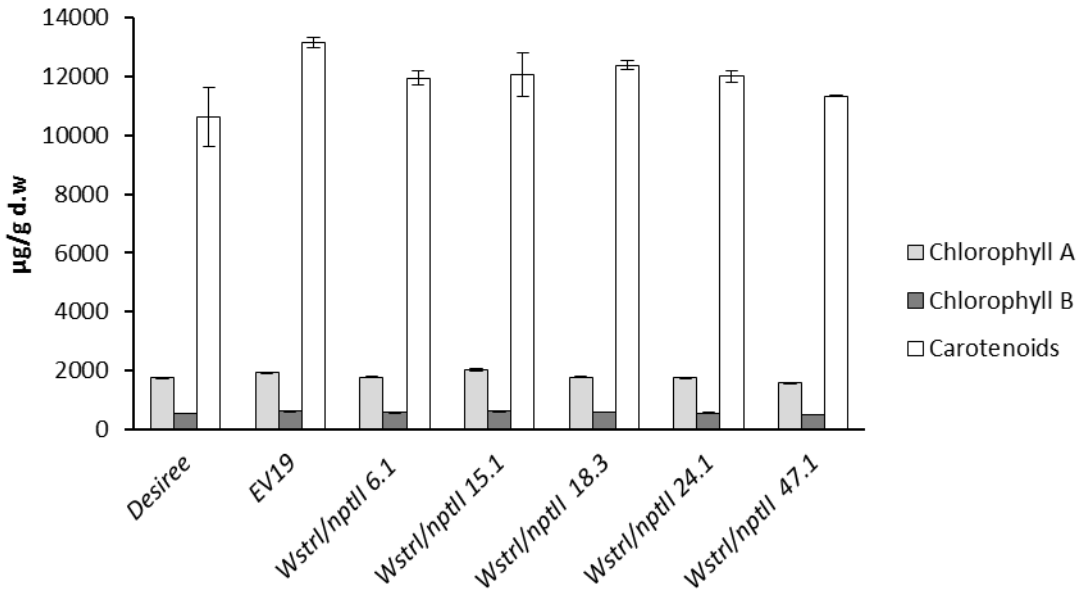

Figure 5.3.8: Analysis of growth characteristic.

Chlorophyll and Carotenoid levels from harvested leaves during week 12 of their growth, showing no significant difference between the transgenic and control lines (n = 4).

5.3.3 Tuber and Root alkaloid content

The tropane and nortropane alkaloid content of harvested tubers and roots can be seen in Figures 5.3.9 and 5.3.10. From the panel of ten tropane and nortropane alkaloids in the MRM method developed in Chapter 3, only three were detected in the tuber and five in the roots. Whilst the same three metabolites, ornithine and the two calystegine's (A_3 and B_2) were detected in both tissues, the detection of pseudotropine and importantly tropine within the root was an indication that the normal metabolic flux at the tropinone branch point may have been altered, with the addition of an active *trI*.

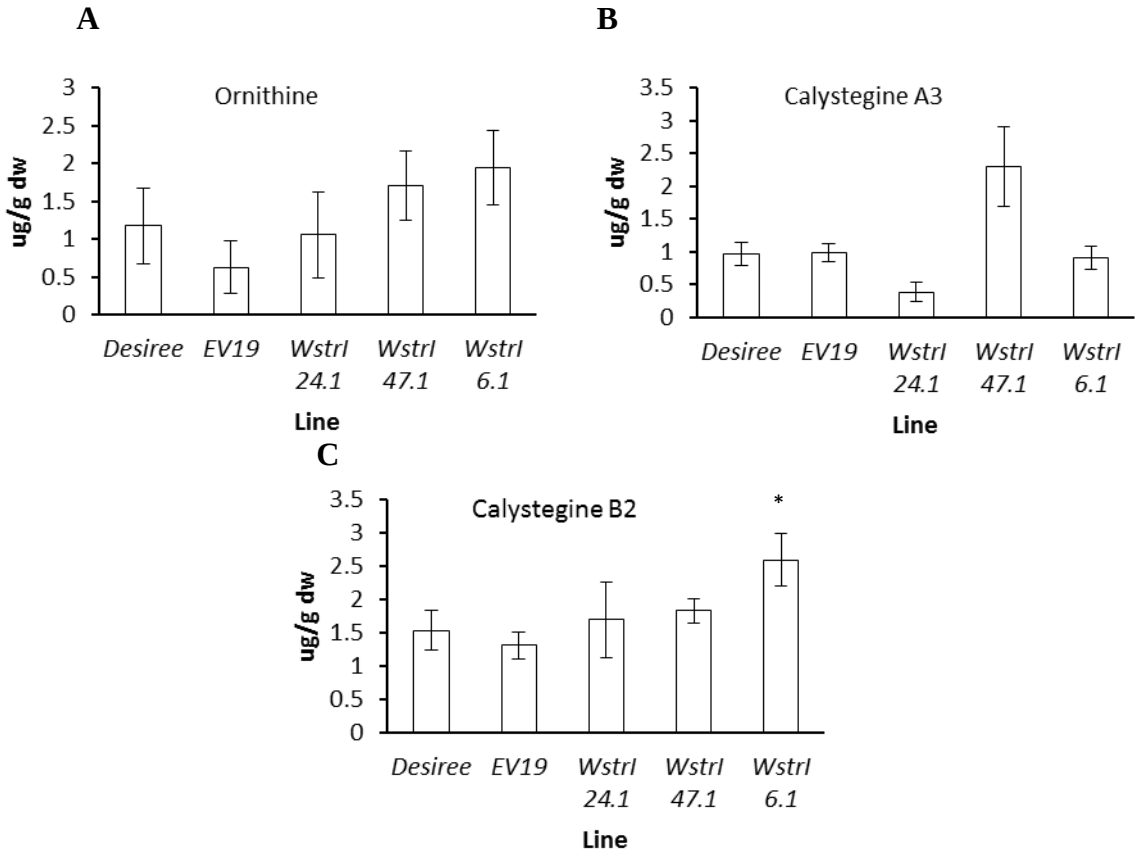

Figure 5.3.9: Tuber metabolite analysis of selected transgenic lines.

Ornithine and tropane alkaloid content of tubers from *WstrI/nptII* transgenic lines compared to controls. Panel A = ornithine, B = calystegine A_3 and C = calystegine B_2. These were the only tropane alkaloid biosynthesis pathway associated metabolites detectable in the tuber. Data generated using the MRM method developed in Chapter 3 and is the result of a single injection from each of the four replicates grown. Control lines in this assay were *Désirée* and EV19 (Empty Vector). * indicates a significant difference where $P < 0.05$ and ** indicates a significance of $P < 0.01$ ($n = 4$) with transgenic lines compared against the controls.

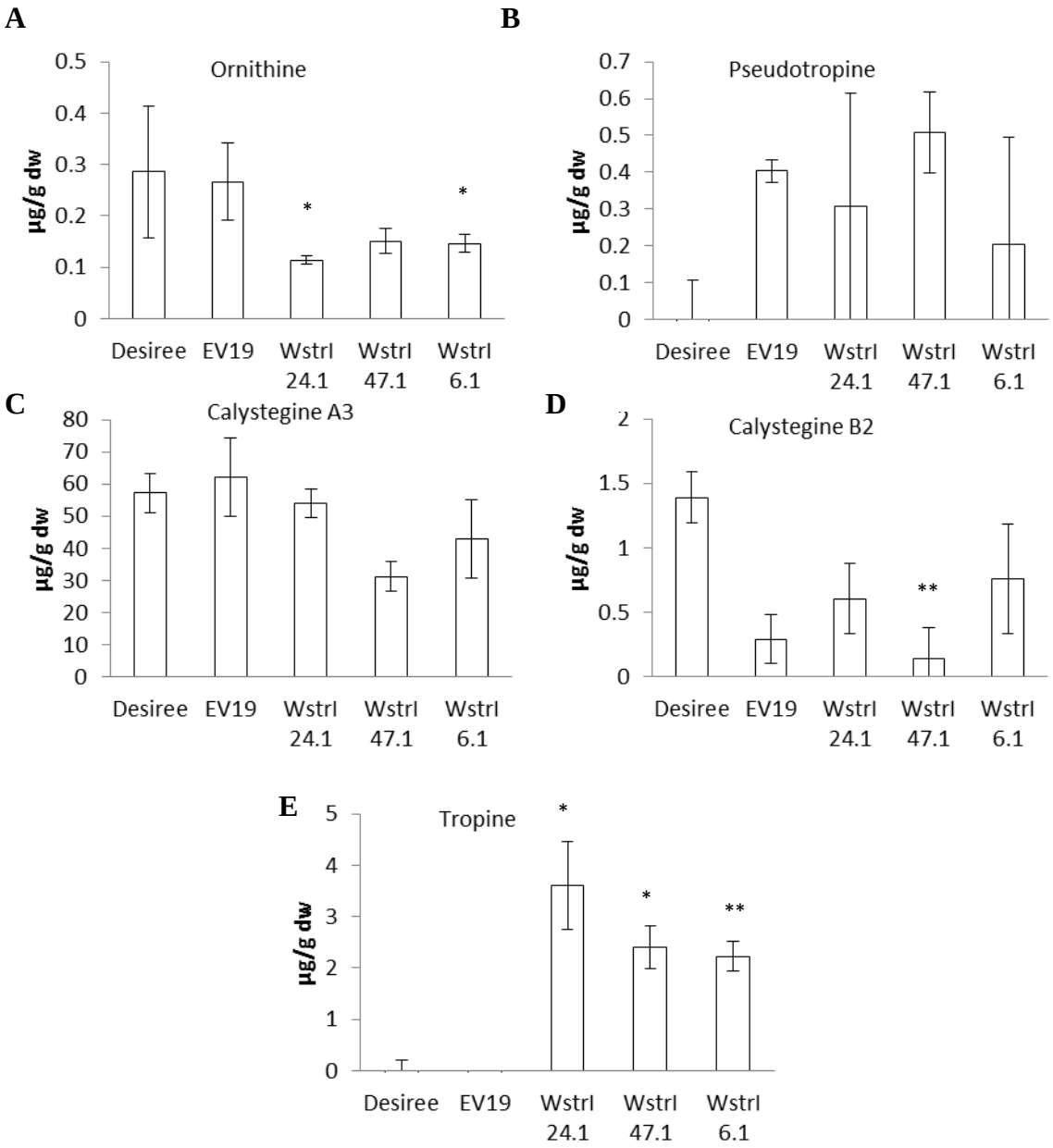

Figure 5.3.10: Root metabolite analysis of selected transgenic lines

Metabolite content of roots harvested from *WstrI/nptII* transgenic lines compared to controls. Panel A = Ornithine, B = Pseudotropine, C = Calystegine A_3, D = Calystegine B_2 and E = Tropine. These were the only tropane alkaloid biosynthesis pathway associated metabolites detectable in the roots. Control lines in this assay were *Désirée* and EV19 (Empty Vector). Data generated using the MRM method developed in Chapter 3 and is the result of a single injection from each of the four replicates grown. The error bars shown is the Standard Error, * indicates a significant difference where $P < 0.05$ and ** indicates a significance of $P < 0.01$ ($n = 4$), with transgenic lines compared against the controls.

5.3.4 Exogeneous tropinone leaf disc assays

Figures 5.3.11 and 5.3.12 show the results from leaf disc assays taken over three different developmental stages for the transgenic and control lines. These time points were at weeks 5, 7 and 11 which correspond to vegetative growth III, tuber initiation I and tuber bulking (Patil *et al*, 2016), which allows for endogenous *trI* expression levels to be compared from cultivar *Désirée* in Figure 5.3.1. With the addition of exogenous tropinone, across all three time points the conversion to pseudotropine is consistent within the lines. The transgenic lines produced significantly less pseudotropine than the control lines (0.61 ± 0.18 µg/g for *WstrI/nptII* 6.1, compared to 5.24 ± 0.44 µg/g FW in cultivar *Désirée* from assay 1). Similarly, with respect to the conversion to tropine, the transgenic lines show increased levels of tropine within the samples. The highest levels of tropine can be seen in the second disc assay where in lines *WstrI/nptII* 6.1 and 24.1 tropine reaches 161.00 ± 3.61 and 156.65 ± 14.52 µg/g FW respectively. In contrast the *Désirée* and empty vector controls contain tropine at levels of 0.63 ± 0.05 and 0.75 ± 0.09 µg/g FW.

RT-qPCR was conducted on the same leaves used in the leaf disc assays to determine the *WstrI* and *SttrII* relative expression levels at these times points. Figure 5.3.12 shows that during the first assay *WstrI* is expressed at twice the level as *ef-1α* for *WstrI/nptII* 6.1 and 24.1, with *WstrI/nptII* 47.1 showing a threefold relative expression increase. For these transgenic lines, in assays 2 and 3 the relative expression levels decrease and are expressed at the same level as *ef-1α*. *SttrII* expression levels appear to fluctuate across the three assays; however, there is no significant difference in the levels of expression between the controls and transgenic lines. Whilst there is expression of *trII* within the transgenic lines, the decrease in pseudotropine in the assays can be attributed to the presence of an active trI resulting in a change in metabolite flux towards tropine.

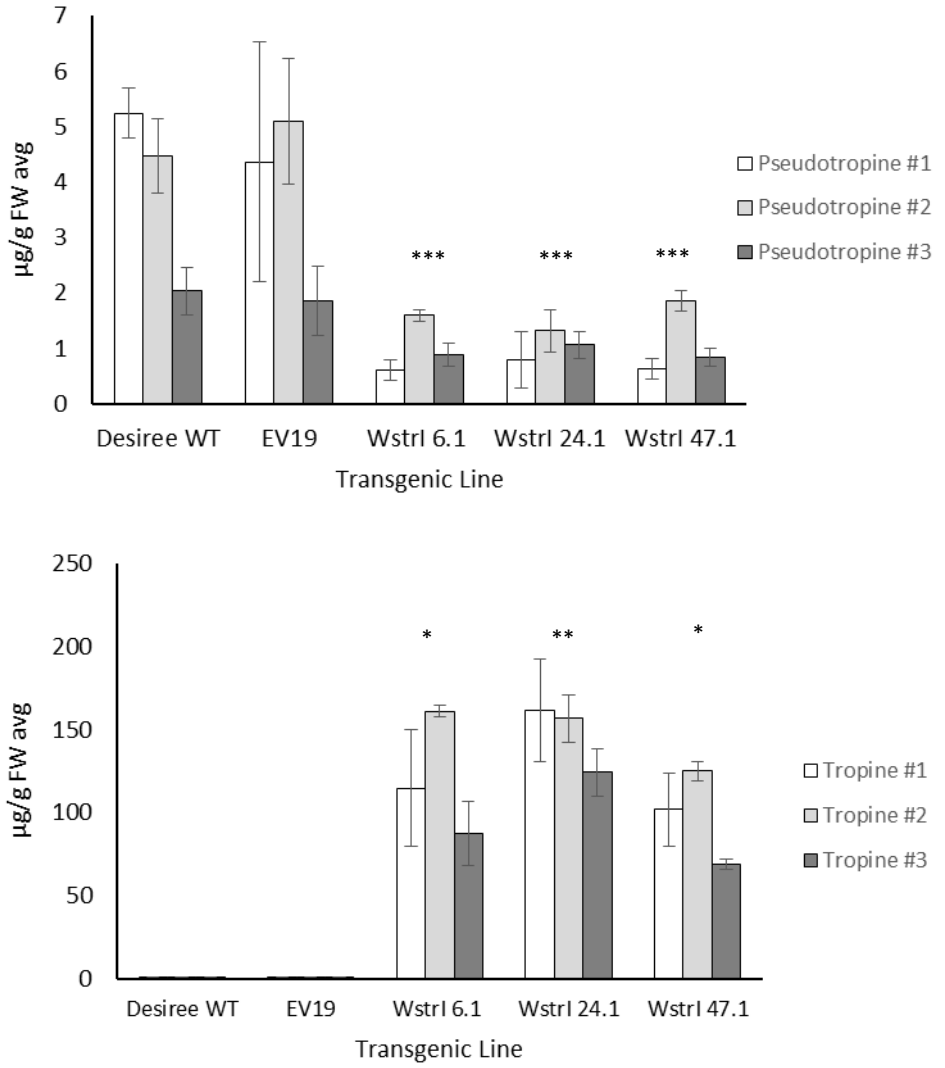

Figure 5.3.11: Pseudotropine and tropine content of *WstrI* transgenic leaf discs. Pseudotropine (top) and tropine (bottom) content of leaf discs from *WstrI/nptII* transgenic lines and controls during three separate assays conducted during plant development. Developmental stages were Vegitative Growth (V.G) III at 5 weeks for assay 1, Tuber Initiation (T.I) I at 7 weeks for assay 2 and Tuber Bulking (T.B) at 11 weeks for assay 3. Exogenous tropinone was applied to these leaf discs, before they were left for 48 hours. Assays were also conducted with KCl applied to leaf discs at the same stages to act as a control (data not shown due to no detectable levels of metabolites from the MRM method). Data generated using the MRM developed in Chapter 3 and is the result of a single injection from each of the four replicates grown. * indicates a significant difference where $P < 0.05$, ** indicates a significance of $P < 0.01$and ** indicates a significance of $P < 0.001$ ($n = 4$) with transgenic lines compared against the controls.

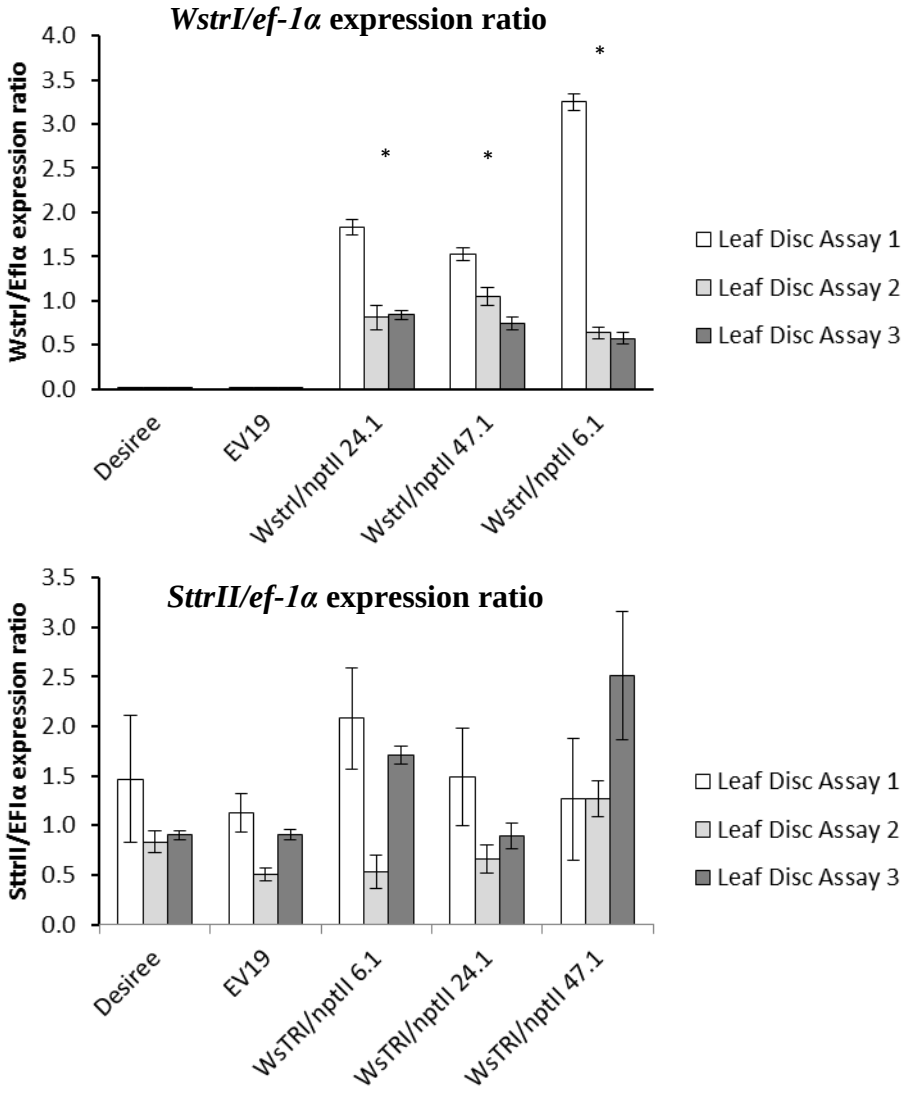

Figure 5.3.12: Tropinone reductase activity from transgenic lines during leaf disc assays. RT-qPCR data showing the *WstrI/ef-1α* (top) and *SttrII/ef-1α* (bottom) expression ratios from *WstrI/nptII* transgenic lines and controls during the three separate leaf disc assays conducted during plant development. Developmental stages were V.G III at 5 weeks for assay 1, T.I I at 7 weeks for assay 2 and T.B at 11 weeks for assay 3. The *WstrI/ef-1α* expression ratio shows that there is a slightly higher level of *WstrI* expression within the leaf tissue during the earlier developmental stages, with this decreasing to a comparable level to *ef-1α* for the latter two assays. *SttrII* was tested to ensure there was no effect on this gene through the transformation process and to ensure that the gene was still expressed during this assay. There is no significant difference in expression ratios between the *WstrI/nptII* transgenics for *trII* when compared to the controls. * indicates a significant difference where $P < 0.05$ ($n = 4$)

5.3.5 Exogeneous tropinone tuber sprout feeding assays

Tuber sprout feeding assays were conducted as this tissue is reported to be the site of nortropane alkaloid biosynthesis and contains a high level of calystegines (Keiner and Dräger, 1999). It is therefore of interest to investigate if the presence of an active *trI* within this tissue influences the nortropane alkaloid content, and if there is an increase in any tropane alkaloid associated metabolites. Exogenous tropinone and KCl were added to sprouts from transgenic and control lines and these sprouts were kept under 16:8 hour light/dark conditions for 48 hours, before undergoing metabolite analysis.

Figure 5.3.13 shows that for the tropinone fed lines there were some significant differences when compared to the control. Detection of pseudotropine for lines *WstrI/nptII* 6.1 and 24.1 indicates that there is a significant difference in the concentration throughout the sprout when compared to the tropinone fed control lines ($P<0.01$). Other significant differences can be seen for line *WstrI/nptII* 24.1 with respect to calystegine B_2 and *WstrI/nptII* 47.1 for tropine ($P<0.05$ in both cases). Tropine levels in the sprouts of the transgenic lines was 62.2 ± 22.9, 71.8 ± 27.3 and 77.7 ± 15.3 µg/g DW for *WstrI/nptII* 6.1, 24.1 and 47.1 respectively. In *WstrI/nptII* 47.1 for metabolites downstream of tropine displayed higher levels compared to the control and other transgenic lines, from both tropinone and KCl fed sprout samples.

There are indications that the downstream tropane alkaloids are detectable with levels variable between the transgenic lines and controls. *WstrI/nptII* 47.1 as well as exhibiting the highest levels of tropine, displayed the highest levels of hyoscyamine, anisodamine and scopolamine when compared to sprouts from the other transgenic lines and *Désirée* control. Variation in tropane alkaloid levels was also detected between the control and tropinone fed sprouts and these can be seen in Figure 5.3.13. The levels of hyoscyamine, anisodamine and scopolamine in the *Désirée* tropinone fed lines are; 0.01 ± 0.00, 0.10 ± 0.01 and 0.19 ± 0.02 µg/g DW. Whereas, in *WstrI/nptII* 47.1 tropinone fed lines the levels of these same three tropane alkaloids was 0.32 ± 0.25, 0.21 ± 0.07 and 0.42 ± 0.14 µg/g DW. This indicates that, at least for this line there is a diversion of tropinone flux along the tropane alkaloid biosynthesis pathway, when in the presence of exogenous tropinone.

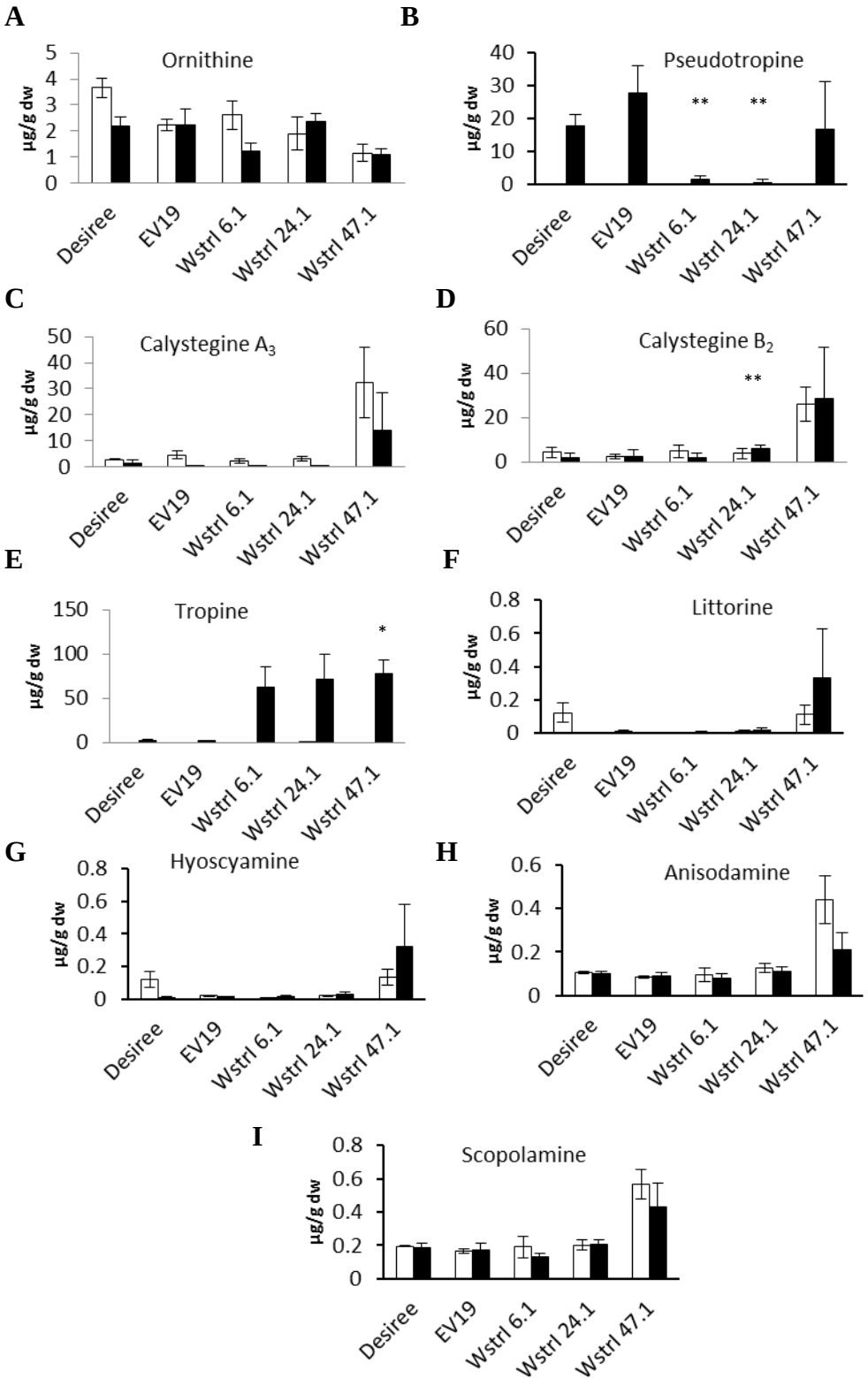

Figure 5.3.13: **Detection of tropane alkaloids in sprouts from exogenous feeding assay**. Detection of metabolites from the tropane and nortropane alkaloid biosynthesis pathway from tuber sprouts which have been fed exogenous tropinone (■) and the controls which were fed KCl (□). Each panel represents a different metabolite with: A = ornithine, B = pseudotropine, C = calystegine A_3, D = calystegine B_2, E = tropine, F = littorine, G = hyoscyamine, H = anisodamine and I = scopolamine. * indicates a significant difference where $P < 0.05$, ** indicates a significant difference where $P < 0.01$ (n = 4).

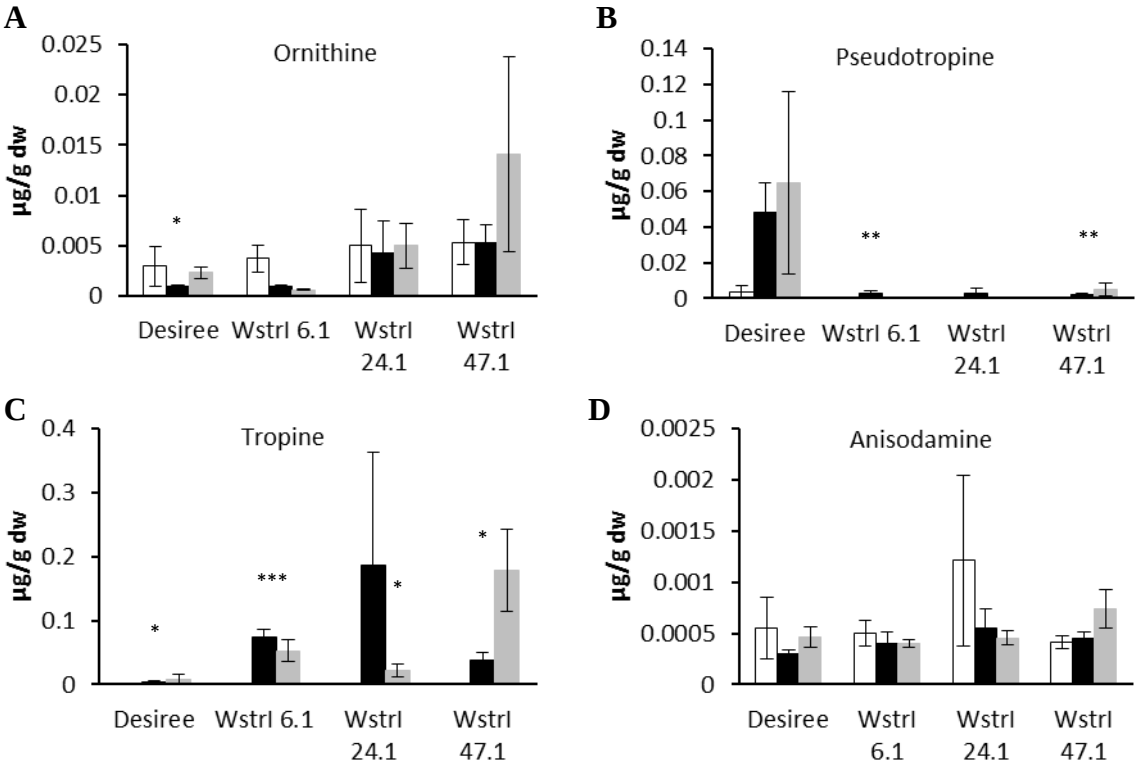

Figure 5.3.14: **Detection of tropane alkaloids in plantlets grown in the presence of methyl jasmonate and tropinone.**

Detection of metabolites from a plantlet feeding assay, where plantlets were grown on MS20 media (□), MS20 + 5 mM tropinone (■) and MS20 + 5 mM tropinone + 1 mM methyl jasmonate (■). Data is shown for the metabolites which were detected within the samples. Each panel represents a different metabolite with: A = ornithine, B = pseudotropine, C = tropine, D = anisodamine. * indicates a significant difference where $P < 0.05$, ** indicates a significant difference where $P < 0.01$, *** indicates a significant difference where $P < 0.001$ ($n = 4$)

Assays which involved feeding plantlets on three different media types (MS20 as a control, MS20 with 5 mM tropinone and MS20 with both 5 mM tropinone and 1 mM methyl jasmonate) were conducted to determine if methyl jasmonate can enhance tropine conversion. Figure 5.3.14, indicates that the plantlets which were grown in the presence of methyl jasmonate, with the exception of *WstrI/nptII* 47.1 in the case of ornithine and tropine do not exhibit an increase in metabolite content. Of the 11 metabolites used in the MRM detection method, only four were detectable within these samples. It can be noted that the plantlets which were grown in the presence of tropinone contained higher levels of tropine and lower levels of pseudotropine

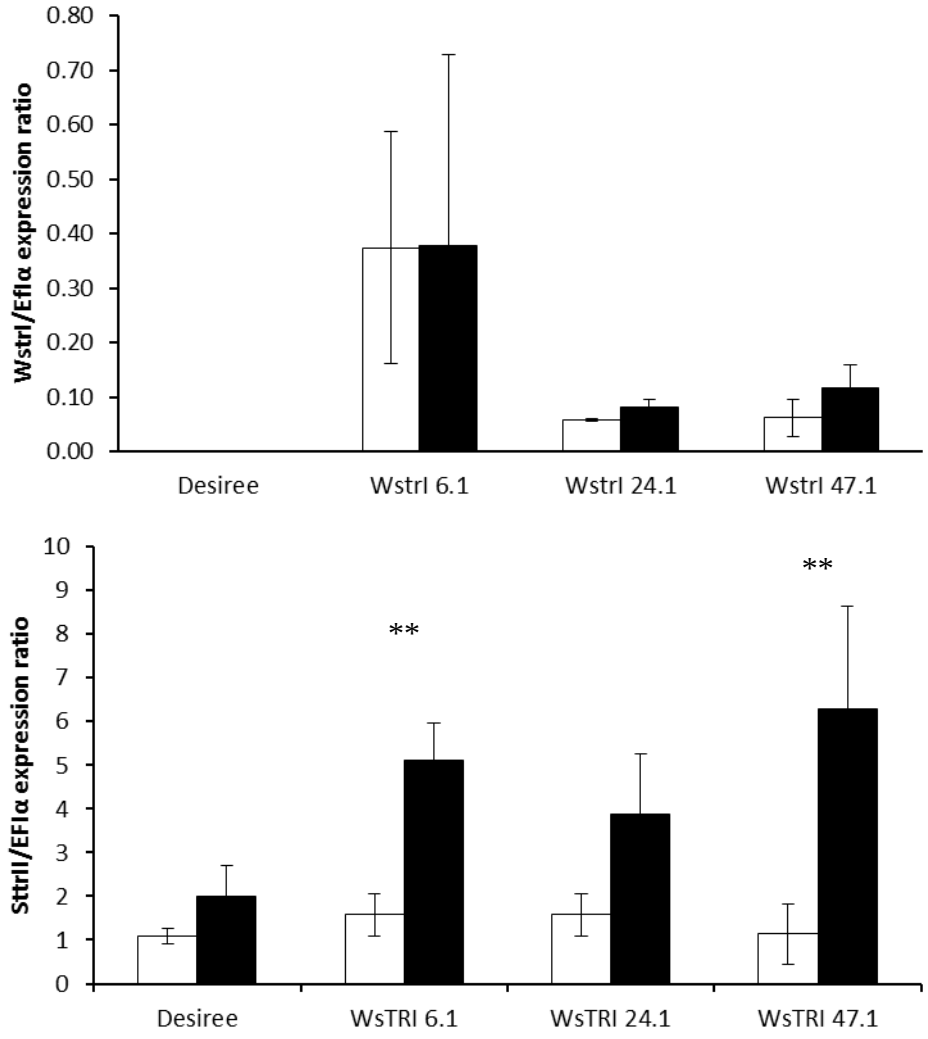

Figure 5.3.15: ***WstrI* and *trII* expression data from methyl jasmonte application assays.** RT-qPCR data showing the *WstrI/ef-1α* (top) and *SttrII/ef-1α* (bottom) expression ratios from *W*strI/nptII transgenic lines and controls for samples from the plantlet feeding assay. Plantlets grown on control (□), and tropinone + methyl jasmonate (■) media were tested to see if the addition of the methyl jasmonate elicitor had any effect upon the expression of *WstrI* and *SttrII*. ** indicates a significance of $P < 0.01$

compared to cultivar *Désirée*. This result supports data seen in the leaf disc and sprout feeding assays (Figures 5.3.11 and 5.3.13). RT-qPCR assays were also undertaken to determine if the addition of methyl jasmonate affected the expression of *WstrI* and *SttrII*. Figure 5.3.15, indicates that *WstrI* expression ratios in plantlets grown in the presence of methyl jasmonate are not different to those grown on the control media, whereas with respect to *SttrII* both the transgenic and *Désirée* plantlets show an increase in *trII e*xpression in the presence of methyl jasmonate compared to those grown on control media.

5.4 Discussion

5.4.1 Patterns of *trI* expression in potato and tropane alkaloid producing plants.

The *trI* expression level within the roots of the current commercial tropane alkaloid production platform *Duboisia myoporoides* has been reported for the 6-week, 3 month and 6 months growth stages (Kohnen *et al*, 2017). Highlighting the level of expression within this species at these time points and within the root tissue is of importance as the roots are the site of tropane alkaloid biosynthesis (Ziegler and Facchini, 2008) and whilst a direct comparison to the expression of *trI* in potato is unable to be inferred, trends in *trI* expression may be identified.

trI expression within *Duboisia* roots has been shown to be 2.5 to 5-fold higher than the endogenous control *gadph* at the 6 week and 3-month time points respectively. Within potato, *trI* expression levels from plants of the same age, show levels which are 25-fold lower at 6 weeks, rising to only 5-fold lower at 6 months. Similarly, *trI* expression from *Withania somnifera*, is higher in the root tissues compared to leaf and stem (Kushwaha *et al*, 2013). Although Kohnen *et al*, (2017) use *gadph* as the endogenous control in their study and *ef-1α* is used in this study, these two housekeeping genes have been shown to exhibit similar gene expression levels and stability. This can be seen from comparative analysis conducted by Rocha *et al* (2016) and Boa *et al*, (2016).

Interestingly, *trI* expression levels within other tissues of potato show a different trend to that seen in the roots. *trI* expression in potato leaves is approximately 3 to 10-fold higher at the 6 week and 6-month time points. The determination that the expression level of *trI* is higher in leaf and stem potato tissues compared to the roots suggests that whilst *trI* may be expressed, tropinone availability in these tissues is a limiting factor. Previously, it was reported that within roots of potato, trII is more active and more highly expressed than trI (Dräger, 2006). trII drives the conversion of tropinone to pseudotropine and suggests that any tropinone present is converted before translocation into the stem or leaves can take place. Therefore, tropine is unable to be accumulated in these tissues. This is important as it aids the understanding of why tropane alkaloids, or at least, tropine does not accumulate in the roots or other tissues of potato.

5.4.2 Phylogenetic analysis of tropinone reductases

The phylogenetic analysis of tropinone reductase enzymes from members of the solanaceae and other plant families which convert tropinone can be seen in Figure 5.3.2. These form three distinct groups. Group I encompass trI proteins, Group II contains the trII proteins and both are from only solanaceous species. Group III contains proteins from other species. From this analysis there is 98 % trI amino acid similarity between potato and Black Nightshade (*Solanum nigrum*), and it has been shown in previous studies that *Solanum nigrum* does not contain tropane or nortropane alkaloids (Dräger *et al*, 1994).

There are regions of similarity within *trI* nucleotide sequences from species which produce tropane alkaloids and those that do not. However, it is the differences which may explain the lack of functionality in non-producers. Comparing the *trI* CDS sequences between *Withania somnifera* and potato there are regions which contain single nucleotide polymorphisms. These polymorphisms result in a change in the amino acid sequence possibly influencing protein structure and function. It should be noted that the amino acid sequences for the conserved SDR motifs, and those relating to tropinone binding are identical. The structural differences which may be presented by these comparatively minor changes and the low expression rates of *trI* within roots, suggests that tropine is not readily formed in potato as trII is more active in this tissue.

5.4.3 Detectable endogenous tropane and associated alkaloid content

Tropine levels within the roots of transgenic lines in this study were found to be 500-fold lower than previously reported levels present in *Withania somnfiera* roots (Kushwaha *et al*, 2013). The levels of calystegine A_3 and B_2 within the roots of *WstrI/nptII* 47.1 is significantly lower than control plants. In these samples there is an almost 50% reduction in calystegine A_3 and a 90% reduction in B_2 per dry weight mass. Küster *et al* (2017) analysed the fresh weight content of calystegines in transgenic tuber sprouts. In *SttrI* over-expressing lines they found that the concentrations of calystegine A_3, B_2 and B_4 were significantly lower than in wild type controls. The reduction in the calystegine content of these tuber sprouts, follows the similar patterns seen in Figure 5.3.10. Although the tuber sprouts and roots are different tissues this is an interesting

finding, suggesting that there has been manipulation of the biosynthetic pathway at the tropinone branch point.

Tubers were analysed for their concentrations of tropane, nortropane and associated metabolites using a targeted MRM approach developed using pure standards. Only three of the ten metabolites targeted were detected; ornithine, calystegine A_3 and B_2. There was a significant reduction in calystegine A_3 levels in line *WstrI/nptII* 24.1, which exhibited a 50% reduction compared to controls. Interestingly in line *WstrI/nptII* 6.1 there was a 30% increase in calystegine B_2 levels compared to controls.

Tropine was not detected in tubers of transgenic lines analysed within this study. Tropine accumulation within the roots of *Duboisia* and other solanaceous species has not been extensively reported due to the rapid conversion towards the tropane alkaloids hyoscyamine and scopolamine. From available literature, the levels of tropine in 31-day root cultures of *Atropa belladonna* is less than 5 µmol g^{-1} (DW). The levels detected within the roots of transgenic line *WstrI/nptII* 47.1 equates to 896 µmol g^{-1}. This shows that the transgenic lines exhibit higher detectable levels of tropine than some known tropane alkaloids producers. However, these producers accumulate the downstream tropane alkaloids suggesting that there are further lesions in the potato pathway downstream of this step.

Previous studies have reported that tropine levels can be enhanced and produced in tuber peel tissue through alterations to carbohydrate metabolism, this was not investigated in this study. Richter *et al*, (2007), demonstrated that in invertase over-expression and down-regulating sucrose synthase lines there was a 2.5 to 3-fold increase in tropine accumulation. These results, as well as others reported in previous literature (Rothe *et al*, 2001) indicate that sucrose presence can influence tropane alkaloid biosynthesis. The addition of sucrose to *Atropa belladonna* root cultures primarily increased calystegine content (Rothe *et al*, 2001), but there was a slight, non-significant increase in hyoscyamine. These data suggest that sucrose is having an effect on the nortropane alkaloid arm, upregulating that side of the pathway.

5.4.4 Tropinone feeding assays

Application of exogenous substrates to determine the functionality of metabolomic pathways is a useful tool, ensuring the required substrate is present in sufficient concentration for potential changes to be detected.

Küster *et al,* (2017) conducted leaf assays on over-expressing *SttrI* lines where they demonstrated that tropine accumulation was between 2 and 5-fold greater than in wild type controls when supplied with exogenous tropinone. As tropine is accumulated in wild type leaves, this increase in tropine accumulation correlates with the higher levels of *trI* expression observed. However, it should be noted that in the wild type, pseudotropine levels were 4-fold greater than detectable tropine. Within the *SttrI* over-expressing lines generated by Küster *et al,* (2017) pseudotropine levels were 4 to 6-fold greater than tropine levels. So, whilst the accumulation of tropine within their *SttrI* transgenics was enhanced, there was no reduction in pseudotropine accumulation.

trI overexpression lines produced within thus study displayed the opposite effect. In the leaf disc assays from all lines, pseudotropine decreased, tropine increased and was significantly higher than in the controls. Although the level of tropine detected in the controls was negligible, the level of tropine accumulation across the leaf disc assays suggests the generated transgenic lines are comparable to Küster *et al,* (2017) on a concentration basis. The reduction of pseudotropine coupled with no significant difference in *trII* expression between the leaf disc assays suggests that the *trI* transgene within the *WstrI/nptII* transgenic lines is more efficient at converting tropinone. Therefore diverting substrate flux away from the nortropane alkaloid biosynthesis arm of the pathway.

The leaf assay experiments described in Küster *et al,* (2017) are not directly comparable to those conducted in this study. Firstly, the leaves used in this study were one week older at the time of the first experimental assay. Secondly, the exogenous tropinone application was applied for 48 hours and not 8 days as in Küster *et al,* (2017). Despite these two differences, the concentration of tropinone used, growth room/ambient light conditions and temperature were all comparable Tropinone application was reduced to 48 hours to reduce the potential risk of bacterial contamination. Whilst the risk of this occurring was low, it was deemed appropriate

with using an unsterile environment, as well as samples being made up of multiple small leaf discs which allowed for maximum tropinone infiltration into the plant tissue. It can be speculated that accumulation of pseudotropine and tropine could have reached comparable levels to that reported in Küster *et al,* (2017) if left for the same amount of time. However, this was not tested.

In tuber sprout assays, transgenic lines exhibited significant differences to the *Désirée* control. Tubers from the *WstrI/nptII* 47.1 contained elevated levels of both calystegines A_3 and B_2, whilst line *WstrI/nptII* 24.1 tubers exhibited a significant difference between the fed and unfed calystegine B_2 content. This difference showed that there was an increase in calystegine B2 content within the tropinone fed lines. Petterson *et al* (2013) show the calystegine A_3 and B_2 content of cultivar *Désirée* sprouts are 15 and 21 µg/g (FW) respectively. In the unfed and fed sprouts of line *WstrI/nptII* 47.1 the A_3 content was 32.4 ± 13.5 and 23.1 ± 14.1 µg/g (DW). The calystegine B_2 content was 26.1 ± 7.7 in unfed sprouts and 28.6 ± 11.5 µg/g (DW) in fed sprouts. Whilst the concentration of the calystegine and other metabolites would be lower in a fresh weight sample (Petterson *et al,* 2013), the indication that calystegine content within this study is higher than the controls is an interesting point differing from previously published research. The levels of pseudotropine in *WstrI/nptII* 47.1 are not different to the levels in the controls. One potential hypothesis to explain why there is greater accumulation of calystegines, but no change to pseudotropine levels within *WstrI/nptII* 47.1 could be that *trII* expression within tuber sprouts has been unaffected by the increase in *trI* expression. With both enzymes competing directly for tropinone, both arms of the tropane alkaloid biosynthesis pathway are not active.

5.4.4.1 Use of elicitors to potentially enhance tropine production.

In previous studies methyl jasmonate has been shown to upregulate the expression of genes along the tropane alkaloid biosynthesis pathway (Kang *et al,* 2004; Deng 2005; Kushwaha et al, 2013). Kushwaha *et al,* (2013) determined that the relative expression of *trI* within *Withania* leaf tissue exposed to methyl jasmonate for 6 hours was between 5 and 8-fold higher after application. However, following 48 hours of exposure, the transgenic and control plantlets did not show any differences in expression (Kushwaha *et al,* 2013). In this study the *WstrI* expression levels in transgenic potato plantlets grown in the presence of methyl jasmonate showed no

significant difference to controls. However, the expression of *trII* in transgenic lines showed between a 2 and 6-fold increase, with a 1-fold increase in cultivar *Désirée*. Deng, (2005) examined the effects of methyl jasmonate upon the formation of tropine and pseudotropine in *Datura stromonium*. Deng (2005) demonstrated the concentration of tropinone, tropine and pseudotropine was enhanced by addition of 1µM methyl jasmonate. The increase in these metabolites was between 1.2 and 1.4-fold change when compared to controls. It was also noted that the levels of *pmt* in the roots were also enhanced following methyl jasmonate addition, which was not investigated within this study. The reported effects on genes upstream of the tropinone branch point by the elicitor could indicate that that there is greater availability of tropinone. This was not tested within the assays conducted in this study, however, could be of interest to see if there is an increase in tropinone/pseudotropine or tropine accumulation within root or tuber sprouts from potato.

Methyl jasmonate has been shown to increase hyoscyamine in *Scopolia* root cultures (Kang *et al*, 2004) as well a decrease in calystegine levels after 48 hours, with a predominant effect being seen on the tropane alkaloid pathway. Coupling the use of methyl jasmonate with manipulation to carbohydrate metabolism may enhance the effects to this pathway and although there does not appear to be a study which looks at both conditions it may provide further insights into the biosynthetic pathway within potato.

5.4.5 Presence of high value tropane alkaloids

In this study high valued tropane alkaloids have been detected within tuber sprout and methyl jasmonate feeding assays. The tropane alkaloids hyoscyamine, anisodamine and scopolamine were detected in tissues from both assays within transgenic and control lines. These alkaloids have not previously been detected within tissues of *Solanum tuberosum* and although the concentrations of these compounds are extremely low, the highly sensitive detection and quantification method which was developed in chapter 3 was sufficient to detect and accurately quantify them.

Anisodamine was the only tropane alkaloid detected in the *Désirée* and *WstrI/nptII* 47.1 plantlets from methyl jasmonate assays. Whereas, tuber sprouts from the same lines contained detectable levels of hyoscyamine, anisodamine and

scopolamine. The *WstrI/nptII* transgenic lines contained between 2 and 135-fold higher levels than measured in the *Désirée* control line.

The detection of these alkaloids is of interest as it suggests there is activity within the tropane alkaloid biosynthesis pathway, in the tuber sprout and young plantlet tissues. With higher levels of these metabolites being detected within tuber sprouts and is the site of the nortropane alkaloid biosynthesis pathway (Keiner and Dräger, 2000), it could be suggested that tuber sprouts are a candidate tissue to undergo further manipulation. This may enhance the production of tropane alkaloids, due to their ability to store these alkaloids at higher concentrations. From the work conducted in chapter 4, which suggests that the two annotated *h6h* genes within *Solanum tuberosum* genome database are non-functional, the development of *WstrI/h6h* transgenics using a bona-fide *h6h* gene may elucidate greater accumulation of the commercially interesting tropane alkaloids.

5.5 Summary

In summary, transgenic potato lines over-expressing *trI* from *Withania somnifera* were generated and underwent analysis to determine if there was any change to the endogenous tropane alkaloid profile. The transgenic lines showed a diversion in the pathway flux of the substrate tropinone, away from pseudotropine and towards tropine, which is a step in the production of downstream alkaloids and one of the primary objectives of this study. There was also a reduction of pseudotropine by almost 80% in some lines, whilst no significant effect upon *trII* expression could be measured. This suggests that the enzyme produced from the *WstrI* transgene outcompetes trII for access to the substrate tropinone.

Moving forward, it would be of scientific and commercial interest to further develop tools which can enhance the production of tropine within the highly efficient potato lines and then couple these with enhancements to the downstream genes. Previous discussion regarding carbohydrate metabolism enhancing the tropane alkaloid biosynthesis pathway more efficiently than methyl jasmonate and other elicitors opens further avenues of pursuit. The over-expression of invertase within potato (Richter *et al*, 2007) and information published on the effects of additional sucrose over elicitors in *Atropa belladonna* upon tropane alkaloid biosynthesis (Rothe *et al*, 2001), suggest that changing multiple conditions to elicit the best enhancement may be of interest. If this approach was to be taken, there is potential to achieve enhancement across the whole pathway in a simple step.

Chapter 6: Effects of *tropinone reductase II* down-regulation and the simultaneous effects of *tropinone reductase II* down-regulation and *WstrI* overexpression in *Solanum tuberosum.*

6.1 Introduction:

Tropinone reductase II (trII) is known to be active within potato tissues, and in particular sprouting tubers (Kaiser *et al*, 2006), which contain high levels of calystegines. *trII* expression and enzymatic activity has been shown to be higher than *trI* (331,000 pk_at/mg compared to 530 pk_at/mg protein, respectively (Kaiser *et al*, 2006)) in most tissues of potato plants. As tropinone does not accumulate Richter *et al*, (2007) concluded that it is the availability of tropinone and not trII activity which is the rate limiting factor in the formation of calystegines.

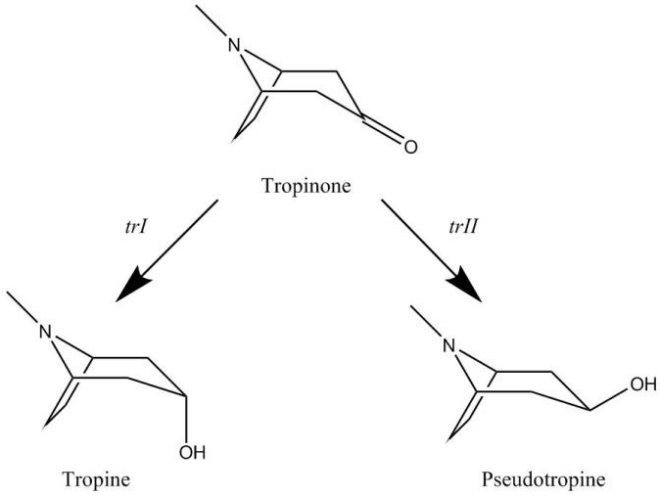

Figure 6.1.1: **The tropinone branch point**.

Schematic representation of the tropinone branch point, with the point of emphasis being trII catalysing the conversion of tropinone to pseudotropine.

Calystegines are polyhydroxy alkaloids (shown through the structure of calystegine A_3 within the biosynthetic pathway in Figure 1.2). As well as displaying glycosidase inhibiting activity, calystegines have also been investigated due to indications that they have antiviral and immunostimulatory activity (Molyneux *et al*, 1993). Calystegines have been found within members of the Solanaceae, the Convolvulaceae, and the unrelated family, the Moraceae (Schimming *et al*, 2005). The Solanaceae and the Convolvulaceae are two plant families which belong to the Solanales. Within the Solanaceae, Bekkouche *et al*, (2001) determined the distribution of eight nortropane alkaloids within eight different species, from seven genera. It was determined that from the calystegines being investigated there were differences to the overall profile exhibited. For example, the profile from aerial parts of *Atropa belladonna* and *Hyoscyamus albus* were identical (with A_3, B_1, B_2, B_3 and N_1 being

found), whereas, within *Withania frutescens* and *Withania somnifera* there were major differences with the profiles of calystegine found. Only B_2 and C_1 were detected in *Withania somnifera* and A_3, B_1, B_2, B_3, C_1 and N_1 were detected in *Withania frutescens*. It was also noted that calystegine B_2 was found in seven of the eight genera studied, which aligns with the finding of Friedman *et al*, (2003) and Petersson *et al*, (2013) where calystegine B_2 was the most abundant nortropane alkaloid within potato tuber.

Keiner *et al*, (2000) demonstrated that in sprouting potato tubers, the highest calystegine content occurs five months after being kept in cold storage within the sprouting eyes of the tuber. The sprouting eyes are when there is < 1 mm of white shoot appearing from eyes. As sprout length increased over a further three months, calystegine content decreased by approximately 50 %. This decrease, as the authors state, is on a fresh mass basis and not solely due to the increase in water content within the sprouts. Other potato tissues have shown that calystegine content varies across developmental stage and tissue type. Primary aerial leaves and roots of emerging small plants contain approximately the same concentration and profile of calystegines (Keiner and Dräger, 2000). The highest concentrations are seen when tuber initiation begins. As maturation and senescence occurs, calystegine content across all tissues decreases. The role of calystegines is to attract root rhizobia to help promote growth in early plant development (Höke and Dräger, 2004). Thus, the requirements for nortropane alkaloids within plant tissues, particularly the roots decreases throughout plant development.

The aim of this study is to inhibit the conversion of tropinone into the nortropane alkaloids providing a greater substrate concentration for conversion towards the tropane alkaloid biosynthesis pathway. This will be accomplished through the generation of independent antisense *SttrII* transgenic lines (As*trII*), as well as transgenic lines which over-express *WstrI* whilst downregulating *SttrII.* Within the *SttrII* down-regulated lines, it is of interest to see if tropinone flux is diverted away from conversion to pseudotropine and if there is any endogenous *trI* activity resulting in tropine formation. With the co-transformed *WstrI* and As*trII* lines it is of interest to investigate whether *WstrI* activity can disrupt the flux of tropinone towards pseudotropine more efficiently than the *SttrII* down-regulating lines, and whether there is a resultant increase in concentration of tropine.

6.2 Materials and Methods

6.2.1 Production of plasmid and trasngenics

As in chapter 5, the vector was confirmed by restriction endonuclease digest and Sanger sequencing before being electroporated into *Agrobacterium tumefaciens* (section 2.5.4.2). *Agrobacterium* mediated transformation into *Solanum tuberosum* cultivar *Désirée* (in the case of 3Ω1 Tnos:*nptII*:Pnos 35sCaMV:As*trII*:Tnos and of 3Ω1 Tnos:*nptII*:Pnos 35sCaMV:*WstrI*:Tnos to produce single As*trII* lines and co-transformed As*trII/WstrI* lines) or in cultivar *Bintje* to produce single As*trII* lines. Figures 6.2.1 through 6.2.3 show the same methodology for the production of transgenic lines as seen in Chapter 5, through the extraction of genomic DNA and testing for the presence of *nptII* (with *ef-1α* as a loading control). For the positive lines from this analysis, further PCR analysis was undertaken to the determine if the 35sCaMV:As*trII*:Tnos cassette was present in the single As*trII* transgenic lines, and if both the 35sCaMV:As*trII*:Tnos and 35sCaMV:*WstrI*:Tnos were present in the co-transformed lines.

6.2.2 Biological replication

Within most assays, there were 4 biological replicates per line. The only deviation from this was for line *WstrI*/As*trII*/*nptII* 3.2 in the exogeneous tropinone leaf assay where n = 2, and for *Wstr*I/As*trII*/*nptII* 3.1 and 3.2 in the exogeneous tropinone tuber sprout assay where n = 2 and n = 1 respectivley.

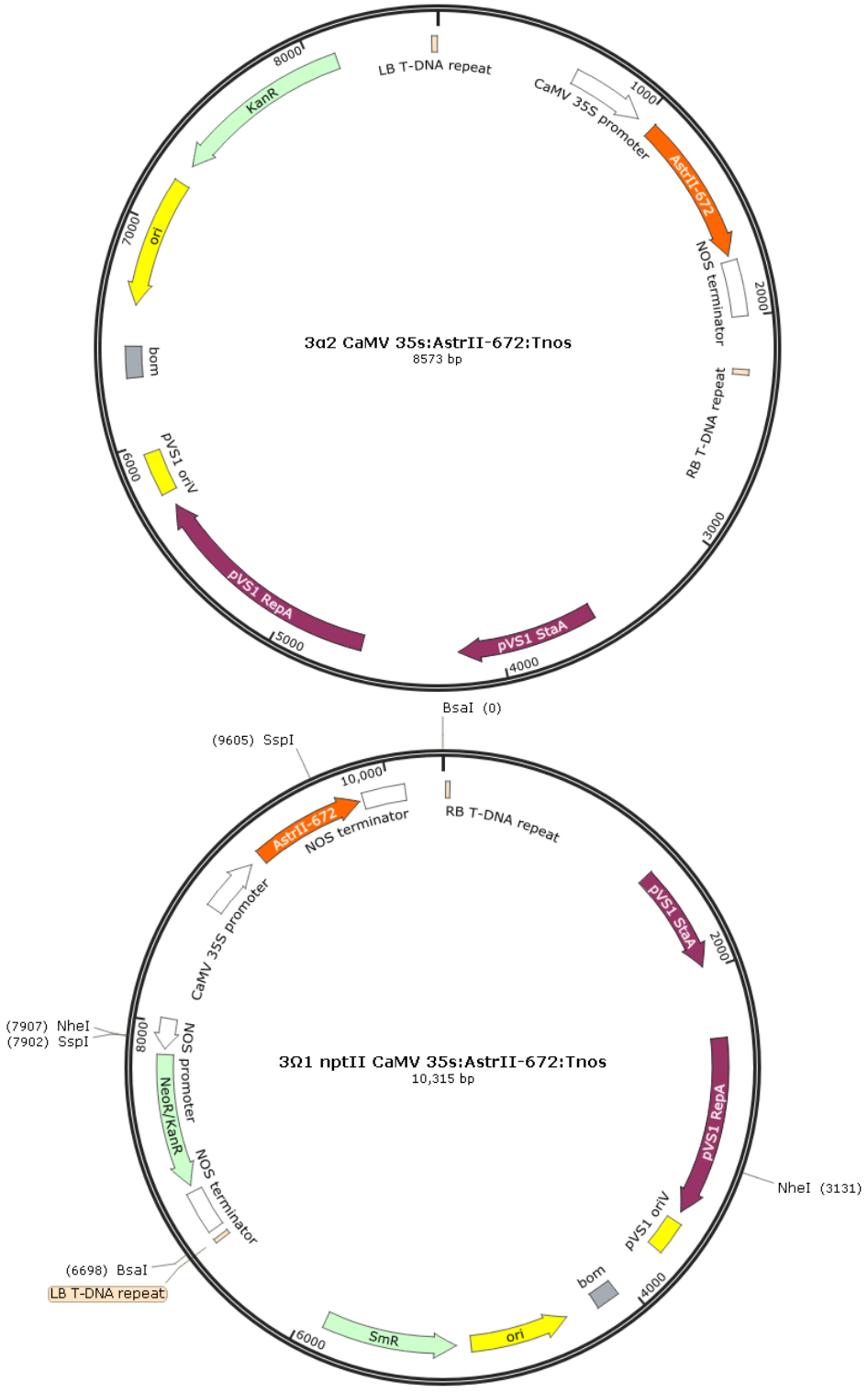

Figure 6.2.1: Diagrammatic representation of vectors for production of transgenics. Top: Complete 3α2 destination vector containing the 35sCaMV:A*strII*:Tnos gene cassette. Bottom: Final 3Ω1 destination vector containing the transgenic selectable marker gene *nptII* as well as the 35sCaMV:A*strII*:Tnos gene cassette from the 3α2 vector. The vector diagram also includes the diagnostic restriction endonuclease cut sites for SspI, NheI and BsaI which will be used to determine if the recombinant ligation reaction has been successful. These two vectors were generated using the GoldenBraid cloning methodology detailed in chapter 1.11 and 2.5.3.4.3. Vector maps generated using SnapGene® Viewer 3.2.1

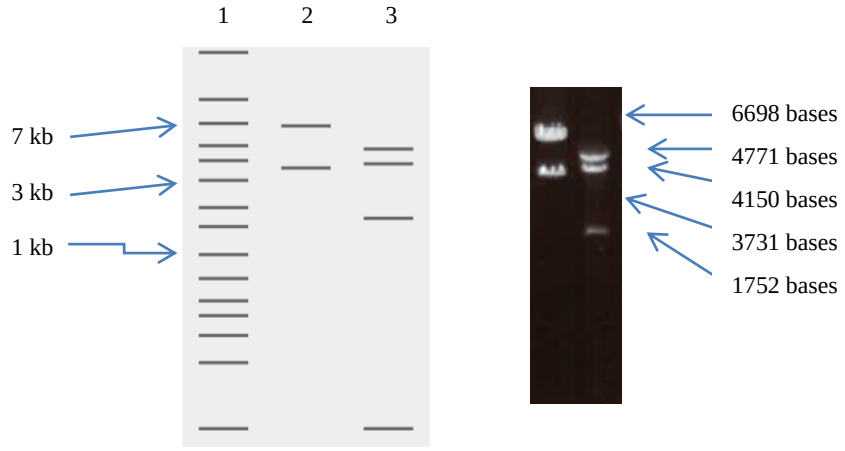

Figure 6.2.2: Predicted and actual enzymatic digest of produced transformation vectors. Left: Predicted restriction digestion map for the finalised 3Ω1 Tnos:*nptII*:Pnos 35sCaMV:A*strII*:Tnos transformation vector using BsaI in a single digestion reaction and then double digestion reaction using SspI and NheI. Lane 1 - DNA ladder; Lane 2 - BsaI restriction digest (yielding band sizes of 6698/3731) Lane 3 – SspI and NheI restriction digest (yielding band sizes of 4771/4150/1752/5) .Right: Image of ethidium bromide stained electrophoresis gel showing the expected banding pattern of the complete transformation vector. The 5 bases band is too small to be resolved and imaged on the gel. There are two bands visible at the top of the image which represents the 4771/4150 fragments. Predicted digestion image was generated using Benchling online software (www.benchling.com).

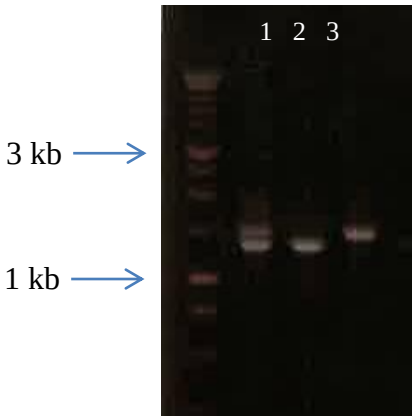

Figure 6.2.3: **Electrophoresis gel of transgenic cassette.**
Image of ethidium bromide stained electrophoresis gel showing the results of a PCR using a primer pair designed for regions within the 35sCaMV promoter and Tnos terminator. This pair of primers was used, as it allowed for the differentiation of the two gene cassettes being used in a single reaction due to the 200bp difference. Lane 1 – 1kb DNA marker (Promega, UK), Lane 2 – Co-transformed transgenic line, Lane 3 – A*strII* positive transgenic, Lane 4 – *WstrI* positive transgenics.

6.3 Results:

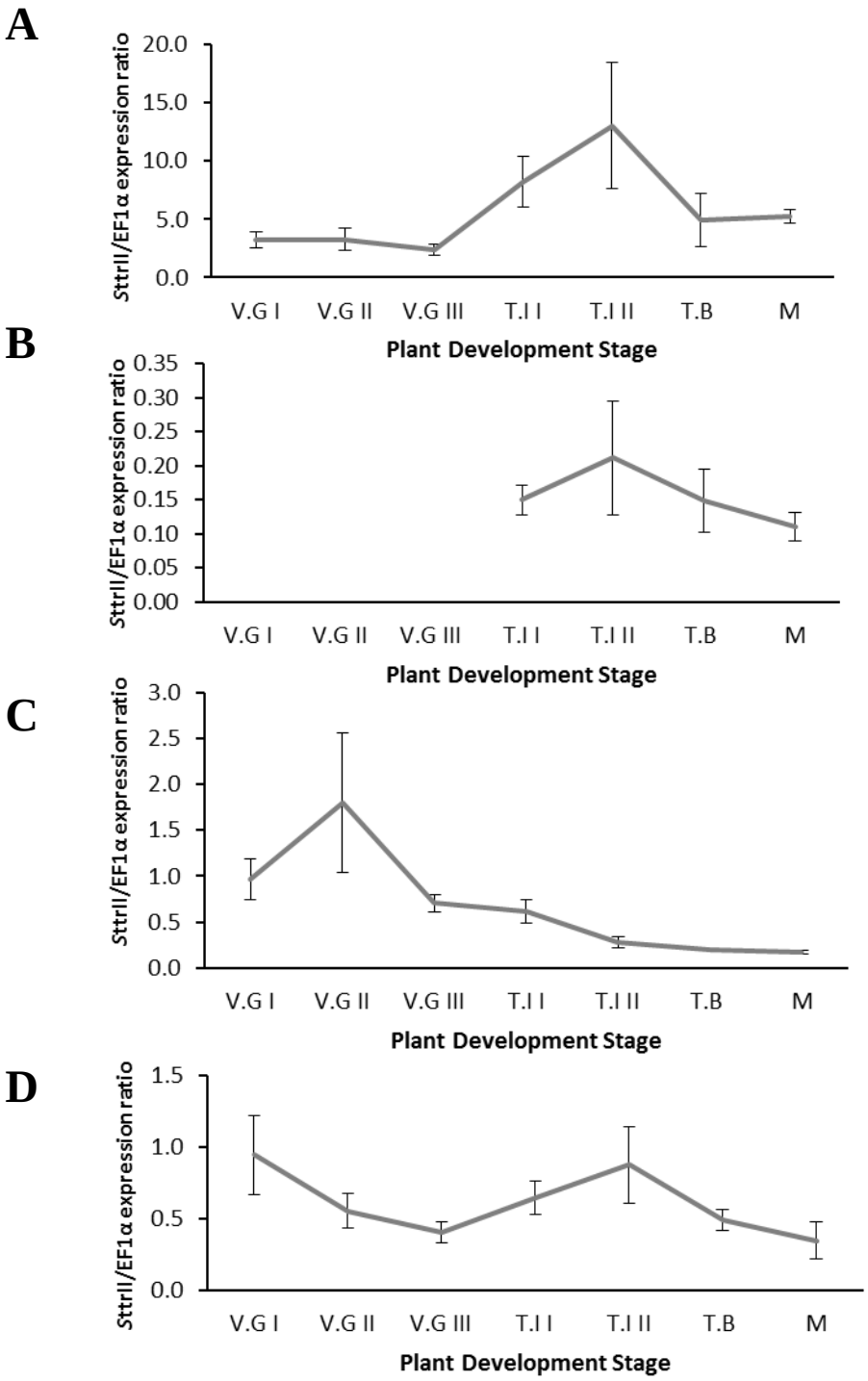

Figure 6.3.1: ***trII* time course expression data from four tissues**

RT-qPCR expression data for *SttrII* from four different tissues during seven stages of plant development. Each panel represents a different tissue, with A – root; B – tuber; C – stem and D – leaf. Developmental stages relate to the following with average height given as an indicator: V.G – Vegetative Growth (stage I (27.0 cm) to III (61.8 cm)), T.I – Tuber Initiation (stage I (93.2 cm) and II (109.5 cm)), T.B – Tuber Bulking (131.6 cm) and M – Maturation/Senescence (128.2 cm). Growth stage definitions taken from Patil *et al*, (2016). Three replicates were used at each growth stage, with the standard error represented by the error bars.

RT-qPCR analysis of *trII* from four tissues during the growth and development of potato can be seen in Figure 6.3.1. The levels of expression in the four tissues investigated indicate that *trII* is expressed at different levels when compared to the endogenous control, *ef-1α.* The highest expression levels are seen within the roots, with the lowest expression ratio being 2.4:1 (± 0.5) during V.G III and the highest 13.1:1 (± 5.4) during T.B II. In other tissues levels also varied with developmental stage but were generally 1.8 and 14.8 fold lower than the levels seen in roots at V.G II and T.B II respectively.

6.3.1 Transgene characterisation.

After initial characterisation for the presence of the transgene, lines found to be positive for the either the As*trII* or As*trII/WstrI* constructs, continued to be grown on MS20 kanamycin media. RNA was extracted from these lines with the same process followed as in Chapter 5 Figures 5.2.4 and Table 5.2.1. Once RNA was extracted cDNA was synthesised and RT-qPCR was used to check the relative expression ratios for *StrII* and *WstrI* against *ef-1α.* Initially 21 lines were tested, with two of these being positive for As*trII* and *WstrI* in cultivar *Désirée*, two As*trII* positive lines in cultivar *Bintje* and 17 As*trII* lines in cultivar *Désirée*. The results from this RT-qPCR analysis can be seen in Figure 6.3.2A (*StrII*/*ef-1α* expression ratio) and Figure 6.3.2B (*WstrI*/*ef-1α* expression ratio).

Figure 6.3.2 shows that there is variation in the *SttrII*/*ef-1α* and *WstrI*/*ef-1α* expression ratios for the down-regulating and the co-transformed transgenic lines produced. Expression of *trII* within the down-regulating (As*trII/nptII* 26.1) and co-transformed line (*WstrI*/As*trII/nptII* 3.1), give a comparative expression level of 0.05 ± 0.00 and 0.53 ± 0.06 respectively when compared to *trII* expression within the cultivar *Désirée* control. *WstrI* expression of the two co-transformed lines when compared to the constitutively expressed *ef-1α* is 0.22 ± 0.02 and 1.20 ± 0.06 for *WstrI*/As*trII*/*nptII* 3.1 and 3.2 respectively. This indicated that for line 3.1, *WstrI* expression is not as high as *ef-1α,* and that line 3.2 exhibits almost a 6 fold increase in expression compared to 3.1. The impact of these different expression levels on metabolite levels will be elucidated later in the study.

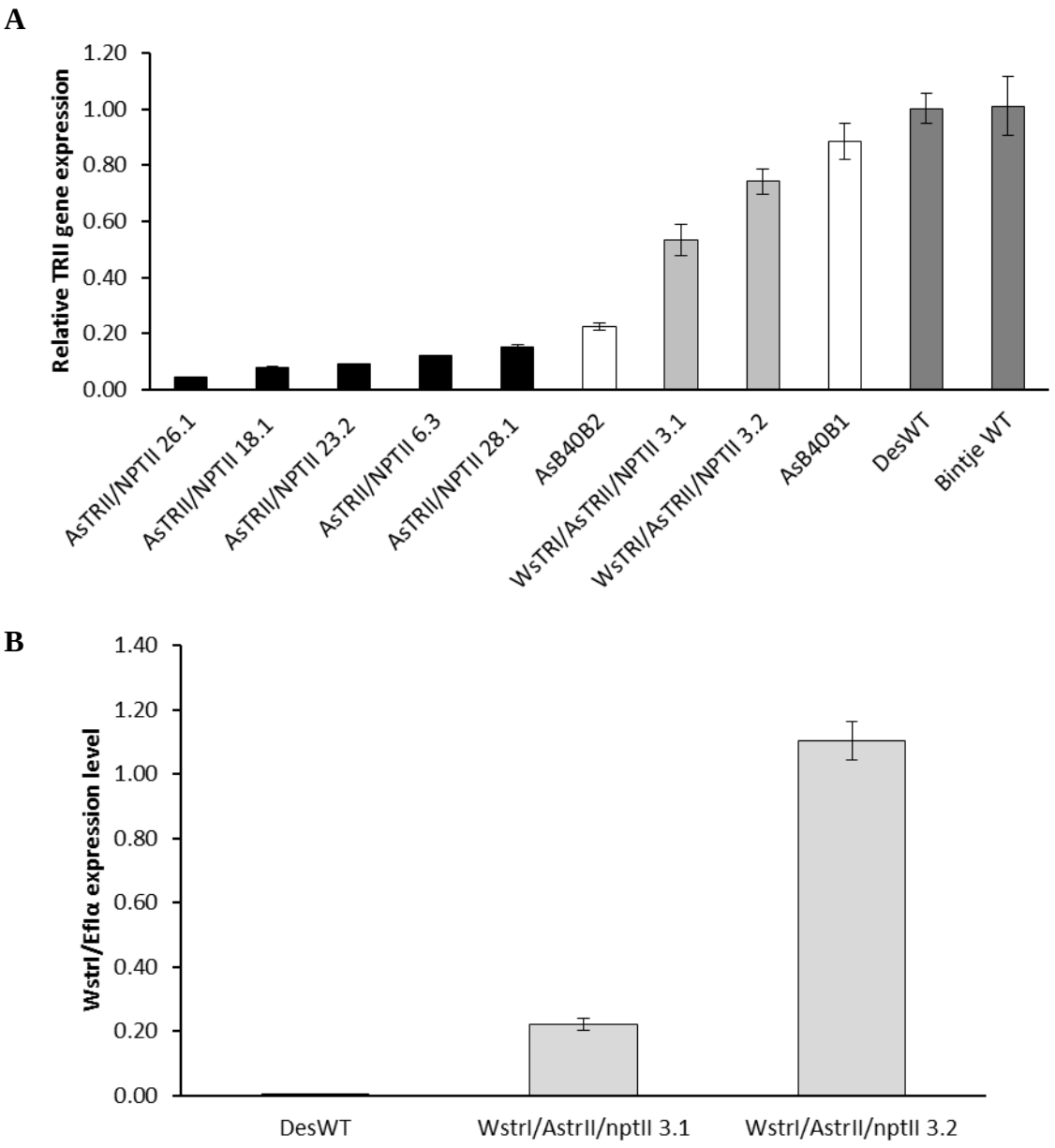

Figure 6.3.2: Transgene expression data from characterisation of initial trasngenics.

A: RT-qPCR expression ratios between *SttrII* and *ef-1α* from the nine transgenic lines which are being investigated further due to exhibiting the highest level of *trII* expression down-regulation. Expression levels from 21 plantlets were initially tested. The data from the other 12 plantlets is shown in appendix A.6.2.2. B: RT-qPCR expression ratios between *WstrI* and *ef-1α* from the co-transformed transgenic lines which are being investigated further due to exhibiting *WstrI* expression and *SttrII* down regulation. In both cases the error bars represent the standard error between technical replicates in the RT-qPCR analysis (n = 3). A*strII*/*nptII* lines are in cultivar *Désirée*, AsB40 lines are in cultivar *Bintje* and the *WstrI*/A*strII*/*nptII* lines are in cultivar *Désirée*.

The lines in Figure 6.3.2 were grown in the glasshouse as detailed in Chapter 2.4 during the summer months of 2017, in a randomised block design with four biological replicates alongside the *trI* over-expression transgenics discussed in Chapter 5. Height measurements were taken weekly for all plants grown during this period, with the average height of the transgenic lines grown seen in Figure 6.3.3. Of the down-regulating transgenics, one of the seven lines exhibited stunting. This line As*trII/nptII* 6.3 reached a maximum height of 110.9 ± 7.3 cm. The co-transformed lines also experienced stunting in their growth, reaching 115.8 ± 11.7 and 127.5 ± 9.1 cm for *WstrI*/As*trII/nptII* 3.1 and 3.2 respectively. This is compared to the *Désirée* and Empty Vector controls grown, which reached a height of 156.5 ± 5.2 for cultivar *Désirée* and 149.5 ± 5.8 for the Empty Vector lines.

The growth parameters measured in Figures 6.3.5 and 6.3.6 indicate that for As*trII/nptII* 6.3 and the two co-transformed lines within this study, there were significant differences in the development of these plants. Across the four organs examined, the fresh weight for the tissues harvested from these three lines, was consistently and significantly lower than the other transgenics lines and controls. Whilst, there did not appear to be any difference in carotenoid or chlorophyll content between any of the transgenic lines compared to the controls, after exogenous tropinone leaf assays discussed in Figure 6.3.8, further analysis for As*trII/nptII* 6.3 will not be shown, as interpretation of the results would be confounded by the general differences in growth characteristics.

6.3.2 Growth and phenotypic characterisation

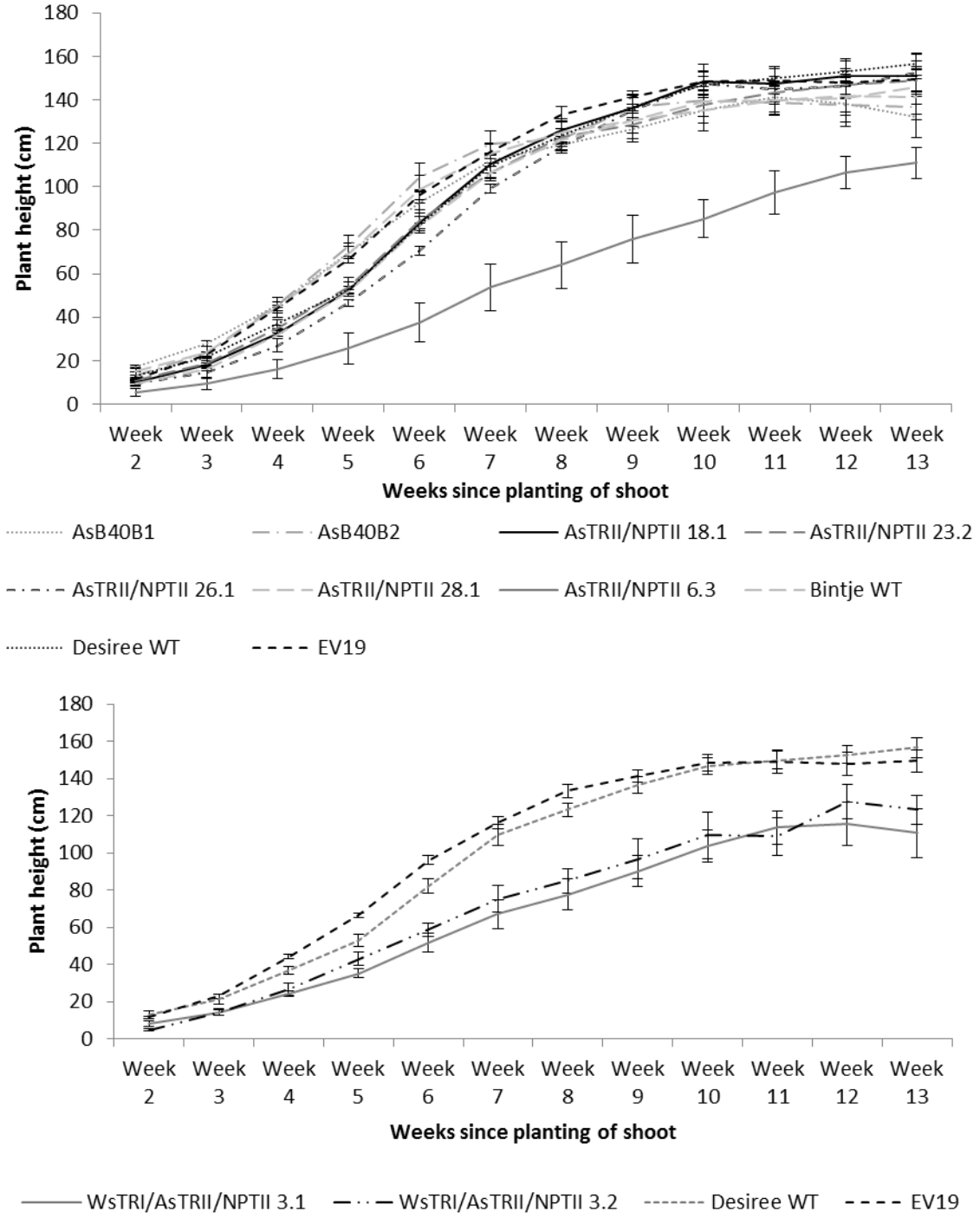

Figure 6.3.3: **Height measurements during growth of A*strII and WstrI/AstrII* transgenics**
Top: Average weekly plant height measurements for the seven A*strII/nptII* transgenics lines within both cultivars and controls grown in glasshouse conditions. This indicates that six of the seven lines grown did not exhibit any adverse growth effects such as stunting when compared to the controls, whilst there was one line (A*strII/nptII* 6.3) that only grew to an average height of 110.9 ± 14.5 cm. Bottom: Average weekly height measurements for the two *WstrI*/A*strII/nptII* lines in cultivar *Désirée*. These are the average of the four biological replicates with the Standard Error being shown (n = 4). Cultivar *Désirée*, *Bintje* and an Empty Vector (EV) transgenic were grown as experimental controls.

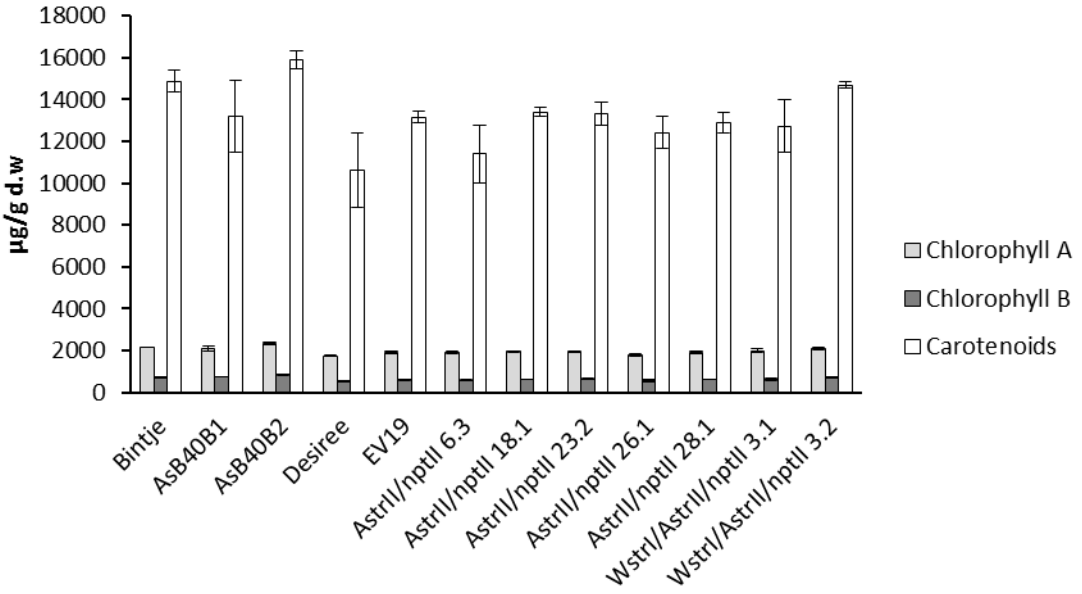

Figure 6.3.4: Growth characteristics.

Chlorophyll and carotenoid levels from harvested leaves during week 12 of their growth, showing no significant difference between the transgenic and control lines (n = 4).

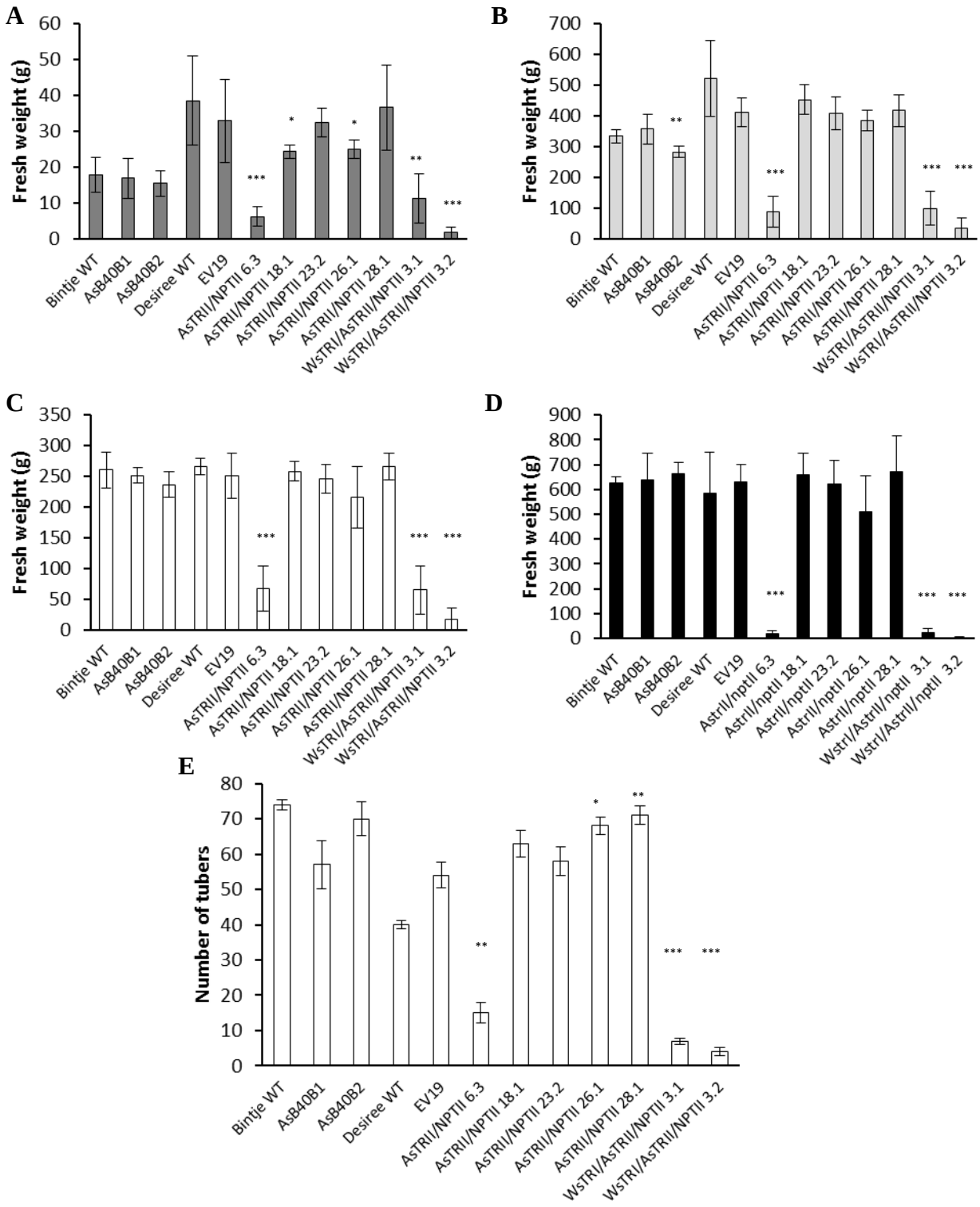

Figure 6.3.5: Biomass of tissues from harvested transgenic lines.

Harvested potato organ fresh weight data from: A = root, B = stem, C = leaf, D = tuber mass, E = tuber number. A*strII/nptII* 6.3 and the two co-transformed lines show a highly significant decrease in fresh weight when compared to the control lines, which correlates with the average height achieved across the replicates (Figure 6.3.4). * indicates a significant difference where $P < 0.05$ ** indicates a significance of $P < 0.01$ and *** indicates a significance of $P < 0.001$ (n = 4). A*strII*/*nptII* lines are in cultivar *Désirée*, AsB40 lines are in cultivar *Bintje* and the *WstrI*/A*strII/nptII* lines are in cultivar *Désirée*

6.3.3 Tuber and Root alkaloid content

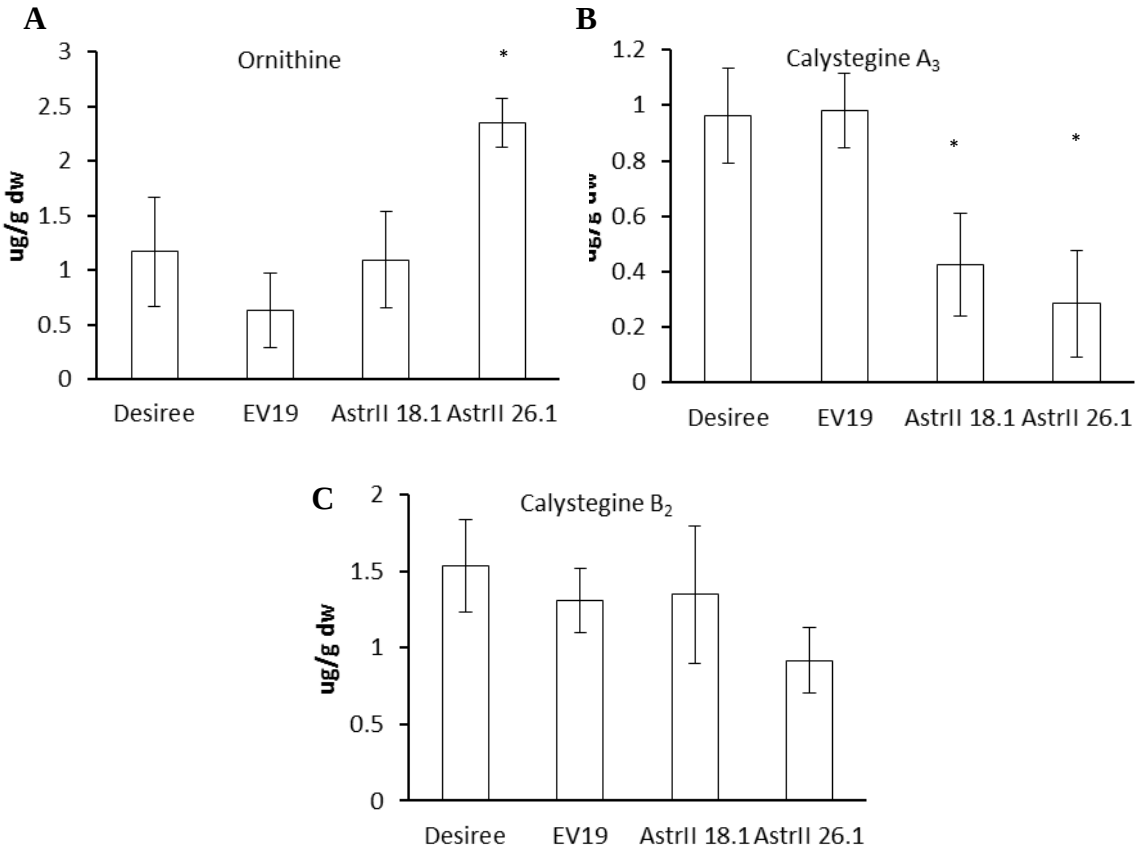

Figure 6.3.6: **Tuber tropane and nortropane alkaloid metabolite content.**
Metabolites associated with the tropane and nortropane alkaloids detected within tubers from A*strII/nptII* transgenic lines compared to controls. Panel A = ornithine, B = calystegine A_3 and C = calystegine B_2. These were the only metabolites of the ten from along the tropane and nortropane alkaloid biosynthesis pathway detectable. Data was generated using the MRM developed in Chapter 3, and is the result of a single injection from each of the four replicates grown. * indicates a significant difference to control lines where $P < 0.05$ ($n = 4$).

The tropane and nortropane alkaloid content of harvested tubers and roots can be seen in Figures 6.3.6 and 6.3.7. From the panel of ten tropane and nortropane alkaloids within the MRM developed in chapter 3, only three were detected in the tuber and five in the roots. Whilst the same three metabolites, ornithine and the two calystegines (A_3 and B_2) were detected in both tissues, the detection of pseudotropine and importantly elevated levels of tropine within the root was an indication that through the addition of an active trI the normal metabolic flux at the tropinone branch point may have been altered.

The tubers from the *WstrI*/A*strII*/*nptII* lines were not analysed due to poor tuberisation and development, as indicated from the tuber fresh weight and count in Figure 6.3.5 (panel D and E). There was a significant reduction in calystegine A_3 content in the two A*strII/nptII* lines analysed with line 18.1 containing 0.42 ± 0.18 and 26.1 having 0.28 ± 0.19 µg/g DW compared to 0.96 ± 0.17 and 0.98 ± 0.13 µg/g DW in the controls (P = 0.038). Although there is no significant difference in the calystegine B_2 content within these lines (P = 0.45), there appears to be a slight reduction in A*strII/nptII* 26.1. The roots of *WstrI*/A*strII*/*nptII* 3.1 and A*strII/nptII* 26.1 were analysed for their tropane and nortropane alkaloid profile along with controls. There was no significant difference in the levels of the precursor ornithine (P = 0.24 and 0.35 respectivley), as well as no detectable level of the metabolites pseudotropine and tropine in A*strII/nptII* 26.1 and cultivar *Désirée*, calystegine B_2 in *WstrI*/A*strII*/*nptII* 3.1 and tropine in the Empty Vector control. *WstrI*/A*strII*/*nptII* 3.1 showed significant difference in the content of calystegine A_3 (4.73 ± 1.14 µg/g DW, P = 0.00005) and tropine (0.87± 0.34 µg/g DW, P = 0.047) when compared to the controls used (cultivar *Désirée* contained 52.27 ± 6.01 µg/g DW calystegine A_3 and no detectable tropine).

The reduction in calystegine A_3 and slight difference in B_2 within tubers for A*strII/nptII* 18.1 and 26.1, suggests that there has been manipulation in the synthesis and storage of calystegines within these down-regulating lines. Similarly, the reduced calystegine A_3 and elevated tropine levels in the roots of *WstrI*/A*strII*/*nptII* 3.1 suggests together there may have been a change in the tropane and nortropane alkaloid biosynthesis pathway at the tropinone reductase branch point.

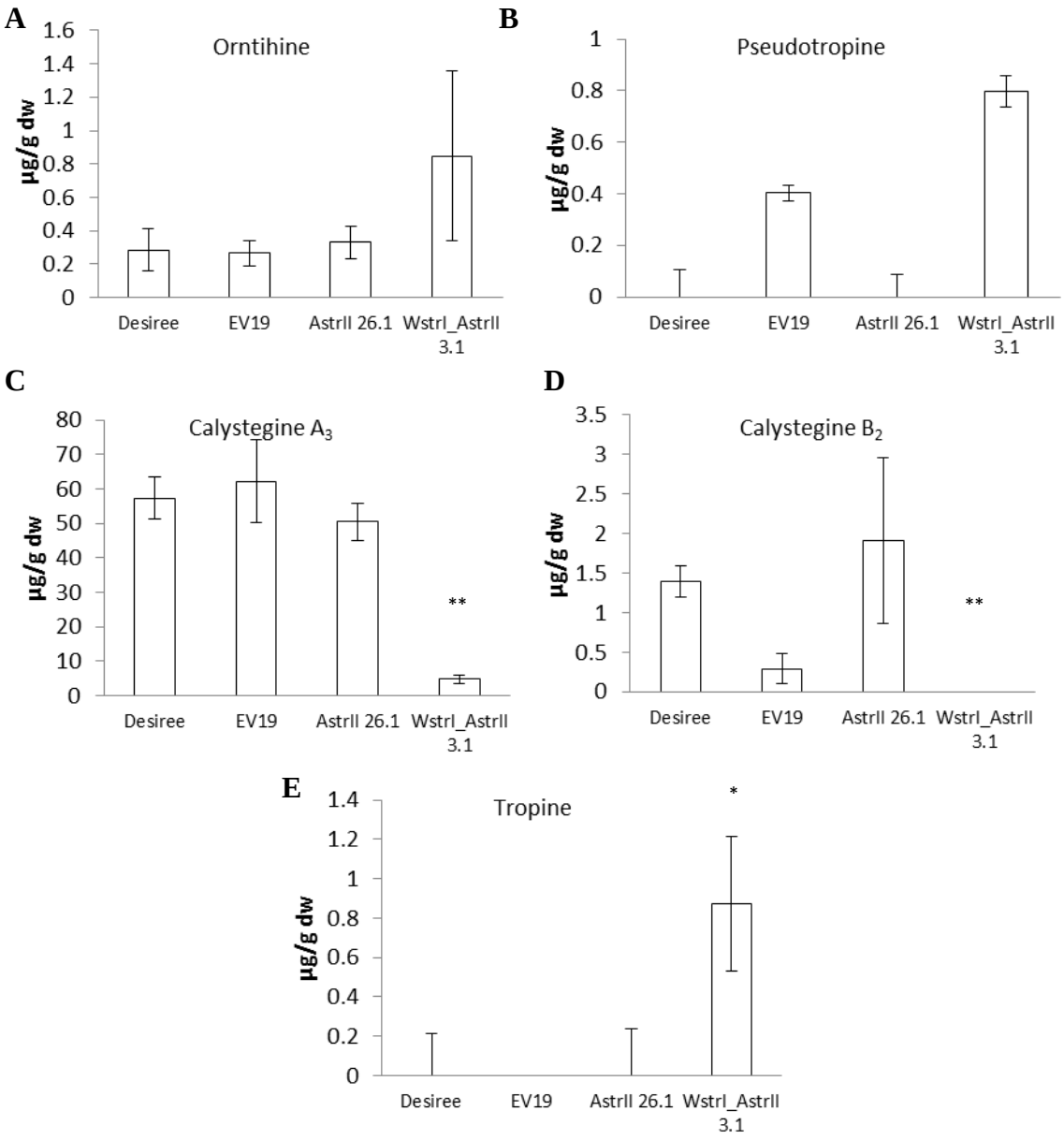

Figure 6.3.7: Root tropane and nortropane alkaloid metabolite content.

Metabolites associated with the tropane and nortropane alkaloids which were detected within roots from A*strII/nptII* and *WstrI*/A*strII/nptII* transgenic lines where available compared to controls. Panel A = ornithine, B = pseudotropine, C = calystegine A_3, D = calystegine B_2 and E = tropine. These were the only metabolites of the ten from along the tropane and nortropane alkaloid biosynthesis pathway detectable. Data generated using the MRM method developed in Chapter 3, and is the result of a single injection from each of the four replicates grown. The error bars shown is the standard error, * indicates a significant difference to control lines where $P < 0.05$ ($n = 4$).

6.3.4 Exogeneous tropinone leaf disc assays

Figure 6.3.8 and 6.3.10 show the results of leaf disc assays from two different developmental stages for the down-regulating, co-transformed transgenic and control lines in both cultivar *Désirée* and *Bintje*. As with the leaf disc assays described in Chapter 5, these time points were at weeks 5 and 7, which correspond to vegetative growth III and tuber initiation I. Exogenous tropinone was applied to the leaf discs, and across the two time points the conversion to pseudotropine is variable between the analysed lines. A*strII/nptII* 26.1 (1.64 ± 0.27 µg/g and 2.43 ± 0.31 µg/g FW) shows a significant difference (P = 0.0195) across the time points compared to the control lines (5.24 ± 0.44 µg/g and 4.47 ± 0.66 µg/g FW) for assays 1 and 2 respectively. *WstrI*/A*strII/nptII* 3.1 and 3.2 exhibited similar levels of pseudotropine within the leaf disc assays. The highest level was seen within *WstrI*/A*strII/nptII* 3.2 for leaf disc assay 2, at 0.54 ± 0.01 µg/g FW (P = 0.0011). The was no significant difference in the conversion to tropine within the A*strII/nptII* transgenic compared to controls (P = 0.28 and 0.22 for *AstrII/nptII* 18.1 and 26.1 respectivley), whereas, the *WstrI*/A*strII/nptII* lines showed elevated levels of tropine within the samples. The highest levels of tropine can be seen in the second disc assays for these lines, where it reaches 37.99 ± 11.95 and 40.73 ± 6.90 µg/g FW respectively (P = 0.015), with the *Désirée* control in the same assays containing 0.63 ± 0.05 and 0.46 ± 0.04 µg/g FW. The *Bintje* down-regulated *trII* lines showed no significant difference in the concentration of pseudotropine and tropine between the control and transgenic lines assayed.

RT-qPCR was used to determine the *SttrII* and *WstrI* relative expression levels of lines used in the leaf disc assays at the time points. Figure 6.3.9 and 6.3.11 shows that *trII* expression levels in the co-transformed lines were significantly different across the two time points analysed for the lines derived from cultivar *Désirée*, with P values given being <0.05 and <0.01 for *WstrI*/A*strII/nptII* 3.1 and 3.2 respectively. Across the two assays of the A*strII/nptII* lines there was no significant difference (P values varied between 0.19 amd 0.34) in the relative expression levels of *trII* when compared to *ef-1α*. Similarly, for the A*strII Bintje* transgenic lines there was no significant difference between the *SttrII/ef-1α* expression ratios for the first two leaf disc assays (P values between 0.13 and 0.34).

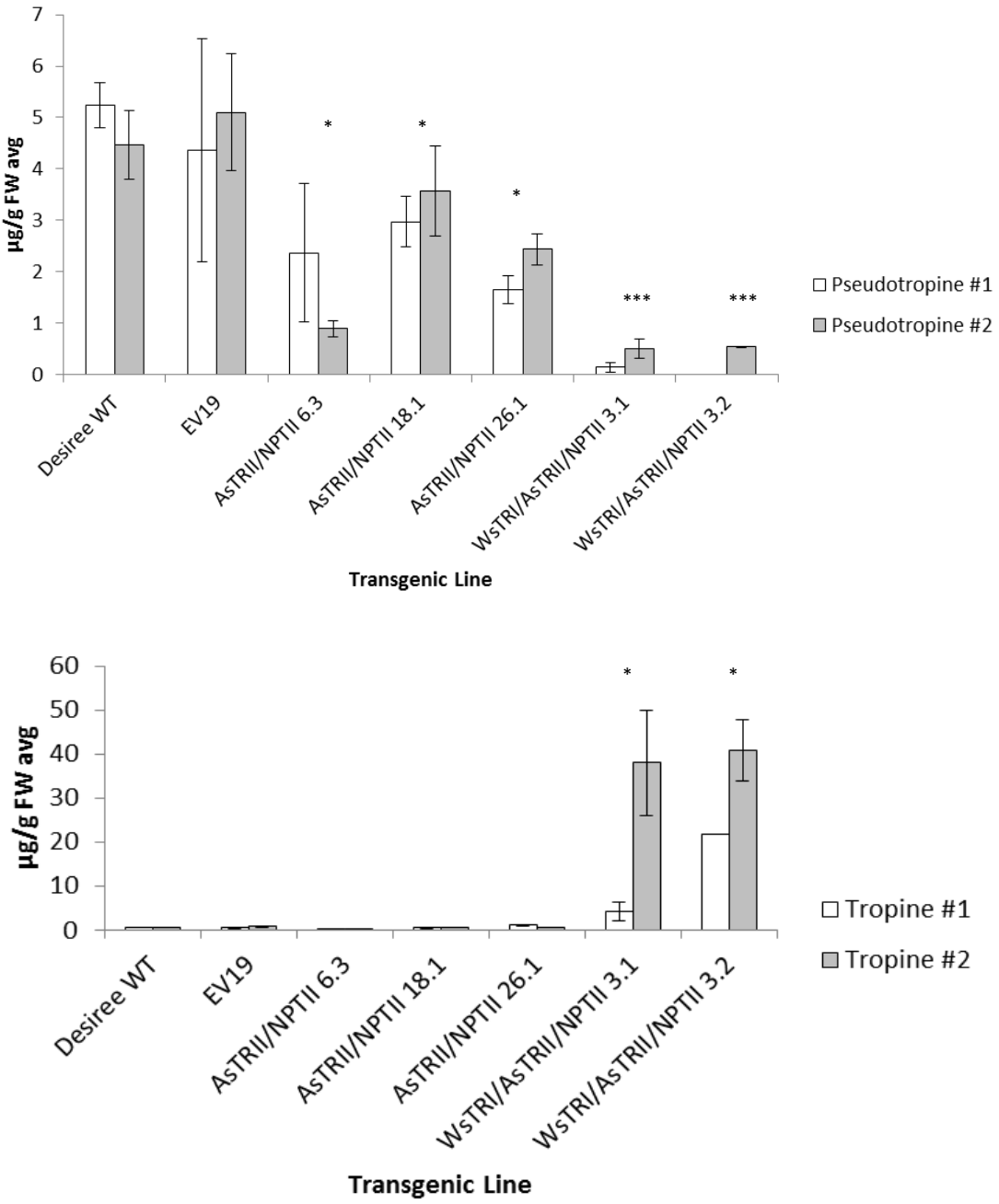

Figure 6.3.8: **Pseudotropine and tropine content from *Désirée* transgenic leaf disc assays.** Pseudotropine (top) and tropine (bottom) content of leaf discs from down-regulating and co-transformed transgenic and control lines during three separate assays, at three stages during plant development. Exogenous tropinone and KCl (as a control – data not shown) was applied to the leaf discs, before they were left for 48 hours. Data was generated using the MRM method developed in Chapter 3, and is the result of a single injection from each of the four replicates grown. * indicates a significant difference where $P < 0.05$, ** indicates a significance of $P < 0.01$and *** indicates a significance of $P < 0.001$ when compared to control lines (n = 4 except in *WstrI*/A*str**II/nptII* 3.2 where n = 2).

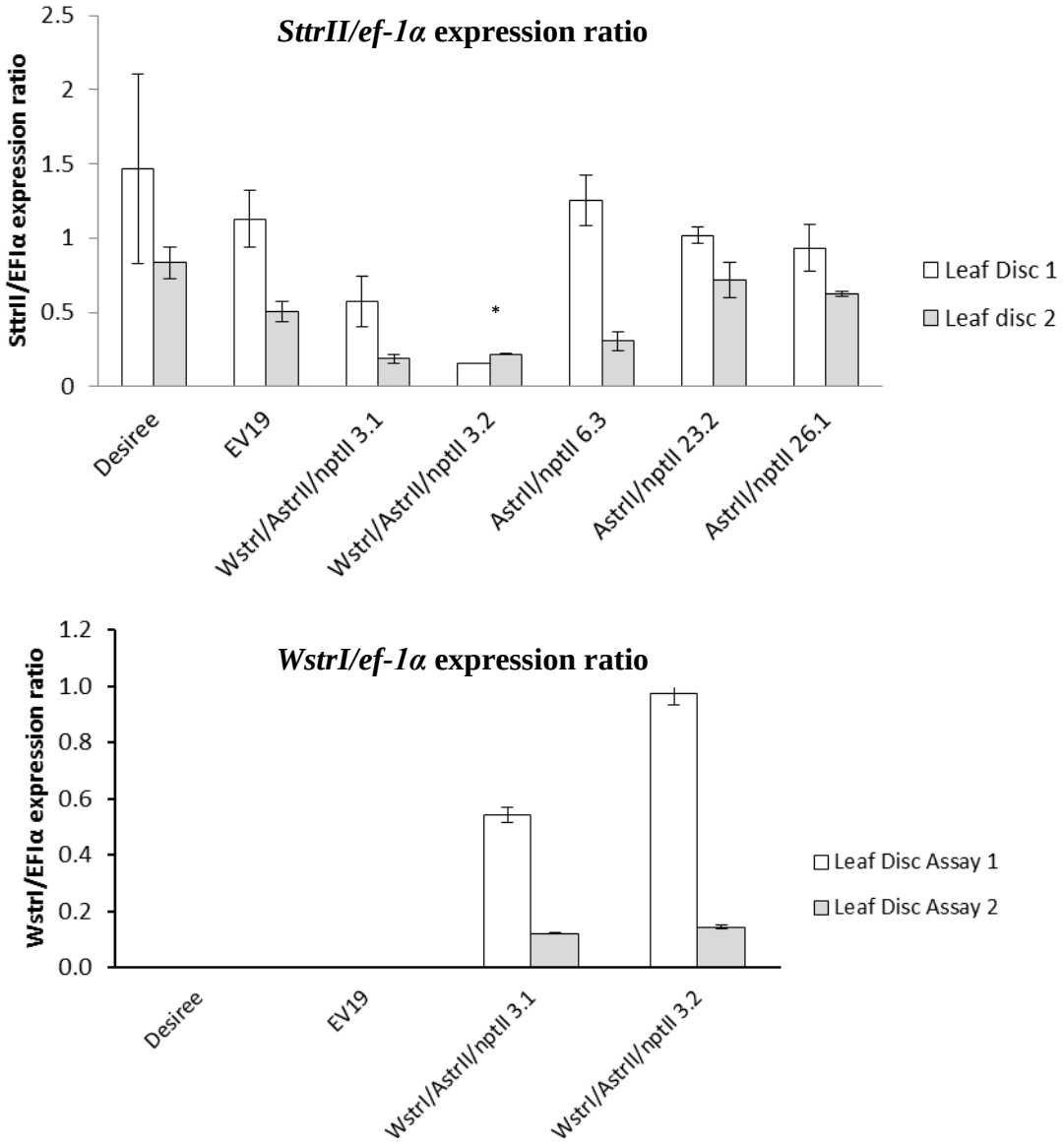

Figure 6.3.9: Tropinone reductase gene expression during *Désirée* leaf discs assays.

RT-qPCR data showing the *SttrII*/*ef-1α* (top) and *WstrI*/*ef-1α* (bottom) expression ratios from the A*strI/nptII*, and co-transformed transgenic lines and controls during the three separate leaf disc assays.. *SttrII* was tested to ensure there was no effect on this gene through the transformation process and to ensure that the gene was still expressed during this assay. The *WstrI*/*ef-1α* expression ratio shows *WstrI* is not expressed to the same levels as *ef-1α* within the leaf tissue, with the exception of leaf disc assay 1 for *WstrI*/A*strII/nptII* 3.2. After leaf disc assay 1 the *WstrI* expression levels between the two co-transformed lines are comparable to each other. There is no significant difference in expression ratios between the *WstrI/nptII* transgenics for *trII* when compared to the controls. * indicates a significant difference where $P < 0.05$ ($n = 4$).

For the co-transformed lines during the first assay seen in Figure 6.3.9, *WstrI* is expressed at twice the level seen in the latter two assays (P = 0.04). This follows what was seen with the *WstrI* relative expression pattern in the single *WstrI* over-expression lines discussed in Chapter 5. However, the overall expression ratio is lower than in the single over-expression transgenics. They exhibited a ratio of 0.54 ± 0.03 (for *WstrI*/A*strII/nptII* 3.1) and 0.97 ± 0.04 (for *WstrI*/A*strII/nptII* 3.2) to 1.00 when compared to *ef-1α*. Within leaf disc assay 2 and 3 the *WstrI*/ *ef-1α* expression ratios display the same pattern, with the lowest ratio being in leaf disc assay 3 at 0.09 ± 0.00 and 0.10 ± 0.01 for the two lines.

The lower expression levels of *WstrI* seen in the co-transformed transgenic lines when compared to the single *WstrI* over-expression lines in Chapter 5 could explain why the accumulation of tropine is not as high in the co-transformed lines. Whilst the expression of *trII* within these lines is significantly reduced, being coupled with the presence of the active *WstrI,* the changes in the metabolite flux away from pseudotropine and towards tropine can be explained.

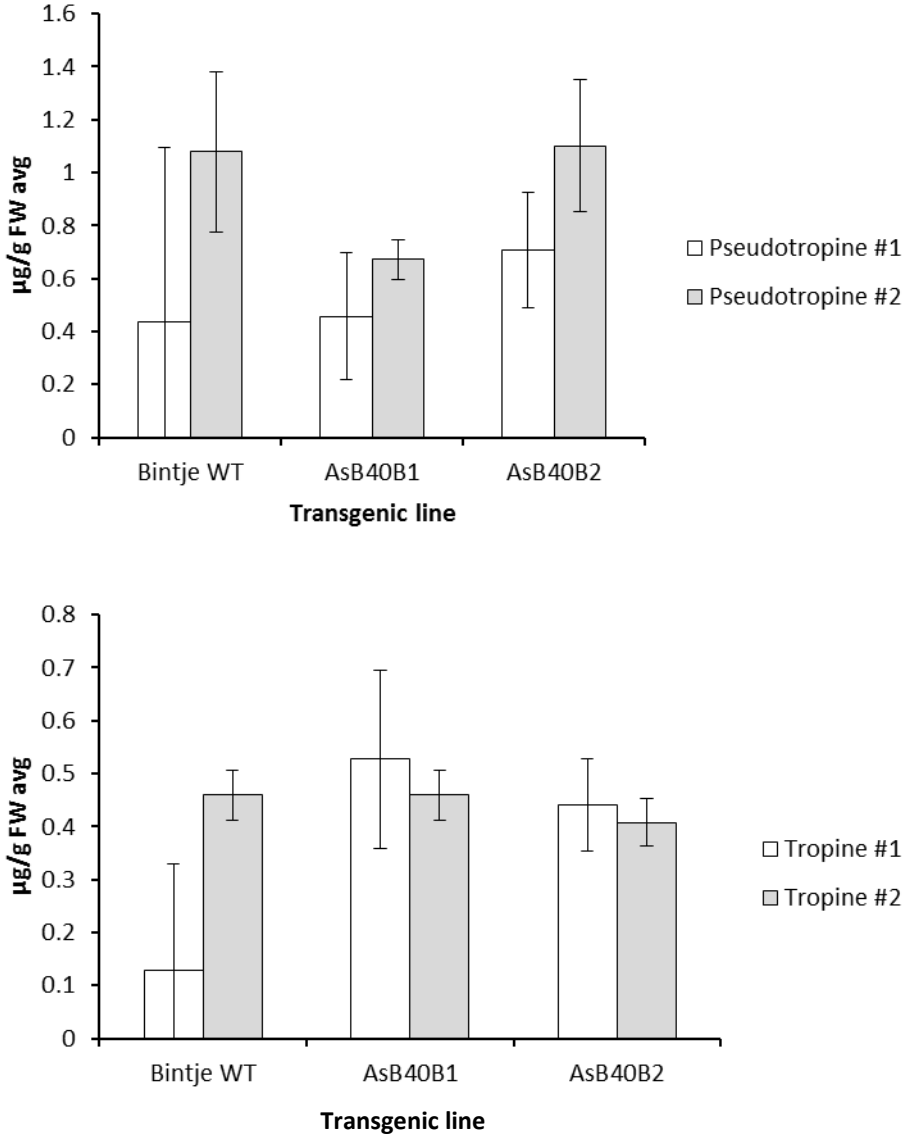

Figure 6.3.10: **Metabolite content from *Bintje AstrII* leaf disc assays.**

Pseudotropine (top) and tropine (bottom) content of leaf discs from down-regulating transgenic and control lines during three separate assays, at three stages during plant development in cultivar *Bintje*. Exogenous tropinone and KCl (as a control – data not shown) was applied to the leaf discs, before they were left for 48 hours. There was no significant difference between the controls and *SttrII* transgenic *Bintje* lines for the amount of pseudotropine and tropine detected by the MRM method developed in chapter 3.

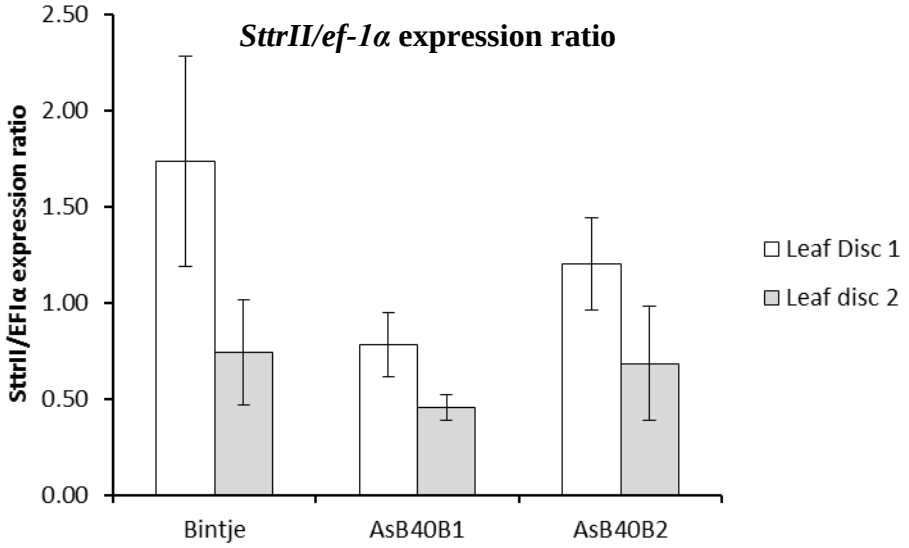

Figure 6.3.11: ***trII* gene expression during *Bintje* leaf discs assays.**

RT-qPCR data showing the *SttrII*/*ef-1α* ratio of the As*trII* cultivar *Bintje* lines. As with the cultivar *Désirée* lines, *SttrII* was tested to ensure there was no effect on this gene through the transformation process and to ensure that the gene was still expressed during this assay. There was no significant difference across in expression levels for leaf disc assay 1 and 2. (n = 4).

6.3.5 Exogeneous tropinone tuber sprout feeding assays

Tuber sprout feeding assays were used to determine if there was any manipulation to the tropinone branch point within this tissue, as it has been shown to have high calystegine content and is the site of nortropane biosynthesis (Keiner and Dräger, 2000). Exogenous tropinone and KCl was added to sprouts from transgenic and control lines, with these being kept under 16:8 hour light/dark conditions for 48 hours, before metabolite analysis. Figure 6.3.12 shows the tropinone fed lines exhibited significant differences when compared to the KCl fed controls. Detection of pseudotropine for the co-transformed line *WstrI/*A*strII/nptII* 3.1 was significantly lower than that of the *Désirée* and Empty Vector lines when fed both tropinone and KCl ($P = 0.013$). There was not a significant difference for the concentration of tropine detected in the co-transformed line *WstrI/AstrII/nptII* 3.1 ($P = 0.54$), although the levels of tropine detected within the tuber sprouts was 58.72 ± 37.10 ug/g DW. When the results for these two metabolites are analysed together they provide evidence that the metabolite flux has been diverted away from the nortropane alkaloid pathway and towards the tropane alkaloid biosynthesis pathway within these lines. There was also a significant increase in tropine formation within A*strII/nptII* 26.1 compared to control lines. As this line did not undergo transformations which would affect trI, the increase in tropine seen within A*strII/nptII* 26.1 is due to the action of the endogenous trI from potato converting tropinone. Within the two A*strII/nptII* lines that had tuber sprouts tested, there was no significant difference in the pseudotropine accumulating in tropinone fed lines compared with controls ($P = 0.11$ and 0.06 for *AstrII/nptII* 18.1 and 26.1 respectivley).

In the co-transformed and A*strII/nptII* lines the accumulation of downstream tropane alkaloids can be seen within sprouts which were fed KCl and tropinone. Although the levels seen for the metabolites littorine, hyoscyamine, anisodamine and scopolamine within these lines are not as high as those detected for pseudotropine or tropine, their presence is of interest (P values in most cases were > 0.05, except for hyoscyamine in A*strII/nptII* 18.1 where $P = 0.007$, and scopolamine in A*strII/nptII* 26.1 where $P = 0.032$).

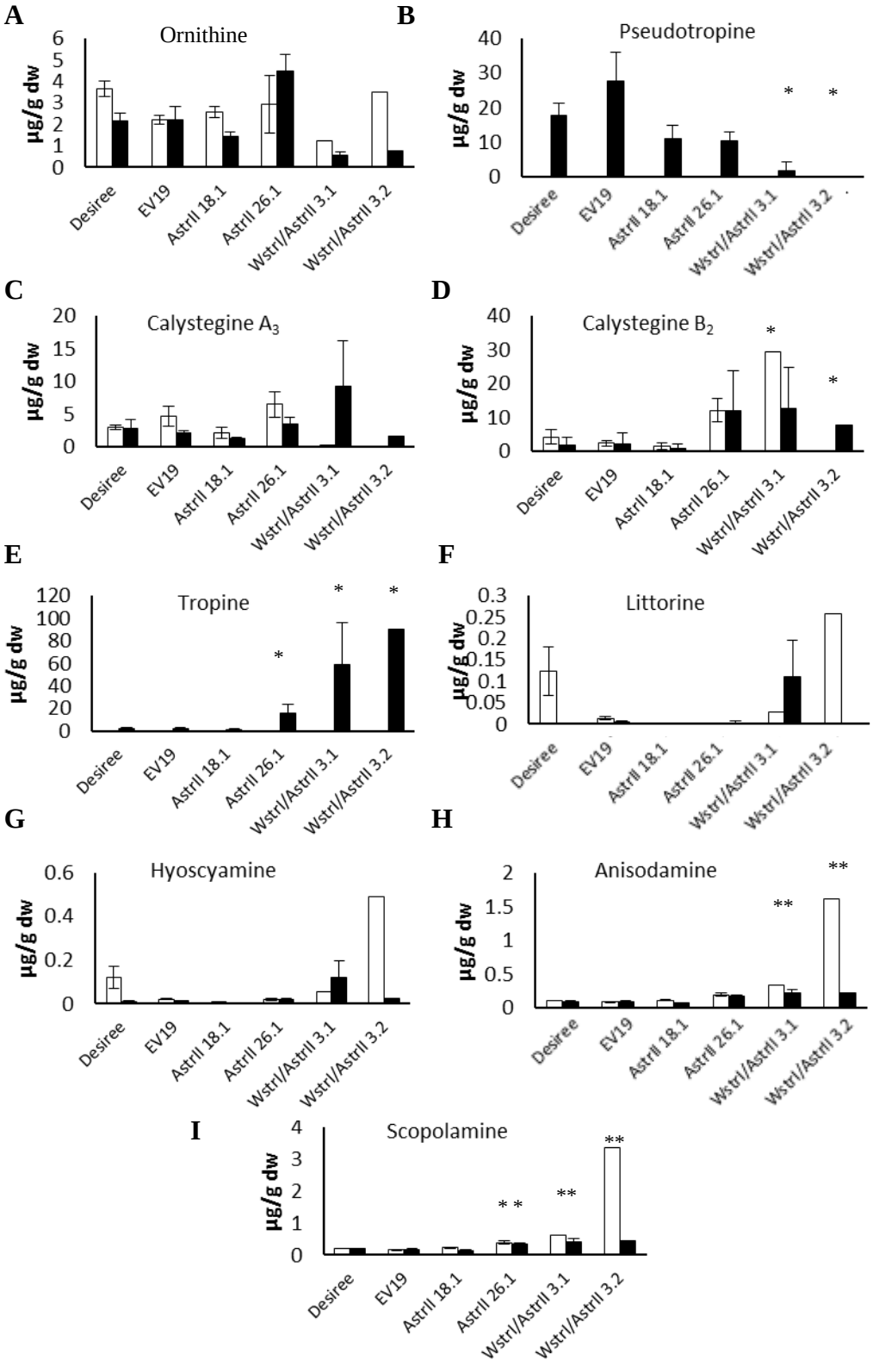

Figure 6.3.12: Alkaloid metabolite content in transgenic tuber sprouts during feeding assays.
Detection of metabolites from the tropane and nortropane alkaloid biosynthesis pathway from sprouts which have been fed exogenous tropinone (■) and the KCl fed controls (□). Each panel represents a different metabolite with: A = ornithine, B = pseudotropine, C = calystegine A_3, D = calystegine B_2, E = tropine, F = littorine, G = hyoscyamine, H = anisodamine and I = scopolamine. * indicates a significant difference where $P < 0.05$, ** indicates a significant difference where $P < 0.01$ (n = 4, except for *WstrI*/A*strII/nptII* 3.1 where n = 2 and *WstrI*/A*strII/nptII* 3.2 where n = 1)

6.3.6 Effects of methyl jasmonate on tropinone conversion

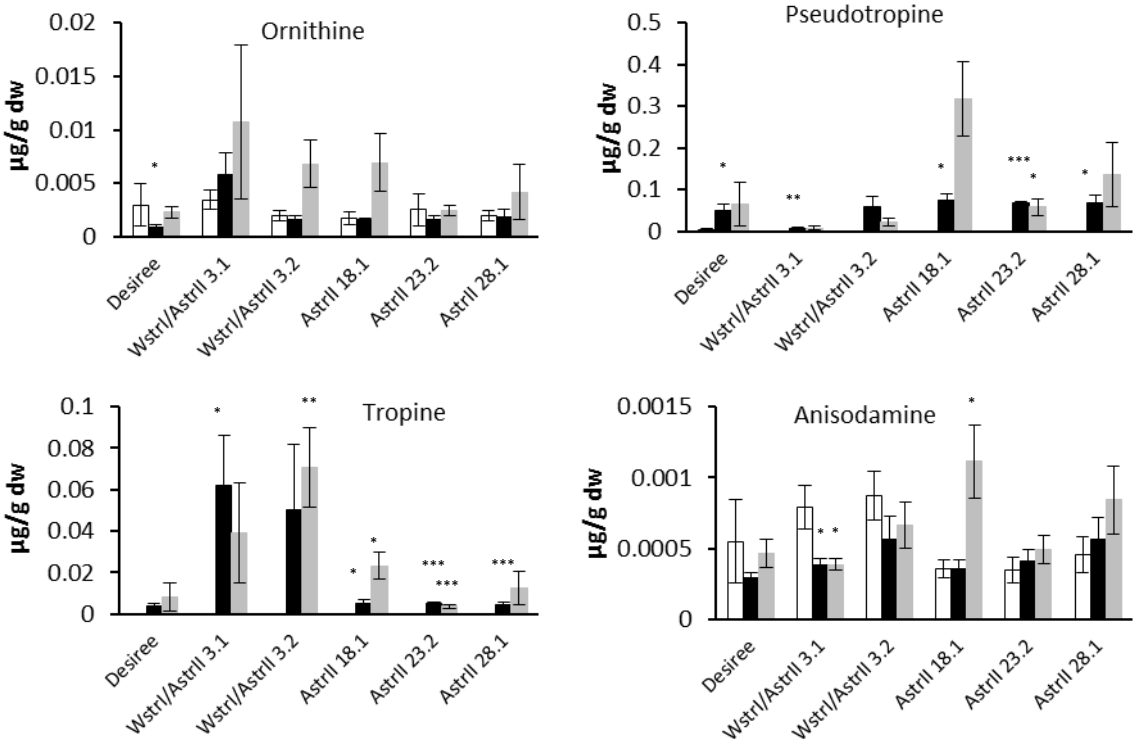

Figure 6.3.13: **Detected tropane alkaloids in transgenic plantlets grown in the presence of methyl jasmonate and tropinone.**

Detection of metabolites from a plantlet feeding assay, where plantlets were grown on MS20 media (□), MS20 + 5 mM tropinone (■) and MS20 + 5 mM tropinone + 1 mM methyl jasmonate (■). Data is shown for the metabolites which were detected within the samples. Each panel represents a different metabolite with: A = ornithine, B = pseudotropine, C = tropine, D = anisodamine. * indicates a significant difference where $P < 0.05$, ** indicates a significant difference where $P < 0.01$, *** indicates a significant difference where $P < 0.001$ ($n = 4$)

Hyoscyamine, anisodamine and scopolamine are detected at 0.49, 1.62 and 3.34 µg/g DW respectively in *WstrI*/Ast*rII/nptII* 3.2 in the presence of KCl, surprisingly, the levels of these tropane alkaloids is not as high in sprouts which were fed tropinone. Although in the case of *WstrI*/Ast*rII/nptII* 3.2 there was only one tuber sprout available for each experimental condition, due to the poor tuberisation and development of these lines, however the indication that these metabolites are present offers a potential avenue for further consideration.

As in Chapter 5, assays were conducted which involved feeding plantlets on three different media types to determine if methyl jasmonate can enhance tropinone conversion to tropine and how it affects the down-regulation of *trII*. Figure 6.3.13, indicates that the plantlets which were grown in the presence of tropinone and methyl jasmonate had higher levels of the four metabolites detected from the ten in the MRM developed.

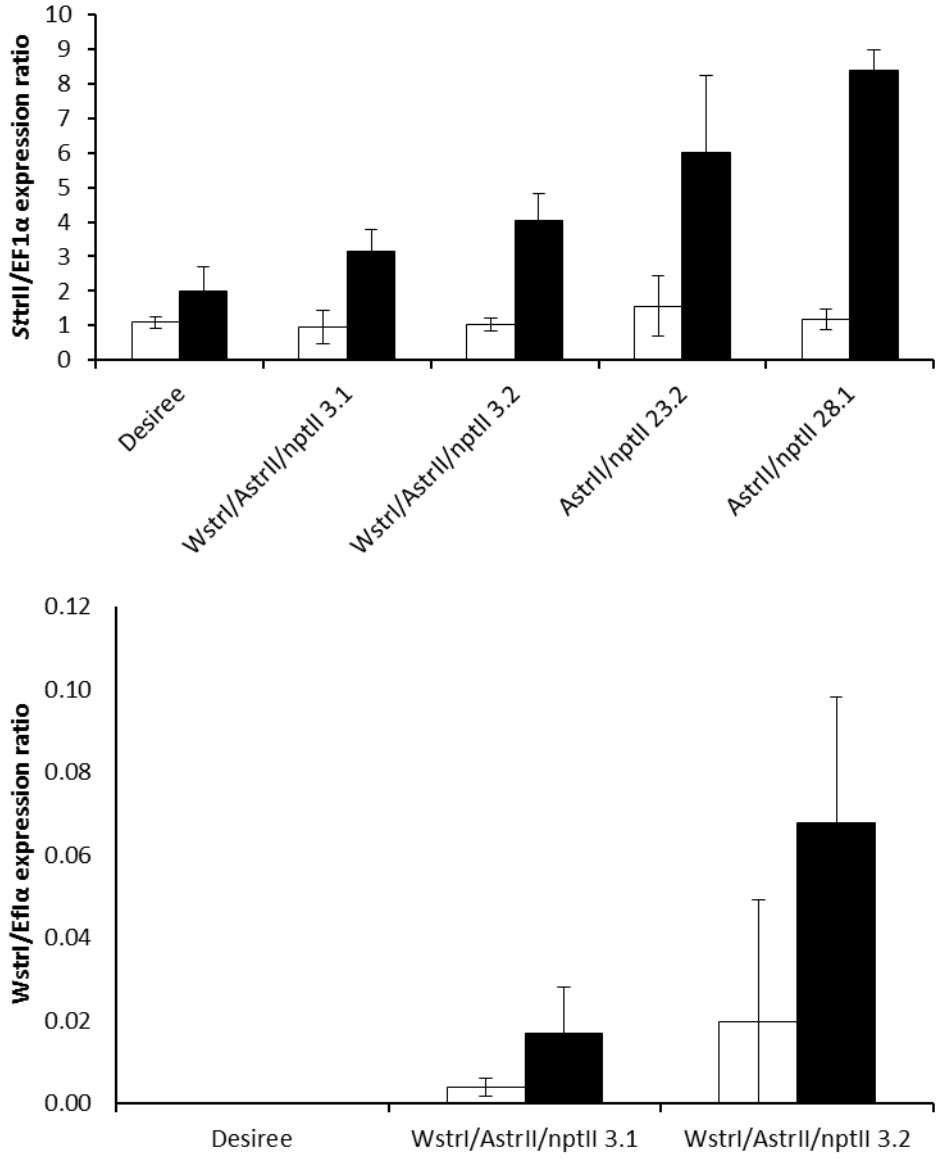

Figure 6.3.14: ***WstrI* and *trII* expression data from As*trI*I and *WstrI*/*AstrII* methyl jasmonte application assays**

RT-qPCR data showing the *SttrII*/*ef-1α* (top) and *WstrI*/*ef-1α* (bottom) expression ratios from As*trII/nptII* and *WstrI*/A*strII/nptII* transgenic lines and controls for samples from the plantlet feeding assay. Plantlets grown on control (□), and tropinone + methyl jasmonate (■) media were tested to see if the addition of the methyl jasmonate elicitor had any effect upon the expression of *WstrI* and *SttrII*.

The two co-transformed lines exhibited the greatest effect upon pseudotropine and tropine accumulation. *WstrI*/Ast*rII/nptII* 3.1 showed a very significant decrease in the accumulation of pseudotropine and a significant increase in tropine accumulation. This pattern can be seen in both the tropinone and tropinone plus methyl jasmonate conditions. Interestingly Ast*rII/nptII* 18.1 grown in the presence of tropinone and methyl jasmonate shows the highest accumulation of both pseudotropine and tropine amongst the down-regulating lines. Unfortunately for this line, the *trII* gene expression data is unavailable due to poor RNA quality.

Gene expression analysis was conducted for the lines which were grown on the control and the tropinone plus methyl jasmonate media, for *SttrII* and *WstrI* (when applicable). As shown in Figure 6.3.14, for both *SttrII* and *WstrI* the expression levels appear to be higher in plantlets which were grown in the presence of the elicitor methyl jasmonate and this follows previous research concerned with the effects of methyl jasmonate upon *pmt* and *h6h* (Kang *et al*, 2004). This does however, appear to reverse the down-regulatory effects on *trII*. Although *trII* is expressed at a higher level, in the co-transformed lines, *WstrI* expression is also increased. This offers an explanation as to why there is not a greater accumulation of pseudotropine, with tropinone flux continuing towards the more active trI.

6.4 Discussion:

6.4.1 Expression patterns of *trII*

The pattern of *trII* gene expression in the Solanaceae has previously been determined using northern blot analysis. Northern blot analysis can be used to visually investigate gene expression by detecting RNA using a hybridisation probe after separation by electrophoresis. Kaplan *et al*, (1995) have shown that qRT-PCR and Northern Blot analysis offer similar results in quantitifying gene expression levels, however, qRT-PCR offers a more direct means of quanitifcation, with fewer environmental impacts. Solanaceous tropane alkaloid producers exhibit the highest *trII* expression profiles within the roots, followed by leaves and stem tissue. This was demonstrated to be the case in *Anisodus acutangulus* (Kai *et al*, 2009). The study conducted by Kai *et al*, (2009) corroborated the earlier analysis by Keiner *et al*, (2002) which showed *trII* is expressed highest in the roots, with limited expression in stem and leaf tissues. As well as these three tissues, Keiner *et al*, (2002) also showed there was high *trII* expression in tuber sprouts seven months post-harvest. This supports the evidence described by Keiner and Dräger, (1999) that tuber sprouts are the sites of nortropane alkaloid biosynthesis.

Whilst the studies conducted by Keiner *et al*, (2002) and Kai *et al*, (2009) do not give a numerical value for the expression profile, visually, the expression pattern is readily discernible. The expression profile described in Figure 6.3.1 shows that the *trII* expression ratio fluctuates from three to thirteen fold higher than the ubiquitous *ef-1α* in roots throughout the growth and development of the potato plants. Within the stem and leaf, the expression ratio is generally below 1 compared to *ef-1α,* however, it does peak at 1.8 during early plant growth. *trII* expression within tubers is consistently low at a ratio of 0.2:1. The expression patterns generated by northern blot analysis within *Anisodus acutangulus* and potato support the expression profile described in Figure 6.3.1. This demonstrates that *trII* expression profiles within potato follow similar patterns to that seen within tropane alkaloid producing species.

Transgenic lines generated were characterised by RT-qPCR for their *trII* expression levels within young leaves. Keiner *et al*, (2002) have shown that in young leaves, *trII* expression is low, so strong expression of *trII* is not to be expected.

Comparison to untransformed cultivars *Désirée* and *Bintje* shows that generated transgenics displayed a varying degree of *trII* down-regulation relative to *ef-1α*. The levels seen in the untransformed controls correlate to the levels seen in the *trII* analysis within 6.2.1 during V.G. I. The strongest expression levels seen within this study also follow the pattern of reduction of *trII* transcript levels seen in Küster *et al*, (2017). In the roots and tuber sprouts examined by Küster *et al*, (2017) it was reported that *trII* expression when compared to controls was 4% and 0.4% respectively. Therefore, whilst the expression in the transgenics generated in this study were from leaf tissue, the similarity to effects seen in the Küster *et al* (2017) study was of interest.

6.4.2 Phenotypic differences

From the growth data shown in Figure 6.3.4 and the harvest data in Figure 6.3.5 there were clear abnormalities in one of the down-regulating lines (A*strII/nptII* 6.3) as well as the two co-transformed lines.

The phenotype exhibited by these lines show similarities to phenotypes described in the review by Barrel *et al*, (2013). The phenotypes described were because of the transformation and re-generation process. As *Solanum tuberosum* is clonally propagated, sometimes unexpected mutagenic events may occur when transgenes are inserted. Within the review it was identified that the generation of these abnormal lines could be because of somaclonal variation. That is variation which occurs during the regeneration from cell culture. Although *AstrII/nptII* 6.3 underwent leaf feeding assays as shown in Figure 6.3.8, from further analysis was not conducted on this line so that any potential deleterious effects the phenotype may have caused were removed.

6.4.3 The detectable endogenous nortropane and tropane alkaloid content

The calystegine content of potato tubers has previously been determined by Friedman *et al*, (2003) and Petersson *et al*, (2013) who examined a variety of potato cultivars as shown in Figures 1.8 and 1.9. Reported levels of calystegines within the cultivar *Désirée* from Petersson *et al*, (2013) can not be directly compared to the levels seen within this study, due to differences in sample preparations. However, examining calystegine A_3 and B_2 ratios within *Désirée* it has been shown to be 1:1.40. In the control lines of this study the ratio is 1:1.54 for cultivar *Désirée* and 1:1.62 for the

Empty Vector. While the ratio is slightly higher in controls from this study, they exhibit a similar trend when compared to the ratio in Petterson *et al* (2013). It can therefore be suggested that the results from the transgenics are comparable to calystegine levels in commercial cultivars.

The tuber calystegine concentrations within A*strII/nptII* 26.1 showed there was a reduction of 74% in A_3 and 40% in B_2 concentration compared to cultivar *Désirée*. Whilst this level of reduction was not seen in other transgenic lines, there was a 60% reduction in calystegine A_3 concentration in *AstrII/nptII* 18.1. This represents a significant reduction in calystegine A_3 accumulation across the two transgenic lines. This suggests there has been manipulation of the nortropane alkaloid biosynthetic pathway and to the storage of these metabolites within transgenic potato lines. The calystegine content in A*strII/nptII* 26.1 roots was not significantly different to levels seen in the control lines. However, as accumulation within tubers is reduced it can be suggested that there has been manipulation to the nortropane alkaloid biosynthesis pathway within the roots.

Detectable tropine within roots of *WstrI*/A*strII/nptII* 3.1 indicates that the *WstrI* transgene is influencing the endogenous metabolite flux across the tropinone branch point. Tropine levels within the root medulla and bark of *Withania somnifera*, have been reported to be 2096.85 ± 10.98 and 1966.10 ± 8.87 µg/g DW respectively (Kushwaha *et al*, 2013). Whilst the levels of tropine within *WstrI*/A*strII/nptII* 3.1 are not as high as those found within *Withania*, (0.87 ± 0.34 µg/g DW) the detection of tropine in a previously inactive producer is of interest. There is little information available with regards to the natural tropine levels found within potato tubers. Richter *et al* (2007) dissected the tuber into three different tissues and determined the levels of tropine accumulation after application of tropinone. They reported levels of approximately 30 µmol/g DW, this equating to around 4.70 µg/g. This shows that when in the presence of exogenous tropinone, tropine levels in *Désirée* lines are approximately 5-fold higher than in *WstrI*/A*strII/nptII* 3.1.

There also appears to be a highly significant difference in calystegine A_3 and B_2 content of line *WstrI*/A*strII/nptII* 3.1. Calystegine A_3 content is 4.73 ± 1.14 µg/g DW which is significantly lower than the levels detected within *Désirée*. Calystegine B_2 was not detected within this line, which suggests that this was not accumulated. It is unclear

as to why elevated levels of pseudotropine were detected within roots of *WstrI*/A*strII/nptII* 3.1. This does indicate that reductions in calystegine content may be due to other factors as the precursor to these nortropane alkaloids is clearly present. It can be speculated that the defects which have been seen during the growth and development of this co-transformed line may be a cause for the differences in nortropane alkaloid content.

6.4.4 Tropinone feeding assays

Tropinone feeding assays have been used in this study to exacerbate the manipulation across the tropinone branch point within the transgenics.

Single transgenic lines in the cultivar *Désirée* and *Bintje* exhibited different effects in levels of pseudotropine and tropine accumulated. Across the tropinone leaf feeding assays, the A*strII/nptII Désirée* lines showed significant reduction in the levels of pseudotropine detected, whereas there was no difference in the levels within the *Bintje* background. Kuster *et al*, (2017) demonstrate in leaf assays that there was a highly significant difference in the accumulation of pseudotropine across the five *SttrII* down-regulating lines developed. The decrease they reported was from 600 µg/g in control lines to < 10 µg/g DW in the transgenics. They also describe that there was no change in tropine accumulation.

Decreasing pseudotropine accumulation was seen in the *AstrII/nptII Désirée* transgenic lines generated in this study. However, the effects on accumulation were not as dramatic when compared to the results from Kuster *et al*, (2017). *SttrII* expression levels within the leaves from the assays in this study were analysed to elucidate potential differences. *trII* expression levels were shown to be the same as the respective control lines. This would explain why the expected effects at the tropinone branch point have not been seen within the single A*strII/nptII* down-regulation lines.

Co-transformed *WstrI*/A*strII/nptII* lines displayed a decrease in pseudotropine and an increase in tropine accumulation through the two leaf assays. *trII* and *WstrI* gene expression in these lines was as hypothesised, with a 5-fold decrease in *trII* expression. Comparing the *WstrI*/A*strII/nptII* lines to the single *WstrI/nptII* transgenics (from chapter 5), the accumulation of pseudotropine in the co-transformed lines is reduced by

approximately 50%. However, the single *WstrI/nptII* lines display a 3 fold increase in tropine accumulation. Differences in *WstrI* gene expression between these single and co-transformed lines can explain these differences. The co-transformed lines exhibited lower *trII* and *trI* expression when compared to the single *WstrI/nptII* lines. This suggests that whilst the co-transformed lines displayed growth and phenotypic effects from the transformation process, they offer an insight into the simultaneous disruption of both arms of the tropane and nortropane biosynthesis pathway.

The calystegine content of the tuber sprouts from *WstrI*/A*strII/nptII* 3.1 indicates that in the unfed lines, there was a 150-fold difference in the concentration of B_2 when compared to A_3. The B_2 content of this line was also significantly higher than that seen in the *Désirée* and Empty Vector. Whereas, in the presence of tropinone, pseudotropine and calystegine accumulation were significantly different to the *Désirée* and Empty Vector. There was a significant decrease in the build-up of pseudotropine in both *WstrI*/A*strII/nptII* lines. However, there was an unexpected increase in the accumulation of calystegine A_3 in line 3.1 as well as B_2 across both lines. Pseudotropine and calystegine levels in the single A*strII/nptII* lines did not exhibit any significant difference when compared to *Désirée* and untransformed controls.

The levels of pseudotropine, and the two calystegines (A_3 and B_2) when related to reported levels within Küster *et al* (2017), suggest that the effects on the nortropane alkaloid arm are not as pronounced within this study. The total calystegine content seen within control sprouts from Küster *et al* (2017) is reported at 3000 µg/g, however the content is only 7 µg/g in the controls from this study. Total calystegine content reported by Küster *et al* (2017) are also supported by the levels reported by Keiner and Dräger (2000). The discrepancy in the total calystegine content could be due to the differences in storage conditions during dormancy. Whilst the lines in this study were stored at 4^{o}C for 4 months before being left at room temperature for 5 weeks to sprout, Küster *et al* (2017) stored their tubers at 7^{o}C for 5 months or at 7^{o}C for 4 weeks then 2 months at room temperature.

Keiner and Dräger (2000) demonstrated that the highest levels of calystegines can be found in tubers 5 months after harvest. Calystegine B_2 levels were found to be 6 to 7-fold higher at this point, than directly after harvest. They also showed that single sprouts appeared on tubers after 2 weeks at room temperature if the tubers were stored

at 4^{o}C for 3 months. The sprouting exhibited by tubers within this study developed slowly which may have impacted the accumulation of calystegines.

6.4.4.1 The potential enhancement of transgene expression through the application of an elicitor

Methyl jasmonate application has been shown to increase the expression of *trI* within *W. somnifera* 8-fold after 6 hours (Kushwaha *et al,* 2013), as well as having a weak effect on *A. acutangulus trI* expression in roots (Kai *et al*, 2009). Kai *et al*, (2009) reported that *trII* expression in *A. acutangulus* can also be enhanced when in the presence of methyl jasmonate. Zabetakis *et al,* (1999) demonstrated that in *Datura stramonium* root cultures there was an increase in tropine (4-fold), hyoscyamine (1.8-fold) and scopolamine (2.5-fold) accumulation after 7 days of methyl jasmonate application, when compared to control cultures. This reported change in gene expression level and the increase in metabolite content suggested that methyl jasmonate may enhance changes to the transgenic lines developed within this study.

Utilising the MRM method developed in chapter 3, only four metabolites were detected in plantlet samples when grown in the presence of tropinone and methyl jasmonate. In the *AstrII/nptII* lines, there was a significant difference in the accumulation of pseudotropine. *AstrII/nptII* 18.1 when grown in the presence of methyl jasmonate and tropinone showed an increase in pseudotropine accumulation compared to the control and tropinone fed plantlets. There was also significant difference in accumulation of tropine within all the *AstrII/nptII* lines, compared to the control plantlets. Tropine accumulation within *Désirée* controls indicate that endogenous *SttrI* displayed a degree of activity. As with pseudotropine, *AstrII/nptII* 18.1 showed an increase in tropine concentration within plantlets grown in the presence of methyl jasmonate.

SttrII RT-qPCR analysis for control and methyl jasmonate grown plantlets indicates there was up to a 4-fold increase in *AstrII/nptII* 28.1, and the *Désirée* control showing a 2-fold increase in *trII* expression. Kai *et al*, (2009) showed that *trII* expression increased in the presence of methyl jasmonate. Although there was an increase in *trII* expression in plantlets which were grown in the presence of methyl jamonate, there does not appear to be an increase in pseudotropine accumulation

compared to plantlets grown in tropinone. The quality of extracted RNA from *AstrII/nptII* 18.1 which was grown in the presence of methyl jasmonate was unsuitable for analysis, so whilst it showed a 4-fold increase in pseudotropine accumulation, the underlying gene expression can not be determined. Although these lines showed low *trII* expression levels when they were initially characterised, it appears *trII* expression levels increased through-out plant development to that seen in controls.

There was a decrease in pseudotropine and increase in tropine within co-transformed transgenic plantlets grown in the presence of tropinone, when compared controls. The application of methyl jasmonate on these lines elicited no significant difference in the levels of pseudotropine and tropine accumulated. *WstrI* expression showed a non-significant increase within the methyl jasmonate grown plantlets. The expression levels seen within the lines exhibiting the highest levels of expression was less than a tenth of the *ef-1α* expression. There was also an increase in the *trII* expression levels within these co-transformed lines; however, the activity of *WstrI* appears to have been sufficient to drive metabolite flux towards tropine formation. Anisodamine detection in Ast*rII/nptII*, *WstrI/AstrII/nptII* and control lines although at relatively small levels suggests that there may be limited functionality of the downstream pathway.

6.4.5 The detectability of the high valued tropane alkaloids

The detection of the downstream tropane alkaloids within tissues examined through various feeding assays is of particular note. These tropane alkaloids have not been previously reported within tissues of potato (Kaiser *et al*, 2006). The four tropane alkaloids which are synthesised downstream of tropine were all seen in tuber sprout samples analysed from both tropinone fed and unfed assays. Whilst these metabolites were detected, the total tropane alkaloid concentration within the tuber sprouts was 0.066% of the level found within the current commercial source of these compounds *Duboisia myoporoides* (Kohnen *et al*, 2017). As the tropane alkaloids can be detected, it suggests that there is some limited functionality of the downstream biosynthesis pathway within potato.

6.5 Summary

Whilst it appears that the single *trII* down-regulating transgenic lines did not exhibit the hypothesised effect upon the tropinone branch point, the co-transformed transgenic lines could open potential avenues for further development. Taking into consideration potential plasmid manufacture issues which may explain the phenotypic characteristics displayed within the co-transformed lines shown in Figure 6.3.4 and 6.3.5 and re-developing the strategy to utilise a single plasmid rather than two may lead to stronger plant growth and development.

The characterisation of the endogenous metabolites within *WstrI*/A*strII/nptII* 3.1 roots has shown that there is manipulation across the tropinone branch point. Tropine levels were detected at 0.87 ± 0.37 μg/g DW and Calystegine A_3 was detected at 4.73 ± 1.14 μg/g DW. These levels are significantly differnet to the *Désirée* controls used. Coupled with the exogeneous tropinone assay which showed that there was a decrease in pseudotropine in all lines in these studies, whereas in the co-transformed lines there was an increase in detectable tropine levels.

This approach may develop robust adaptations and manipulation to the tropinone branch point and it is an avenue of pursuit worth following. With the detection of economically important tropane alkaloids, the potential enhancement to tropine accumulation and introduction of genes which display higher functionality to this region of the pathway could lead to a better platform for the production of these tropane alkaloids.

Chapter 7: General Discussion

7.1 General discussion

Whilst tropane alkaloids have been used within medicine for almost 5000 years (Griffin and Lin, 2000), the improvement and commercialisation of these plant natural products has only been studied since the early 1950's (Bernard, 1952). Because of this, the tropane alkaloid biosynthesis pathway has been elucidated in members of the solanaceae, (Nakajima *et al*, 1993; Kaiser *et al*, 2006; Kohnen *et al*, 2017) but how the pathway is regulated in potato is poorly understood. Previous research conducted by Kaiser *et al*, (2006) and Richter *et al*, (2007) have shown that trII is more active than trI in potato tissues. Limited trI activity therefore represents a lesion in the tropane alkaloid biosynthesis pathway in potato preventing the formation and accumulation of TA's formed downstream.

The main aims of the study can be summarised into three different areas. Firstly a robust detection method for tropane alkaloids and associated metabolites employing the Agilent QqQ-LC-MS/MS was developed. Secondly, a transgenic approach was used to manipulate the tropinone flux towards tropine biosynthesis. Finally, using recombinant protein assays, determine the functionality of annotated tropane alkaloid biosynthesis genes present downstream of the known pathway lesion points within the potato genome.

A robust quantification detection method was developed using a combination of the ThermoFischer Orbitrap™ and Agilent QqQ-LC-MS/MS systems. The fragmentation patterns of the tropane and nortropane alkaloids as well as associated metabolites have not been extensively reported in the literature. The development of a targeted quantification method for metabolites along the tropane alkaloid biosynthetic pathway using the QqQ-LC-MS/MS was pivotal to discerning metabolite variability between the transgenic lines and for the recombinant protein assays. The fragmentation pattern for the three high value tropane alkaloids, hyoscyamine, anisodamine and scopolamine have been reported by Chen *et al*, (2017) and Zhou *et al*, (2017) and can be seen in Table 3.1.1. The fragmentation products detected for these alkaloids in this study are in agreement with results previously reported in earlier studies; however, there are slight differences in the number of fragments produced. These differences could be attributed to variability in machine, separation column matricies and chromatography conditions. Previously reported studies detected a greater number of fragments for the

tropane alkaloids atropine (racemic hyoscyamine) and scopolamine (Chen *et al*, 2017; Zhou *et al*, 2017). The overlap displayed between fragments produced for these metabolites in the development of the method in this study was important. The similarities in fragmentation patterns for these metabolites, gives confidence in the fragments produced for the other metabolites along the pathway as well as the overall MRM which has been used in associated assays.

Using a transgenic approach, this study has shown it is possible to influence the partitioning of substrate within the biosynthetic pathways at the tropinone branch point. The introduction of a known active *trI* gene from *Withania somnifera* has potential significantly enhanced endogenous tropine accumulation in the roots of transgenic potato lines.

In previous studies, manipulation of the tropinone branch point in potato has been studied to try and reduce the accumulation of calystegines and promote the accumulation of tropine within tissues (Keiner and Dräger, 2000; Richter *et al*, 2007). These studies were primarily concerned with the *trII* (nortropane alkaloid) arm of the pathway and through a transgenic approach and mechanical wounding assays, attempted to understand the distribution and mechanisms behind calystegine formation. Building on these studies, Küster *et al*, (2017) generated transgenic lines which impacted both arms of the pathway independently. In this study, transgenic lines were developed disrupting the endogenous tropinone reductase activity and any metabolite changes quantified. This study also demonstrated that the endogenous potato *trI* gene catalysed the conversion of tropinone to tropine, and by down-regulating *trII* reducing the concentration of the calystegines. Whilst Küster *et al* (2017) enhanced the accumulation of tropine through over-expression of the endogenous *trI* gene the pseudotropine concentration in all transgenic lines bar one showed no significant variation.

Within this study, the introduction of an active *trI* gene from *Withania somnifera* resulted in an almost two fold increase in tropine accumulation compared to the *SttrI* lines overexpressing the endogenous potato *SttrI* lines reported in the Küster *et al* (2017) study. Therefore, the introduction of the *WstrI* gene into the potato genome enhances the ability of potato to produce and accumulate tropine compared to the endogenous gene. Conversely, in the *WstrI* overexpression lines from this study, the pseudotropine levels in leaf disc assays were reduced by ca. 50 % suggesting that whilst

the endogenous potato trI catalyses the conversion of tropinone to tropine the accumulation compared to an exogenous trI within potato is lower.

Transgenic lines down-regulating the potato gene, *SttrII*, used in this study did not exhibit the same degree of manipulation on the formation of pseudotropine as shown in Küster *et al,* (2017). In that study, pseudotropine levels in the generated transgenics were < 10 µg/g (FW) compared to 600 µg/g (FW) seen in the control lines. Here, A*strII/nptII* transgenic line which showed greatest manipulation to the tropane alkaloid biosynthesis pathway, showed pseudotropine levels of 1.6 µg/g (FW), whereas the *Désirée* controls contained 5 µg/g (FW) when exogenous tropinone was applied in leaf feeding assays. Single A*strII/nptII* transgenic lines did exhibit a reduction in endogenous tuber calystegine content, but there was no significant reduction in content within the roots. Pseudotropine accumulation in the presence of exogenous tropinone within these A*strII/nptII* lines was reduced, but this was not as dramatic as the levels seen in the transgenics developed by Küster *et al* (2017).

Metabolite results from the *Désirée* A*strII/nptII* lines indicate that *trII* activity was disrupted. However, *trII* expression levels within the leaf disc assays were not significantly different compared to the controls although a reduction in levels of pseudotropine across these lines indicates a reduction in enzyme activity. The *WstrI*/A*strII/nptII* co-transformed lines, which have not previously been generated in previous studies manipulating the TA biosynthetic pathway, demonstrated that both arms of the pathway can be manipulated simultaneously. Although these lines did not accumulate tropine to the levels comparable with single *WstrI/nptII* lines, the co-transformed lines exhibited a greater reduction in pseudotropine accumulation. The generated co-transformed lines offer a different point of view compared to the single transgenics for the overall enhancement of the tropinone branch point within the pathway. These *WstrI*/A*strII/nptII* transgenic lines also exhibited a phenotype which was detrimental to the growth of the plants, but still allowed for metabolite effects along the pathway to be measured. If future investigation of this pathway were to be undertaken, it would be best practice to re-manufacture a single transformation vector which can manipulate both arms of the pathway and re-transform *Solanum tuberosum*.

The use of elicitors, such as methyl jasmonate, in an attempt to upregulate the genes at the tropinone branch point of the pathway and enhance gene expression did not have the hypothesised effects nor replicated the effects described in Zabetakis *et al*,

(1999) and Kai *et al,* (2009). Previously methyl jasmonate has been shown to increase the expression of *pmt* and *h6h* which led to an increase in the associated metabolites around these areas of the tropane alkaloid biosynthesis pathway (Kang *et al*, 2004; Ryan *et al*, 2015). This avenue of investigation, whilst not giving the anticipated results may still be enhanced through the manipulation of carbohydrate metabolism (Richter *et al*, 2007), however this would require the generation of further transgenic lines. Transgenic lines which have had their carbohydrate metabolism manipulated have been shown to have a 2 to 3-fold increase in tropine accumulation (Richter *et al*, 2007). The increase in tropine present, coupled with the methyl jasmonate enhancement of downstream tropane alkaloid biosynthesis genes could further increase the accumulation of the economically important tropane akaloids.

Due to the economic importance of the tropane alkaloids, alternative methods for the manufacture of these compounds are of commercial interest. Recent advances have used *S. cerevisiae* in the manufacture of intermediates of benzylisoquinoline alkaloids (these are plant-secondary metabolites which include codeine and morphine) (DeLoache *et al,* 2015). This approach offers an interesting avenue for overcoming yield and alkaloid variability in the current commercial production platform. Although the recombinant protein assays, expressing the native h6h genes from potato did not show any conversion of hyoscyamine to scopolamine, the biotransformation of hyoscyamine in *E. coli* using *h6h* from *Datura*, would be of interest to move into a yeast system. Using a microbial system to produce these metabolites would allow for an increase in efficiency and yield with each step being able to be strictly regulated, maximising output. This would allow large scale fermentation to occur and could be a potential platform to generate the whole pathway in a cell culture system which industrially produces tropane alkaloids.

As well as regulating reaction conditions, moving to a yeast or microbial system has advantages over a transgenic approach, as food sources are not being removed from the food chain. This can have similar conotations to the usage of food sources in the manufacture of first generation biofuels. These ethical implications aside, through this project the accumulation of downstream tropane alkaloids has been shown within the tubers of transgenic lines. Although the main site of accumulation is the leaves, the detection of these drugs within the tubers of transgenic lines, which are the parts of *Solanum tuberosum* which are consumed can be problematic if levels of tropane

alkaloids are enhanced. Therefore, if any further enhancement of the tropane alkaloid pathway in *Solanum tuberosum* was to be undertaken this issue would need to be overcome.

Results of this study have shown that through the introduction of a functional trI gene the utilisation of the substrate, tropinone, can be diverted towards tropane alkaloid biosynthesis and away from the nortropane alkaloids. However, conversion of tropine to the economically important tropane alkaloids hyoscyamine and scopolamine is limited within potato. Whilst a relatively small concentration of tropane alkaloids is detected within tuber sprout and plantlet tissues, for potato to be considered a viable platform to produce tropane alkaloids, further research would need to be conducted to overcome lesions identified within this study such as the *h6h* lesion as well develop an understanding of any potential lesions between *trI* and *h6h*. Recent advances in the genome editing technology CRISPR and particularly the potential time and accuracy benefits it offers would be of interest. CRISPR coupled with the development of high throughput spectrophotmetirc techniques can increase the understanding and knowledge around these other potential lesions.

References:

Abdel-lateif, K.S. Maghrabi, I.A. Eldaeb, H.A. (2016) *The Plant Natural Products: Their Antioxidants, Free Radical Scavengers, DNA Protection and Antimicrobial Activities.* Journal of Bioprocessing & Biotechniques. 6(9): doi: 10.4172/2155-9821.1000293

Amirkia, V. Heinrich, M. (2014) *Alkaloids as drug leads – A predictive structural and biodiversity-based analysis*. Phytochemistry Letters. **10** xlviii – liii.

Arab, A. Alves, MN. Sartoratto, A. Ogasawara, DC. Trigo, J.R. (2012) *Methyl jasmonate increase the TA scopolamine and reduced natural herbivory in Brugmansia suaveolens: Is scopolamine responsible for plant resistance?* Neotropical Entomology. **41**: 2-8

Asano, N. Kato, A. Oseki, K. Kizu, H. Matsui, K. (1995) *Calystegins of Physalis alkekengi var. francheti (Solanaceae). Structure determination and their glycosidase inhibitory activities.* European Journal of Biochemistry. **229(2):** 369-376

Barnard, C. (1952). *The Duboisias of Australia*. Economic Botany. **6(1):** 3-17

Barrell, P.J. Meiyalaghan, S. Jacobs, J.M.E. Conner, A.J. (2013) *Application of biotechnology and genomics in potato improvements*. Plant Biotechnology Journal. **11:** 907-920

Bekkouche, K. Daali, Y. Cherkaoui, S. Veuthey, J-L. Christen, P. (2001) *Calystegine distribution in some solanaceous species*. Phytochemistry **58:** 455-462

Boa, W. Qu, Y. Shan, X. Wan, Y (2016) *Screening and Validation of Housekeeping Genes of the Root and Cotyledon of Cunninghamia lanceolate under Abiotic Stresses by Using Quantitative Real Time PCR.* International Journal of Molecular Sciences. **17:**1198

Booth, W.T. Schlachter, C.R. Pote, S. Ussin, N. Mank, N.J. Klapper, V. Offermann, L.R. Tang, C. Hurlburt, B.K. Chruszsz, M. (2018). *Impact of an N-terminal Polyhistidine Tag on Protein Thermal Stability*. ACS Omega**. 3**: 760-768

Brock, A. Brandt, W. Dräger, B. (2008). *The functional divergence of short-chain dehydrogenases involved in tropinone reduction.* The Plant Journal. **54:** 388-401

Brown, C.R. (1993) *Origin and history of the Potato*. American Potato Journal 70: 363-372

Cardillo A.B., Perassolo M., Sartuqui M., Talou J.R., Giulietti A.M. (2017) *Production of tropane alkaloids by biotransformation using recombinant Escherichia coli whole cells*. Biochemical Engineering Journal. **125**; 180-189

Chen, W. Cheng, X. Zhou, Z. Liu, J. Wang, H. (2013). *Molecular cloning and characterisation of a tropinone reductase from Dendrobium nobile Lindl*. Molecular Biology Reports. **40:** 1145-1154

Chen H., Marin-Saez J., Romero-Gonzalez R., Frenich A.G, (2017) *Simultaneous determination of atropine and scopolamine in buckwheat and related products using modified QuEChERS and liquid chromatography tandem mass spectrometry*. Food Chemistry. **218**, 173-180

Christen, P. (2000) *Tropane alkaloids: Old drugs used in modern medicine.* Studies in Natural Products Chemistry. **22**: 717-749

Cirlini M., Bemuth T.M., Biancardi A., Rychlik M., Dall'Asta C., Bruni R. (2018) *Are tropane alkaloids present in organic foods? Detection of scopolamine and atropine in organic buckwheat (Fagopyron esculentum L.) products by UHPLC-MS/MS*. Food Chemistry. **239**, 141-147

Coa Y-D., He Y-C., Li H., Kai G-Y., Xu J-H., Yu H-L. (2015) *Efficient biosynthesis of rare natural product scopolamine using E. Coli cells expressing a S14P/K97A mutant of hyoscyamine-6β-hydroxylase AaH6H.* Journal of Biotechnology. **211**, 123-129

DeLoache, W.C. Russ, Z.N. Narcross, L. Gonzales, A.M. Martin, V.J.J. Dueber, J.E. (2015). *An enzyme-coupled biosensor enables (S)-reticuline production in yeast from glucose.* Nature Chemical Biology. **11:** 465-471

Deng, F. (2005) *Effects of glyphosate, chlorsulfuron and methyl jasmonate on growth and alkaloid biosynthesis of jimsonweed (Datura stramonium L.).* Pesticide Biochemistry and Physiology. **82:** 16-26

Doncheva, T. Berkov, S. Philipov, S. (2006) *Comparative study of the alkaloids in the tribe Datureae and their chemosystematic significance*. Biochemical Systematics and Ecology. **34:** 478-488

Dräger, B. Funck, C. Höhler, A. Mrachatz, G. Nahrstedt, A. Portsteffen, A. Schaal, A. Schmidt, R. (1994) *Calystegines as a new group of tropane alkaloids in Solanaceae*. Plant Cell, Tissue and Organ Culture. **38**: 235-240

Dräger B., (1995) *Identification and Quantification of Calystegines, Polyhydroxyl Nortropane Alkaloids*. Phytochemical Analysis. **6**, 31-37. .

Dräger B., (2002) *Analysis of tropane and related alkaloids*. Journal of Chromatography A. **978**, 1-35.

Dräger, B. (2006) *Tropinone reductases, enzymes at the branch point of tropane alkaloid metabolism*. Phytochemistry **67:** 327-337

Ducreux, L.J. Morris, W.L. Hedley, P.E. Shepard, T. Davies, H.V. Millam, S. Taylor, M.A. (2005). *Metabolic engineering of high carotenoid potato tubers containing enhanced levels of β-carotene and lutein.* Journal of Experimental Botany **56(409):** 81-89.

Dutt M., Dhekney S.A., Soriano L., Kandel R., Grosser J.W. (2014) *Temporal and spatial control of gene expression in horticultural crops*. Horticultural Research **1,** 14047; doi.10.1038/hortres.2014.17

El Bazaoui A., Stambouli H., Bellimam M.A., Soulaymani A., (2009). *Determination of tropane alklaoids in seeds of Datura stromonium L. by GC/MS and LC/MS*. Annales de Toxicologie Analytique. **21(4).** 183-188

Felsenstein, J. (1985). *Confidence Limits on Phylogenies: An Appraoch Using the Bootstrap.* Evolution **39(4):** 783-791

Freitas, A.V.L. Trigo, J.R. Brown, K.S. Witte, L. Hartmann, T. Barata, L.E.S. (1996) *Tropane and pyrrolizidine alkaloids in the ithomiines Placidula euryanassa and Miraleria cymothe (Lepidoptera: Nymphalidae).* Chemoecology **7:** 61-67

Friedman, M. Roitman, J.N. Kozuke, N. (2003) *Glycoalkaloid and calystegine contents of eight potato cultivars.* Journal of Agricultural Food Chemistry. **51:** 2964-2973

Griffin, W.J and Lin, G.D. (2000) *Chemotaxonomy and geographical distribution of tropane alkaloids*. Phytochemistry **53:** 623-637

Griffiths, D.W. Shepard, T. Stewart, D. (2008) *Comparison of the calystegine composition and content of potato sprouts and tubers from Solanum tuberosum group Phureja and Solanum tuberosum group Tuberosum*. Journal of Agricultural and Food Chemistry. **56:** 5197-5204

Gritsanapan, W. Griffin, W.J. (1991) *Alkaloid variation within Duboisia myoporoides*. Phytochemistry. **30(8):** 2667-2669.

Grynkiewicz, G. Gadzikowska, M. (2008) *Tropane alkaloids as medicinally useful natural products and their synthetic derivatives as new drugs*. Pharmacological Reports. **60:** 439-463

Hashimoto, T. Yukimune, Y. Yamada, Y. (1986) *Tropane Alkaloid Production in Hyoscyamus Root Cultures*. Journal of Plant Physiology. **124(2):** 61-75

Hashimoto, T. Yukimune, Y. Yamada, Y. (1989) *Putrescine and putrescine N-methyltransferase in the biosynthesis of tropane alkaloids in cultured roots of Hyoscyamus albus*. Planta. **178:** 131-137

Hashimoto, T. Mitani, A. Yamada, Y. (1990) *Diamine oxidase from cultured roots of Hyoscyamus niger*. Plant Physiology. **93:** 216-221

Hashimoto, T. Hayashi, A. Amano, Y. Kohno, J. Iwanari, H. Usuda, S. Yamada, Y. (1991). *Hyoscyamine-6β-hydroxylase, an Enzyme Involved in Tropane Alkaloid Biosynthesis, Is Localized at the Pericycle of the Root.* The Journal of Biological Chemistry. **266(7):** 4648-4653

Hashimoto, T. Matusda, J. Yamada, Y. (1993) *Two-step epoxidation of hyoscyamine to scopolamine is catalysed by bifunctional hyoscyamine-6β-hydroxylase.* FEBS Letters **329(1-2)**; 35-39

Hashimoto,T. Yun, D-J. Yamada, Y. (1993) *Production of tropane alkaloids in genetically engineered root cultures*. Phytochemistry **32(3):** 713-7188

Hashimoto, T. Yamada, Y. (2003) *New genes in alkaloid metabolism and transport*. Current opinion in Biotechnology. **14:** 163-168

Hawkes, J.G. Francisco-Ortega, J. (1993). *The early history of the potato in Europe*. Euphytica **70:** 1-7

Hichri, I. Barrieu, F. Bogs, J. Kappel, C. Delrot, S. Lauvergeat, V. (2010) *Recent advances in the transcriptional regulation of the flavonoid biosynthetic pathway*. Journal of Experimental Botany**.** Doi: 10.1093/jxb/erq442

Höke, D. Dräger, B (2004) *Calystegines in Calystegia sepium do not Inhibit Fungal Grwoth and Invertase Activity but Interact with Plant Invertase*. Plant Biology **6**: 206-213

Humphrey, A. O'Hagan, D. (2001) *Tropane alkaloid biosynthesis. A century old problem resolved*. National Product Report. **18:** 494-502

Jaber-Vazdekis, N. González, C. Ravelo, Á, Zárate, R. (2009) *Cloning, characterisation and analysis of expression profiles of a cDNA encoding a hyoscyamine-6β-hydroxylase (H6H) from Atropa baetica Willk.* Plant Physiology and biochemistry. **47:** 20-25

Jakabova S., Vincze L., Farkas A., Kilar F., Boros B., Felinger A., (2012*) Determination of tropane alkaloids atropine and scopolamine by liquid chromatography-mass spectrometry in plant organs of Datura species*. Journal of Chromatography A. **1232**, 295-301

Jaremicz, Z. Luczkiewicz, M. Kokotkiwicz, A. Krolicka, A. Sowinski, P. (2014) *Production of tropane alkaloids in Hyoscyamus niger (black henbane) hairy roots grown in bubble-column and spray bioreactors*. Biotechnology Letters. **36:** 843-853

Jirschitzka, J. Schmidt, G.W. Reichelt, M. Schneider, B. Gershenzon, J. D'Auria, J.C. (2012) *Plant tropane alkaloid biosynthesis evolved independently in the Solanaceae and Erythroxylaceae*. PNAS. **109(26):** 10304-10309

Jouhikainen, K. Lindgren, L. Jokelainen, T. Hiltunen, R. Teeri, T.H. Oksman-Caldentey, K-M. (1999) *Enhancement of scopolamine production in Hyoscyamus muticus L. hairy root cultures by genetic engineering.* Planta. **208**: 545-551

Juhascik M.P., Jenkins A.J. (2009). *Comparison of Liquid/Liquid and Solid-Phase Extraction for Alkaline Drugs*. Journal of Chromatographic Science. **47**, 553-557

Kai, G. Li, L. Jiang, Y. Yan, X. Zhang, Y. Lu, Xuan. Liao, P. Chen, J. (2009). *Molecular cloning and characterisation of two tropinone reductases in Anisodus acutangulus and enhancement of tropane alkaloid production in AaTRI-transformed hairy roots.* Biotechnology and Applied Biochemistry. **54**: 177-186.

Kai, G. Liu, Y. Wang, X. Yang, S. Fu, X. Luo, X. Liao, P. (2011) *Functional identification of hyoscyamine-6β-hydroxylase from Anisodus acutangulus and overproduction of scopolamine in genetically-engineered Escherichia coli.* Biotechnology Letters. **33**; 1361-1365

Kai, G. Zhang, A. Guo, Y. Li, L. Cui, L. Luo, X. Liu, C. Xiao, J. (2012) *Enhancing the production of tropane alkaloids in transgenic Anisodus acutangulus hairy root cultures by over-expressing tropinone reductase I and hyoscyamine-6β-hydroxylase*. Molecular Biosystems **8**:2883-2890

Kaiser, H. Richter, U. Keiner, R. Brabant, A. Hause, B. Dräger, B. (2006) *Immunolocalisation of two tropinone reductases in potato (Solanum tuberosum L.) root, stolon, and tuber sprouts*. Planta. **225:** 127-137

Kallberg Y., Oppermann U., Jörnvall H., Persson B. (2002) *Short-chain dehydrogenase/reductase (SDR) relationships: A large family with eight clusters common to human, animal, and plant genomes*. Protein Science. **11:** 636-641

Kanegae T., Kajiya H., Amano Y., Hashimoto T., Yamada Y. (1994) *Species-Dependent Expression of the Hyoscyamine 6β-Hydroxylase Gene in the Pericycle*. Plant Physiology. **105**:483-490

Kang S-M., Jung H-Y., Kang Y-M., Yun D-J., Bahk J-D., Yang J-K., Choi M-S. (2004) *Effects of methyl jasmonate and salicylic acid on the production of tropane alklaoids and the expression of PMT and H6H in adventitious root cultures of Scopolia parviflora.* Plant Science **166:** 745-751

Kaplan L.A.E., Van Cleef K., Wirgin I., Crivello J.F. (1995) *A Comparison of RT-PCR and Northern Blot Analysis in Quantifying Metallothionein mRNA Levels in Killifish Exposed to Waterborne Cadmium*. Marine Environametnal Research **39:** 137-141

Keiner R., Dräger B. (1999) *Calystegine distribution in potato (Solanum tuberosum) tubers and plants*. Plant Science. **150**; 171-179.

Keiner, R. Nakajima, K. Hashimoto, T. Dräger, D. (2000). *Accumulation and Biosynthesis of Calystegine in Potato*. Journal of Applied Botany **74:**122-125

Keiner, R. Kaiser, H. Nakajima, K. Hashimoto, T. Drager, B. (2002). *Molecular cloning, expression and characterisation of tropinone reductase II, an enzyme of the SDR family in Solanum tuberosum (L.).* Plant Molecular Biology. **48:** 299-308

Khanam, N. Khoo, C. Close, R. Khan, A.D. (2001) *Tropane alkaloid production by shoot culture of Duboisia myoporoides R. Br*. Phytochemistry **56:** 59-65

Kitteringham N.R, Jenkins R.E, Lane, C.S, Elliott V.L, Park B.K. (2009). *Multiple reaction monitoring for quantitative biomarker analysis in proteomics and metabolomics*. Journal of Chromatography B. **877**, 1229-1239

Knight, T. (2003) *Idempotent vector design for standard assembly of BioBricks.* Boston, MA, USA: MIT Synthetic Biology Working Group, MIT Artificial Intelligence Laboratory.

Kohnen, K.L. Sezgin, S. Spiteller, M. Kayser, O. (2017) *Localisation and Organisation of Scopolamine Biosynthesis in Duboisia myoporoides R.Br.* Plant and Cell Physiology. **59(1):** 107-118

Kokotkiewicz A., Migas P., Stefanowicz J., Luczkiewicz M., Krauze-Baranowska M., (2017) *Densitometric TLC analysis for the control of tropane and steroidal alkaloids in Lycium barbarum.* Food Chemistry. **221**, 535-540

Kushwaha A.K., Sangwan N.S., Trivedi P.K., Negi A.S., Misra L., Sangwan R.S. (2013) *Tropine Forming Tropinone Reductase Gene from Withania somnifera (Ashwagandha): Biochemical Characteristics of the Recombinant Enzyme and Novel Physiological Overtone of Tissue-Wide Gene Expression Patterns*. PloS one. **8(9);** e74777

Küster N., Rosahl S., Dräger B. (2017) *Potato plants with genetically engineered tropane alkaloid precursors.* Planta. **245(2);** 355-365

Lanoue, A. Boitel-Conti, M. Portais, J.C. Laberche, J.C. Barbotin, J.N. Christen, P. Sangwan-Norreel, B. (2002) *Kinetic study of Littorine Rearrangement in Datura inoxia Hairy Roots by 13C NMR Spectroscopy.* Journal of Natural Products **65:** 131-1135

Lantin S., O'Brien M., Matton D.P. (1999) *Pollination, wounding and jasmonate treatments induce the expression of a developmentally regulated pistil dioxygenase at a distance, in the ovary, in the wild potato Solanum chacoense Bitt*. Plant Molecular Biology. **41**: 371-386

Lee, M.S.Y. (2000) *Tree robustness and clade significance*. Systems Biology. **49(4):** 829-836

Leete, E. (1990) *Recent developments in the biosynthesis of tropane alkaloids*. Planta medica. **56:** 339-352.

Li R., Reed D.W., Liu E., Nowak J., Pelcher L.E., Page J.E. (2006) *Functional Genomic Analysis of Alkaloid Biosynthesis in Hyoscyamus niger Reveals a Cytochrome P450 Involved in Littorine Rearrangement*. Chemistry & Biology. **13**; 513-520

Li J., van Belkum M.J., Vederas J.C. (2012) *Functional characteriation of recombinant hyoscyamine-6β-hydroxylase from Atropa belladonna*. Bioorganic and Medicinal Chemistry. **20;** 4356-4363

Liu T., Zhu P., Cheng K., Meng C., He H. (2005) *Molecular Cloning, Expression and Characterisation of Hyoscyamine-6β-Hydroxylase from Hairy Roots of Anisodus tanguticus*. Planta Medica. **71(3)**; 249-253

Magallon, S. Castillo, A. (2009). *Angiosperm diversification through time*. American Journal of Botany **96:1**, 349-365

Makarov A., (2000). *Electrostatic Axially Harmonic Orbital Trapping: A High-Performance Technique of Mass Analysis.* Analytical Chemistry. **72**, 1156-1162

Makarov A., Scigelova M., (2010). *Coupling liquid chromatography to Orbitrap mass spectrometry*. Journal of Chromatography A. **1217**, 3938-3945

Mano Y., Nabeshima S., Matsui C., Ohkawa H. (1986*) Production of tropane alkaloids by hairy root cultures of Scopolia japonica*. Agricultural and Biological Chemistry. **50**(11), 2715-2722

March R.E. (1997) *An Introduction to Quadrupole Ion Trap Mass Spectrometry*. Journal of Mass Spectrometry. **32**, 351-369

McKibbin, R.S. Muttucumaru, N. Paul, M.J. Powers, S.J. Burrell, M.M. Coates, S. Purcell, P.C. Tiessen, A. Geigenberger, P. Halford, N.G. (2006) *Production of high-starch, low-glucose potatoes through over-expression of the metabolic regulator SnRK1*. Plant Biotechnology Journal. **4:** 409-418

Miazek, K. Ledakowicz, S. (2013) *Chlorophyll extraction from leaves, needles and microalagae: A kinetic approach*. International Journal of Agricultural and Biological Engineering. **6(2):** 107-115.

Molyneux, R.J Pan, Y.T. Goldmann, A. Tepfer, D.A. Elbein, A.D. (1993) *Calystegins, a Novel Class of Alkaloid Glycosidase Inhibitors.* Archives of Biochemistry and Biophysics. **304(1):** 81-88

Molyneux, R.J. Gardner, D.R. James, L.F. Colegate, S.M. (2002) *Polyhydroxy alkaloids: chromatographic analysis*. Journal of Chromatography A. **967:** 57-74

Moummou H., Kallber Y., Tonfack L.B., Persson B., van der Rest B. (2012) *The Plant Short-Chain Dehdrogenase (SDR) superfamily: Genome-wide inventory and diversification patterns*. BMC Plant Biology **12:** 219

Moyano, E. Fornale, S. Palazon, J. Cusido, R.M. Bagni, N. Pinol, M.T. (2002) *Alkaloid production in Duboisia hybrid hairy root cultures overexpressing pmt gene.* Phyotochemistry. **59:** 697-702

Mroczek T., Glowniak K., Kowalska J. (2006) *Solid-liquid extraction and cation-exchange solid-phase extraction using a mixed-mode polymeric sorbent of Datura and related alkaloids*. Journal of Chromatography A. **1107**, 9-18.

Murashige, T. Skoog, F. (1962) *A revised medium for rapid growth and bioassays with tobacco tissue cultures*. Physiologia Plantarum **15:** 473-497

Nakajima, K. Hashimoto, T. Yamada, Y. (1993) *Two tropinone reductases with different stereospecificities are short-chain dehydrogenases evolved from a common ancestor*. Proceedings of the National Academy of Science. **90:** 9591-9595

Nakane, E. Kawakita, K. Doke, N. Yoshioka, H. (2003) *Elicitation of primary and secondary metabolism during defense in the potato.* Journal of General Plant Pathology **69**: 378-384

Nash, R.J. Watson, A.A. (1995). *Inhibition of glycosidases by Lepidoptera; roles in the insects' leads to novel compounds.* Chemoecology **3/4:** 167-171

Nicot, N. Hausman, J-F. Hoffmann, L. Evers, D. (2005) *Housekeeping gene selection for real-time RT-PCR normalisation in potato during biotic and abiotic stress.* Journal of Experimental Botany. doi:10.1093/jxb/eri285 Page 1-8

Oksman-Caldentey, K-M. Inzé, D. (2004) *Plant cell factories in the post-genomic era: new ways to produce designer secondary metabolites.* TRENDS in Plant Science **9(9):**433-440

Oksman-Caldentey, K-M. (2007) *Tropane and Nicotine Alkaloid Biosynthesis-Novel Approaches towards Biotechnological Production of Plant-Derived Pharmaceuticals*. Current Pharmaceutical Biotechnology. **8:** 203-210

Ollagnier, S. Kervio, E. Retey, J. (1998) *The role and source of 5'-deoxyadenosyl radical in a carbon skeleton rearrangement catalysed by a plant enzyme*. FEBS Letters **437:** 309-312

Palazon, J. Moyano, E. Cusido, R.M. Bonfill, M. Oksman-Caldentey, K.M. Pinol, M.T. (2003). *Alkaloid production in Duboisia hybrid hairy roots and plants overexpressing the h6h gene*. Plant Science. **165:** 1289-1295

Park, W-J. You, S-H. Choi, H-a. Chu, Y-J. Kim, G-J. (2015). *Over-expression of recombinant proteins with N-terminal His-tag via subcellular uneven distribution in Escherichia coli*. Acta Biochim et Biophysica Sinica. **47(7):** 488-495

Patil, V. Siddappa, S. Kawar, P. Bhardwaj, V. (2016) Biology of Solanum tuberosum (Potato). Series of Crop Specific Biology Documents. Ministry of Environment, Forest and Climate Change, Government of India.

Patron, N. J. Orzaez, D. Marillonnet, S. Warzecha, H. Matthewman, C. Youles, M. Raitskin, O. Laveau, A. Farre, G. Rogers, C. Smith, A. Hibberd, J. Webb, A.A.R. Locke, J. Schornack, S. Ajioka, J. Daulcombe, D.C. Zipfel, C. Kamoun, S. Jones, J.D.G. Kuhn, H. Robatzek, S. Van Esse, H.P. Sanders, D. Oldroyd, G. Martin, C. Field, R. O'Connor, S. Fox, S. Wulff, B. Miller, B. Breakspear, A. Radhakrishnan, G. Delaux, P.M. Loque, D. Granell, A Tissier, A. Shih, P. Bruntell, T.P. Quick, W.P. Rischer, H. Fraser, P.D. Aharoni, A. Raines, C. South, P.F. Ane, J.M. Hamberger, B.R. Langdale, J. Stougaard, J. Bouwmeester, H. Udvardi, M. Murray, J.A.H. Ntoukakis, V. Schafer, P. Denby, K. Edwards, K.J. Osbourn, A. Haseloff, J. (2015) *Standards for plant synthetic biology: a common syntax for exchange of DNA parts*. New Phytologist doi: 10.1111/nph.13532

Perchalskl R.J., Yost R.A., Wilder B.J. (1982). *Structural Elucidation of Drug Metabolites by Triple-Quadrupole Mass Spectrometry*. Analytical Chemistry. **54**, 1466-1471

Petersson E.V., Arif U., Schulzova V., Krtková V., Hajšlová J., Meijer J., Andersson H.C., Jonsson L., Sitbon F. (2013) *Glycoalkaloid and Calystegine Levels in Table Potato Cultivars Subjected to Wounding, Light and Heat Treatments*. Journal of Agricultural and Food Chemistry. **61:** 5893-5902

Pfaffl, M.W (2001) *A new mathematical model for relative quantification in real-time RT-PCR*. Nucleic Acids Research. **29(9):** 2002-2007

Philipov, S. Doncheva, T. (2013) *Alkaloids derived from Ornithine: Tropane Alkaloids*. Natural Products. pp 343-385

Pietsch, J.; Günther, J.; Henle, T.; Dreβler, J. (2008) *Simultaneous determination of thirteen plant alkaloids in a human specimen by SPE and HPLC*. Journal of Separation Science **31:** 2410-2416

Plunkett, A.O. (1992) *Pyrrile, Pyrrolidine, Pyridine, Piperidine and Axepine Alkaloids*. Natural Product Reports. **9:** 491

Pramod K.K., Singh S., Jayabaska ran C. (2010a) *Expression of hyoscyamine 6β-hydroxylase in the root pericycle cells and accumulation of its product scopolamine in leaf and stem tissues of Datura metel L*. Plant Science. **178(2);** 202-206

Pramod K.K., Singh S., Jayabaskaran C. (2010b) *Biochemical and structural characterisation of recombinant hyoscyamine-6β-hydroxylase from Datura metel L*. Plant Physiology and Biochemistry. **48**; 966-970

Rahman, L.u. Kitamura, Y. Yamaguchi, J. Mukai, M. Akiyama, K. Yamamoto, H. Muranaka, T. Ikenaga, T. (2006) *Exogeneous plant h6h but not bacterial hchl gene is expressed in Duboisia leichhardtii hairy roots and affects tropane alkaloid production.* Enzyme and Microbial Technology. **39(6):** 1183-1189

Reinhardt N., Fischer J., Coppi R., Brandt W., Dräger B. (2014) *Substrate flexibility and reaction specificity of tropinone reductase-like short-chain dehydrogenases*. Bioorganic Chemistry. **53**: 37-49

Richter, U. Rothe, G. Fabian, A-K. Rahfeld, B. Dräger, B. (2005) *Overexpression of tropinone reductases alters alkaloid composition in Atropa belladonna root cultures*. Journal of Experimental Botany. **65(412):** 645-652

Richter, U. Sonnewald, U. Dräger, B. (2007) *Calystegines in potatoes with genetically engineered carbohydrate metabolism.* Journal of Experimental Botany. **58(7):** 1603-1615

Robins, R.J Bachmann, P. Robinson, T. Rhodes, M.J.C. Yamada, Y. (1991) *The formation of 3α- and 3β- acetoxytropanes by Datura stramonium transformed root cultures involves two acetyl-CoA-dependent acyltransferases*. FEBS Letters **292(1):** 293-297

Robins, R.J. Bachmann, P. Woolley, J.G. (1994) *Biosynthesis of Hyoscyamine involves an Intramolecular Rearrangement of Littorine*. Journal of the Chemical Society Perkins Transactions 1. **(6):** 615-619

Rocha. P. Stenzel, O. Parr, A. Walton, N. Christou, P. Dräger, B. Leech, M.J. (2002) *Functional expression of tropinone reductase I (trI) and hysocyamine-6β-hydroxylase (h6h) from Hyoscyamus niger in Nicotiana tabacum*. Plant science. **162:** 905-913

Rocha, A.J. Maranhão, P.A, Silva, R.O. Pohl, S. Fonteles, C.S.R. (2016) *Identification of suitable reference genes for gene expression normalisation in Jatropha curcas L during development and under stress conditions using Real Time Quantitative PCR.* Brazilian Archives of Biology and Technology. **59**: e16150396

Romera-Torres, A. Romero-González, R. Vidal, J.L.M. Garrido-Frenich, A. (2018) *Simultaneous analysis of tropane alkaloids in teas and herbal teas by liquid chromatography coupled to high-resolution mass spectrometry (Orbitrap*). Journal of Separation Science. **41(9):** 1938-1946

Ross, H.A. Wright, K.M. McDougall, G.J. Roberts, A.G. Chapman, S.N. Morris, W.L. Hancock, R.D. Stewart, D. Tucker, G.A. James, E.K. Taylor, M.A. (2011) *Potato tuber pectin structure is influenced by pectin methyl esterase activity ad impacts on cooked potato texture*. Journal of Experimental Botany. **62(1):** 371-381

Rothe, G. Garske, U. Dräger, B. (2001). *Calystegines in root cultures of Atropa belladonna respond to sucrose, not to elicitation*. Plant Science **160**: 1043-1053

Ryan S.M., DeBoer K.D., Hamill J.D. (2015) *Alkaloid production and capacity for methyljasmonate induction by hariy roots of two species in Tribe Anthocercideae, family Solanaceae*. Functional Plant Biology **42:** 792-801

Sanger, F., Donelson, J.E., Coulson, A.R., Kösse, I.H., Fischer, D. (1974) *Determination of a nucleotide sequence in bacteriophage f1 DNA by primed synthesis with DNA polymerase*. Journal of Molecular Biology **90(2):** 315-333

Sarrion-Perdigones, A. Vazquez-Vilar, M. Palaci, J. Castelijns, B. Forment, J. Ziarsolo, P. Blanca, J. Granell, A. Orzaez, D. (2013) *GoldenBraid 2.0: A comprehensive DNA assembly framework for plant synthetic biology*. Plant Physiology. **162:** 1618-1631

Schimming, T. Jenett-Siems, K. Mann, P. Tofern-Reblin, B. Milson, J. Johnson, R.W. Deroin, T. Austin, D.F. Eich, E. (2005). *Calystegines as chemotaxonomic markers in the Convolvulaceae*. Phytochemistry. **66:** 469-480

Schmidt, G.W. Jirschitzka, J. Porta, T. Reichelt, M. Luck, K. Torre, J.C.P. Dolke, F. Veresio, E. Hopfgartner, G. Gershenzon, J. D'Auria, J.C. (2015) *The last step in cocaine biosynthesis is catalysed by a BAHD acyltransferase*. Plant Physiology **167(1):** 89-101

Schmittgen, T.D. Livak, K.J. (2008) *Analysing real-time PCR data by the comparative C_T method.* Nature Protocols. **3(6):**1101-1108

Simo, C. Ibanez, C. Valdes, A. Cifuentes, A. Garcia-Canas, V. (2014) *Metabolomics of Genetically Modified Crops*. International Journal of Molecular Sciences. **15**: 18941-18966

Springer, N.M. Ying, K. Fu, Y. Ji, T. Yeh, C-T. jia, Y. Wu, W. Richmond, T. Kitzman, J. Rosenbaum, H. Iniguez, A.L. Barbazuk, W.B. Jeddolah, J.A. Nettleton, D. Schnable, P.S. (2009) *Maize Inbred Exhbit High Levels of Copy Number Variation (CNV) and Presence/Absence Variation (PAV) in Genome Content*. PLoS Genetics **5(11):** e1000734

Sramska P., Maciejka A., Topolewska A., Stepnowski P., Halinski., (2017) *Isolation of atropine and scopolamine from plant material using liquid-liquid extraction and Extrelut® columns.* Journal of Chromatography B. **1043**, 202-208

Steenkamp P.A., Harding N.M., van Heerden F.R., van Wyk B.E. (2004) *Fatal Datura poisoning: identification of atropine and scopolamine by high performance liquid chromatography/photodiode array/mass spectrometry*. Forensic Science International. **145**, 31-39

Stenzel, O. Teuber, M. Dräger, B. (2006). *Putrescine N-methyltransferase in Solanum tuberosum L., a calystegine-forming plant.* Planta. **223:** 200-212

Stürzenbaum, S.R. Kille, P. (2001) *Control genes in quantitative molecular biological techniques: the variability of invariance*. Comparative Biochemistry and Physiology Part B. **130:** 281-289

Tamura K, Stecher G, Peterson D, Filipski A, and Kumar S (2013) *MEGA6: Molecular Evolutionary Genetics Analysis Version 6.* Molecular Biology and Evolution **30:** 2725-2729

Temerdashev A.Z., Kolchev I.A., Kiseleva N.V. (2012). *Chromatographic Determination of Some Tropane Alkaloids in Datura metel*. Journal of Analytical Chemistry. **67:12**, 960-966

Tepfer, D. Goldmann, A. Pamboukdjian, N. Maille, M. Lepingle, A. Chevalier, D. Dénarié, J. Rosenberg, C. (1988) *A Plasmid of Rhizobium meliloti 41 Encodes Catabolism of Two Compounds from Root Exudate of Calystegium sepium.* Journal of Bacteriology **170(3):** 1153-1161

The Potato Genome Sequencing Consortium (2011). *Genome sequence and analysis of the tuber crop potato*. Nature **475:** 189-194

Vorst O., de Vos C.H.R., Lommen A., Staps R.V., Visser R.G.F., Bino R.J., Hall R.D, (2005) *A non-directed approach to the differential analysis of multiple LC-MS-derived metabolic profiles*. Metabolomics **1(2),** 169-180

Wink, M. (1988) *Plant breeding: importance of plant secondary metabolites for protection against pathogens and herbivores*. Theoretical Applied Genetics. **75:** 225-233

Yang, F. Zhao, H. Carroll, A.R. (2017) *Tropane alkaloids from the Australian plant Triunia montana (Proteaceae).* Tetrahedron Letters. **58**: 736-739

Zabetakis, I. Edwards, R. O'Hagan, D. (1999) *Elicitation of tropane alkaloid biosynthesis in transformed root cultures of Datura stramonium*. Phytochemistry **50:** 53-56

Zhou M., Ma X., Sun J., Ding G., Cui Q., Miao Y., Hou Y., Jiang M., Bai G. (2017) *Active fragments-guided drug discovery and design of selective tropane alkaloids using ultra-high performance liquid chromatography-quadrupole time-of-flight tandem mass spectrometry coupled with virtual calculation and biological evaluation*. Analytical and Bioanalytical Chemistry. **409**, 1145-1157

Ziegler, J. Facchini, P.J. (2008) *Alkaloid Biosynthesis: Metabolism and Trafficking*. Annual Review of Plant Biology **59:** 735-769

Bibliography

Applied Biosystems (2009) *DNA sequencing by Capillary Electrophoresis: Applied Biosystems Chemistry Guide*. Second Edition.

Christen P., Bieri S., Veuthey J-L., *Analysis of Tropane Alkaloids in Biological Matrices*. Modern Alkaloids: Striucture, Isolation, Synthesis and Biology. Wiley (2007) Chapter 12, pg 343-369

Dewick, P. M. (2009). *Medicinal Natural Products*. Chichester: Wiley-Blackwell. ISBN 978-0-470-74276-1

El-Sakka M.A., Phytochemistry (3) Alkaloids. Al Azhar University; Third Edition (2010).

Kumar, K.P. Bhowmik, D. Chandira, C.B.R. (2010). *Transdermal Drug Delivery System – A Novel Drug Delivery System and its Market Scope and Opportunities*. International Journal of Pharma and Bio Sciences. V1 (2)

NanoDrop® Technologies, Inc. (2007) *NanoDrop® ND-1000 Spectrophotometer V3.5 User's Manual*. **Rev 7/2007**

NSW Government – Office of Environment and Heritage (2011). *Observed Changes in New South Wales climate 2010*. ISBN 9781742932033

Ohlendorf, W. (1996) *Domestication and crop development of Duboisia spp. (Solanaceae) In: Domestication and commercialisation of non-timber forest products in agroforestry systems.* Non-Wood Forest Products 9 (Chapter 16) 183-187

Ortiz, O. Mares, V. (2017) *The Historical, Social and Economic Importance of the Poato Crop.* Chapter 1, The Potato Genome. Springer Nature, Switzerland. ISBN 978-3-319-66135-3.

Roberts, M.F. Wink, M. (1998) *Alkaloid: Biochemistry, Ecology and Medicinal Application*. Plenum Press, New York. pp 1-7

Springob, K. Kutchan, T.M. (2009) *Plant Derived Natural Products*. Chapter 1, Introduction to the Different Classes of Natural Product. Springer, New York. ISBN 978-0-387-85497-7

Vanhaelen, M. Lejoy, J. Hancoq, M. Molle, L. (1991) *Climatic and geographical aspects of medicinal plant constituents.* Chapter 5, The Medicinal Plant Industry, CRC Press, London. ISBN 978-0-849-36669-7

Wink, M. (1998) *Alkaloids: Biochemistry, Ecology and Medicinal Applications*. Plenum Press, New York. pp. 11-44

Yamada, Y. Hashimoto, T. (1988) *Biosyntehsis of tropane alkaloids. Application of plant cell and tissue culture.* Ciba Foundation Symposium 137, Wiley, Chichester pp 199-212

Web pages

Food and Agriculture Organisation of the United Nations (FAO) (2018) www.fao.org/faostat/en Accessed 16/02/2018

International Association for Plant Taxonomy (IAPT) (2012*) Chapter I: Taxa and their ranks*. Article 4. www.-iapt-taxon.org/nomen.main.php?page=art4. Accessed 11/8/2015

Markets and Markets (2018) https://www.marketsandmarkets.com/PressReleases/BRIC-Diabetes-Drugs.asp Accessed 07/03/2018

Appendix:

	Parts Per Million (ppm) Standard Mix Concentration															
	0.01		0.1		0.5		1		2		5		10		20	
Compound	Avg.	Sdev	Avg.	Sdev	Avg.	Sdev	Avg.	Sdev	Avg.	Sdev	Avg.	Sdev	Avg.	Sdev	Avg.	Sdev
Ornithine	1796.333	131.535	1581.000	54.028	2554.000	263.369	5141.667	129.867	9769.667	344.218	27899.333	706.451	59759.333	530.852	112200.333	2437.363
Labelled Ornithine	792.000	336.822	1710.000	621.935	6321.333	249.963	11921.667	312.862	20998.000	229.541	61375.667	2334.737	119831.667	2990.460	229319.000	13269.316
Tropinone	1727.667	600.733	8172.000	157.645	35140.667	7050.209	80791.000	3248.542	85099.333	2456.506	160541.667	4525.840	262176.333	2709.470	473105.000	2190.190
Calystegine A_3					8143.000	19.799	17551.333	1254.577	26926.000	1176.626	65011.000	6888.427	105057.333	3145.069	310084.000	3221.124
Tropine	4385.667	2100.104	7615.667	520.187	37335.667	1881.449	78944.333	3514.418	128097.333	2528.809	153227.000	4366.381	235155.667	3115.159	670399.667	18770.466
Phenylalanine	7057.000	2750.770	10842.000	48.570	53993.333	1573.347	111588.333	9924.114	228994.000	4117.850	571100.333	5393.993	1103925.333	12926.450	2146811.000	23108.958
Littorine	2518.000	1224.074	9339.333	86.674	49072.667	795.309	90695.000	1473.512	166087.667	420.430	365085.667	2357.849	651888.333	3703.724	1107416.000	15231.721
Hyoscyamine	2505.667	64.501	26179.667	797.111	124392.333	2095.223	239857.667	7448.937	448174.000	11258.852	995357.000	24642.031	1739404.667	53034.701	2996481.667	77332.261
Anisodamine	1887.667	144.905	15112.000	404.063	63077.333	1384.270	113110.333	2813.646	197478.000	2739.668	400096.333	6807.915	676562.333	16332.870	1186683.333	28145.544
Scopolamine	1599.667	87.831	15712.333	319.691	69714.000	779.024	125758.333	2430.271	222348.333	2740.211	453268.000	3638.078	764212.667	13173.208	1296115.333	20032.013

Table A.3.1: Average relative abundance and Standard deviation of compounds used in the early development of the MRM method

Standard	Product Ions	Collision Energy	Abundance	Buffer Ratio (A/B)
Ornithine	70.1	16	6770	100/0
	116.1	4	4132	
	115.1	4	1501	
Tropinone	98.1	20	78750	100/0
	57.1	36	44868	
	56.1	48	25199	
	82.1	20	26010	
Pseudotropine	96.1	21	79234	100/0
	67.1	29	25817	
	124.1	17	49742	
	42.2	45	14532	
Calystegine A_3	142.1	8	22080	100/0
	79.1	20	8928	
	77.1	36	5790	
	98.1	16	5115	
Calystegine B_2	140.1	8	19553	100/0
	158.1	4	9235	
Tropine	98.1	24	35960	100/0
	58.2	28	27963	
	57.1	36	28898	
	56.1	52	16787	
Phenylalanine	120.1	8	132080	65/35
	77.1	44	45788	
	103.1	28	43711	
	51.1	72	24069	
Littorine	142.1	28	153128	50/50
	93.1	32	197007	
	77.1	60	122601	
	124.1	24	404892	
Hyoscyamine	124.1	24	494919	50/50
	93.1	32	252103	
	77.1	68	174560	
	91.1	48	119048	
Anisodamine	140.1	24	477875	50/50
	77.1	80	76020	
	91.1	44	68738	
	58.2	44	47005	
Scopolamine	138.1	12	396847	50/50
	156.1	12	408702	
	77.1	72	207672	
	103.1	4	233802	

Table A.3.2: Data for metabolites associated with the tropane and nortropane alkaloid biosynthesis pathway used in the generation of the MRM.

	Datura Leaf		Potato Sprout	
Metabolite	**ng/mg DW**	**st.dev**	**ng/mg DW**	**st.dev**
Ornithine	0.01731815	0.000717269	0.484461236	0.017539583
Tropinone	0.000584393	0.000312652	0.000626943	0.000144902
Calystegine A_3	0.005797557	0.000735296	0.03095444	0.005437381
Tropine	0.000937892	0.00053239	0.000190937	1.03666E-05
Phenylalanine	0.023147082	0.000769118	0.289143578	0.001754108
Littorine	0.032198174	0.000390754	-0.003076015	8.24471E-06
Hyoscyamine	0.013527441	0.000329121	-0.001562105	1.88645E-05
Anisodamine	0.078729797	0.001208632	-0.003233839	0.000306518
Scopolamine	0.149712454	0.002380208	-0.004312895	0.000153176

Table A.3.3: Numerical representation of the metabolites being detected in the samples from Figure 3.3.8 showing that although in minute quantities, metabolites of interest are able to be detected within the Datura leaf sample and that the metabolites up to the tropinone branch point and associated with the NTA arm are detectable in the potato sprout tissue.

Primer	Sequence (5'-3')	UPL Probe
pET-Dsh6h-NheI_F	GCT AGC ATG GCT ACT TTT GTC TCA AA	
pET-Dsh6h-EcoRI_R	GAA TTC TTA ACA GAA GAA CCA ACA CA	
pET-Sth6h-NdeI_F	CAT ATG ATG GCA TCA CTA GTT TCA AG	
pET-Sth6h-BamHI_R	GGA TCC TTA GAG CTT ATA TGG TTT CA	
pET-Sth6h_u743-NdeI_F	CAT ATG GAT GGA AAA TAA TTT AGT GTC	
pET-Sth6h_u743-BamHI_R	GGA TCC TTA GAG CTT GTA AGA CTG AAG	
pET-T7_ter	GCT AGT TAT TGC TCA GCG G	
Sth6h_qPCR_F	TGG TGA CCC ATC ACT ACC C	122
Sth6h_qPCR_R	GCA CCA TCA CAA TGT TCA CC	122
Sth6h-u743_qPCR_F	GCC TGA AAG TTA CAT ATT CCC AGA	80
Sth6h-u743_qPCR_R	TGG ACT GCT ACC ACT TAA AGG AA	80

Gene	I.D
Dsh6h	KR006982.1
Sth6h_u743	XM_006352681.2
Sth6h	XM_006340300.2

Table A.4.2.1: Primers used in the synthesis and sequencing of recombinant protein vectors, as well as RT-qPCR analysis for the two annotated h6h sequences within potato. GenBank Accession numbers for the genes used in this study are also given.

Primer	Sequence (5'-3')	UPL Probe
Ws_trI-syn-F	GCG GGT CTC GAA TGG ATG AAT CAA G	
Ws_trI-syn-R	GCG CGG TCT CGA AGC TTA AAA TCC A	
Ws_trI-F	CGA ATG GAT GAA TCA AGC GTT T	
Ws_trI-R	AGC TTA AAA TCC ACC ATT AGC T	
Ws_trI-Trans-F	CCA TGG AAG ATC TAG ATG GAG TC	
Ws_trI-Trans-R	TTG CAC CTT TGG AAG CAG AAT AA	
Ws_trI_Tnos_Seq_F	TCA ATT CAG TTG CTC CAG GA	
Ws_trI_35s_Seq_R	AGT TCA TTT TCA TTA CGT GAA C	
Ws_trI_qPCR-F	CGA AGA AGT CGC TGC AGT AAT	18
Ws_trI_qPCR-R	TAT AAT CTG GCC CGT TAC ATA AGA	18

Gene	I.D
Ws_trI	KF360055.1

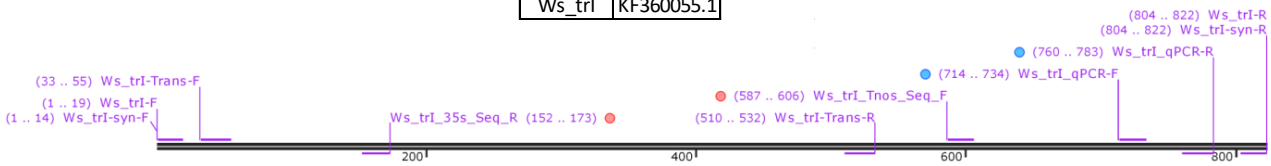

Table A.5.2.1: Primer sequences and location of primer binding upon *WstrI* coding sequence used in this study.

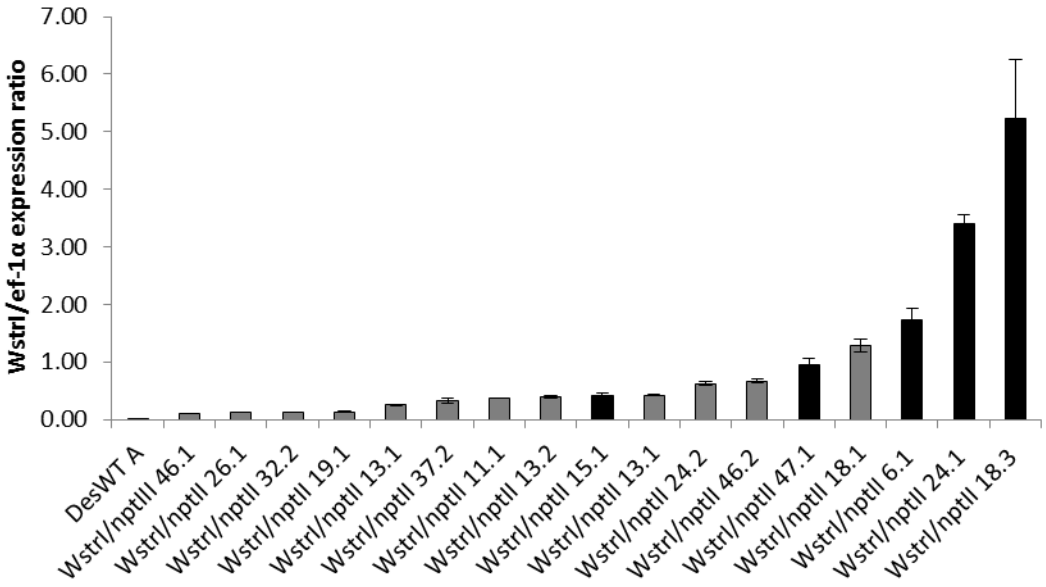

Figure A.5.2.1: *WstrI/ef-1α* expression ratios for all plant lines characterised prior to the best performers being grown out in the glasshouse.

Primer	Sequence (5'-3')	UPL Probe
As_trII-672-F	GCG CCG TCT CGC TCG AAT GGA AGC AGC AGG AAA ACA A	
As_trII-672-R	GCG CCG TCT CGC TCG AAG CTT AAG GCA TTG GGT ATG GGA T	
trII-5UTR-F	AAA TCA ATT GGA GGC TTC ATT	
trII-5UTR-R	GCA GCC TTC AAG ATT CC	
35s-AS-Trans-R	GGG TCT TGC GAA GGA TAG TG	
As-35stoNPTII-R	TAG ATC GTC TTG ATC AGA CC	
As_trII_35s_Seq_R	TCT ACA TAG AAT GGG TGA GC	
As_trII_Tnos_Seq_F	TGA TTA CGT GAA CAT GTA TA	
qPCR-trII-5U_74F	CCC ATT TTT CAA GTC TTG TGC	74
qPCR-trII-5U_74R	GCA GCC TTC AAG ATT CCA TC	74
qPCR-As_trII-138_F	TGC TGC TTC ATA TGT CAC TGG	138
qPCR-As_trII-138_R	TGA TTA AAA GCC ACC ATT AGC C	138

Gene	I.D
St_trII	AJ292343.1

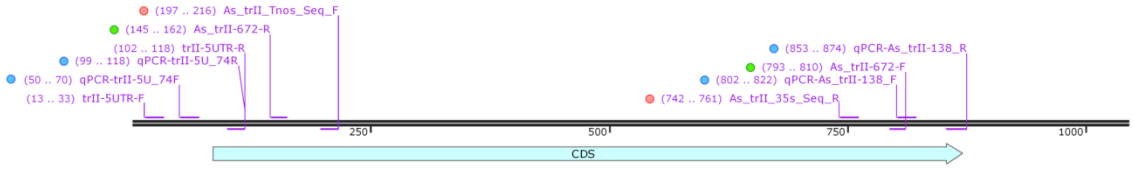

Table A.6.2.1: Primers used in the production of down-regulation vector, sequencing and characterisation of transgenics within this study

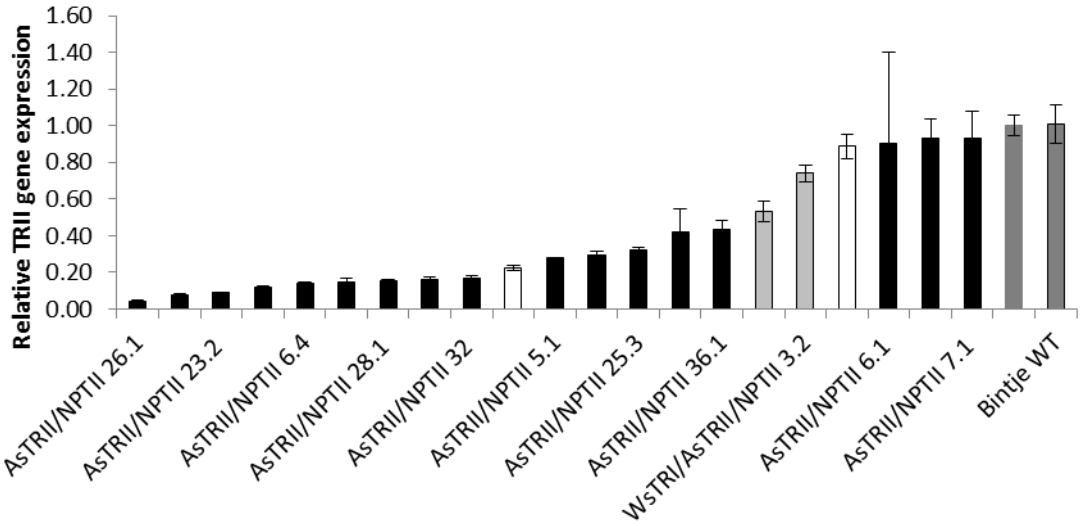

Figure A.6.2.1: RT-qPCR analysis for all *SttrII* down-regulating lines prior to the best lines being grown out in the glasshouse**.**